FLOW OVER SIDE WEIRS

by D.J. Balmforth. B.Sc.

Submitted for the Degree of

DOCTOR OF PHILOSOPHY

UNIVERSITY OF SHEFFIELD

Department of Civil and Structural Engineering

AUGUST 1978

CONTENTS

TABLES

FIGURES

ACKNOWLEDGEMENTS

The author wishes to thank Dr E.J. Sarginson for his help and encouragement as supervisor, Mr B. Wardle for his assistance in the construction of the experimental apparatus, and Mrs J. Patrick for typing this script.

NOMENCLATURE

A	Cross-sectional area of flow; constant in the law of curvature distribution.
A_m	Average value of A.
AJ	Value of surface curvature in iteration j.
AJ1	Value of surface curvature for the previous step (x_{n-1} to x_n).
a	Streamline constant = $c.\cos\psi$
B	Width of rectangular section channel.
B_w	Width of the channel at crest level (Allen[13]).
b	Streamline constant = $c.\sin\psi$
C	Weir coefficient (Ackers[5]) = $^2/_3 \sqrt{2g}\ C_D$
C'	Dimensionless constant (Allen[13]).
C_D	Coefficient of discharge.
C_{II}	Constant (Frazer[15]).
c	Height of weir crest above channel bed; streamline constant
c_r	Ratio $^c/_{y_c}$.
D	Diameter of circular section.
d	Distance below free surface.
d_r, d_2, d_3, d_4, d_5	Depth ratios (Frazer[15])
E	Specific energy.
E_c	Critical specific energy.
E_1	Specific energy at the upstream end of the weir.
E_2	Specific energy at the downstream end of the weir.
F_r	Froude Number
f	A function
g	A function
g	Gravitational acceleration
h	A function
h	Step Length

h_f	Head loss due to friction.
i	A function.
j	A suffix used as a counter.
K	Pressure force correction factor; streamline constant = $\cos\psi$
K_s	Value of the streamline constant at the water surface.
K_1, K_2	Constants used in modified formula for q.
k_o, k_1, k_2, k_3	Values computed in the Runge Kutta method.
L	Length of the weir.
l	Ratio L/B
M_L	Momentum flux of flow passing over the weir in length Δx.
M_1	Momentum flux of the mainstream at the upstream end of Δx.
M_2	Momentum flux of the mainstream at the downstream end of Δx.
m	Indice in curvature distribution law.
m_o, m_1, m_2, m_3	Values computed in the Runge Kutta method.
n	Manning roughness value; a suffix used as a counter; indice in velocity distribution law; side slope of trapezoidal section; proportional depth = z/y.
P	Wetted perimeter; pressure force.
p	Pressure.
Q	Discharge.
Q_a	Available flow (Allen[13]).
Q_w	Discharge over the side weir.
Q_1	Discharge in the upstream channel; discharge at the upstream end of a short length of channel.
Q_2	Discharge in the downstream channel; discharge at the downstream end of a short length of channel.

q	Discharge over the side weir per unit length.
$q_2, q_3, q_4, q_5, q_\infty$	Discharge ratios (Frazer[15]).
R	Hydraulic mean depth.
R_e	Reynolds' number.
R_m	Average hydraulic mean depth.
r	Radius of curvature.
r'	Radius of curvature of the water surface.
s_f	Friction gradient.
s_o	Slope of the channel bed.
t	Curvature of the water surface $= d^2y/dx^2 = dz/dx$
u	Longitudinal component of velocity at a distance d below the water surface.
u_o	Longitudinal component of velocity at the water surface.
$\bar{u}$	Longitudinal component of the side spill flow.
v	Mean longitudinal component of velocity at a section.
v_m	Mean value of v, $= \frac{1}{2}(v_1 + v_2)$
v_1	Value of v at the upstream end of the weir; value of v at the upstream end of a short length of channel.
v_2	As v_1 but at the downstream end.
W	Width of the water surface.
w	Discharge per unit width of channel $= vy$.
x	Distance along the channel bed.
y	Depth of flow.
y_c	Critical depth.
y_m	Mean value of y, $= \frac{1}{2}(y_1 + y_2)$
y_1	Depth of flow at the upstream end of weir; depth of flow at the upstream end of a short length of channel.

y_2	As y_1 but at the downstream end.
z	Slope of the water surface = dy/dx; distance above the channel bed.
α	Velocity energy coefficient.
β	Momentum flux correction factor.
γ	Indice in Engels' formula[8], and Coleman and Smith formula[9].
ΔM	Change in momentum flux over length Δx.
ΔQ	Discharge passing over the weir in length $\Delta x = Q_2 - Q_1$.
Δv	$v_2 - v_1$.
Δx	Short length of channel.
Δy	Increase in y over Δx.
δ	Indice in Engels' formula and the Coleman and Smith formula.
ζ	A function (Schmidt[12]).
η	Constant = $(n + 1)^2 / (m + 2n + 1)$.
θ	Constant = $2y_1/y_c + (y_c/y_1)^2$; angle of inclination of bed to horizontal
λ	Friction factor.
μ	Weir coefficient (De Marchi[3,4]).
μ_s	Empirical value of μ.
ν	Kinematic viscosity of water.
ρ	Density of water.
τ_{ox}	Shear stress at the boundary.
ϕ	Slope angle of a streamline; potential function; a function.
ψ	Stream function; a function.

SUMMARY

A literature survey has been carried out to assess the merits of the diverse methods of analysis of side weir flow previously available. Two of these appeared to have potential as practical methods of analysis and they were tested against the data obtained during this investigation.

A momentum analysis of the flow in the main channel yielded a general differential equation which, for supercritical flow, included terms to allow for the effect of curvature on the vertical pressure distribution. The discharge over the side weir, per unit length, was obtained using the transverse weir equation. These two simultaneous equations formed the basis of a mathematical model incorporating standard integration techniques.

Preliminary tests were conducted in a large rectangular channel which tapered uniformly so as to produce a constant head along the weir. This enabled values of the coefficient of discharge to be obtained for use in the transverse weir equation, and values were found to lie within 2% of those given by the Rehbock equation. Velocity distributions were measured to establish values of the momentum flux correction factor, and these were found to correspond to normal values.

In the main experimental investigations five side weirs were tested in a prismatic rectangular channel. The most significant parameters that affected the discharge over the weir were the settings of the channel controls and the crest height. Substantial variations in the weir length were required to affect the side spill discharge significantly, whilst the effect of the channel slope was almost negligible.

A comprehensive set of experimental data was obtained and this was used to test the accuracy of the mathematical model. It was found to give extremely good simulation of the flow with both mean and standard deviation of errors in the computed discharge less than 5% in all cases.

CHAPTER 1. INTRODUCTION

1.1 Introduction

1.1.1 The side weir and side spillway have been widely used since the end of the 19th century for diverting a proportion of the mainstream flow in a channel or watercourse into a secondary chamber alongside. By far the most common application has been as storm sewage overflows and Victorian engineers were responsible for the construction of a large number of such overflows on combined sewer systems in most cities and towns in the British Isles. Originally these overflows consisted of no more than a slot in the side of the sewer pipe, but soon they developed into proper side weirs constructed in special chambers. The channel was normally rectangular in section with either a single side weir, or double side weirs where space was restricted. More recently side weirs have been used to distribute flows to settling tanks in sewage treatment works and side spillways can be seen let into river banks as part of flood relief schemes.

1.1.2 In the majority of cases the use of a side weir as a storm sewage overflow has proved unsatisfactory in the long term. There are several reasons for this:-

(a) The existing sewers now carry flows well in excess of their original design values.

(b) The inability of the traditional side weir overflow to provide a separation of solid particles.

(c) A lack of understanding of the various characteristics of side weir flow.

(d) The absence of a satisfactory theoretical or empirical treatment to enable the engineer to design a new installation or analyse an existing system.

1.1.3 Accurate prediction of sewer flows and redesigning of overflow chambers has done much to alleviate the problems listed under (a) and (b) above, but despite numerous published works on the subject the engineer was still without proper means of design or analysis unless he resorted to an over-simplified theoretical or limited empirical approach. Naturally this led to errors in design.

It is the purpose of this investigation, therefore, to develop a satisfactory theoretical analysis of side weir flow and provide the engineer with a design method capable of dealing with a wide variety of side weir and spillway configurations and flow conditions.

1.2 Review of Previous Work

1.2.1 Over the past eighty years there have been a large number of contributions to the field of side weir flow. Some have been similar in nature to more major works whilst others have been limited to very specific applications. In general these works have been excluded from this review. The more significant contributions have been divided, for ease of reference, into empirical and theoretical categories, though in a few cases this is somewhat arbitrary as both approaches have been considered.

(a) Theoretical

1.2.2 Parmley W.C.[1]

By assuming that the discharge per unit length over a side weir is given by the transverse weir equation Parmley developed an expression for the time required to reduce the head on the weir by a given amount:-

$$t = \frac{B}{0.294\sqrt{g}} \left\{ \frac{1}{\sqrt{y_2 - c}} - \frac{1}{\sqrt{y_1 - c}} \right\} \qquad \text{............(1.1)}$$

He then assumed that the longitudinal velocity v along the weir was constant, and thus the length of weir required is

$$L = \frac{vB}{0.294\sqrt{g}} \left\{ \frac{1}{\sqrt{y_2 - c}} - \frac{1}{\sqrt{y_1 - c}} \right\} \qquad \text{............(1.2)}$$

Parmley did not support this equation by experimental data nor did he indicate how the value of v was to be determined. Since the formula may only be applied to supercritical flow conditions (Fig. 2.1), where the mean velocity varies substantially along the length of the weir, it is unlikely to give accurate results.

1.2.3 Nimmo W.H.R.[2]

A detailed momentum analysis is given for a trapezoidal section by considering the channel to be divided into a number of small finite sections each Δx in length. The discharge over the weir is computed for each section from the transverse weir equation

$$Q = C\,(y - c)^{3/2}\,\Delta x \qquad \text{............(1.3)}$$

and a finite difference formula is derived for computing the changes in depth, and hence in discharge, along the length of the weir:-

$$\frac{\Delta y}{\Delta x} = \left\{ s_f - s_o - \frac{Q}{g\,(by + ny^2)^2} \cdot \frac{\Delta Q}{\Delta x} + \frac{Q^2}{g} \cdot \frac{y}{(by + ny^2)^3} \cdot \frac{\Delta b}{\Delta x} + \frac{Q^2}{g} \cdot \frac{y^2}{(by + ny^2)^3} \cdot \frac{\Delta n}{\Delta x} \right\} \Big/ \left\{ 1 - \frac{Q^2}{g} \cdot \frac{(b + 2ny)}{(by + ny^2)^3} \right\} \qquad \text{.............(1.4)}$$

The validity of the method was determined by comparing computed longitudinal surface profiles and discharges with those measured in a 54m trapezoidal timber flume, and there was found to be a reasonably good correlation. The value of the weir coefficient C used in equation (1.3) was first obtained by measuring the mean head and discharge over each 1.2m length of flume. For general application of the method the same value of C as used for a transverse weir of the same type is suggested but this is not supported by experimental data.

1.2.4 De Marchi G. [3,4]

The discharge per unit length of weir is given by a form of the transverse weir equation, such that

$$q = -\frac{dQ}{dx} = \mu\sqrt{2g}\,(y - c)^{3/2} \quad \text{..............(1.5)}$$

The same value for μ as a transverse weir could be used, in which case $\mu = \frac{2}{3} C_D$, although no recommendation is given by De Marchi. By neglecting energy losses and slope of the channel bed the following differential equation is derived

$$\frac{dy}{dx} = \frac{y\,Q}{Q^2 - gB^2y^3} \cdot \frac{dQ}{dx} \quad \text{..............(1.6)}$$

Inspection of this equation enabled De Marchi to distinguish between the falling supercritical flow profiles (Figs. 2.1 and 2.4) and the rising subcritical profile (Fig. 2.2). After substituting the terms of the transverse weir equation for $^{dQ}/_{dx}$ in equation (1.6), the latter is integrated to

$$L = \frac{B}{\mu}\left\{ \phi\left(\frac{y_2}{E}\right) - \phi\left(\frac{y_1}{E}\right)\right\} \quad \text{..............(1.7)}$$

where

$$\phi\left(\frac{y}{E}\right) = \frac{2E - 3c}{E - c}\sqrt{\frac{E - y}{y - c}} - 3\sin^{-1}\sqrt{\frac{E - y}{E - c}} \quad \text{.....(1.8)}$$

Values of $\phi\left(\frac{y}{E}\right)$ are given graphically enabling the method to be used easily for analysing existing weirs or for computing the length of a weir required to remove a given proportion of the mainstream flow. Although it has been shown to give good results in certain cases[11] (section 6.13) significant errors have also been observed with this method, particularly when applied to supercritical flow (section 6.13).

1.2.5 Ackers P. [5]

This method also neglects energy losses and the effect of a sloping channel bed. In this case energies are related to the weir crest and similar equations for side spill discharge and surface slope are derived to those given by De Marchi. The equations are integrated using a similar integration function to that given in equation (1.8) and it may be concluded that there is no advantage to be gained in using this method over the one summarised in the previous section. A number of important conclusions are drawn by Ackers however.

By inspection of the theoretical equations it was shown that the subcritical flow upstream of the weir would be drawn down sufficiently to form supercritical flow on the weir itself (Fig. 2.1) if the crest height was less than a half of the specific energy at the upstream end of the weir. This has been verified by the current investiation (section 6.4).

It was also shown that if energy losses and bed slope are neglected then the condition for a constant head along the weir is

$$\frac{dB}{dx} = -C\,\frac{(y-c)^{3/2}}{yv} \qquad \text{.............(1.9)}$$

It follows that if a constantly tapering channel is used to produce a constant head then the mean velocity remains constant along the length of the weir (ref: section 4.2). Ackers recommended that no allowance for longitudinal velocity should be made in computing the value of the weir discharge coefficient which should be the same as if the weir were transverse. This has also been verified during the present investigation (section 6.1)

1.2.6 Chow V.T. [6]

By dividing the channel into small finite sections Δx in length, and applying a momentum analysis, Chow developed a numerical integration technique in which the rise in water surface elevation $\Delta y'$ is given by the equation

$$\Delta y' = \frac{\alpha Q_1 (v_1 + v_2)}{g (Q_1 + Q_2)} \quad \Delta v \left\{ 1 - \frac{\Delta Q}{2Q_1} \right\} - s_f . \Delta x \quad \ldots\ldots\ldots (1.10)$$

Suffixes 1 and 2 refer respectively to the upstream and downstream ends of the section under consideration. The side spill discharge ΔQ is computed from a form of the transverse weir equation;

$$\Delta Q = \frac{2}{3} \sqrt{2g} \; C_D \left\{ \frac{y_1 + y_2}{2} - c \right\}^{3/2} . \Delta x \quad \ldots\ldots\ldots (1.11)$$

and the gradient of the total energy line s_f may be computed from the Manning equation or by any other suitable method. The performance of Chow's Numerical Integration Method has been studied as part of this investigation and the findings are discussed in section 6.13. Although Chow makes no recommendation for values of C_D or α the method was found to work reasonably well in most cases when the normal values of C_D and α were used. It is recommended for use when a digital computer is not available as the computations can easily be arranged into tabular form. The method is applicable to both subcritical and supercritical flow profiles where a hydraulic jump is not formed along the weir section.

1.2.7 Smith K.V. [7]

A general differential equation for spatially varied flow over side weirs is derived from energy considerations:

$$\frac{dy}{dx} = \frac{s_o - s_f - \frac{\alpha Q}{gA^3} \cdot \frac{dQ}{dx} + \frac{\alpha Q^2 y}{gA^3} \cdot \frac{dB}{dx}}{1 - \frac{\alpha Q^2 W}{gA^3}} \qquad \text{............(1.12)}$$

where $\frac{dQ}{dx}$ is given by the transverse weir equation,

$$\frac{dQ}{dx} = -\frac{2}{3}\sqrt{2g}\; C_D \;(y - c)^{3/2} \qquad \text{............(1.13)}$$

Equation (1.12) is applicable to most artificial sections, and an extended form of the equation is given for irregular section natural channels.

The solution of equations (1.12) and (1.13) is simultaneously effected by dividing the channel into small incremental lengths and working along the weir in steps from known conditions at one end. Each step length is dealt with successively and solutions obtained iteratively for that length. Although tedious by long hand calculation the method is readily handled by a digital computer. It is claimed that convergence to a solution is rapidly reached at each step for both subcritical and supercritical flows, although difficulty is experienced in the region of critical flow. Worked examples are included but the results are not supported by experimental data. No recommendations are given for suitable values of the weir coefficient C_D or the velocity energy coefficient α.

This is the first method to apply a generalised theoretical approach to the problem of flow over side weirs.

(b) Empirical

1.2.8 Engels H. [8]

By neglecting the effects of friction and channel slope Engels suggests a simple formula for the side spill discharge,

$$Q_w = \frac{2}{3}\sqrt{2g} \; . \; C_D \, L^{\gamma} \quad (y_2 - c)^{\delta} \qquad \text{.............(1.14)}$$

in which the indices γ and δ are related by the equation

$$\gamma + \delta = 2.5 \qquad \text{.............(1.15)}$$

Equation (1.15) ensures that equation (1.14) is dimensionally homogenous.

A series of 25 tests were performed on a wide variety of side weirs in prismatic rectangular channels, in which the flow was subcritical throughout (Fig. 2.2). From the results Engels concludes that γ should have a value of 0.831 and δ a value of 1.669. The data from these tests has been used in section 6.12 to help to evaluate the performance of the mathematical model developed as a part of the current investigation.

Engels undertook a further series of tests on weirs set in a tapering rectangular channel. Values of γ and δ were found to be 0.9 and 1.6 respectively, and these values were not affected by the ratio of upstream to downstream width. However, since a prismatic channel can be thought of as a special case of a tapering channel, there is clearly some inconsistency in the recommended values for γ and δ.

A value of C_D of 0.855 is recommended for a round crested weir and 0.735 for a sharp crested weir, which do not agree with accepted values for transverse weirs.

1.2.9 Coleman S. and Smith D. [9]

The usual form of the transverse weir equation is abandoned in favour of an empirical equation of the type

$$Q_w = C\,L^{\gamma}\,(E_1 - c)^{\delta} \qquad \text{.............(1.16)}$$

where the upstream specific energy E_1 is computed by adding the velocity head $\frac{v_1^2}{2g}$ to the depth at the start of the weir, y_1. The formula is only applied to cases where supercritical flow occurs along the length of the weir (Fig. 2.1) and having conducted a series of tests for that condition Coleman and Smith suggest suitable values for C, γ and δ such that

$$Q_w = 0.316\,L^{0.72}\,(E_1 - c)^{1.645}\ \mathrm{m^3/s} \qquad \text{.............(1.16.1)}$$

This is further developed by including the channel width B,

$$Q_w = 2.583\,B\,L^{0.72}\,(E_1 - c)^{1.645}\ \mathrm{m^3/s} \qquad \text{.............(1.17)}$$

although this is not supported by experimental data.

Finally, by a semi-empirical analysis, a formula for the length of weir is obtained:

$$L = 1.158\,B\,v\,(y_2 - c)^{0.13}\left\{\frac{1}{\sqrt{y_1 - c}} - \frac{1}{\sqrt{y_2 - c}}\right\}\ \mathrm{m} \qquad \text{.(1.18)}$$

It can be seen that equation (1.18) is similar to that developed by Parmley (equation (1.2)). Again no indication is given as to how the value of v is to be calculated. Furthermore, none of the equations given above allow for the draw-down effects in the upstream channel. Despite these drawbacks, however, the equations were used as the principal design method in Great Britain for a number of years.

1.2.10 Favre H. and Braendle F. [10]

By applying a momentum analysis to a short length of channel the following differential equation for spatially varied flow with decreasing discharge is developed:

$$- dy = s_f \, dx + \frac{v \, dv}{g} + \left\{1 - \frac{\bar{u}}{v}\right\} \frac{Q \, dQ}{gA^2} \qquad \text{.........(1.19)}$$

where $\bar{u}$ represents the longitudinal component of the side spill flow. Since equation (1.19) cannot be integrated directly it is written as a difference equation relating to a small finite length of channel Δx, with the friction gradient s_f computed from the Manning equation:

$$- \Delta y = \frac{n^2 v_m^{\,2}}{R^{4/3}} \Delta x + \frac{v_2^{\,2} - v_1^{\,2}}{2g} + \left\{1 - \frac{\bar{u}}{v_m}\right\} \cdot \left\{\frac{Q_2^{\,2} - Q_1^{\,2}}{2gA_m^{\,2}}\right\} \qquad \text{.............(1.20)}$$

A preliminary series of 9 tests were undertaken to establish suitable roughness values n for the channel and to determine the head/discharge characteristics for the side weirs. The latter was achieved by testing the weirs as transverse weirs under constant head.

A second series of 19 tests were conducted on 2m long round crested weirs in a 201m wide horizontal rectangular channel. The first 9 tests used a double side weir installation. In each case the flow was subcritical throughout (Fig. 2.2).

Data from the preliminary tests was used for computing n and $(Q_2 - Q_1)$ for use in equation (1.20). The velocities $\bar{u}$ and v_m were assumed to be the same, thus putting the last term in equation (1.20) equal to zero, and theoretical longitudinal profiles were computed by applying equation (1.20) to successive short increments of channel along the weir. At the same time the side spill discharge was computed.

Computed longitudinal surface profiles are found to lie within about ± 10% of measured values, while computed discharges differ by about ± 5%. The effect of friction is found to be small. The effect of a sloping channel bed is not considered and the tests have not been extended to different sized weirs or channels, nor to cover supercritical flow. The validity of this method for general application is therefore uncertain.

1.2.11 Gentilini B.[11]

Gentilini conducted a series of 12 experiments in a 214mm wide rectangular channel in order to assess the validity of De Marchi's theory[3,4]. The first 8 tests were conducted with subcritical flow along the weir (Fig. 2.2) and the remainder with supercritical flow occurring (Fig. 2.4). De Marchi's assumption that energy losses along the weir were negligible is investigated by plotting values of $100\left\{\frac{E_1 - E_2}{E_2}\right\}$ against $\frac{C}{E_2}$ for subcritical flow. Values of $100\left\{\frac{E_1 - E_2}{E_2}\right\}$ are found to reduce from 2.80 to zero as $\frac{C}{E_2}$ increases.

from 0.70 to 0.95. Gentilini concludes therefore that the assumption of zero energy loss is reasonable for subcritical flow. He further substantiates this by computing mean values for the weir discharge coefficient μ (equation (1.5)) and comparing them with measured values.

$$\text{Theoretical} \quad \mu = \frac{B}{L} \left\{ \phi \left(\frac{y_2}{E}\right) - \phi \left(\frac{y_1}{E}\right) \right\} \qquad \text{.........(1.7.1)}$$

$$\text{Experimental} \quad \mu_s = \frac{Q_1 - Q_2}{\sqrt{2g} \int_L (y - c)^{3/2} \, dx} \qquad \text{.........(1.21)}$$

For subcritical flow the ratio μ_s/μ varies from 0.903 to 0.981 as y_2 increases.

For supercritical flow, however, the ratio μ_s/μ varies from 0.381 to 0.575 showing a substantial discrepancy between theoretical and experimental values. It is concluded that De Marchi's method is not suitable for application to supercritical flow. The experimental work was not extended to investigate the effect of sloping the channel bed, although this has subsequently been found to introduce further errors into De Marchi's method (section 6.13). The data from Gentilini's experiments has been used in section 6.12.

1.2.12 Schmidt M. [12]

Schmidt identifies four possible flow cases as shown in Figs. 2.1 to 2.4, and investigates the value of the weir discharge coefficient and energy loss along the length of the weir using the results of a series of tests undertaken in a large rectangular channel.

Using an average value for the head on the weir, $y_m - c$, the discharge over the side weir is obtained from the formula

$$Q_w = \frac{2}{3} \sqrt{2g} \quad C_D L (y_m - c)^{3/2} \qquad \text{...........(1.22)}$$

Values of the coefficient of discharge, C_D, are found to be well scattered within $\pm$ 5% of Rehbock's[19] values.

The energy of the flow is represented by the dimensionless function ζ, such that

$$\zeta = \frac{y_2 - y_1}{\frac{\alpha_1 V_1^2}{2g} - \frac{\alpha_2 V_2^2}{2g} - h_f} \qquad \text{...........(1.23)}$$

where α_1 and α_2 are taken as 1.1 and h_f is an average head loss for the main channel computed from a form of the Manning equation:

$$h_f = \frac{n^2 v_m^2 L}{R_m^{4/3}} \qquad \text{...........(1.24)}$$

Values of ζ are plotted against $\frac{y_m - c}{y_m}$ for various conditions of flow and the data of Engels [8] and Gentilini [9] are also included. Although relationships are indicated on the graphs the points are far too scattered for reliable conclusions to be drawn. This is not surprising since in many cases a hydraulic jump formed on the weir.

1.2.13 Allen J.W. [13]

Experiments were conducted on a side weir formed in the side of a 150mm circular pipe. The main channel, therefore, had a circular invert which was adjusted to slopes varying between horizontal and 1 in 70. Weir lengths varied from 235mm to 762mm.

The tests were only conducted for supercritical flow along the weir (Fig. 2.1) and the subcritical flow in the upstream channel was observed to draw down by up to 30%.

Allen considers the flow in the upstream pipe as being made up of two parts, namely the 'unavailable' flow which passes along the main channel below the crest, and can be computed from proportional depth-discharge curves, and the remainder which he terms the 'available' flow, Q_a. He shows that the discharge over the weir, Q_w is proportional to Q_a and deduces the following formula for computing its value:

$$\frac{Q_w}{Q_a} = C' \left\{\frac{L}{D}\right\}^{2/3} \qquad \ldots\ldots\ldots\ldots(1.25)$$

where C' is a dimensionless constant. The effect of channel slope is found to be negligible.

An attempt is made to correlate the experimental results with a simple theory. The shape of the water surface profile is approximated by a square law of the type

$$(y - c) \propto \frac{1}{\sqrt{x}} \qquad \ldots\ldots\ldots\ldots(1.26)$$

where x = distance from the upstream end of the weir.

Equation (1.26) does not give good agreement with the measured water surface profile at the upstream end of the weir and it leads to an expression for side spill flow per unit length of the form

$$dQ = C\,(y - c)^{2/3}\,d\,L \qquad \ldots\ldots\ldots\ldots(1.27)$$

It can be seen that equation (1.27) is contrary to the findings of previous research where the value of the head over the weir $(y - c)$ is raised to the power $3/2$.

Finally an empirical formula is deduced for computing the value of the coefficient C' in equation (1.25):

$$C' = \frac{0.22\,D}{B_W} \qquad \text{...........(1.28)}$$

where B_W is the width of the channel at crest level.

Although the formulae above are given in dimensionless form there is no reason to suppose that they will give good correlation with wiers of different proportions to those used for the experiments, particularly bearing in mind the novel form of equation (1.27).

1.2.14 Collinge V.K. [14]

Collinge conducted tests in a 102mm and a 305mm wide flume in order to observe the types of water surface profiles that could occur, to check if the De Marchi theory could be applied to side weirs and the limits of its applicability, to determine whether the coefficient of discharge of the weir is affected by the longitudinal velocity, and to determine the nature of the bed load movement.

Measurements of discharges and surface profile co-ordinates were made for a variety of flows in each flume for both subcritical and supercritical conditions (Figs. 2.1 and 2.2), although from the observations recorded it would appear that an unbroken hydraulic jump occurred on the weir in a number of cases (Fig. 1.3).

A preliminary series of tests were undertaken to establish values of the weir coefficient μ (equation (1.5)) for use with the De Marchi method. The downstream channel was sealed and an average head over the crest determined from equations (1.29) and (1.30) below.

For small variations of head,

$$\text{Mean head} = \frac{y_1 + y_2}{2} - c \qquad \text{..........(1.29)}$$

For larger variations of head,

$$\text{Mean head} = \left\{ \frac{1}{L} \int_0^L (y - c)^{3/2} \, . \, dx \right\}^{2/3} \qquad \text{...(1.30)}$$

The mean head is then used in equation (1.5) to obtain a value of μ. Since equation (1.5) is strictly only applicable to short lengths of weir where the head may be considered constant, its use with equation (1.30) to produce a value of weir coefficient must be questioned, and it is not surprising that the test results produce values of weir coefficients of 0.352 and 0.374 for the 305mm and 102mm flumes respectively which are substantially different from the usual transverse weir coefficient of 0.415 recommended by De Marchi. A value of μ of 1.33 is obtained for a clinging nappe using the 102mm flume, but the value of the indice in equation (1.5) rises from 1.5 to 1.8 in this case.

In the main programme of tests the measured discharge is compared with computed values using the empirical weir coefficients obtained from the preliminary tests. For subcritical flow (upstream Froude Number ranging from 0.3 to 0.98) the computed side spill discharges are about 20% greater than the measured values but this rises to over 150% greater as the flow becomes supercritical ($Fr_1 = 1.0$) and then falls to about 30% greater as the upstream Froude Number rises to 1.3. It is unfortunate that the theoretical discharges were computed using the empirical weir coefficients since the more generally accepted value of of 0.415 would have given better correlation.

Collinge, however, attributed the discrepancies to the effects of longitudinal velocity on the weir coefficient and proceeded to obtain values for μ from the main series of tests in the same manner used for the preliminary tests. The values of μ thus produced are found to be up to 20% less than those previously computed and a graph showing the percentage reduction in μ with longitudinal velocity is given. Although relationships are indicated for both free and clinging nappes on the graph there is too much scatter and insufficient data for firm conclusions to be reached.

The present investigation has shown the weir coefficient to be unaffected by longitudinal velocity and the discrepancies between theoretical and measured values that Collinge observed can be wholly attributed to the inability of the De Marchi method to take friction and channel slope into account, as discussed in section 6.13.

1.2.15 Frazer W. [15]

Frazer was the first investigator to identify all of the five possible flow types that can occur in a channel fitted with a side weir. He denotes the types as Cases I to V and they are shown in Figures 2.1 to 2.5 respectively.

After a series of qualitative tests on a small pilot rig the main investigations were carried out in a rectangular flume with a width that could be varied up to a maximum of 229mm. This was fitted with a sharp crested weir whose length and crest height were varied during the course of the experiment.

An attempt at a conventional analysis of side weir flow is made but it amounts merely to a statement of constant specific energy when applied to a prismatic channel. Further attempts at a theoretical analysis are abandoned in favour of a semi-empirical approach.

The experimental results are shown in dimensionless form and for each flow case an attempt is made to give a correlation of quantity with depth of flow, and quantity with length of weir.

The following dimensionless parameters are defined:-

$$q_5 = \frac{\text{Discharge at Downstream End of Weir}}{\text{Discharge at Upstream End of Weir}}$$

$$d_5 = \frac{\text{Depth at Downstream End of Weir}}{\text{Critical Depth at Upstream End of Weir}}$$

q_∞ = q_5 for infinitely long weir.

For supercritical flow (Case I) the relationship between quantity and depth of flow is shown to be

$$q_5 = d_5 \sqrt{2.5 - 1.5\, d_5} \qquad \text{...........(1.31)}$$

and the relationship between quantity and length

$$\frac{1 - q_5}{1 - q_\infty} = 1 - 10^{-\frac{L}{8B}} \qquad \text{...........(1.32)}$$

Equation (1.31) implies an energy loss of $\frac{1}{4}(y_1 - y_2)$.

For subcritical flow (Case II) equation (1.31) becomes

$$q_5 = d_5 \sqrt{0.99\theta - 2d_5} \qquad \text{...........(1.33)}$$

where $\theta = \frac{2y_1}{yc} + \left\{\frac{yc}{y_1}\right\}^2$

In order to correlate quantity with weir length the transverse weir equation is assumed to apply

$$Q_1 - Q_2 = C_D \cdot \frac{2}{3}\sqrt{2g}\,(y_m - c)^{3/2} \cdot L$$

where y_m represents the mean depth of flow along the weir.

In dimensionless form,

$$1 - q_5 = C_{II} \ (d_r - c_r)^{3/2} \ . \ l \qquad \text{..........(1.34)}$$

where $C_{II} = C_D \frac{2}{3} \sqrt{2g}$, $d_r = \frac{y_m}{yc}$

$c_r = \frac{c}{yc}$ and $l = \frac{L}{B}$

Values of C_{II} are shown graphically and vary between 0.3 and 0.6, but there is too much scatter for reliable values of C_{II} to be obtained. In addition, all the tests were conducted on a horizontal channel so the effect of channel slope was not observed. This limits the range of application of the method considerably.

Perhaps the most interesting aspect of Frazer's work was his attempt to deal with the formation of an hydraulic jump on a side weir (Case III) and he is the only person known to have included this case in his investigations. It is considered as a combination of Cases I and II. Suffixes 1 and 2 refer to the upstream and downstream end of the weir respectively in this case, and suffixes 3 and 4 to the upstream and downstream ends of the hydraulic jump. The latter is assumed to occur instantaneously and the sequent depth formula is therefore applied. In dimensionless form this states that

$$d_4 = \frac{d_3}{2} \left\{ \sqrt{\frac{8q_3^{\,2}}{d_3^{\,3}} + 1} - 1 \right\} \qquad \text{...........(1.35)}$$

This is clearly a simplification of the phenomenon since it was observed during the present investigation that a significant flow passed over the weir along the length of an hydraulic jump.

The flow downstream of the jump is treated as a Case II profile, and upstream of the jump as Case I where equations (1.31) and (1.32) can be used to compute d_3 and q_3. d_4 is obtained from equation (1.35) and the dimensionless specific energy just downstream of the jump is defined as

$$\psi = 2d_4 + \frac{q_3^2}{d_3^2} \qquad \text{............(1.36)}$$

The conditions at the downstream end of the weir are computed from the following expressions

For $0.882 > q_2 > 0.700, \quad q_2 = d_2 \sqrt{(1.01\psi - 2d_2)}$ ....(1.37)

For $0.700 > q_2 > 0.478, \quad q_2 = d_2 \sqrt{(0.383\psi^2 - 2d_2)}$ ....(1.38)

Equations (1.37) and (1.38) are obtained by curve fitting data which exhibits a good deal of scatter, and it is questionable whether they are applicable even within their limited ranges of q_2. Furthermore, an attempt to obtain a weir discharge coefficient for the section downstream of the jump by a similar method to that used with the Case II profile met with the same problem of widely scattered results. This coefficient is required to provide the additional relationship between q_2 and d_2 needed for the solution of equation (1.37) or (1.38).

1.2.16 El-Khashab A. and Smith K.V.H. [16]

The experimental work reported by El-Khashab and Smith was undertaken concurrently with the present investigation.

Side weir flow is analysed using both an energy and a momentum approach in a similar fashion to the more detailed analysis attributed to Yen and Wenzel[18]. The energy analysis yields an equation identical to that already proposed by Smith but simplified for a prismatic channel:-

$$\frac{dy}{dx} = \frac{s_o - s_f - \frac{\alpha Q}{gA^2} \cdot \frac{dQ}{dx}}{1 - \alpha \frac{Q^2 W}{gA^3}} \qquad \text{...........(1.39)}$$

Results of the experimental tests, which were conducted in a 0.46m wide rectangular flume, show the total energy line to deviate considerably from the theoretical line even after allowing for friction losses. This was at first thought to be due to the effect of secondary flows induced by the flow over the weir but three dimensional velocity measurements, used to compute the total kinetic energy at each section, did little to alleviate the problem. The discrepancy was finally attributed to the acceleration of the flow passing over the weir where the longitudinal velocity component of $\bar{u}$ was observed to be greater than the mean velocity v in the main channel at that section.

A momentum approach was therefore adopted which yielded the following differential equation:

$$\frac{dy}{dx} = \frac{s_o - s_f - \frac{1}{gA}(2\beta v - \bar{u})\frac{dQ}{dx}}{1 - \beta \frac{Q^2 W}{gA^3}} \qquad \text{...........(1.40)}$$

This equation was solved by the step by step procedure of Smith[7] in which the discharge over the weir per unit length is computed from the transverse weir equation (1.13). No recommendation is given for a suitable value of the coefficient of discharge however.

The value of $\bar{u}$ used in equation (1.40) was first obtained experimentally. For subcritical flow the value of $\bar{u}$ is obtained from one of two relationships, shown graphically. For $Q_W/Q_1 < 0.5$ the ratio $\bar{u}/v$ is shown to be proportional to y/c, and for $Q_W/Q_1 > 0.5$ the ratio $v_1/\bar{u}$ is shown to be proportional to $(y - c)/(y_1 - c)$. For supercritical flow a single relationship between $\bar{u}/v$ and the upstream Froude Number Fr_I is concluded from the results.

There are two important drawbacks to the use of these relationships in computing side spill discharges and surface profiles. Firstly there is no reason to suppose that these empirical correlations can be extrapolated for weirs whose dimensions differ appreciably from those used in the experiments. Secondly, for subcritical flow a preliminary computation is required to estimate $\bar{u}$. Neither of these drawbacks apply to the mathematical model developed as the result of the present investigation.

It is also doubtful whether it is correct to distinguish between the longitudinal component of the side spill flow $\bar{u}$ and the mean velocity of the mainstream v in equation (1.40). The momentum analysis is conducted along the centre line of the channel and the longitudinal velocity of particles which ultimately pass over the weir, as they initially deviate from the mainstream, is clearly equal to the mean velocity of the mainstream at that point (i.e. $\bar{u} = v$). Once a particle has passed over the weir, however, it will have travelled some distance downstream and the mean velocity in the mainstream will be less at that downstream section in most cases. At that point the particle is remote from the mainstream flow and no longer involved in the analysis.

For supercritical flow (Case I) an upstream depth of y_1 equal to 0.93 y_c is recommended as a starting value for computations, but results of the present investigation showed y_1 to vary between $0.84y_c$ and $0.98y_c$, which has a significant effect on any computed values.

El-Khashab and Smith state that their method of analysis showed "excellent agreement" with observations but no values for the mean or standard deviation of errors are quoted. A discussion on this published paper has been submitted by the author[17], and a copy is contained in Appendix I.

CHAPTER 2. THEORY

2.1 Classification of Side Weir Flow

2.1.1 Before conducting an investigation into the behaviour of flow over side weirs it is important to identify the various flow categories that can occur. There are five possible flow configurations and these were first classified by Frazer[15] who denoted them as Cases I to V respectively. The flow profile for each case is shown in Figures 2.1 to 2.5 and the conditions under which each occurs are discussed below.

2.1.2 Case I (Fig. 2.1)

If a low side weir is installed in a channel where the flow regime is normally subcritical then the water surface will be drawn down as the flow approaches the weir and the Froude Number progressively increases until critical conditions are reached a short distance upstream of the weir. The surface continues to fall so that at the start of the weir the depth is a little less than the critical depth (normally between 0.84 and 0.98 of the critical depth).

The flow along the weir is supercritical for the whole length, with a falling profile, and despite the discharge over the weir the flow accelerates in the main channel and the Froude Number progressively increases. Initially the curvature of the water surface is negative, but a point of contraflecture is reached a short distance downstream of the start of the weir and the curvature becomes positive (a sag-curve profile) for the remainder of the length of the weir.

Due to the high longitudinal velocities the side spill flow makes a small angle with the weir as it passes over the crest, and the magnitude of the angle reduces progressively as the flow passes downstream.

The flow is entirely controlled by the conditions that exist at the upstream end of the weir and the surface profile along the upstream section of the weir is not affected by the length of the weir. With long weirs the water surface may fall sufficiently for the nappe to cling at the downstream end of the weir and in extreme cases side spill may cease altogether before the downstream end of the weir is reached. If the downstream channel cannot sustain supercritical flow an hydraulic jump will form in the downstream channel.

It is shown in section 6.4 that the Case I condition only occurs if the crest height is less than half of the Specific Energy of the flow at the upstream end of the weir.

2.1.3 Case II (Fig. 2.2)

In the case where the flow in the channel upstream of the weir is subcritical, but the crest height is greater than a half of the Specific Energy at the upstream end of the weir, subcritical flow will occur along the whole length of the weir. The entire flow in the channel is controlled by conditions in the downstream channel and the water surface rises along the weir despite the reduction in discharge due to the side spill flow. The surface curvature is negative over virtually the whole length of the weir and the Froude Number progressively decreases along the weir.

The longitudinal velocities are much less than those observed with Case I flows and the angle that the side spill flow makes with the weir is correspondingly greater and increases progressively as the flow passes downstream.

The water surface in the upstream channel is again drawn down as the flow approaches the weir but this is not as severe as in Case I, and the critical depth is not reached.

In practical applications this flow case often occurs when there is a control structure, such as a weir or sluice, in the downstream channel. It is possible in such a case to vary the downstream depth by adjusting the settings of the control structure thereby regulating the proportion of flow that passes over the weir. This is dealt with in more detail in section 6.3.

2.1.4 Case III (Fig. 2.3)

This case is strictly a combination of the Case I and Case II profiles. Like the Case I flow it can only occur if the crest height is less than a half of the Specific Energy of the flow at the upstream end of the weir, and in fact the two cases are identical up to the hydraulic jump. However in this case the downstream flow is throttled, either by a control structure or by the downstream channel itself, so that the hydraulic jump, which occurred downstream of the weir in Case I, now moves upstream to form on the weir. The flow profile on the latter part of the weir is essentially the same as the Case II profile and is regulated by the downstream control in exactly the same fashion.

A slight relaxing of the downstream throttle causes the jump to move downstream and less flow passes over the weir. Conversely increased throttling moves the jump upstream and increases the side spill discharge. In many cases the jump is observed to oscillate in position resulting in fluctuating side spill and downstream discharges. For this reason, and because of the difficulty in analysis, it is advisable to avoid this case in practice.

2.1.5 Case IV (Fig. 2.4)

In certain circumstances supercritical flow will occur upstream of a side weir, for example, when the channel is steep sloping or when the upstream flow is regulated by a sluice. If the downstream channel does not throttle the flow then supercritical flow will occur along the whole length of the weir with a falling profile similar to that of Case I. In this case, however, the depth at the start of the weir is not directly related to the critical depth, but is regulated by the upstream channel control which governs the whole of the flow along the weir. If the downstream channel cannot sustain supercritical flow an hydraulic jump will form in the downstream channel.

2.1.6 Case V (Fig. 2.5)

In the same way as the Case III profile is formed by a combination of Case I and Case II so the Case V profile is formed by a combination of Case IV and Case II. The supercritical profile upstream of the hydraulic jump is regulated by the upstream channel control and is identical to the corresponding Case IV profile. The subcritical profile downstream of the hydraulic jump is regulated by the downstream channel control and is identical to the corresponding Case II profile. The Case V profile is formed because the downstream throttle is sufficiently severe to move the hydraulic jump upstream so that it forms on the weir. The jump has also been observed to oscillate in position in this situation, and again it is advisable to avoid this case in practice.

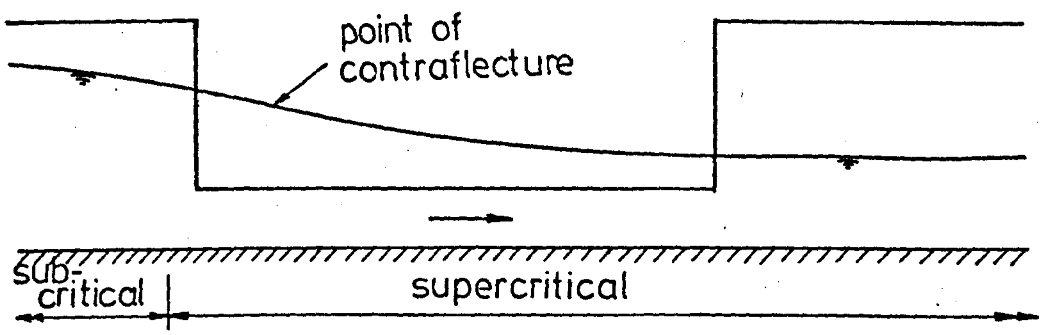

CASE I. MILD SLOPE, LOW WEIR

fig. 2.1

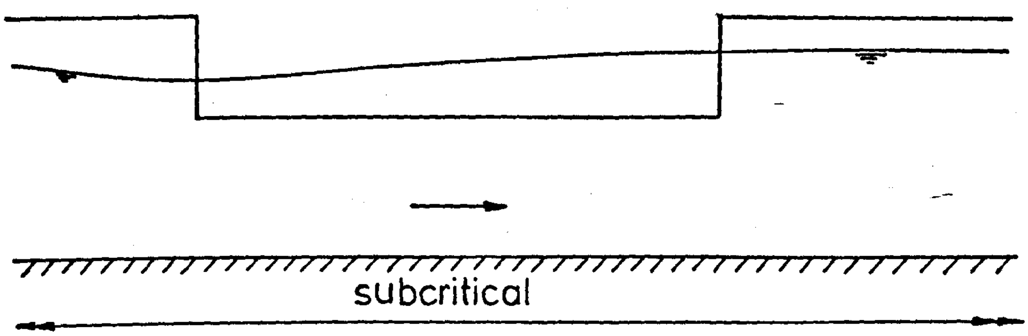

CASE II. MILD SLOPE, HIGH WEIR, DOWNSTREAM CONTROL

fig. 2.2

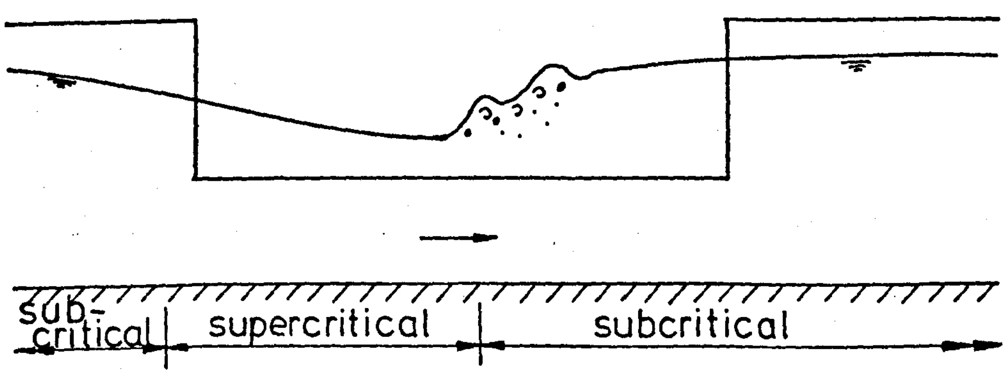

CASE III. MILD SLOPE, LOW WEIR, DOWNSTREAM CONTROL

fig. 2.3

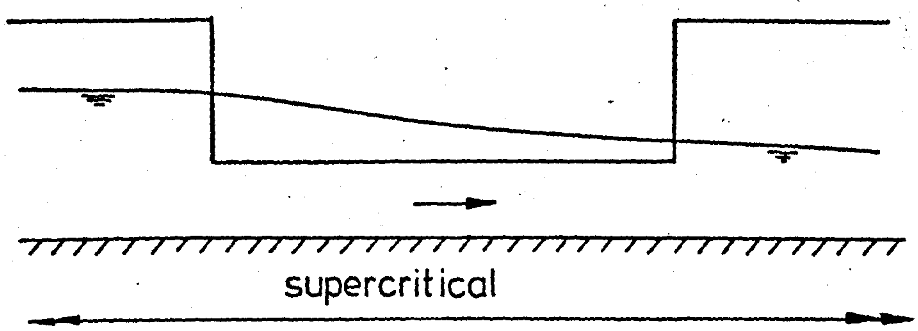

CASE IV. STEEP SLOPE, LOW WEIR

fig. 2.4

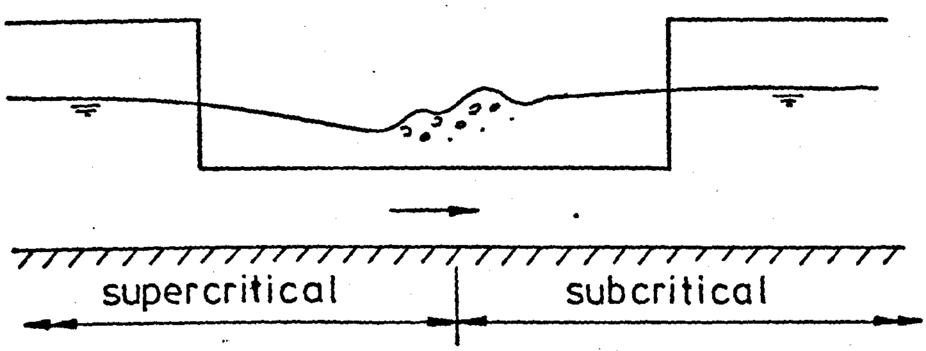

CASE V. STEEP SLOPE, LOW WEIR, DOWNSTREAM CONTROL

fig. 2.5

2.2. Development of the General Differential Equation

2.2.1 The analysis that follows is based on the Principles of Conservation of Momentum and Continuity and is similar to a more general analysis of spatially varied flow performed by Yen and Wenzel[18].

Figure 2.6 shows a small finite length of channel, length Δx, with the upstream and downstream cross-sections defined as sections 1 and 2 respectively.

If q = discharge passing over the weir per unit length of channel

then $$\frac{dQ}{dx} = -q \qquad \text{............(2.1)}$$

The change in momentum over the length Δx is given by the equation

$$\Delta M = (M_2 + M_L) - M_1 \qquad \text{............(2.2)}$$

where M_L is the momentum of the water lost over the weir between sections 1 and 2.

$$M_2 - M_1 = \Delta(\rho \beta A v^2) \qquad \text{............(2.3)}$$

where β is the momentum flux correction factor (or momentum coefficient) defined by

$$\int_A \rho u^2 \, dA = \rho \beta A v^2$$

If each particle that ultimately passes over the weir initially deviates from the mainstream with a longitudinal velocity equal to the mean velocity at that section then

$$M_L = \rho q \Delta x \, v \qquad \text{............(2.4)}$$

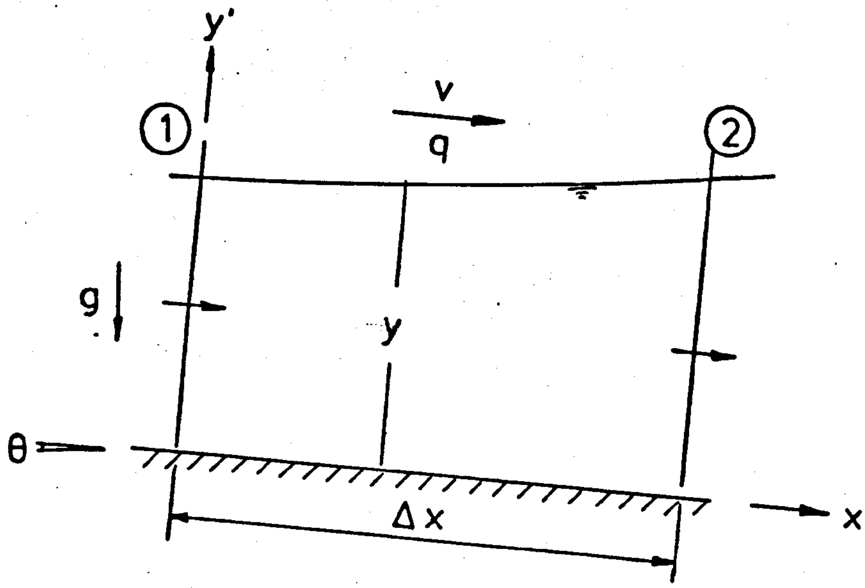

fig. 2.6

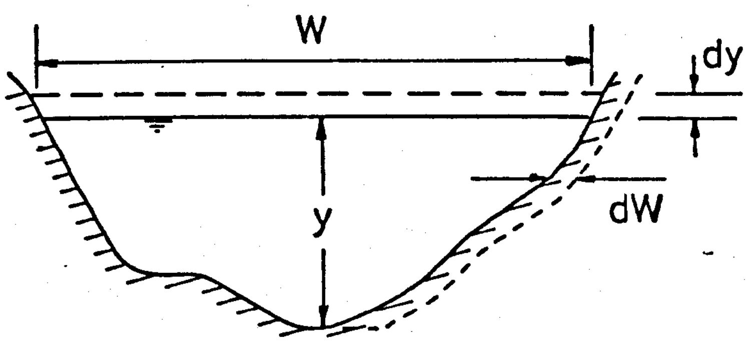

fig. 2.7

According to Newtons Second Law of Motion the rate of change of momentum is balanced by three forces. These are:-

(a) The component weight of water between sections 1 and 2

$$= \rho g\ A \sin \Delta x = \rho g\ A\ S_o \Delta x \qquad \text{............(2.5)}$$

(b) The opposing effect of friction

$$= -\tau_{ox} P \Delta x$$

where P is the wetted perimeter.

$$s_f = \frac{\tau_{ox}}{\rho g R} \qquad \text{............(2.6)}$$

$$\therefore\ -\tau_{ox} P \Delta x = -\rho g A\ s_f \Delta x \qquad \text{............(2.7)}$$

(c) The change in pressure force, including the force exerted by the tapering channel walls in the direction of flow

$$= -\Delta(\rho g\ KAy \cos\theta) + \rho g K y^2 \Delta W \cos\theta \qquad \text{.........(2.8)}$$

where K is the pressure force correction factor defined by

$$\int_A p\ dA = K \rho g A y \cos\theta$$

Putting equations (2.5), (2.7), (2.8), and (2.3) and (2.4) into equation (2.2) gives

$$\rho g A\ s_o \Delta x - \rho g A\ s_f \Delta x - \Delta(\rho g\ KAy \cos\theta) + \rho g K y^2 \Delta W \cos\theta$$
$$= \Delta(\rho \beta A v^2) + \rho q v \Delta x$$

$$\rho g A\ s_o \Delta x - \rho g A\ s_f \Delta x - \rho q v \Delta x = \Delta(\rho \beta A v^2) + \Delta(\rho g K A y \cos\theta)$$
$$+ \rho g K y^2 \Delta W \cos\theta$$

In the limit as Δx tends to zero,

$$\frac{d}{dx}\left\{\rho\beta A v^2 + \rho g K A y \cos\theta\right\} - \rho g K y^2 \cos\theta . \frac{dW}{dx} = \rho g A . (s_o - s_f) - \rho q v \quad ..(2.9)$$

Expanding equation (2.9)

$$\rho A v^2 . \frac{d\beta}{dx} + \rho\beta v^2 . \frac{dA}{dx} + 2\rho\beta A v . \frac{dv}{dx} + \rho g A y . \frac{d(K \cos\theta)}{dx}$$

$$+ \rho g K y \cos\theta . \frac{dA}{dx} + \rho g K A \cos\theta . \frac{dy}{dx} - \rho g K y^2 . \cos\theta . \frac{dW}{dx}$$

$$= \rho g A \, (s_o - s_f) - \rho q v$$

Dividing throughout by $\rho g A$

$$\frac{v^2}{g} . \frac{d\beta}{dx} + \frac{\beta v^2}{gA} . \frac{dA}{dx} + 2\frac{\beta v}{g} . \frac{dv}{dx} + y . \frac{d(K \cos\theta)}{dx}$$

$$+ \frac{K y \cos\theta}{A} . \frac{dA}{dx} + K \cos\theta . \frac{dy}{dx} - \frac{K y^2 \cos\theta}{A} . \frac{dW}{dx}$$

$$= s_o - s_f - \frac{qv}{gA} \quad ....(2.10)$$

For the generalised cross-section shown in figure 2.7

$$\frac{dA}{dx} \approx W . \frac{dy}{dx} + y . \frac{dW}{dx} \quad ....(2.11)$$

$$Q = vA$$

$$\therefore \frac{dQ}{dx} = v . \frac{dA}{dx} + A . \frac{dv}{dx} = -q$$

$$\therefore \frac{dv}{dx} = -\frac{1}{A} . \left\{ q + v \frac{dA}{dx} \right\}$$

$$\frac{dv}{dx} = -\frac{1}{A} . \left\{ q + v \left(W . \frac{dy}{dx} + y . \frac{dW}{dx} \right) \right\} \quad ....(2.12)$$

Substituting equations (2.11) and (2.12) into equation (2.10)

$$\frac{v^2}{g} \cdot \frac{d\beta}{dx} + \frac{\beta v^2}{gA}\left(W . \frac{dy}{dx} + y . \frac{dW}{dx} \right) - \frac{2\beta v}{gA}\left\{ q + v\left(W . \frac{dy}{dx} + y . \frac{dW}{dx} \right) \right\}$$

$$+ \; y . \frac{d(K \cos\theta)}{dx} + \frac{Ky \cos\theta}{A} . \left(W . \frac{dy}{dx} + y . \frac{dW}{dx} \right) + K \cos\theta \; . \frac{dy}{dx}$$

$$- \; \frac{Ky^2 \cos\theta}{A} . \frac{dW}{dx} = s_o - s_f - \frac{qv}{gA}$$

$$\frac{v^2}{g} . \frac{d\beta}{dx} + \frac{\beta v^2 W}{gA} . \frac{dy}{dx} + \frac{\beta v^2 y}{gA} . \frac{dW}{dx} - \frac{2\beta qv}{gA} + \frac{qv}{gA} - \frac{2\beta v^2 W}{gA} . \frac{dy}{dx}$$

$$- \; \frac{2\beta v^2 y}{gA} . \frac{dW}{dx} + y . \frac{d(K \cos\theta)}{dx} + \frac{KWy \cos\theta}{A} . \frac{dy}{dx} + \frac{Ky^2 \cos\theta}{A} . \frac{dW}{dx}$$

$$+ \; K \cos\theta \; . \frac{dy}{dx} - \frac{Ky^2 \cos\theta}{A} . \frac{dW}{dx} = s_o - s_f$$

$$\frac{dy}{dx}\left(\frac{\beta v^2 W}{gA} - \frac{2\beta v^2 W}{gA} + \frac{KWy \cos\theta}{A} \right) + \frac{dW}{dx}\left(\frac{\beta v^2 y}{gA} - \frac{2\beta v^2 y}{gA} \right)$$

$$+ \; \frac{v^2}{g} . \frac{d\beta}{dx} + y . \frac{d(K \cos\theta)}{dx} = s_o - s_f - \frac{qv}{gA} . (1 - 2\beta)$$

$$\frac{dy}{dx} = \frac{s_o - s_f - \frac{qv}{gA} . (1 - 2\beta) - \frac{v^2}{g} . \frac{d\beta}{dx} - y . \frac{d(K \cos\theta)}{dx} + \frac{\beta v^2 y}{gA} . \frac{dW}{dx}}{K \cos\theta \; . \left(1 + \frac{Wy}{A} \right) - \frac{\beta v^2 W}{gA}}$$

..................(2.13)

Equation (2.13) is the general differential equation for steady spatially varied flow with decreasing discharge over a side weir in a non-prismatic channel with a varying bed slope.

2.2.2. Equation (2.13) may be simplified for different applications as follows.

For a constant bed slope

$$\frac{d\,(K\cos\theta)}{dx} = \cos\theta \cdot \frac{dK}{dx}$$

Equation (2.13) becomes

$$\frac{dy}{dx} = \frac{s_o - s_f - \frac{qv}{gA}\cdot(1 - 2\beta) - \frac{v^2}{g}\cdot\frac{d\beta}{dx} - y\cos\theta\cdot\frac{dK}{dx} + \frac{\beta v^2 y}{gA}\cdot\frac{dW}{dx}}{K\cos\theta\left(1 + \frac{Wy}{A}\right) - \frac{\beta v^2 W}{gA}}$$

For a shallow sloping rectangular section, where the curvature of the flow is small,

$W = B = \frac{A}{y}$, $\frac{d\beta}{dx} = 0$, $\frac{dK}{dx} = 0$, $K = \frac{1}{2}$, and

$$\frac{dy}{dx} = \frac{s_o - s_f - \frac{qv}{gBy}\cdot(1 - 2\beta) + \frac{\beta v^2}{gB}\cdot\frac{dB}{dx}}{\cos\theta - \frac{\beta v^2}{gy}} \qquad \text{.............(2.14)}$$

For a rectangular prismatic channel

$$\frac{dy}{dx} = \frac{s_o - s_f - \frac{qv}{gBy}\cdot(1 - 2\beta)}{\cos\theta - \frac{\beta v^2}{gy}} \qquad \text{.............(2.15)}$$

Equation (2.15) is the form of the general differential equation used for formulating the model for applications where the curvature of the water surface is negligible. Note that this equation reduces to the general differential equation for gradually varied flow when q is put equal to zero:-

$$\frac{dy}{dx} = \frac{s_o - s_f}{\cos\theta - \frac{\beta v^2}{gy}} \qquad \text{.............(2.16)}$$

2.3 Computation of the Side Spill Discharge

2.3.1 Before equation (2.14) can be used as a basis for a mathematical model an expression for q, the discharge over the weir per unit length, has to be derived.

The complex three dimensional flow over the weir may conveniently be considered as consisting of two parts; the longitudinal flow passing down the main channel, and a transverse flow passing over the weir. The latter may be considered as being independent of the mainstream flow in that it is determined at any section solely by the head over the crest at that section and the geometric characteristics of the weir (excluding length). In other words, the discharge per unit length over the side weir may be computed from the transverse weir equation.

$$q = \frac{2}{3} \sqrt{2g} \quad C_D \quad (y - c)^{3/2} \qquad \text{............(2.17)}$$

2.4 Allowance for Channel Roughness

2.4.1 The term s_f in equation (2.15) also has to be computed at each point along the channel. It accounts for the resistance due to boundary shear stress in the x direction, τ_{ox}, and is related to the latter by equation (2.6).

Ideally τ_{ox} should be measured directly or computed from the velocity profile near the boundary. However, in practical applications the necessary information is not usually available and the value of s_f must be estimated by other means. It is normal practice to assume s_f to be equal to the gradient of the total energy line and to compute its value from the Chezy, Manning, or Darcy-Weisbach formulae.

For the smooth channels used in the experimental tests the Darcy-Weisbach equation was chosen:

$$s_f = \frac{\lambda}{4R} \cdot \frac{v^2}{2g} \qquad \text{............(2.18)}$$

in which the friction factor λ was computed from the Blasius formula:

$$\lambda = \frac{0.3164}{R_e^{\frac{1}{4}}} \qquad \text{............(2.19)}$$

where R_e = Reynolds Number = $\frac{4vR}{\nu}$

For larger channels with rougher walls constructed in brick or concrete the Chezy or Manning equations would be more appropriate.

$$\text{Chezy} : s_f = \frac{v^2}{C^2 R} \qquad \text{............(2.20)}$$

$$\text{Manning} : s_f = \frac{n^2 v^2}{R^{4/3}} \qquad \text{............(2.21)}$$

The Mathematical Model was also tested with s_f computed by the Manning equation and a comparison of the results is made in section 6.11.

2.5 The Effect of Curvature of the Water Surface

2.5.1 When supercritical flow forms along all or part of the weir there is an appreciable curvature of the water surface in the vicinity of the upstream end of the weir. This is particularly significant for the Case I and III profiles due to the draw-down of the water surface upstream of the weir. The curvature of the streamlines has the effect of modifying the pressure distribution and the magnitude of the pressure force. For a negative curvature (hog-curve) the centrifugal effects of curvature reduce pressures below their hydrostatic values, and for positive curvature (sag-curve) the pressures increase. The assumptions inherent in equation (2.15) no longer apply and a further analysis of the flow is required to incorporate curvature effects.

2.5.2 Consider a small elemental cuboid of width B, length dx and height dd, a distance d below the water surface, as shown in Figure 2.8. The element is travelling, at the instant considered, with a velocity u in the direction of flow.

Equating the forces acting on the element in a direction perpendicular to the channel bed

$$(p + dp)\, B.dx - (p)\, B.dx - \rho g\, B.dd.dx.\cos\theta = \rho g\, B.dd.dx.\frac{u^2}{r}\cos\phi$$

$$dp = \rho g.dd.\cos\theta + \rho\frac{u^2}{r}.dd.\cos\phi$$

It can be seen from Fig. 2.8 that ϕ varies from a maximum at the surface to zero at the channel bed. Since the maximum surface slope recorded during the experiments was -0.2, corresponding to a $\cos\phi$ of 0.98 at the water surface, the value of $\cos\phi$ is nearly

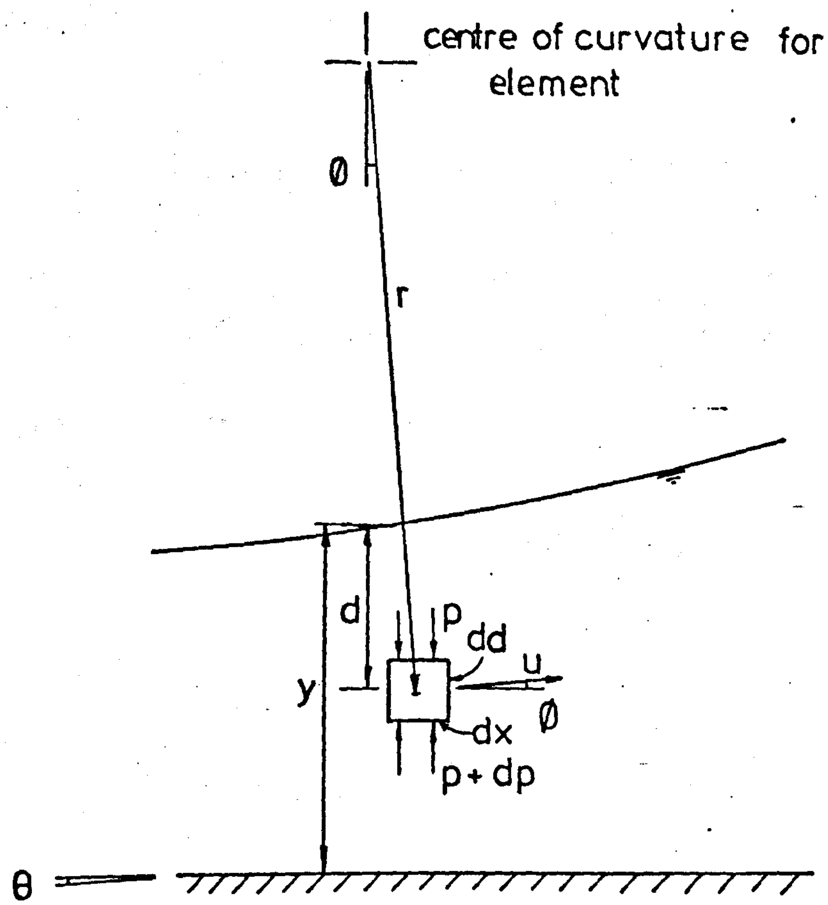

fig. 2.8

always very close to 1.0, so that

$$dp \simeq \rho g . dd . \cos\theta + \rho \frac{u^2}{r} . dd \quad \ldots\ldots\ldots\ldots(2.22)$$

2.5.3 Assume now that the velocity distribution is of the form

$$\frac{u}{u_o} = \left\{1 - \frac{d}{y}\right\}^n$$

where u_o is the velocity at the water surface.

The discharge passing any one section can be computed by integration,

$$Q = \int_o^y u_o \left\{1 - \frac{d}{y}\right\}^n B.dd$$

$$= \frac{u_o \, B \, y}{n + 1} \quad \text{for a rectangular section.}$$

Now $Q = v \, By$

$$\therefore \quad u_o = (n + 1) \, v$$

$$\text{and} \quad u = (n + 1) \, v \left\{1 - \frac{d}{y}\right\}^n \quad \ldots\ldots\ldots\ldots(2.24)$$

2.5.4 Assume also that the distribution of curvature $({}^1/_r)$ is of the form

$$\frac{1}{r} = \frac{1}{r'} \left\{1 - \frac{d}{y}\right\}^m \quad \ldots\ldots\ldots\ldots(2.25)$$

where r' is the radius of curvature of the water surface.

The radius of curvature of the water surface is given by the expression

$$r' = \frac{\left\{1 + ({}^{dy}/_{dx})^2\right\}^{3/2}}{d^2y/dx^2} \quad \ldots\ldots\ldots\ldots(2.26)$$

In practice the value of dy/dx is small so that

$$r' \approx \frac{1}{d^2y/dx^2} \qquad \text{............(2.27)}$$

Specimen computations were made using both equation (2.26) and (2.27). The mathematical model was found to perform equally well with either equation, the results being virtually indistinguishable. Equation (2.27) was therefore adopted for general application, so that

$$\frac{1}{r} = \frac{d^2y}{dx^2} \left\{1 - \frac{d}{y}\right\}^m \qquad \text{............(2.28)}$$

2.5.5 Equation (2.22) now becomes

$$dp = \rho g.dd.\cos \quad + \rho(n+1)^2 v^2 . \frac{d^2y}{dx^2}\left\{1 - \frac{d}{y}\right\}^{m+2n} . dd \quad \text{..(2.29)}$$

At a distance d below the water surface

$$p = \int dp$$

$$= \int\left\{\rho g \cos\theta + \rho(n+1)^2 v^2 . \frac{d^2y}{dx^2}\left(1 - \frac{d}{y}\right)^{m+2n}\right\} dd$$

$$= \rho g d \cos\theta - \frac{\rho(n+1)^2 v^2}{(m+2n+1)} y . \frac{d^2y}{dx^2}\left(1 - \frac{d}{y}\right)^{m+2n+1} + \text{Constant}$$

When $d = 0$, $p = 0$

$$\therefore \text{ Constant} = \frac{\rho(n+1)^2 v^2 y}{(m+2n+1)} . \frac{d^2y}{dx^2}$$

and $$p = \rho g d \cos\theta + \frac{\rho(n+1)^2 v^2 y}{(m+2n+1)} . \frac{d^2y}{dx^2}\left\{1 - \left(1 - \frac{d}{y}\right)^{m+2n+1}\right\}$$

$$\text{............(2.30)}$$

Pressure force $P = \int_0^y p\,B.dd$

For a rectangular section, therefore,

$$P = \frac{1}{2}\rho g B y^2 \cos\theta + \frac{\rho(n+1)^2 v^2\, yB}{(m+2n+1)} \cdot \frac{d^2y}{dx^2} \cdot \left[d + \frac{y}{(m+2n+2)}\left(1 - \frac{d}{y}\right)^{m+2n+2} \right]_0^y$$

$$= \frac{1}{2}\rho g B y^2 \cos\theta + \frac{(n+1)^2}{(m+2n+1)}\; \rho v^2 yB \cdot \frac{d^2y}{dx^2} \left\{ y - \frac{y}{(m+2n+2)} \right\}$$

$$= \frac{1}{2}\rho g B y^2 \cos\theta + \frac{(n+1)^2}{(m+2n+2)}\; \rho B v^2 y^2 \cdot \frac{d^2y}{dx^2} \qquad \text{............(2.31)}$$

Let $$\eta = \frac{(n+1)^2}{(m+2n+2)} \qquad \text{............(2.32)}$$

$$\therefore \; P = \frac{1}{2}\rho g B y^2 \cos\theta + \eta B v^2 y^2 \cdot \frac{d^2y}{dx^2} \qquad \text{............(2.33)}$$

2.5.6 The change in pressure force over a finite length of channel Δx now becomes

$$\Delta\left(\frac{1}{2}\rho g B y^2 \cos\theta + \eta\rho B v^2 y^2 \cdot \frac{d^2y}{dx^2}\right)$$

Equation (2.9) may thus be rewritten to incorporate the effects of curvature. For a rectangular section channel

$$\frac{d}{dx}\left\{ \rho\beta B y v^2 + \frac{1}{2}\rho g B y^2 \cos\theta + \eta\rho B v^2 y^2 \cdot \frac{d^2y}{dx^2} \right\}$$

$$= \rho g B y\,(s_o - s_f) - \rho q v \qquad \text{............(2.34)}$$

Equation (2.34) may be expanded and the terms regrouped in the same generalised way as equation (2.9) in section 2.2.1. However β and η may be assumed to be sensibly constant, and limiting the application of equation (2.34) to a prismatic channel with a constant bed slope gives

$$\rho\beta Bv^2 \cdot \frac{dy}{dx} + 2\rho\beta Bvy \cdot \frac{dv}{dx} + \rho gBy\cos\theta \cdot \frac{dy}{dx} + \eta\rho Bv^2y^2 \cdot \frac{d^3y}{dx^3}$$

$$+ 2\eta\rho Bv^2y \cdot \frac{d^2y}{dx^2} \cdot \frac{dy}{dx} + 2\eta\rho Bvy^2 \cdot \frac{d^2y}{dx^2} \cdot \frac{dv}{dx}$$

$$= \rho gBy\,(s_o - s_f) - \rho qv \qquad \text{.............(2.35)}$$

For a prismatic rectangular channel equation (2.12) becomes

$$\frac{dv}{dx} = -\frac{q}{By} - \frac{v}{y} \cdot \frac{dy}{dx} \qquad \text{.............(2.12.1)}$$

Substituting into equation (2.35),

$$\rho\beta Bv^2 \cdot \frac{dy}{dx} - 2\rho\beta vq - 2\rho\beta Bv^2\frac{dy}{dx} + \rho gBy\cos\theta \cdot \frac{dy}{dx}$$

$$+\eta\rho Bv^2y^2 \cdot \frac{d^3y}{dx^3} + 2\eta\rho Bv^2y \cdot \frac{d^2y}{dx^2} \cdot \frac{dy}{dx} - 2\eta\rho vyq \cdot \frac{d^2y}{dx^2}$$

$$- 2\eta\rho Bv^2y \cdot \frac{d^2y}{dx^2} \cdot \frac{dy}{dx} - \rho gBy\,(s_o - s_f) + \rho qv = 0$$

$$\eta \rho B v^2 y^2 \cdot \frac{d^3y}{dx^3} - 2\eta \rho v y q \cdot \frac{d^2y}{dx^2} + \left(\rho g B y \cos\theta - \rho\beta B v^2\right) \cdot \frac{dy}{dx}$$

$$- \rho g B y \,(s_o - s_f) + \rho q v \,(1 - 2\beta) = 0 \qquad \text{............}(2.36)$$

Dividing equation (2.36) by ρgBy,

$$\eta \frac{v^2 y}{g} \cdot \frac{d^3y}{dx^3} - 2\eta \frac{vq}{gB} \cdot \frac{d^2y}{dx^2} + \left(\cos\theta - \frac{\beta v^2}{gy}\right) \cdot \frac{dy}{dx}$$

$$- (s_o - s_f) + \frac{qv}{gBy} \,(1 - 2\beta) = 0 \qquad \text{............}(2.37)$$

Equation (2.37) is the general differential equation for spatially varied flow in a prismatic rectangular channel where the curvature of the water surface is significant. It can be seen, by comparison with equation (2.15) that curvature has the effect of raising the order of the differential equation from 1st to 3rd.

2.5.7 When curvature ceases to be significant both $\frac{d^3y}{dx^3}$ and $\frac{d^2y}{dx^2}$ tend to zero, so that equation (2.37) reduces to equation (2.15).

For gradually varied flow $q = 0$, and equation (2.37) reduces to

$$\eta \frac{v^2 y}{g} \cdot \frac{d^3y}{dx^3} + \left(\cos\theta - \frac{\beta v^2}{gy}\right) \cdot \frac{dy}{dx} - (s_o - s_f) = 0 \quad \text{...}(2.38)$$

Assuming a linear distribution of curvature ($m = 1$) and uniform velocity ($n = 0$), $\eta = \frac{1}{3}$, so that equation (2.38) becomes

$$\frac{1}{3}\ \frac{v^2y}{g} \cdot \frac{d^3y}{dx^3} + \left(\cos\theta - \frac{\beta v^2}{gy}\right) \frac{dy}{dx} - (s_o - s_f) = 0 \qquad \ldots.(2.39)$$

which is essentially the same as the equation given by Jaeger[20].

Before equation (2.37) can be used in a mathematical model a value of η must be established. This entails obtaining values of m and n by determining the distributions of curvature and velocity over the depth of flow.

2.6 Distribution of Curvature

2.6.1 If potential flow is assumed then curvature distributions can be obtained by producing flow nets for varying degrees of surface curvature. Although this is possible by graphical construction or electrical analogue the direct measurement of curvature of a streamline is open to substantial errors and an analytical representation of the flow net was therefore established.

For positive surface curvature the streamlines at any section are approximated to hyperbolae, and hence the equipotential lines are represented by ellipses. It should be noted that this approximation is only made over a very short length of channel (Fig. 2.9).

For negative surface curvature the streamlines at any section are approximated to ellipses, and hence the equipotential lines become hyperbolae.

2.6.2 Positive Surface Curvature

For the streamlines $$\frac{z^2}{c^2\cos^2\psi} - \frac{x^2}{c^2\sin^2\psi} = 1 \qquad \ldots(2.40)$$

where c is a constant and ψ is the stream function.

Along a particular streamline

$$\frac{z^2}{a^2} - \frac{x^2}{b^2} = 1 \qquad \ldots\ldots\ldots(2.41)$$

where $a = c\cos\psi$ and $b = c\sin\psi$

$$\therefore\ z^2 = a^2\left(1 + \frac{x^2}{b^2}\right)$$

$$z = a\left(1 + \frac{x^2}{b^2}\right)^{\frac{1}{2}}$$

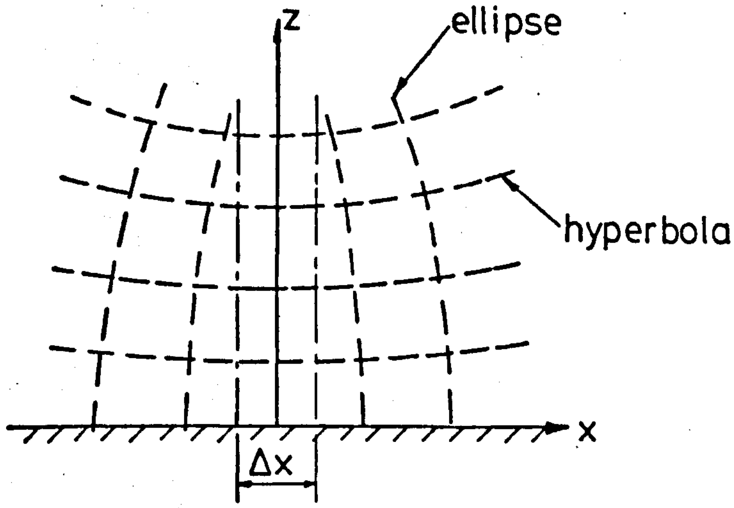

FLOW NET FOR POSITIVE CURVATURE

fig. 2.9

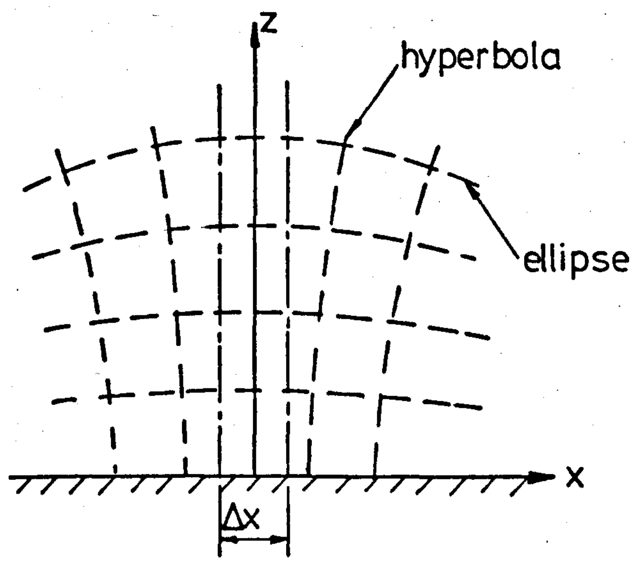

FLOW NET FOR NEGATIVE CURVATURE

fig. 2.10

$$\frac{dz}{dx} = \frac{ax}{b^2}\left(1+\frac{x^2}{b^2}\right)^{-\frac{1}{2}}$$

$$\frac{d^2z}{dx^2} = -\frac{ax^2}{b^4}\left(1+\frac{x^2}{b^2}\right)^{-3/2} + \frac{a}{b^2}\left(1+\frac{x^2}{b^2}\right)^{-\frac{1}{2}}$$

Along the centreline of the element Δz (the z axis)

$x = 0$

$$\therefore \quad \frac{d^2z}{dx^2} = \frac{a}{b^2}$$

$$= \frac{c\cos\psi}{c^2\sin^2\psi}$$

$$\frac{d^2z}{dx^2} = \frac{\cos\psi}{c\,(1-\cos^2\psi)} \qquad \text{............(2.42)}$$

and $z = a = c\cos\psi$ ....(2.43)

Let $K = \cos\psi$,

K_s = value of K at the water surface,

and $K = nK_s$

Substituting into equations (2.42) and (2.43)

$$z = cK = cnK_s$$

At the water surface

$$y = cK_s$$

$$\therefore \quad z = ny \qquad \text{............(2.44)}$$

$$c = \frac{y}{K_s} \qquad \text{............(2.45)}$$

$$\frac{d^2z}{dx^2} = \frac{nK_s^{\,2}}{y\,(1 - n^2K_s^{\,2})} \qquad \text{.........(2.42.1)}$$

and at the water surface, $n = 1$

$$\therefore \quad \frac{d^2y}{dx^2} = \frac{K_s^{\,2}}{y\,(1 - K_s^{\,2})} \qquad \text{.........(2.42.2)}$$

For a given depth y and surface curvature $\frac{d^2y}{dx^2}$, the value of K_s may be computed by inverting equation (2.42.2),

$$K_s = \left\{\frac{y\,.\,{d^2y}/{dx^2}}{1 + y\,.\,{d^2y}/{dx^2}}\right\}^{\frac{1}{2}} \qquad \text{.........(2.46)}$$

Thus for values of n ranging from 0 to 1 the values of z and $\frac{d^2z}{dx^2}$ (the curvature of the streamline) may be computed from equations (2.44) and (2.42.1) respectively.

2.6.3. Negative Surface Curvature

For the streamlines $\frac{z^2}{c^2\sinh^2\psi} + \frac{x^2}{c^2\cosh^2\psi} = 1$ ..(2.47)

Along a particular streamline

$$\frac{z^2}{a^2} + \frac{x^2}{b^2} = 1$$

$$z = a\left(1 - \frac{x^2}{b^2}\right)^{\frac{1}{2}}$$

$$\frac{dz}{dx} = -\frac{ax}{b^2}\left(1 - \frac{x^2}{b^2}\right)^{-\frac{1}{2}}$$

$$\frac{d^2z}{dx^2} = \frac{ax^2}{b^4}\left(1 - \frac{x^2}{b^2}\right)^{-3/2} - \frac{a}{b^2}\left(1 - \frac{x^2}{b^2}\right)^{-\frac{1}{2}}$$

Along the centreline of the element Δz (the z axis),

$x = 0$

$$\therefore \quad \frac{d^2z}{dx^2} = -\frac{a}{b^2}$$

$$= -\frac{c \sinh \psi}{c^2 \cosh^2 \psi}$$

$$\frac{d^2z}{dx^2} = -\frac{\sinh \psi}{c\,(1 + \sinh^2 \psi)} \qquad \text{............(2.48)}$$

and $z = a = c \sinh \psi$ ....(2.49)

Let $K = \sinh \psi$

K_s = value of K at the water surface

and $K = nK_s$

Substituting into equations (2.48) and (2.49)

$$z = cK = cnK_s$$

At the water surface

$$y = cK_s$$

$$\therefore \quad z = ny \qquad \text{............(2.44)}$$

$$c = \frac{y}{K_s} \qquad \text{............(2.45)}$$

$$\frac{d^2z}{dx^2} = -\frac{nK_s^{\,2}}{y\,(1 + n^2K_s^{\,2})} \qquad \text{............(2.48.1)}$$

and at the water surface, n = 1

$$\therefore \quad \frac{d^2y}{dx^2} = -\frac{K_s^{\,2}}{y\,(1 + K_s^{\,2})} \qquad \text{..........(2.48.2)}$$

Inverting equation (2.48.2) to give the required expression for computing K_s

$$K_s = \left\{ \frac{- y \,.\, d^2y/dx^2}{1 + y \,.\, d^2y/dx^2} \right\}^{\frac{1}{2}} \qquad \text{..........(2.50)}$$

For values of n ranging from 0 to 1 the values of z and $\frac{d^2z}{dx^2}$ may be computed from equations (2.44) and (2.48.2) respectively.

2.6.4 Two computer programs were written to calculate curvature distributions for positive and negative surface curvatures. The listings of these programs are given in Appendix II.

Curvature distributions were computed for surface curvatures ranging from + 1.0 to - 1.0 for a standard depth of 0.1m, which well covers the range of measured values. The distributions are tabulated in Appendix II also.

The tabulated curvature distributions show that the curvature of the streamlines is distributed approximately linearly with depth. This is well illustrated by Fig. 2.11 which shows the proportional curvature $\frac{d^2z/dx^2}{d^2y/dx^2}$ plotted against the proportional depth $n = z/y$.

Thus the value of m in equation (2.25) is 1.

FIG. 2.11 GRAPH OF PROPORTIONAL CURVATURE AGAINST PROPORTIONAL DEPTH

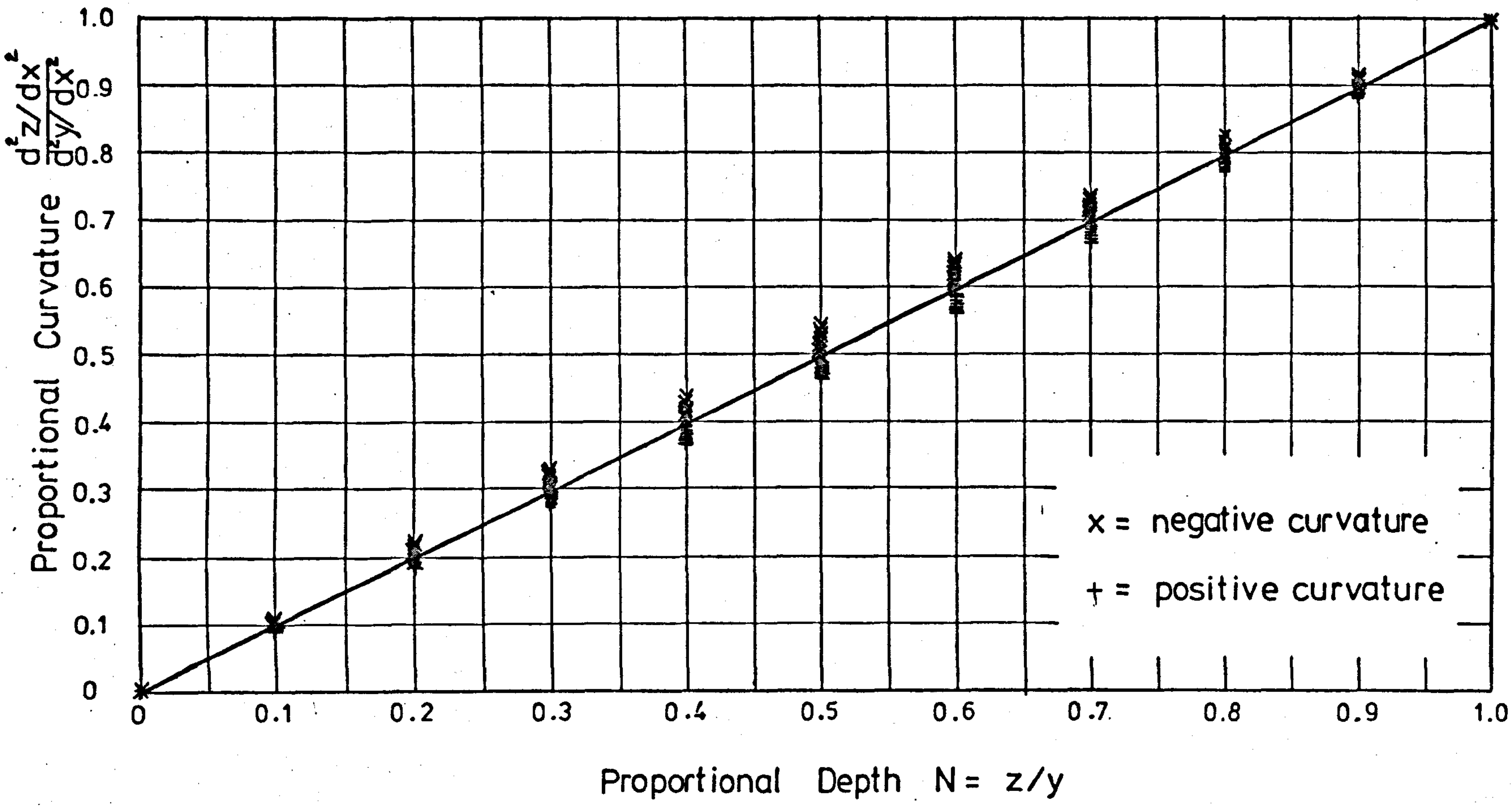

2.7 Distribution of Velocity

2.7.1 Velocity distributions can also be obtained from the flow net method described in section 2.6.

For two adjacent depths z_n and z_{n-1} the respective stream function values ψ_n and ψ_{n-1} can be computed from

$$\psi_n = \cos^{-1} K_n \quad \text{for positive curvatures}$$

and

$$\psi_m = \sinh^{-1} K_n \quad \text{for negative curvatures.}$$

For positive curvatures, therefore,

$$u_n = \frac{\psi_{n-1} - \psi_n}{z_n - z_{n-1}}$$

$$u_n = \frac{\cos^{-1} K_{n-1} - \cos^{-1} K_n}{z_n - z_{n-1}} \qquad \text{............(2.51)}$$

and for negative curvature,

$$u_n = \frac{\psi_n - \psi_{n-1}}{z_n - z_{n-1}}$$

$$= \frac{\sinh^{-1} K_n - \sinh^{-1} K_{n-1}}{z_n - z_{n-1}} \qquad \text{............(2.52)}$$

2.7.2 Velocity distributions were also calculated by the computer programs mentioned in section 2.6 and they are included in the tables in Appendix II. Although the mean velocity does not correspond directly with any measured value, all the velocities may be scaled up or down without affecting the velocity distributions.

There is clearly little change in the value of u over the depth and the velocity distribution may be assumed to be uniform, i.e. $n = 0$ in equation (2.24).

2.7.3 With values of $m = 1$ and $n = 0$, equation (2.32) gives a value of η of $\frac{1}{3}$. This value is therefore used in equation (2.37) in the mathematical model.

2.8 Modification of the Side Spill Discharge Equation to Allow for Curvature Effects

2.8.1 The transverse weir equation (2.17) used to compute the side spill discharge per unit length of the weir is derived assuming a hydrostatic pressure distribution. When curvature significantly alters the pressure distribution an allowance must be made and equation (2.17) modified.

2.8.2 Consider a small element dd in depth and Δx in length (Fig. 2.12)

Mean velocity through element $= \sqrt{2g\,(P/\rho g)}$

Discharge through element $= \sqrt{2g\,(P/\rho g)}\;.\;\Delta x\;dd$

Total discharge through section $\Delta x = \int_0^h \sqrt{2g\,(P/\rho g)}\;.\;\Delta x\;dd$

$$- \Delta Q = \Delta x\,\sqrt{2g}\int_0^h \left(P/\rho g\right)^{\frac{1}{2}}\,.\,dd \qquad \text{........(2.53)}$$

As $\Delta x \rightarrow 0$, and applying a coefficient of discharge,

$$q = -\frac{dQ}{dx} = C_D\,\sqrt{2g}\int_0^h \left(P/\rho g\right)^{\frac{1}{2}}\,dd \qquad \text{........(2.54)}$$

From equation (2.30), with $m = 1$ and $n = 0$,

$$p = \rho g d\cos\theta + \frac{1}{2}\rho v^2 y\,.\,\frac{d^2y}{dx^2}\left\{1 - \left(1 - \frac{d}{y}\right)^2\right\} \qquad \text{........(2.30.1)}$$

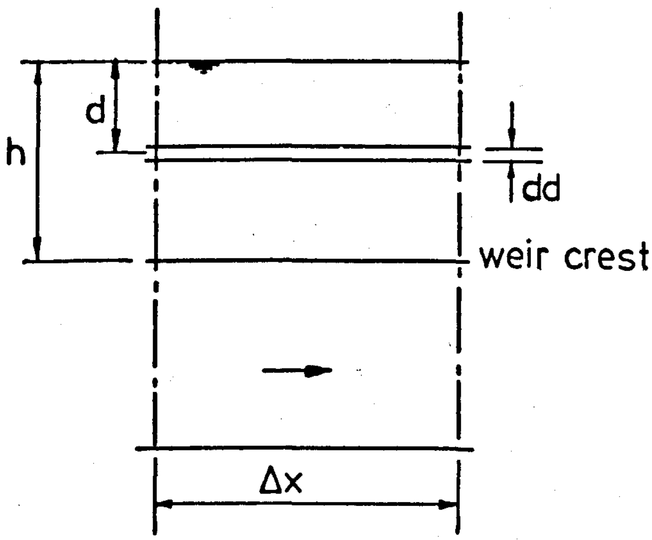

fig. 2.12

$$\therefore \quad \frac{p}{\rho g} = d\left\{\cos\theta + \frac{v^2}{g} \cdot \frac{d^2y}{dx^2}\right\} - d^2\left\{\frac{1}{2}\,\frac{v^2}{gy} \cdot \frac{d^2y}{dx^2}\right\} \quad \text{.....(2.30.2)}$$

2.8.3 Negative Curvature.

Let
$$K_1 = \left\{\cos\theta + \frac{v^2}{g} \cdot \frac{d^2y}{dx^2}\right\}$$
$$K_2 = -\left\{\frac{1}{2}\,\frac{v^2}{gy} \cdot \frac{d^2y}{dx^2}\right\}$$

Then from equation (2.30.2)

$$\frac{p}{\rho g} = K_1 d + K_2 d^2 \quad \text{............(2.30.3)}$$

Substituting into equation (2.54)

$$q = C_D \sqrt{2g} \int_0^h (K_1 d + K_2 d^2)^{\frac{1}{2}}\, dd$$

$$= C_D \sqrt{2g}\; K_2^{\frac{1}{2}} \int_0^h \left(d^2 + \frac{K_1}{K_2} d\right)^{\frac{1}{2}} dd$$

$$= C_D \sqrt{2g}\; K_2^{\frac{1}{2}} \int_0^h \left\{\left(d + \frac{K_1}{2K_2}\right)^2 - \left(\frac{K_1}{2K_2}\right)^2\right\}^{\frac{1}{2}} dd$$

$$= \frac{1}{2} C_D \sqrt{2g}\; K_2^{\frac{1}{2}} \left[\left(d + \frac{K_1}{2K_2}\right)\sqrt{d^2 + \frac{K_1 d}{K_2}} - \left(\frac{K_1}{2K_2}\right)^2 \cosh^{-1}\left(\frac{2K_2 d}{K_1} + 1\right)\right]_0^h$$

$$= \frac{1}{2} C_D \sqrt{2g}\; K_2^{\frac{1}{2}} \left[\left(h + \frac{K_1}{2K_2}\right)\sqrt{h^2 + \frac{K_1 h}{K_2}} - \left(\frac{K_1}{2K_2}\right)^2 \cosh^{-1}\left(\frac{2K_2 h}{K_1} + 1\right)\right]$$

$$q = \frac{1}{2} C_D \sqrt{2g}\ K_2^{\frac{1}{2}} \left[\left(h + \frac{K_1}{2K_2}\right)\sqrt{h^2 + \frac{K_1 h}{K_2}} - \left(\frac{K_1}{2K_2}\right)^2 . \right.$$

$$\left. \ln \left\{ \left(\frac{2K_2 h}{K_1} + 1\right) + \frac{2K_2}{K_1}\sqrt{h^2 + \frac{K_1 h}{K_2}} \right\} \right] \qquad .....(2.55)$$

2.8.4 Positive Curvature

Let
$$K_1 = \left(\cos\theta + \frac{v^2}{g} \cdot \frac{d^2y}{dx^2}\right)$$

$$K_2 = \left(\frac{1}{2}\ \frac{v^2}{gy} \cdot \frac{d^2y}{dx^2}\right)$$

Then from equation (2.30.2)

$$\frac{p}{\rho g} = K_1 d - K_2 d^2 \qquad ....(2.30.4)$$

Substituting into equation (2.54)

$$q = C_D \sqrt{2g} \int_0^h (K_1 d - K_2 d^2)^{\frac{1}{2}}\ dd$$

$$= C_D \sqrt{2g}\ K_2^{\frac{1}{2}} \int_0^h \left(\frac{K_1}{K_2}\ d - d^2\right)^{\frac{1}{2}} dd$$

$$= C_D \sqrt{2g}\ K_2^{\frac{1}{2}} \int_0^h \left\{ \left(\frac{K_1}{2K_2}\right)^2 - \left(d - \frac{K_1}{2K_2}\right)^2 \right\}^{\frac{1}{2}} dd$$

$$= \frac{1}{2} C_D \sqrt{2g} K_2^{\frac{1}{2}} \left[\left(\frac{K_1}{2K_2}\right)^2 \sin^{-1} \left(\frac{2K_2 d}{K_1} - 1\right) + \left(d - \frac{K_1}{2K_2}\right) \sqrt{\frac{K_1 d}{K_2} - d^2} \right]_0^h$$

$$q = \frac{1}{2} C_D \sqrt{2g} K_2^{\frac{1}{2}} \left[\left(\frac{K_1}{2K_2}\right)^2 \left\{ \frac{\pi}{2} + \sin^{-1} \left(\frac{2K_2 h}{K_1} - 1\right) \right\} + \right.$$

$$\left. \left(h - \frac{K_1}{2K_2}\right) \sqrt{\frac{K_1 h}{K_2} - h^2} \right] \qquad \ldots\ldots.(2.56)$$

2.8.5 To show the effect of curvature the following data may be used in equations (2.55) and (2.56) as appropriate and compared with the results obtained from

$v = 1.2$ m/s		$d^2y/dx^2 = -0.5m^{-1}$ and $+0.5m^{-1}$	
$y = 0.105$m			
$c = 0.036$m		$\therefore K_1 = 0.927$ and 1.073	
$h = 0.069$m		$\therefore K_2 = 0.349$	
$s_o = 0.0$			
$C_D = 0.6$			

For Negative Curvature $q = 0.0312m^2/s$ (equation (2.55))

For Positive Curvature $q = 0.0330m^2/s$ (equation (2.56))

For No Curvature $q = 0.0321m^2/s$ (equation (2.17))

Thus, negative curvature of $-0.5m^{-1}$ leads to a 2.8% decrease in q, whilst a positive curvature of $0.5m^{-1}$ leads to a 2.8% increase in q.

CHAPTER 3. THE MATHEMATICAL MODEL

3.1 Arrangement of the General Differential Equations

3.1.1 The general differential equation for gradually varied flow in a prismatic rectangular channel (equation (2.16)) is of the form

$$\frac{dy}{dx} = \psi(y) \qquad \text{..........(3.1)}$$

since the velocity may be expressed as a function of depth at any section, the discharge being constant. This first order differential equation may then be integrated by one of the standard numerical integration methods, such as a Runge Kutta method. This technique was adopted by Humpidge and Moss[21] in formulating a mathematical model describing gradually varied flow.

In spatially varied flow, however, the problem is complicated by the varying channel discharge. The mean velocity at any section v is not only a function of the depth y but also of the discharge Q which is a variable and depends, in this case, on the amount of flow that has passed over the weir up to the section under consideration. The differential equation (2.15) may be written in the form

$$\frac{dy}{dx} = \phi(v, y) \qquad \text{..........(3.2)}$$

where $$v = \frac{Q}{By} \qquad \text{..........(3.3)}$$

At any section, a distance x from the start of the weir

$$Q = Q_1 - \int_o^x q\, dx$$

so that $$v = \frac{Q_1 - \int_o^x q\,dx}{By} \qquad \text{.........(3.4)}$$

Let $w = vy$

$$\therefore \quad w = \frac{Q_1 - \int_o^x q\,dx}{B} \qquad \text{.........(3.4.1)}$$

Differentiating equation (3.4.1) with respect to x.

$$\frac{dw}{dx} = -\frac{q}{B} \qquad \text{.........(3.5)}$$

Substituting for $v = \frac{w}{y}$ in equation (2.15),

$$\frac{dy}{dx} = \frac{s_o - s_f - \frac{qw}{gBy^2}(1 - 2\beta)}{\cos - \frac{\beta w^2}{gy^3}} \qquad \text{.........(2.15.1)}$$

s_f may be computed by making the same substitution into equation (2.18),

$$s_f = \frac{\lambda}{4R} \cdot \frac{w^2}{2gy^2} \qquad \text{.........(2.18.1)}$$

Since q is a function of y only, equations (2.15.1) and (3.5) may be respectively written in the form

$$\frac{dy}{dx} = f(y, w) \qquad \text{.........(3.6)}$$

$$\frac{dw}{dx} = g(y) \qquad \text{.........(3.7)}$$

Equations (3.6) and (3.7) are two simultaneous first order differential equations for y and w, and they may be solved by applying one of the numerical integration techniques suitable for dealing with simultaneous first order differential equations.

3.1.2 When curvature of the water surface is significant, equation (2.15) is replaced by equation (2.37) which is a 3rd order differential equation. Making the substitution $v = \frac{w}{y}$,

$$\frac{\eta w^2}{gy} \cdot \frac{d^3y}{dx^3} - \frac{2\eta wq}{gBy} \cdot \frac{d^2y}{dx^2} + \left(\cos\theta - \frac{\beta w^2}{gy^3}\right) \cdot \frac{dy}{dx}$$

$$- (s_o - s_f) + \frac{qw}{gBy^2} (1 - 2\beta) = 0 \qquad \text{.........(2.37.1)}$$

Let $z = \frac{dy}{dx}$, and $t = \frac{dz}{dx} = \frac{d^2y}{dx^2}$

Equation (2.37.1) becomes

$$\frac{\eta w^2}{gy} \cdot \frac{dt}{dx} - \frac{2\eta wqt}{gBy} + \left(\cos\theta - \frac{\beta w^2}{gy^3}\right) z - (s_o - s_f)$$

$$+ \frac{qw}{gBy^2} (1 - 2\beta) \qquad \text{.........(2.37.2)}$$

$$\therefore \frac{dt}{dx} = \frac{2qt}{wB} - \frac{gyz}{\eta w^2}\left\{\cos\theta - \frac{\beta w^2}{gy^3}\right\} + \frac{gy}{\eta w^2}(s_o - s_f)$$

$$- \frac{q(1 - 2\beta)}{\eta wBy} \qquad \text{.........(3.8)}$$

Hence,

$$\frac{dt}{dx} = f\,(t,\ z,\ y,\ w) \qquad \text{..........(3.9)}$$

$$\frac{dz}{dx} = g\,(t) \qquad \text{..........(3.10)}$$

$$\frac{dy}{dx} = h\,(z) \qquad \text{..........(3.11)}$$

$$\frac{dw}{dx} = i\,(y) \qquad \text{..........(3.7.1)}$$

Equations (3.9), (3.10), (3.11) and (3.7.1) are four simultaneous first order differential equations for t, z, y and w, and again these can be solved using an appropriate numerical integration method.

3.2 Numerical Integration Methods

3.2.1 The simultaneous differential equations arising from the theoretical analysis of the previous chapter may not be solved analytically, and therefore a numerical approximation to the solutions must be made. In choosing an appropriate method consideration must be given to the accuracy and stability of the solution and to the efficiency of the method in terms of computing time and required storage.

Numerical integration methods may be divided into two types:

(i) Runge Kutta methods, which are single step methods using information at the current step only in progressing to the next step,

(ii) predictor-corrector methods, which are multi-step methods using information at a number of locations up to the current step, and normally requiring iteration in in progressing to the next step.

In all the cases considered in this investigation the depth, discharge, slope and curvature of the water surface may all be specified at a particular point along the channel so that, whether curvature effects are included or not, adequate starting values are available and boundary value problems are thus avoided.

3.2.2 Runge Kutta methods have the advantage of being self starting, and the intervals between each step may readily be changed, although this was found to be unnecessary in this case. In general they are particularly straightforward to apply on a digital computer. Also, Runge Kutta methods are comparable in accuracy, and are often more accurate, than predictor-corrector methods of the same order but because of difficulties in estimating the per step error, the step size h must generally be chosen conservatively (i.e. smaller than is actually necessary).

However, once the derivative expressions become anything but simple arithmetical expressions their evaluation becomes the most time consuming part of the computation. A fourth order Runge Kutta method normally requires four evaluations of each derivative expression per step, whereas a predictor-corrector method of the same order will usually require only two. Under these circumstances therefore a predictor-corrector method will be approximately twice as fast at arriving at a solution.

3.2.3 In choosing a suitable predictor-corrector method it is important to carefully consider stability. Two types of instability may be identified: inherent instability and induced instability.

Inherent instability is concerned with the physical problem itself, and occurs when small variations in the conditions of the problem cause large variations in the true solution, and this instability must inevitably be reflected in the numerical solution.

Induced instability of multi-step methods occurs due to the formation of spurious solutions to the equations at each step. Ideally these spurious solutions will be small and will remain small throughout the computations, but in certain cases some predictor-corrector methods produce spurious solutions which accumulate until they dominate the true solution and produce serious errors.

Induced instability may be avoided by using a stable predictor-corrector method. Ralston[22] shows the Manning predictor-corrector method to be stable in virtually all applications. The method makes use of an intermediate 'modifier' between the predictor and corrector stages which leads to rapid convergence and good stability.

Inherent instability cannot be removed by choice of method of solution since it is concerned with the physical problem. It can only be dealt with by reformulating the differential equations in a way that will produce a satisfactory solution.

3.3 The Runge Kutta method

3.3.1 A fourth order Runge Kutta method was chosen for solution where curvature effects are negligible. For the two simultaneous differential equations

$$\frac{dy}{dx} = f(y, w) \qquad \text{..........(3.6)}$$

and

$$\frac{dw}{dx} = g(y) \qquad \text{..........(3.7)}$$

solutions are obtained at a section x_{r+1} ($= x_r + h$) from previously computed values at section x_r only, using the equations

$$y_{r+1} = y_r + \frac{1}{6}(k_o + 2k_1 + 2k_2 + k_3) \qquad \text{..........(3.12)}$$

and

$$w_{r+1} = w_r + \frac{1}{6}(m_o + 2m_1 + 2m_2 + m_3) \qquad \text{..........(3.13)}$$

in which

$$k_o = h.f(y_r, w_r) \qquad \text{..........(3.14.1)}$$

$$m_o = h.g(y_r) \qquad \text{..........(3.14.2)}$$

$$k_1 = h.f(y_r + \tfrac{1}{2}k_o, w_r + \tfrac{1}{2}m_o) \qquad \text{..........(3.14.3)}$$

$$m_1 = h.g(y_r + \tfrac{1}{2}k_o) \qquad \text{..........(3.14.4)}$$

$$k_2 = h.f(y_r + \tfrac{1}{2}k_1, w_r + \tfrac{1}{2}m_1) \qquad \text{..........(3.14.5)}$$

$$m_2 = h.g(y_r + \tfrac{1}{2}k_1) \qquad \text{..........(3.14.6)}$$

$$k_3 = h.f(y_r + k_2, w_r + m_2) \qquad \text{..........(3.14.7)}$$

$$m_3 = h.g(y_r + k_2) \qquad \text{..........(3.14.8)}$$

3.3.2 This method was found to be efficient in both computing time and storage requirements and no instability problems were encountered. In order to determine a suitable step size a step length analysis was undertaken using the data from reading 23 (main series) and step lengths varying between 1mm and 64mm. The results are summarised in Table 3.1 and Figure 3.1.

Table 3.1 Results of Step Length Analysis.

Step Length mm	Computed Upstream Discharge Q_1 l/s	Computed Upstream Depth y_1 mm
1	5.220	92.36
2	5.218	92.39
4	5.218	92.48
8	5.217	92.39
16	5.217	92.39
32	5.215	93.15
64	5.298	93.14

The largest step length consistent with steady computed values was chosen and rounded up to give a step length of 0.02m.

FIG. 3.1 STEP LENGTH ANALYSIS

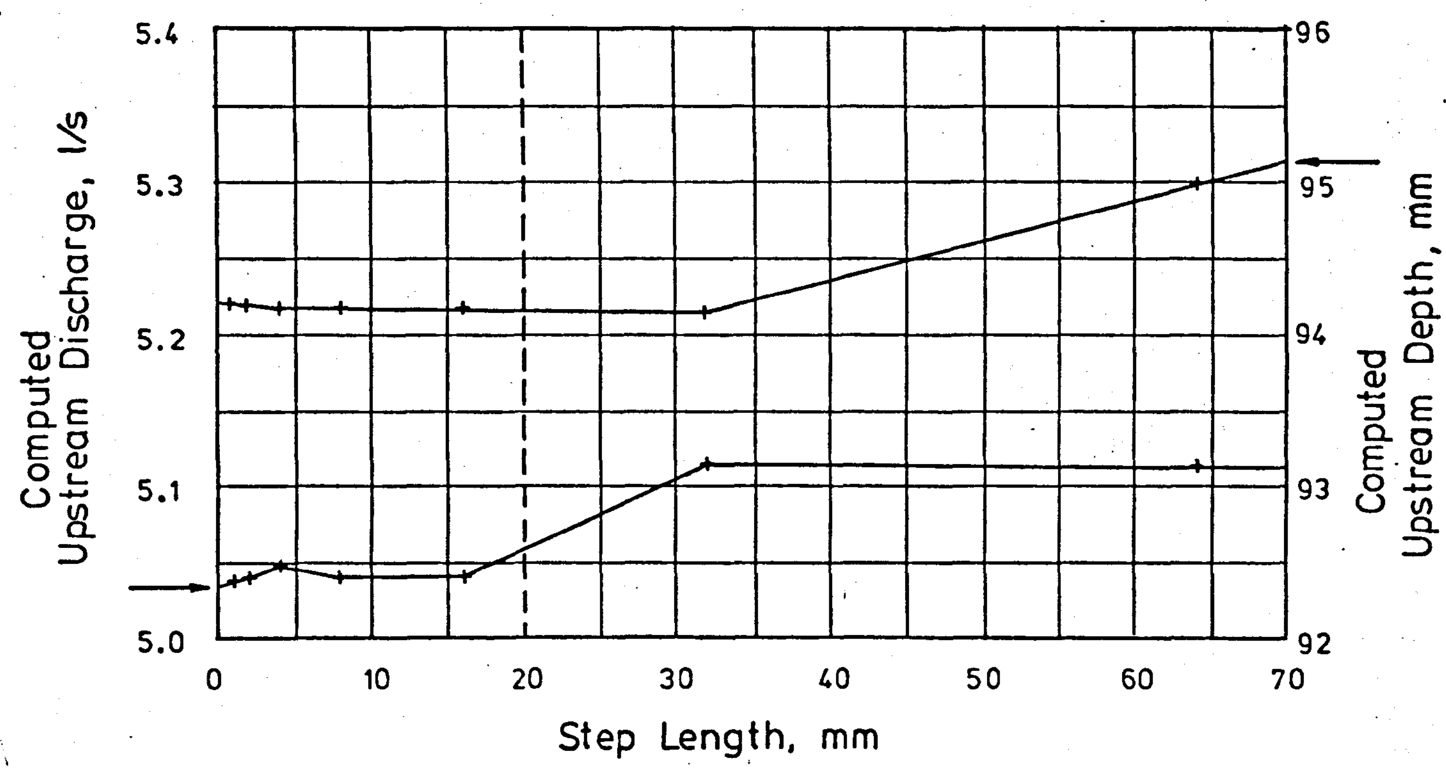

3.4 The Hamming Predictor Corrector Method

3.4.1 When curvature effects become significant, and are included in the analysis (equations (3.9), (3.10), (3.11) and (3.12)), the Hamming Predictor Corrector method is used. Since the fourth order method requires three sets of values prior to the step under consideration another method is required to start the solution. A Runge Kutta method is used for this purpose.

Ralston[22] showed that it is pointless to iterate to a high degree of accuracy at each step and that it is more efficient to achieve the required accuracy by reducing the step size rather than by using a large number of iterations. Also, when the required accuracy is readily attained, rounding errors may be reduced by increasing the step size. A facility for changing the step length was therefore incorporated into this method.

3.4.2 When the Hamming Predictor Corrector method was applied to equations (3.9), (3.10), (3.11) and (3.7.1) the solution rapidly became unstable, the computed water surface diverging from the measured profile with the depth approaching infinity. The instability was identified as inherent instability (section 3.2.3) and it appeared from inspection of the computer printout that unrealistically large values of d^3y/dx^3 (dt/dx) were being calculated. Actual values of d^2y/dx^2 were therefore computed from the measured surface profiles for readings 71 to 76 using the method described in Appendix III. Graphs showing the distribution of curvature along the weir were plotted from these values (Fig. 3.2) and it became apparent that d^2y/dx^2 increases uniformly over the upstream part of the weir (i.e. d^3y/dx^3 is constant).

FIG. 3.2 CURVATURE OF THE WATER SURFACE

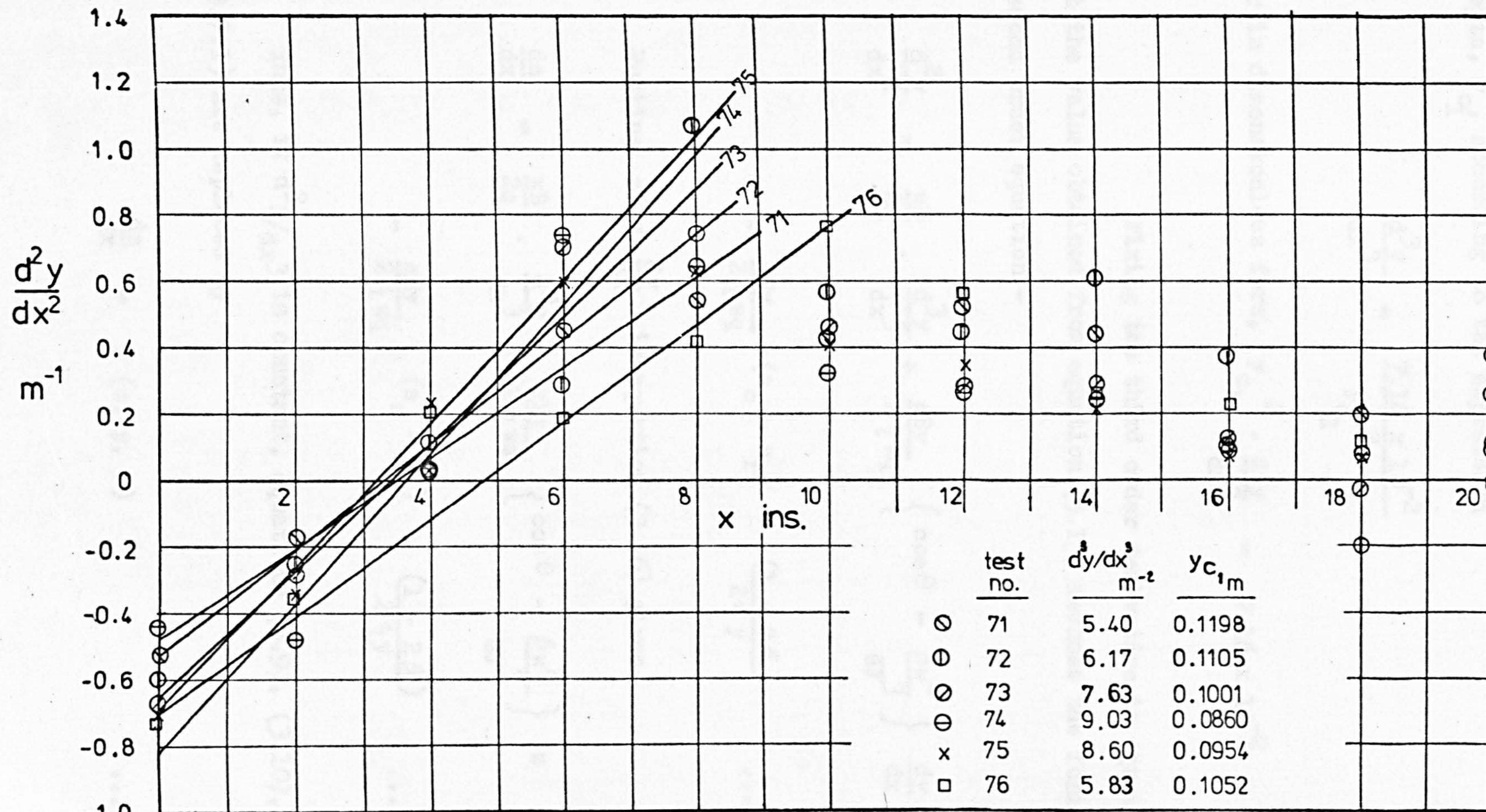

The constant value of d^3y/dx^3 varies from reading to reading, and Figure 3.3 shows that the value depends upon the upstream critical depth, y_{c_1}, according to the expression

$$\frac{d^3y}{dx^3} = \frac{7.16 \times 10^{-2}}{{y_{c_1}}^2}$$

or in dimensionless form, $${y_{c_1}}^2 \cdot \frac{d^3y}{dx^3} = 7.16 \times 10^{-2} \qquad \text{......(3.15)}$$

Fixing the third order derivative in equation (2.37.1) at the value obtained from equation (3.15) reduces the former to a second order equation:-

$$\frac{d^2y}{dx^2} = \frac{wB}{2q} \cdot \frac{d^3y}{dx^3} + \frac{gBy}{2\eta wq}\left\{\cos\theta - \frac{\beta w^2}{gy^3}\right\}\frac{dy}{dx}$$

$$- \frac{gBy}{2\eta wq}(s_o - s_f) + \frac{(1 - 2\beta)}{2\eta y} \qquad \text{............(3.16)}$$

Putting $z = \frac{dy}{dx}$ in equation (3.16) gives

$$\frac{dz}{dx} = \frac{wB}{2q} \cdot \frac{d^3y}{dx^3} + \frac{gBy}{2\eta wq}\left\{\cos\theta - \frac{\beta w^2}{gy^3}\right\} z$$

$$- \frac{gBy}{2\eta wq}(s_o - s_f) + \frac{(1 - 2\beta)}{2\eta y} \qquad \text{............(3.17)}$$

Thus, if d^3y/dx^3 is constant, equations (3.9), (3.10), (3.11) and (3.7.1) are replaced by

$$\frac{dz}{dx} = f(z, y, w) \qquad \text{............(3.18)}$$

FIG.3.3 RATE OF CHANGE OF CURVATURE / UPSTREAM CRITICAL DEPTH

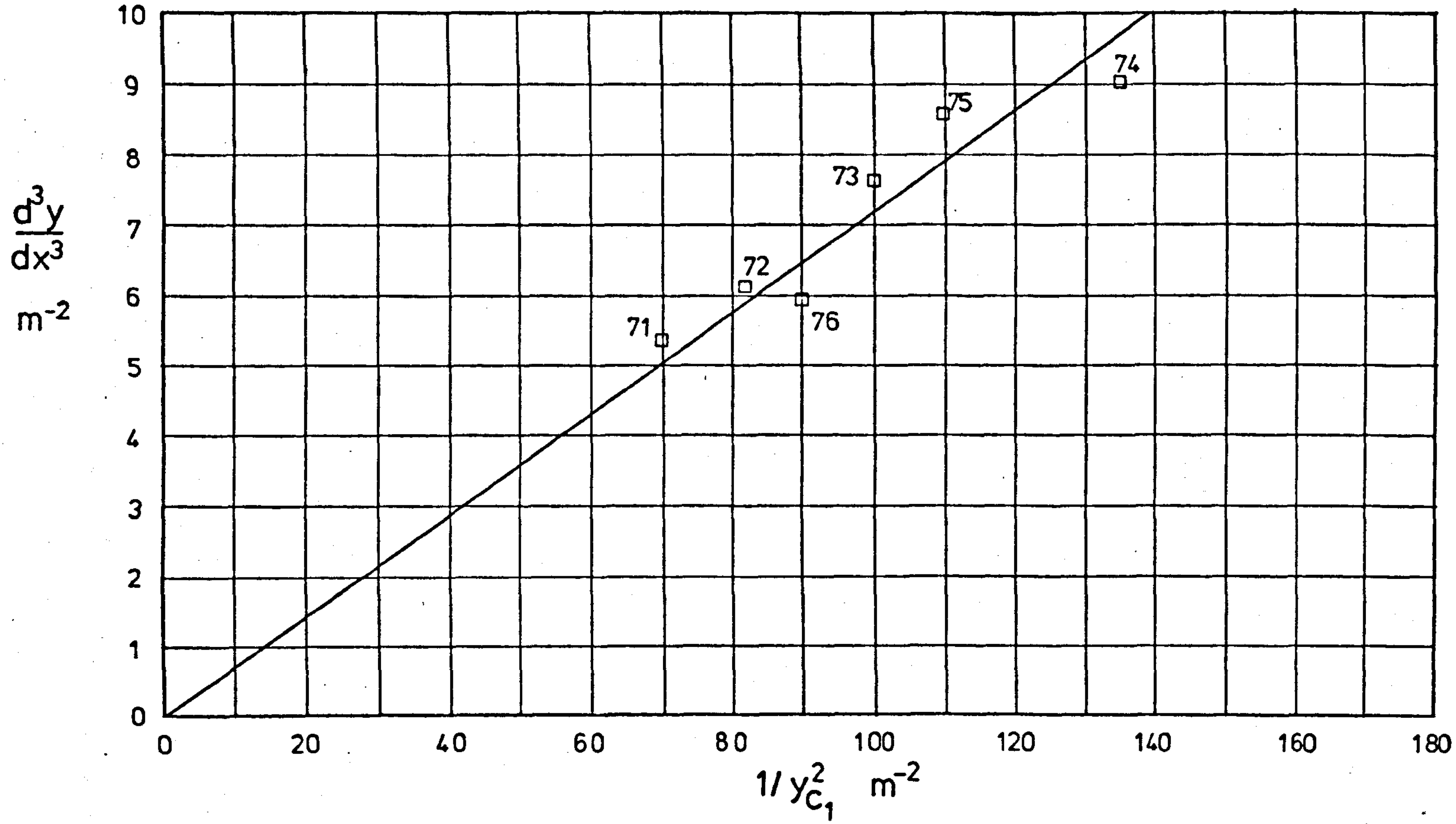

$$\frac{dy}{dx} = g\ (z) \qquad \text{........(3.11.1)}$$

$$\frac{dw}{dx} = h\ (y) \qquad \text{........(3.7.2)}$$

This modification proved successful in removing the inherent instability.

3.4.3 The Hamming Predictor Corrector method uses the following expressions to solve equations (3.18), (3.11.1), and (3.7.2) simultaneously.

Denoting $f\ (z_n, y_n, w_n)$ as f_n

$g\ (z_n)$ as g_n

and $h\ (y_n)$ as h_n

Predictors:-

$$z_{n+1}^{(o)} = z_{n-3} + \frac{4h}{3}\ (2f_n - f_{n-1} + 2f_{n-2}) \qquad \text{....(3.19.1)}$$

$$y_{n+1}^{(o)} = y_{n-3} + \frac{4h}{3}\ (2g_n - g_{n-1} + 2g_{n-2}) \qquad \text{....(3.19.2)}$$

$$w_{n+1}^{(o)} = w_{n-3} + \frac{4h}{3}\ (2h_n - h_{n-1} + 2h_{n-2}) \qquad \text{....(3.19.3)}$$

Modifiers:-

$$\bar{z}_{n+1}^{(o)} = z_{n+1}^{(o)} + \frac{112}{121}\left(z_n - z_n^{(o)}\right) \qquad \text{....(3.20.1)}$$

$$\bar{y}_{n+1}^{(o)} = y_{n+1}^{(o)} + \frac{112}{121}\left(y_n - y_n^{(o)}\right) \qquad \text{....(3.20.2)}$$

$$\bar{w}_{n+1}^{(o)} = w_{n+1}^{(o)} + \frac{112}{121}\left(w_n - w_n^{(o)}\right) \qquad \text{....(3.20.3)}$$

and $$\bar{f}_{n+1}^{(o)} = f\left(\bar{z}_{n+1}^{(o)}, \bar{y}_{n+1}^{(o)}, \bar{w}_{n+1}^{(o)}\right) \quad \text{....(3.21.1)}$$

$$\bar{g}_{n+1}^{(o)} = g\left(\bar{z}_{n+1}^{(o)}\right) \quad \text{....(3.21.2)}$$

$$\bar{h}_{n+1}^{(o)} = h\left(\bar{y}_{n+1}^{(o)}\right) \quad \text{....(3.21.3)}$$

Correctors:- $$z_{n+1}^{(j+1)} = \frac{1}{8}\left(9z_n - z_{n-2}\right) + \frac{3h}{8}\left(f_{n+1}^{(j)} + 2f_n - f_{n-1}\right) \quad \text{..(3.22.1)}$$

$$y_{n+1}^{(j+1)} = \frac{1}{8}\left(9y_n - y_{n-2}\right) + \frac{3h}{8}\left(g_{n+1}^{(j)} + 2g_n - g_{n-1}\right) \quad \text{..(3.22.2)}$$

$$w_{n+1}^{(j+1)} = \frac{1}{8}\left(9w_n - w_{n-2}\right) + \frac{3h}{8}\left(h_{n+1}^{(j)} + 2h_n - h_{n-1}\right) \quad \text{..(3.22.3)}$$

Figure 3.4 indicates the sequence of steps required to use the above formulae in proceeding from x_n to x_{n+1}. The convergence tolerances used in the computation are

$0.0250 \times y_{c_1}$ for f_{n+1}

$0.0085 \times y_{c_1}$ for g_{n+1}

$0.0165 \times y_{c_1}$ for h_{n+1}

Large variations in the tolerance levels were found to have little effect on the computed values and length of computation.

3.4.4 In using this method there is an additional complication arising from the use of equations (2.55) and (2.56) in computing the side spill discharge q. Since the modification to q due to curvature is small it was felt that it would be sufficiently accurate to use the value of curvature from the previous step in computing q. However this led to values of surface curvature oscillating between positive and negative values in the region of the point of contraflecture, instead of producing a smooth transition from negative to positive. To overcome this the actual value pertaining at that point in time in the iterative process of Hamming's method was tried, but this lead to physically unacceptable solutions. Finally an under-relaxation process was adopted, as described below.

Let AJ = value of the surface curvature during a particular iteration j of Hamming's method,

and AJI = value of the surface curvature for the previous step (x_{n-1} to x_n)

Then the value of curvature

for the next iteration $j + 1$ = AJ + 0.5 x (AJI - AJ) ....(3.23)

used in computing q.

Figure 3.4

Flow Chart Showing the Use of the Hamming Predictor Corrector Method

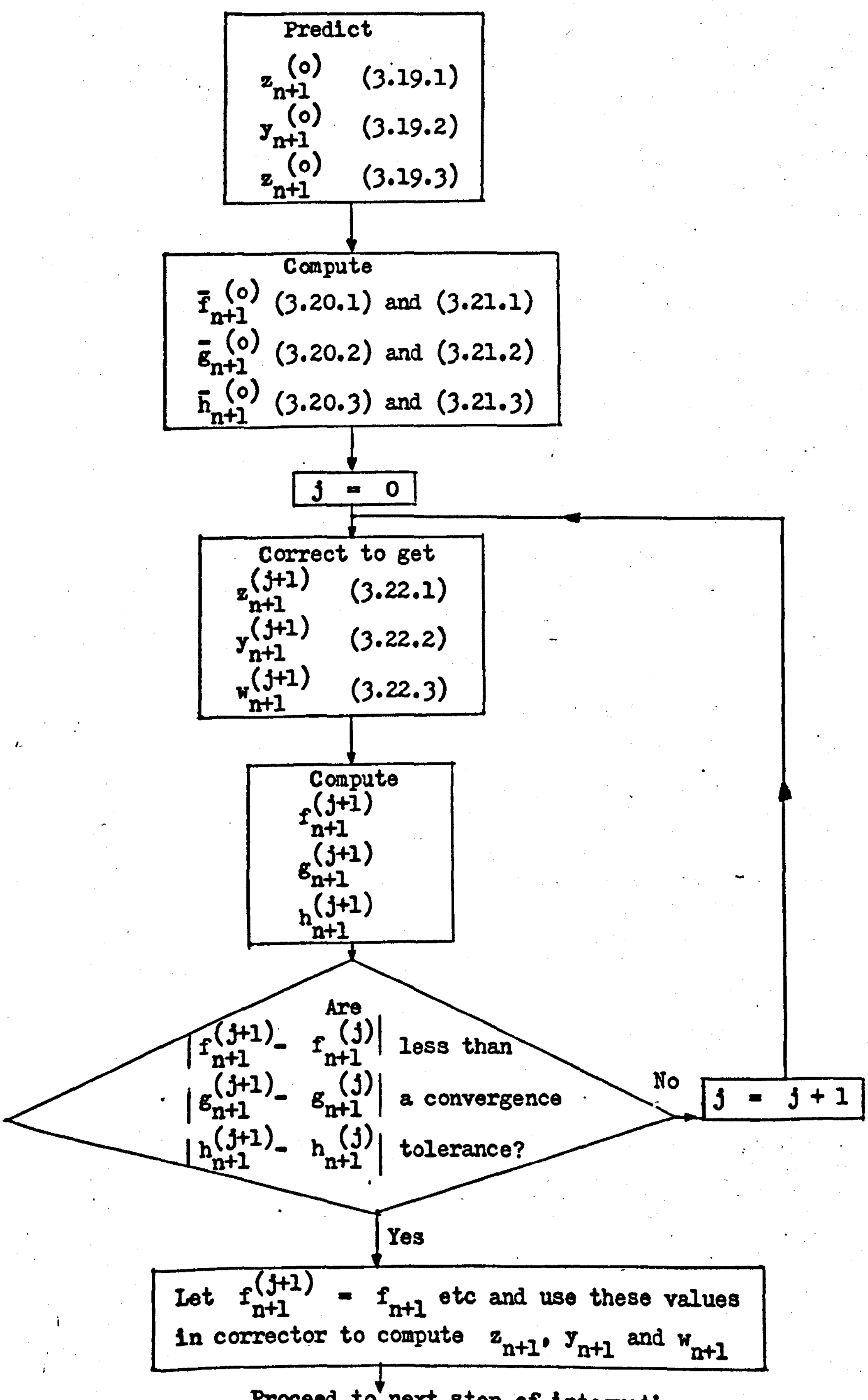

This was found to give good stability and accurate computations.

3.5 Solution for Subcritical Flow

3.5.1 For all subcritical flows the effect of surface curvature is negligible and the model based on equations (3.6) and (3.7) with the Runge Kutta method of integration is used, as described in section 3.3. Starting values are given by the conditions in the downstream channel, as governed by the downstream control, which in this investigation was either an adjustable sluice gate or transverse weir. It was found advantageous to start the computation some distance downstream (usually 428mm downstream) and compute the gradually varied flow profile back as far as the weir, which was achieved by putting the weir discharge coefficient equal to zero up to this point. This overcame the errors in the measured depth at the downstream end of the weir arising from the presence of a small transverse wave caused by the interference of the vertical downstream edge of the weir plate. This phenomenon is discussed more fully in section 6.10.

3.5.2 The computer program consists of a main program which reads and subsequently prints the data, computes starting values and prints the surface profile coordinates and computed discharges. The main program calls the subroutine PROFL which contains the Runge Kutta method of integration, and this in turn makes use of two function subprograms FUN1 and FUN2 which describe the derivative functions of equations (3.6) and (3.7). Figure 3.5 shows the flow chart for the program and a listing and specimen printout are contained in Appendix IV.

Figure 3.5

Flow Chart for Mathematical Model Computer Program - No allowance for curvature

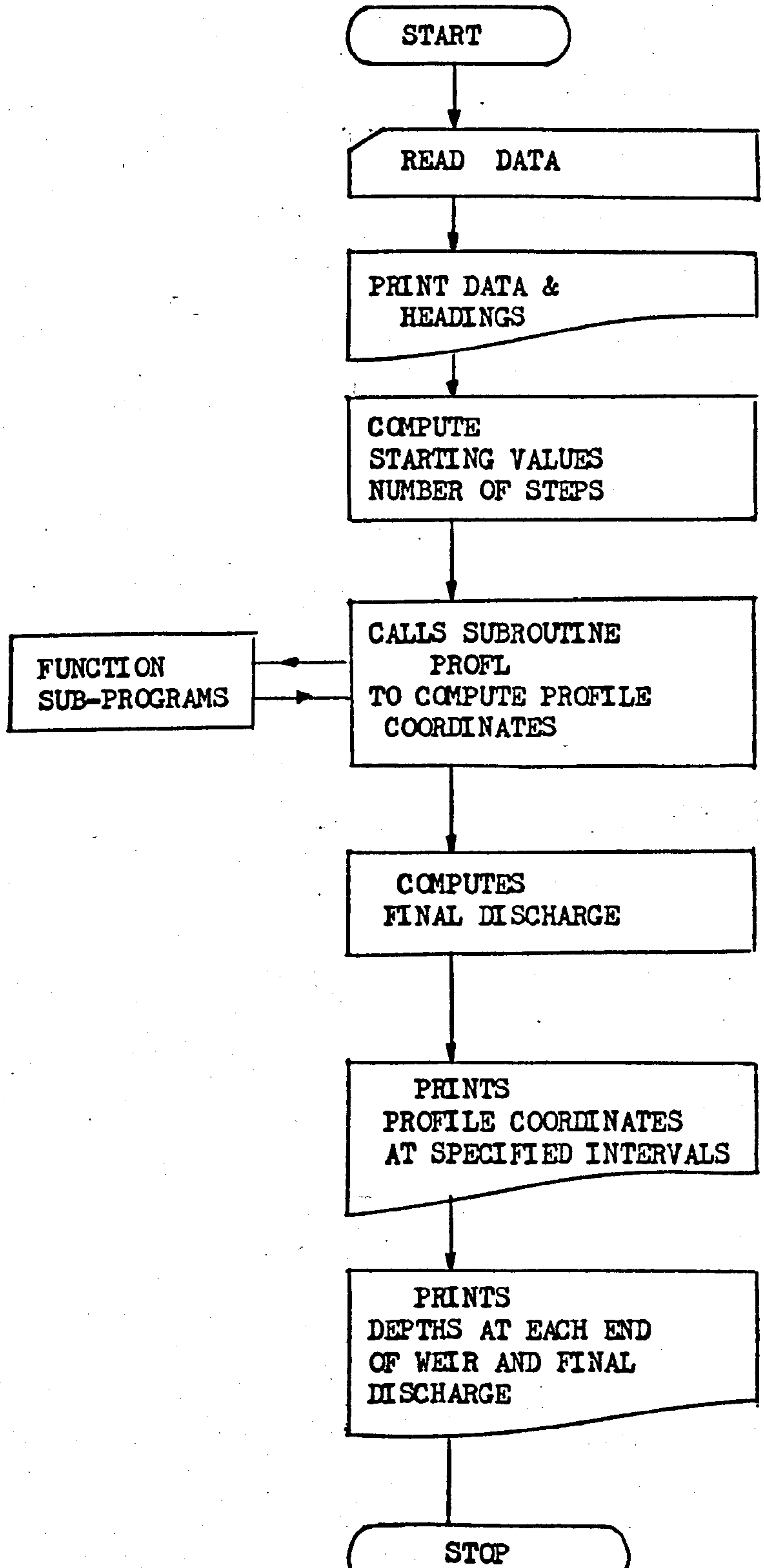

3.5.3 The program requires the following input data:-

Test run number

Channel width (rectangular sections) m

Channel slope (as a real value e.g. 0.003)

Viscosity of the water +

Weir crest height, m

Chainage of the upstream end of the weir, m

Chainage of the downstream end of the weir, m

Chainage at which the computatinn is to start, m ‡

Chainage at which the computation is to finish, m ‡

Depth at the starting point, m

Discharge at the starting point, m^3/s

Step length for the computations, m (negative for subcritical flow)

+ Water may be assumed to be at 15°C for design purposes without significant error.

‡ The program will automatically compute gradually varied flow profiles upstream and downstream of the weir.

3.5.4 Output data is printed as follows:-

A list of all input data

A table of profile coordinates (if desired) consisting of

Station chainage, m

Depth, m

Mean velocity, m/s

Froude number

(This table includes a separate statement of the depths at the start and finish of the weir at the appropriate places).

The discharge, m^3/s, and the depth, m, at the end of the computation (see Appendix IV).

3.5.5 The program uses about 18 seconds C.P.U. time in compilation and about 2 seconds C.P.U. time per test run, depending upon the step size chosen.

3.5.6 In practical application of the program to the design or analysis of subcritical side weir flow several computations will usually be necessary. This is because the conditions in the channel downstream of the weir will not in general be known. Apart from the weir and channel dimensions only the discharge in the upstream channel will be known. It will first be necessary to compute, or estimate the stage-discharge relationship for the downstream channel control. A typical stage-discharge curve is shown in Figure 3.6. The following procedure is then adopted.

Choose at least six points on the downstream stage-discharge curve (Fig. 3.6) and use the corresponding values of Q_2 and y_2 in turn as input data to the model. Use the printed output data to draw the side weir discharge characteristic Q_1 against Q_2 (Fig. 3.7) and the upstream stage-discharge curve Q_1 against y_1 (Fig. 3.8). For any specified upstream discharge, Figure 3.8 can be used to determine the degree of draw down in the upstream channel, followed by Figure 3.7 to obtain the residual flow in the downstream channel (and hence the side spill discharge) and finally Figure 3.6 to obtain the depth in the downstream channel. This graphical approach is considered to be superior to extending the mathematical model to include iterative procedures for such cases.

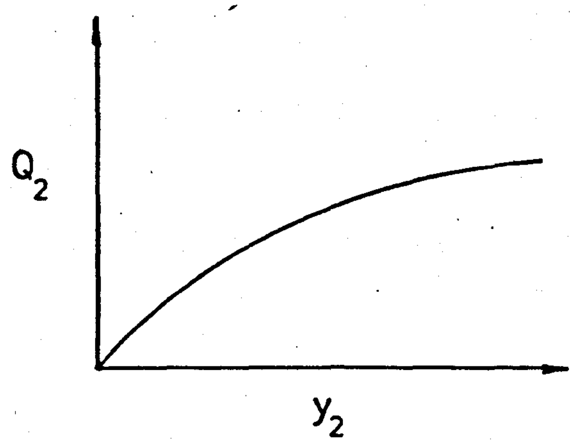

fig. 3.6 Typical stage-discharge curve for downstream channel

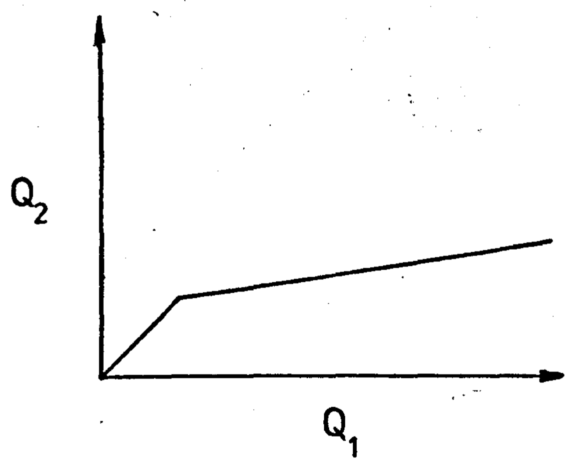

fig. 3.7 Typical side weir discharge characteristic

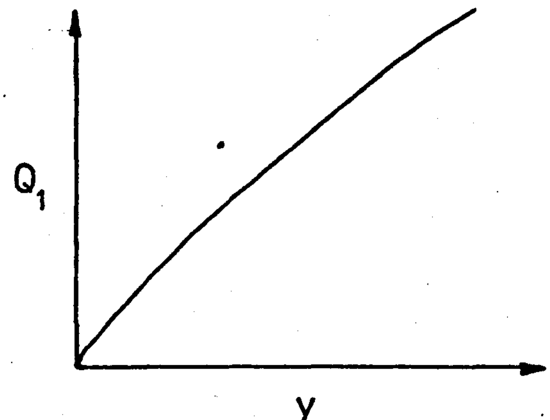

fig. 3.8 Typical stage-discharge curve for the upstream channel

3.5.7 The computer program may easily be modified to enable other crest geometries to be dealt with, including side spillways, providing the transverse discharge properties of such crest shapes are known. The model may also be extended to cover non-rectangular sections.

In all computations it is important to ensure that the results are physically possible and that a Case III profile is not formed in practice. The computed conditions at the upstream end of the weir should therefore be tested to ensure that a subcritical profile will actually form. The conditions under which subcritical profiles form is fully discussed in section 6.4.

3.6 Solution for Supercritical Flow

3.6.1 The program described in section 3.5 above may also be used for computing supercritical flow profiles. The input data is the same, except that the step length is positive as the computation commences from the upstream end of the weir and proceeds in the downstream direction. When curvature of the water surface is significant, errors can be expected using this model, but it was found that when the Froude Number at the start of the weir exceeded 1.5 curvature of the surface was not sufficient to significantly affect the problem, and this model gave acceptable results.

3.6.2 In practical applications the same information listed in section 3.5.6 will be available. In this case, however, this does not present the same problem. Using the known upstream discharge and the known weir and channel dimensions, the depth at the start of the weir may be found using the method described in section 6.10.

Since the starting values are now known the downstream discharge and depth, and hence the side spill discharge, may be computed directly. Only one computation is necessary.

3.6.3 The computed downstream values should be tested to ensure that the supercritical flow can exist in the downstream channel, and that the latter does not throttle the flow causing a Case III or Case V profile to occur along the weir.

3.7 Solution for Supercritical Flow with Curvature

3.7.1 When curvature effects are significant, i.e. when the Froude number at the upstream end of the weir is less than 1.5, the model is based on equations (3.18), (3.11.1), and (3.7.2) and the Hamming Predictor-Corrector method is used, as described in section 3.4.3.

3.7.2 The input data required is identical to that specified for the previous model in sections 3.5 and 3.6 but the method of solution also requires an initial estimate for surface slope. A fixed value of -0.12 is used for this, and the effect of this is fully discussed in section 6.10. Although the input data includes a step length value the program reduces this in size to reach the required accuracy at each step.

3.7.3 Although this method gives good simulation of curvature effects along the upstream section of the weir, errors are introduced along the downstream section because the model uses the fixed value of d^3y/dx^3 obtained from equation (3.15), which is strictly only applicable to the upstream section of the weir. These errors are small, but since curvature effects are not significant along the downstream section the results can be improved by changing over to the no-curvature model once curvature effects have ceased to be significant. This is achieved using the following change-over criteria.

3.7.4 (a) The change over should not occur prematurely, i.e. the Froude Number must be at least 1.2.

(b) The point of contraflecture must have been reached.

(c) The positive curvature must have passed its maximum value.

(d) The surface slopes computed by each model must lie within 10% of each other.

3.7.5 The computer program consists of a main program which reads and writes the input data, computes starting values, and calls the subroutine HPCG containing the Hamming predictor-corrector method. This is generally called twice; firstly for the curvature analysis, where it uses the subroutine FCT to compute the derivative functions, and the subroutine OUTP to print the output data, and secondly for the no-curvature analysis, where it uses subroutines XCT and XUTP in a similar fashion. A flow chart for the program is given in Figure 3.9 and a listing and specimen printout are contained in Appendix IV.

3.7.6 The print-out is essentially the same as that described in section 3.5.4 except that additional information is printed for the curvature analysis, namely,

at each station chainage, the curvature		m^{-1}
	d^3y/dx^3	m^{-2}
	a factor FAC	

FAC denotes the ratio of the value of q computed from equation (2.55) or (2.56), and equation (2.17), thus showing the effect of curvature on the side spill discharge.

3.7.7 The same practical considerations and restraints discussed in sections 3.6.2 and 3.6.3 also apply to this model. The program can be readily adapted to suit different crest geometries and non-rectangular sections.

3.7.8 The program uses about 20 seconds C.P.U. time in compilation and about 5 seconds C.P.U. time per test run depending mainly upon the convergence tolerances chosen.

Figure 3.9

Flow Chart for Mathematical Model Computer Program - with curvature allowance

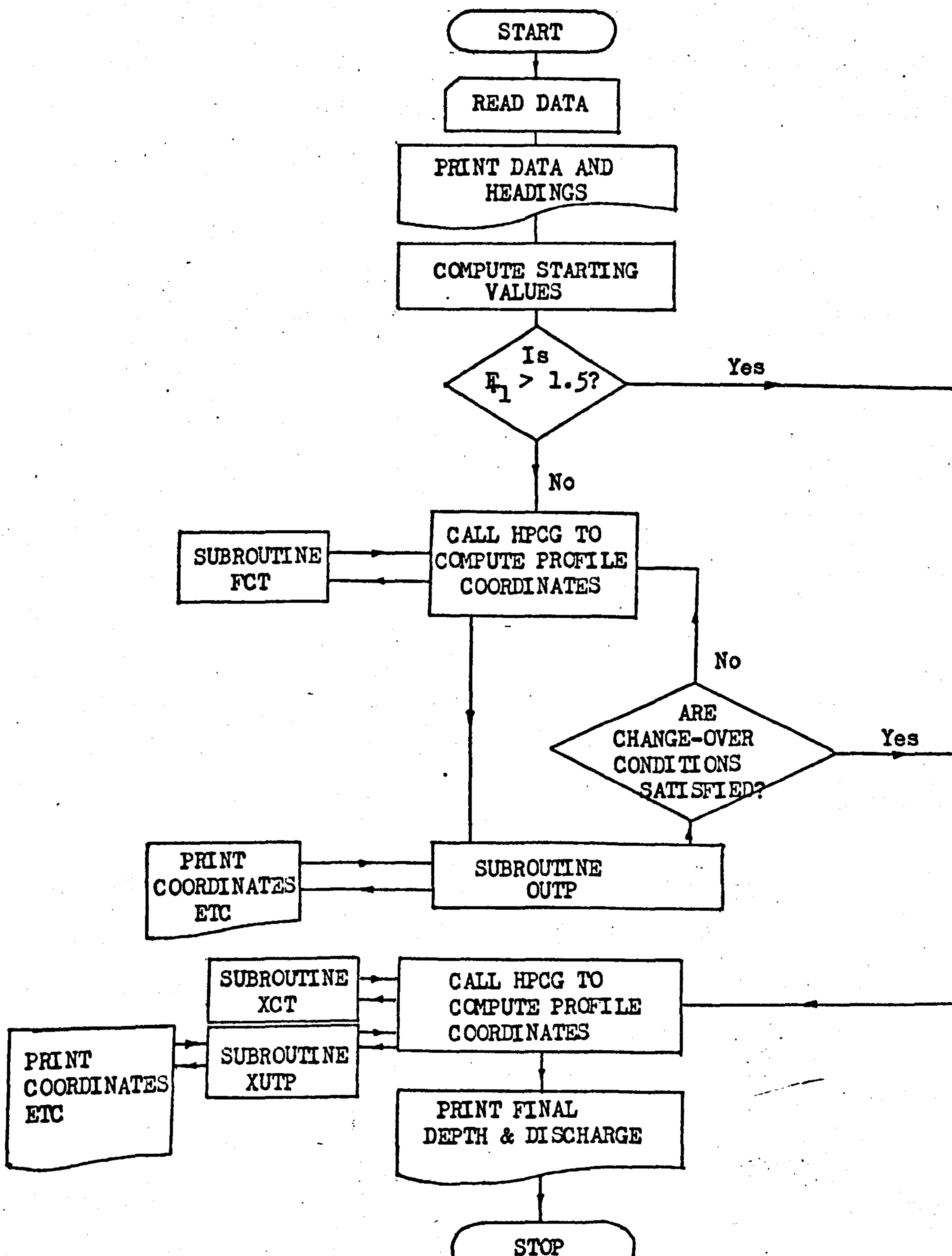

CHAPTER 4. PRELIMINARY EXPERIMENTAL INVESTIGATIONS

4.1 Scope of the Investigation

4.1.1 Before the mathematical model can be used to simulate side weir flow reliable estimates of the coefficient of discharge C_D, and the momentum flux correction factor β, are required. De Marchi[3,4] recommends the use of the same value of C_D as for a transverse weir, but Collinge[14] reports a significant reduction in the value of the coefficient which he attributes to the effects of longitudinal velocity. However, the results of Collinge's tests are based on the application of De Marchi's theory which has been shown to give substantial errors in computation (section 6.13). Thus, it is not clear whether the differences between the computed and measured values of the side spill discharge are due to errors inherent in his method of analysis, or to an actual reducation in the coefficient of discharge.

4.1.2 It is important to remove any such sources of error in determining values of the discharge coefficient and therefore the mathematical model cannot be used to evaluate C_D. Instead a completely independent method of determining C_D values is required.

4.1.3 If the geometric properties of the channel and side weir can be arranged in such a way as to produce a constant head along the length of the weir then the side spill discharge and the head are directly related by the transverse weir equation (2.17). Thus, by measuring the head and the side spill discharge, values of the coefficient of discharge can be obtained without reference to the mathematical model or any other method of side weir analysis.

4.1.4 At the same time the main channel should be sufficiently large in cross-section to enable velocity profiles to be measured from which values of the momentum flux correction factor may be obtained.

4.2 Criterion for a Constant Head

4.2.1 Ackers[5] showed that a constant head will occur along a side weir in a rectangular channel if the width is reduced uniformly along the length of the weir at a rate given by equation (1.9).

$$\frac{dB}{dx} = \frac{-C\,(y-c)^{3/2}}{yv} \qquad \text{........(1.9)}$$

where $C = {}^2/_3 \sqrt{2g}\; C_D$

Although his analysis neglects the effects of friction and channel slope it was found to be reasonably accurate so that only small adjustments were required to achieve a constant head.

4.2.2 Inspection of equation (1.9) shows that if ${}^{dB}/dx$ and y are constant then the mean longitudinal velocity v is also constant, and this was confirmed by the measured velocity profiles.

Let B_1 = width of channel at the upstream end of the weir,

and B_2 = width of channel at the downstream end of the weir.

For a weir of length L,

$$\frac{B_1 - B_2}{L} = -\frac{dB}{dx} = \frac{C\,(y-c)^{3/2}}{yv}$$

Now $Q_1 = B_1 yv$

$$\therefore \quad \frac{B_1 - B_2}{L} = \frac{C\,B_1\,(y-c)^{3/2}}{Q_1}$$

$$(y - c)^{3/2} = \frac{Q_1}{CL}\left(1 - \frac{B_2}{B_1}\right)$$

$$y = c + \left\{\frac{Q_1}{CL}\left(1 - \frac{B_2}{B_1}\right)\right\}^{2/3} \qquad \text{.........(4.1)}$$

4.2.3 Thus for a particular taper and upstream discharge, a constant head may be achieved by regulating the downstream depth to the value given by equation (4.1). In calculating this value, the value of C was obtained by assuming a coefficient of discharge C_D equal to the transverse weir value. Only a small adjustment to the estimated downstream depth was required in practice to achieve a constant head.

4.2.4 It is apparent from equation (4.1) that for a fixed taper a range of upstream discharges Q_1 can be chosen, each with a corresponding value of y (obtained from equation (4.1)), so that a series of values of C_D may be obtained. Further series of C_D values may be obtained for different channel tapers.

4.3 Description of the Apparatus

4.3.1 An existing flume, 15.24m long and with a rectangular section 1.067m wide and 0.914m deep, was adapted to contain both the main channel and the side spill channel, as shown in Figure 4.1. The floor and walls of the flume had a smooth concrete surface and the bed was horizontal. Water entered the flume from a large stilling tank which was connected to the flume by a short uniformly tapering rectangular channel and this effectively stilled the turbulence caused by the jet of water leaving the delivery pipe. The downstream end of the flume was unrestricted and thewater was allowed to flow freely into a vertical shute which transferred the water to the sump tank below.

4.3.2 The water supply for the flume was taken from a large header tank via a 203mm diameter pipe to the stilling tank. The water in the header tank was kept at an approximately constant head by recirculating water from the sump through two rising mains and two overflow pipes. The 203mm delivery pipe was fitted with a control valve adjacent to the flume, and a Dahl tube flow meter. This arrangement was found to give a steady discharge through the flume over long periods of time.

4.3.3 The vertical shute at the downstream end of the weir was fitted with a deflector enabling all of the flow to be diverted into a large measuring tank 2.74m x 3.96m x 3 m deep. This was fitted with a stilling well and float which was connected to a sliding scale adjacent to the flume enabling the water level in the measuring tank to be easily recorded. The tank was fitted with a valve in the floor through which the water could be drained into the sump tank below.

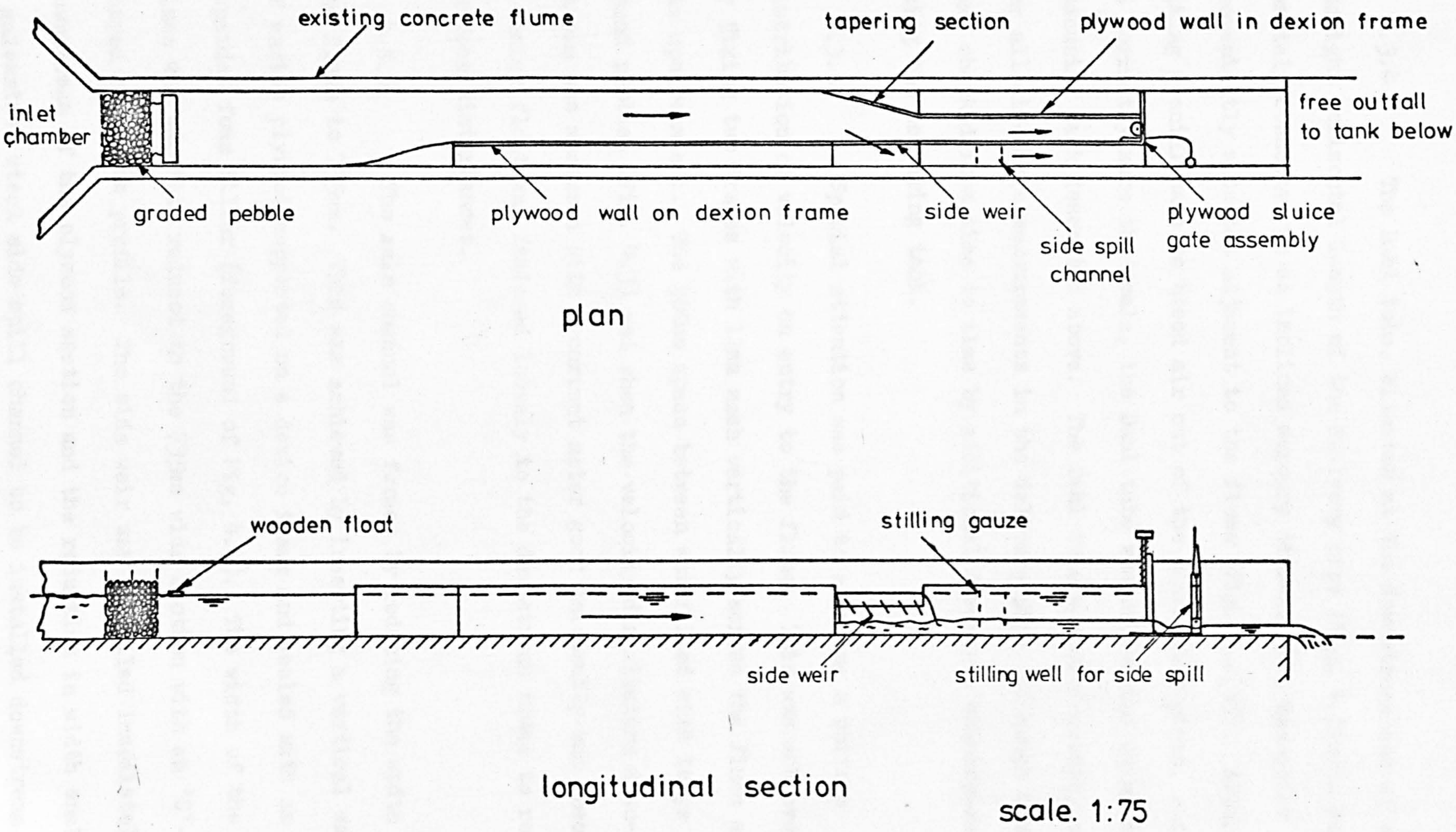

fig. 4.1 General Arrangement of the Preliminary Apparatus

4.3.4 The Dahl tube, situated at the downstream end of a long straight horizontal length of the delivery pipe (Fig. 4.2(a)), was remotely connected to an inclined mercury differential manometer conveniently situated adjacent to the flume (Fig. 4.2(b)). After taking special care to bleed air out of the connecting pipes, and to correctly zero the scale, the Dahl tube was calibrated using the measuring tank described above. The Dahl tube was subsequently used for all discharge measurements in the delivery pipe, although these were checked from time to time by additional discharge measurements using the measuring tank.

4.3.5 Special attention was paid to ensuring a uniform distribution of velocity on entry to the flume. This was achieved by fixing two frames with 12mm mesh vertically across the flume at its upstream end. The 300mm space between was filled with large round pebbles (Fig. 4.3) and when the velocity distribution downstream was measured with a current meter good uniformity was observed. A timber float was fastened loosely to the downstream frame to reduce surface disturbances.

4.3.6 The main channel was formed by reducing the width of the flume to 735mm. This was achieved by inserting a vertical wall of marine plywood supported on a dexion frame and sealed with an expanded foam filler (foreground of Fig. 4.4). The width of the flume was smoothly reduced to the 735mm wide section with an 'S'-shaped aluminium profile. The side weir was installed immediately downstream of the plywood section and the reduction in width enabled a galvanised steel side spill channel to be installed downstream of the weir (Figs. 4.1 and 4.4.)

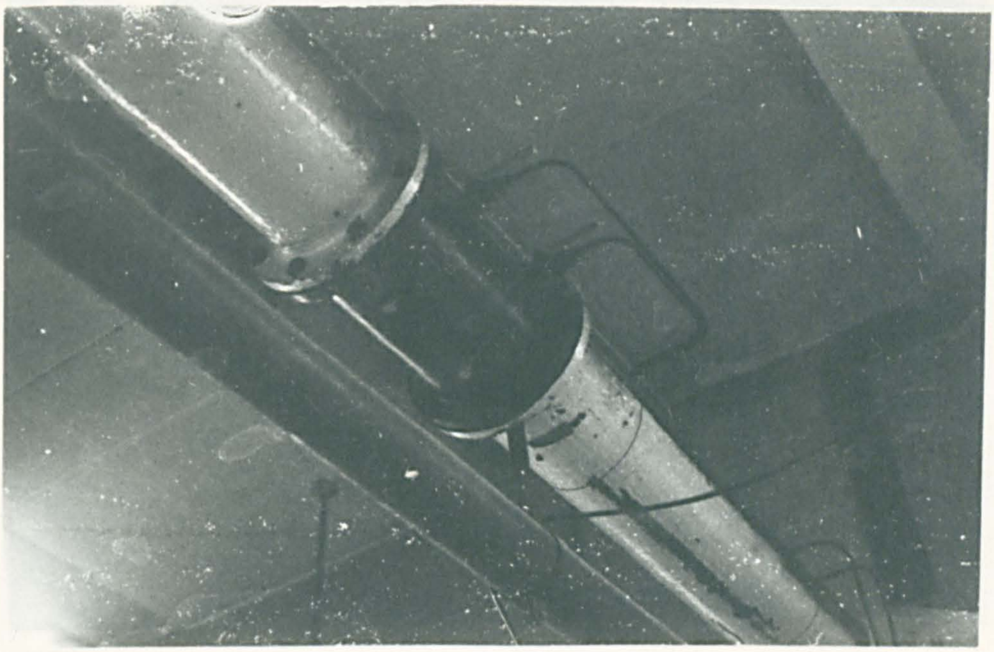

fig. 4.2(a) Dahl Tube FlowMeter on Delivery Pipe.

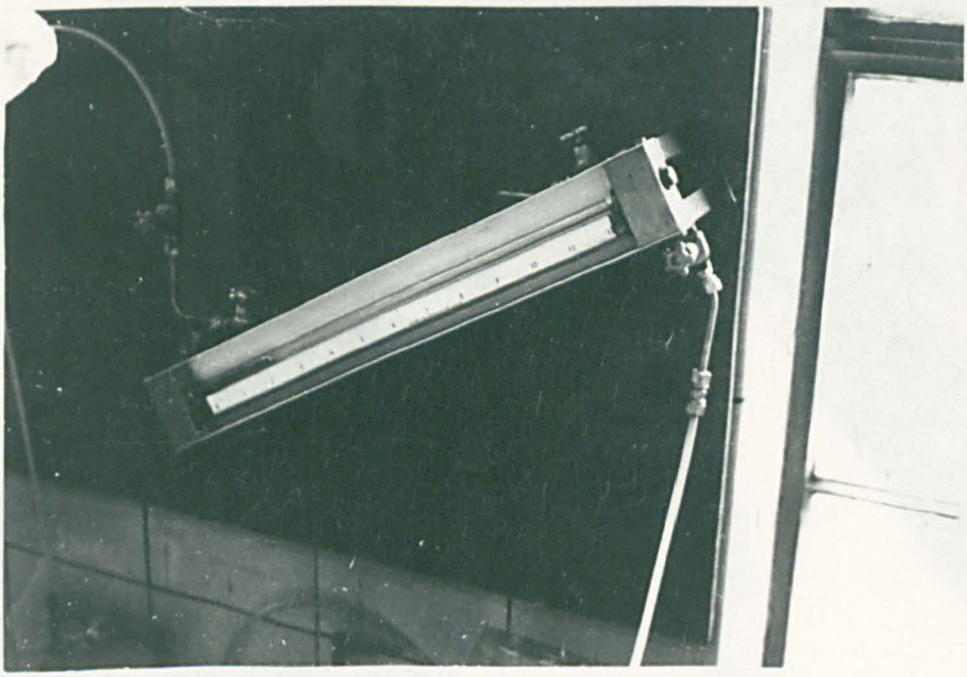

fig. 4.2(b) Dahl Tube Differential Manometer.

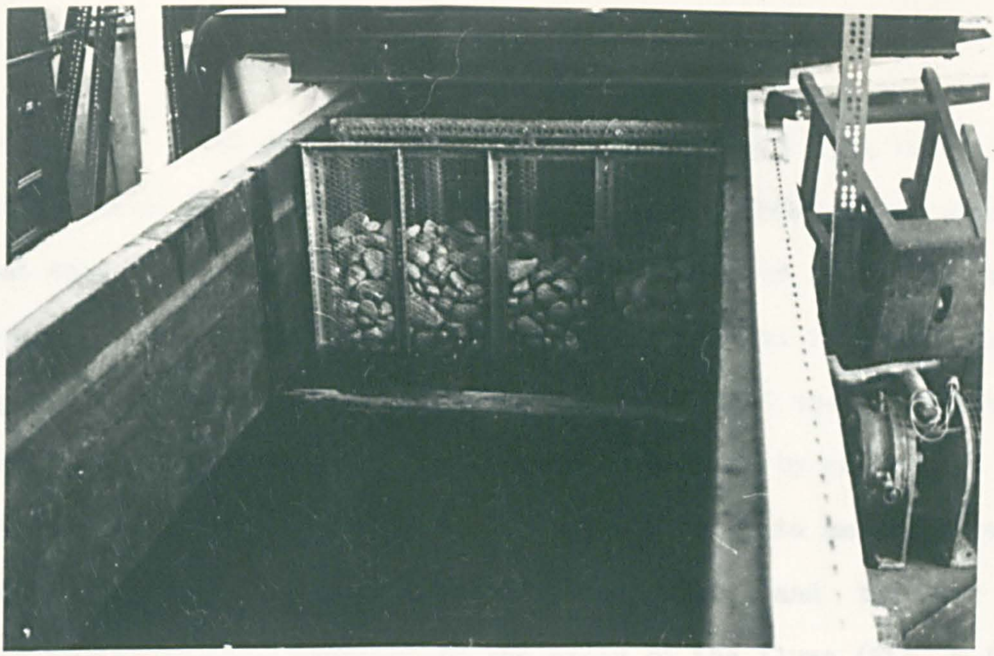

fig. 4.3 Graded Pebble at Inlet to the Flume.

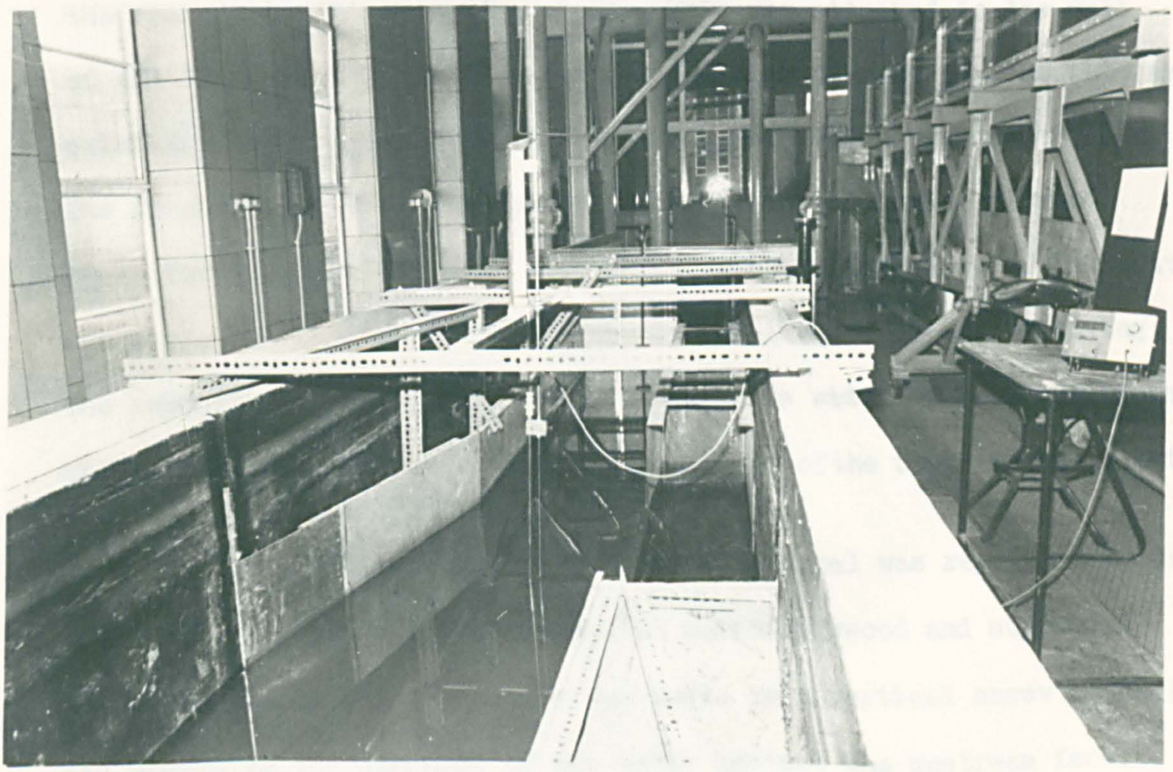

fig. 4.4 General View of the Apparatus used in the Preliminary Investigations, Looking Downstream.

4.3.7 The weir was fabricated from a 50mm x 25mm brass angle section which was set carefully on top of a 19mm thick steel plate. Great care was taken in aligning the outside face of the angle with the surface of the steel to ensure a smooth vertical face with no lips or grooves. The weir crest was machined to BS 3680 specifications[23] as shown in Figure 4.11 and the surface kept clean by careful polishing with a non-abrasive polish. The weir plate assembly was installed in the flume with its back face vertical and the weir crest horizontal and parallel to the walls of the flume (Fig. 4.5). The joints around the weir plate assembly were thoroughly sealed with a flexible sealing compound.

4.3.8 The tapering channel section was constructed by installing a vertical marine plywood board on the opposite side of the channel to the weir (Fig. 4.5). This was attached to the wall of the flume at the upstream end with an aluminium sheet bent into an existing chase in the wall of the flume, and sealed with plasticene. The downstream end of the board was hinged to the marine plywood board forming the left-hand wall of the downstream channel. The latter was supported on transverse dexion runners (Fig. 4.4) and by moving the supporting frames along these runners the width of the downstream channel could be altered, enabling the angle of the taper to be adjusted.

4.3.9 The flow in the downstream channel was regulated by an adjustable sluice gate constructed in marine plywood and supported in aluminium runners. The gate was moved by a vertical screw mechanism and sealed by the pressure of the water against the upstream face. This arrangement enabled the depth in the downstream channel to be accurately regulated.

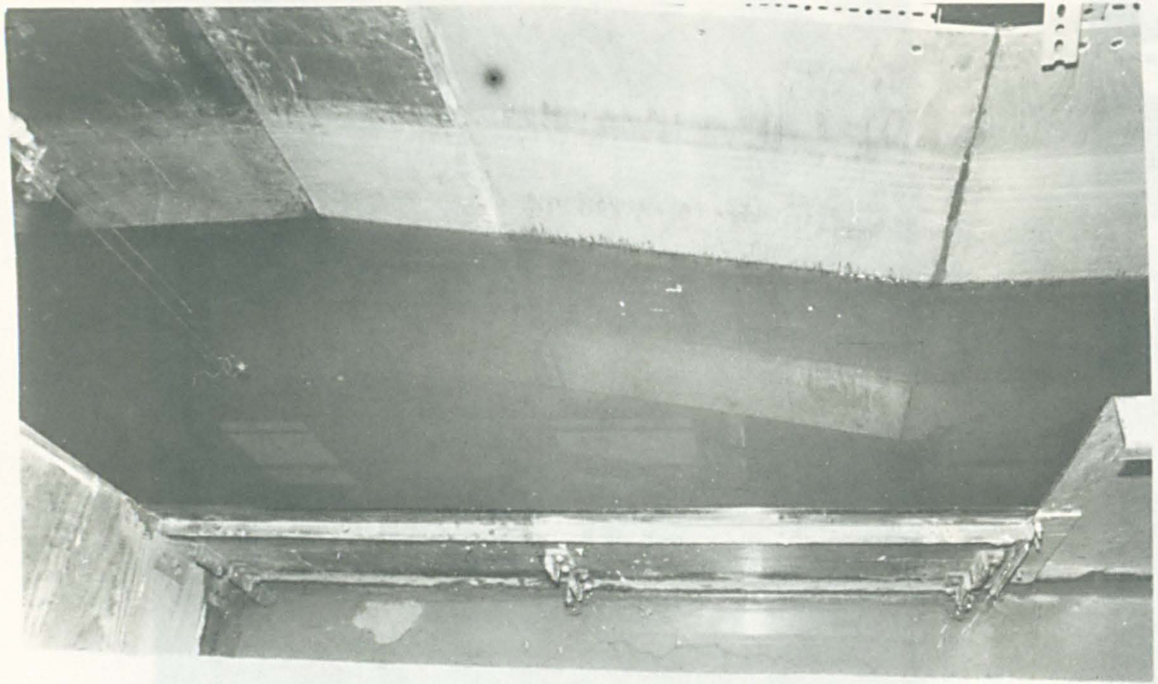

fig. 4.5 The Tapering Channel Section.

fig. 4.6 The Downstream Sluice Gate.

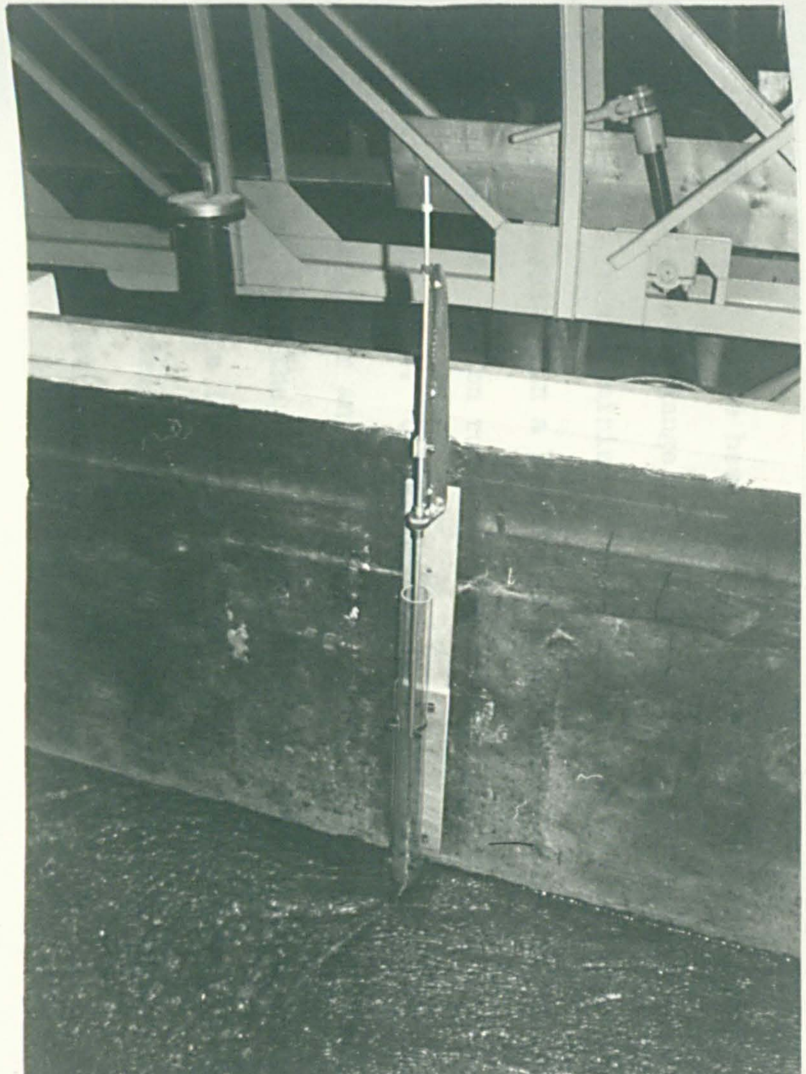

fig. 4.7 The Side Spill Channel Depth Gauge.

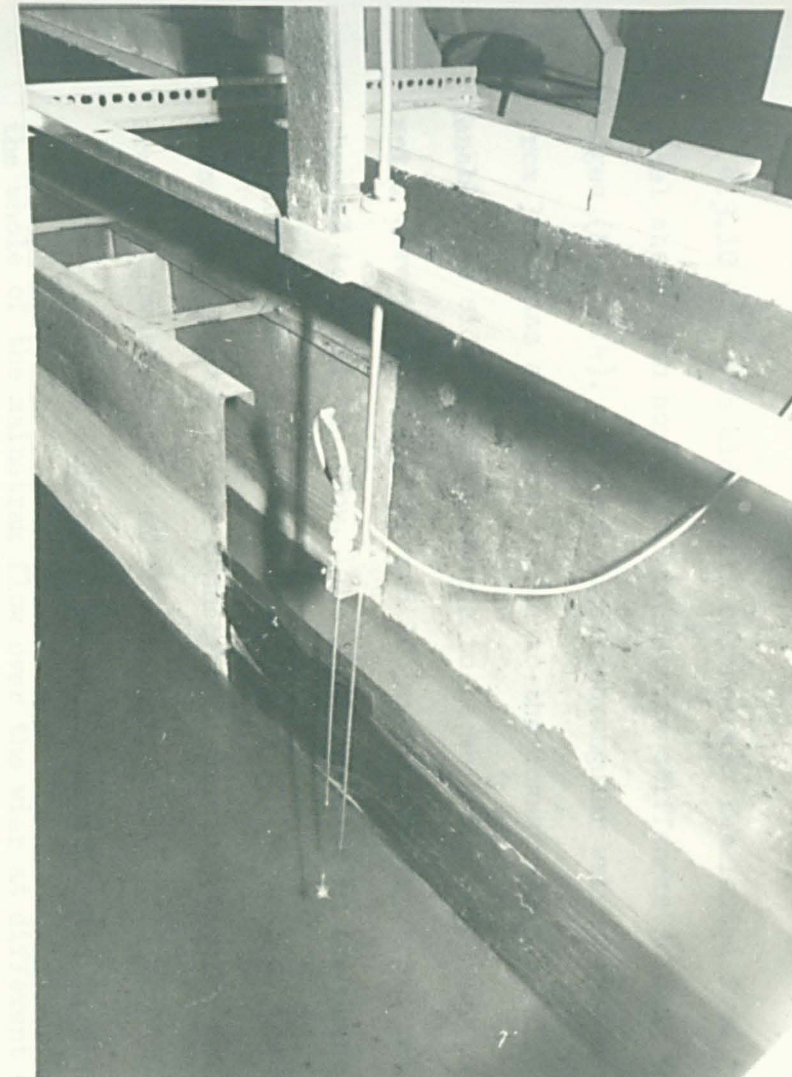

fig. 4.8 The Miniature Current Meter, Depth Gauge and Carriage.

4.3.10 The side spill channel was fabricated from galvanised steel sheet with horizontal transverse stiffeners joining the top edges (Fig. 4.4). A sharp edged rectangular weir plate, machined from 3mm brass sheet was bolted to the downstream end (Fig. 4.6) to enable the side spill discharge to be measured. Two sheets of expanded metal were installed 765mm and 1065mm from the upstream end of the channel to still the flow. The depth of water in the channel was measured using a stilling tube fastened to the wall of the flume downstream (Fig. 4.7) and connected to pressure tapping point 620mm from the downstream end of the channel.

The side spill channel was calibrated by diverting the whole of the mainstram flow over the wier at different discharges and recording the water levels in the stilling tube with a pointer gauge.

4.3.11 The head above the crest of the side weir was measured using a pointer gauge and carriage (Figs. 4.4 and 4.8). The carriage was cut from aluminium channel section and was machined to run smoothly and accurately on a longitudinal aluminium runner supported on two transverse dexion runners. The runners were carefully levelled using aluminium shims. Using the carriage, the pointer gauge could be positioned over any point in the tapering section of channel along the length of the weir. Its exact position was determined from scales fastened to the longitudinal and transverse runners. The pointer gauge was fitted with a vernier scale to ensure accurate recordings of the water surface level.

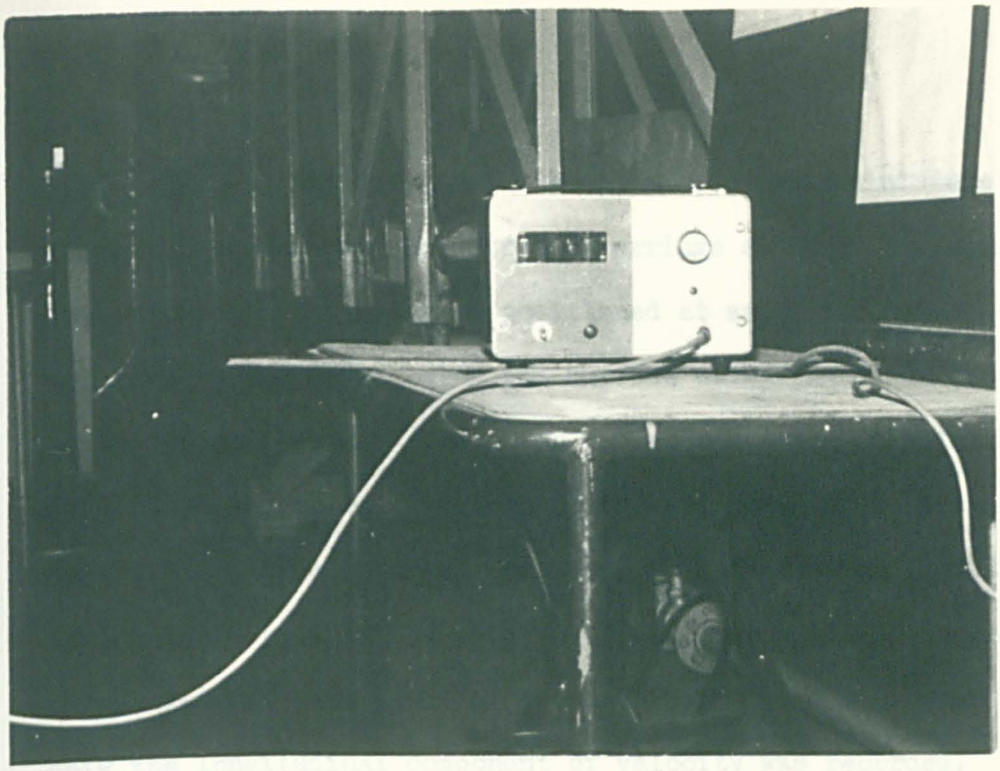

fig. 4.9 The Current Meter Recorder

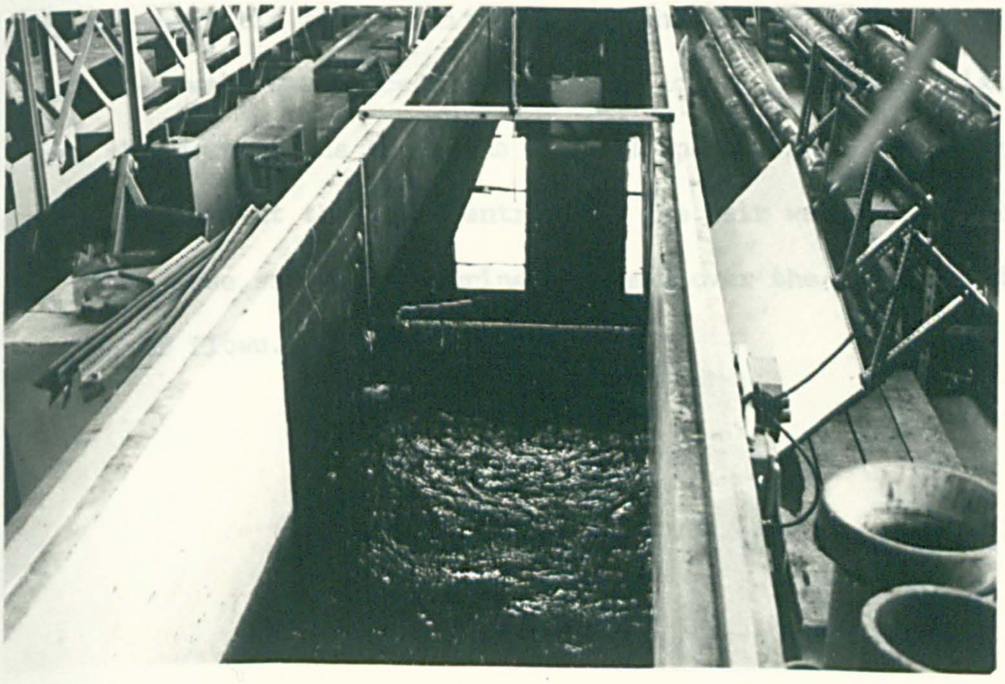

fig. 4.10 Weir being Tested Transversely

4.3.12 In addition to the pointer gauge a miniature propeller current meter was attached to the carriage as shown in Figure 4.8. Not only could the meter be positioned at any point behind the weir, but also at any depth below the surface using the slider mechanism of the pointer gauge. The meter was attached to a digital recorder (Fig. 4.9) and velocity measurements were made by counting revolutions over a fixed time interval and using the calibration formulae provided. Particular attention was paid to the alignment of the current meter whose axis was kept parallel to the crest of the side weir so that only the longitudinal component of velocity was recorded.

4.3.13 The apparatus was found to give good steady flow conditions. Both the head over the crest of the weir and the mean longitudinal velocity were sensibly constant along the length of the weir for all readings, and the apparatus could readily be adjusted to give repeatable test conditions. At the end of the series of tests the side weir was placed transversely across the flume (Fig. 4.10) and the rest of the apparatus removed apart from the stilling arrangements at the flume entrance. The weir was then calibrated as a transverse weir by measuring the head over the crest for the full range of flows.

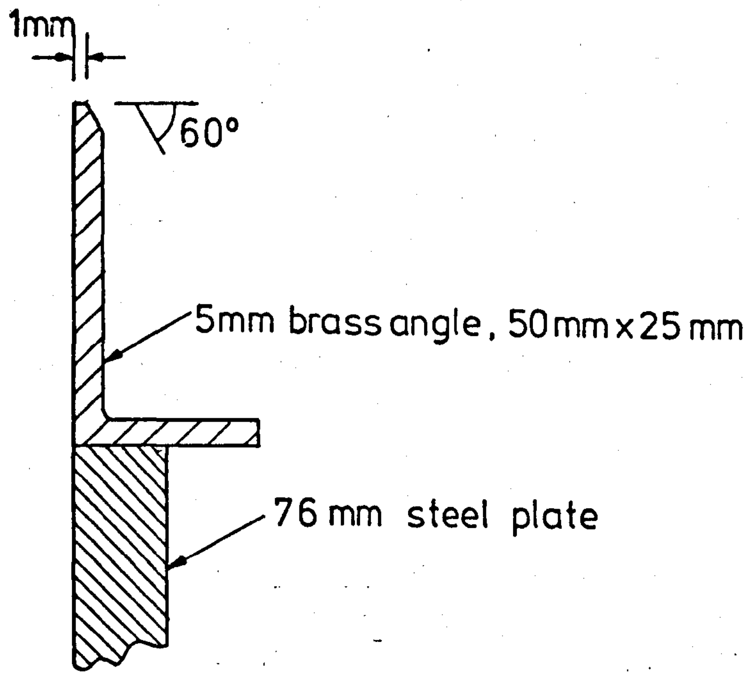

fig. 4.11

Section through Weir Crest

4.4 Experimental Procedure

4.4.1 The channel taper was set approximately in the middle of the range of adjustment at 1 in 4.08.

The pointer gauge was positioned directly over the weir crest at its centre, and the zero of the scale was set by carefully lowering the pointer onto the crest and adjusting the scale zero clamp. The weir crest height was then measured using a steel metre rule.

4.4.2 The range of upstream discharges that could be run satisfactorily through the apparatus was divided into 9 increments. The discharge was adjusted to the first of these values by slowly opening the control valve on the delivery pipe and noting the reading on the Dahl tube manometer.

The pointer gauge carriage was traversed to the centre of the downstream channel, level with the downstream end of the weir, and the pointer set to the level corresponding to the depth of flow computed from equation (4.1). The flow in the downstream channel was then regulated by careful adjustment of the sluice gate until the water surface just touched the pointer.

The gauge carriage was moved to a longitudinal section 300mm behind the weir crest and the pointer moved slowly along the channel to ensure that the water surface was horizontal. If necessary, minor adjustments were made to the downstream sluice gate to ensure that a horizontal water surface (i.e. a constant head) was formed.

4.4.3 The flow was then allowed to settle for a few minutes, after which time the upstream discharge was measured by recording the reading on the Dahl tube manometer, and the side spill discharge was obtained by recording the level in the stilling well attached to the wall of the flume downstream.

4.4.4 Using the gauge carriage the pointer was traversed across the channel at successive cross-sections 200mm apart along the length of the weir, starting at the upstream end. The head was recorded each 100mm behind the weir crest and, when appropriate, a velocity traverse was made over the whole depth immediately after taking a head reading.

4.4.5 The current meter was carefully lowered and velocity readings taken at increments of 50mm starting at 30mm below the crest. Each velocity reading was made by recording the number of propeller revolutions over a period of 15 seconds using the digital recorder and then applying the calibration formulae supplied by the manufacturer. About 10 seconds was allowed after moving the meter before a reading was taken.

4.4.6 After completion of the head recordings and velocity traverses the upstream discharge and side spill discharge were measured again to check that the flow conditions had remained steady during the test. If the readings were found to differ appreciably from those taken at the start of the test, then the test was repeated.

The upstream discharge was then adjusted to each of the remaining 8 flow rates in turn and the above measurements repeated. Two further series of results were obtained for channel tapers of 1 in 3.42 and 1 in 4.90.

4.5 Computation of Results

4.5.1 The discharge in the downstream channel was obtained by deducting the side spill discharge from the upstream discharge.

4.5.2 Although the head over the crest of the weir remained constant along the length of the weir some variation was observed over the cross-sections. This was principally due to the drawdown of the water surface as it passed over the weir causing a reduction in the head in the region immediately behind the weir. Small variations in the head were also observed adjacent to the opposite wall of the channel due to boundary effects. The head over the crest was therefore taken as the mean of the measured values along the 200mm, 300mm and 400mm longitudinal sections.

4.5.3 The results of the velocity traverses are given in Appendix V. Values of velocity energy coefficient and the momentum flux correction factor were obtained by numerical computation with the aid of a programmable calculator. The method of computation is discussed in Appendix V and a table of results is included.

4.5.4 Values of the coefficient of discharge were obtained from the transverse weir equation using the measured values of side spill discharge and mean head over the crest. The results of the preliminary investigations are fully discussed in Chapter 6.

CHAPTER 5. MAIN EXPERIMENTAL INVESTIGATIONS

5.1 Scope of the Investigations

5.1.1 Having obtained reliable values of the Coefficient of Discharge and Momentum Flux Correction Factor the Mathematical Model described in Chapter 3 could now be tested. It was essential that the model be proven for as many different channel configurations as possible. The apparatus was therefore designed with a variable channel slope, a means of controlling the flow upstream and downstream of the weir, and a facility for incorporating a number of weirs of differing dimensions.

5.1.2 Using the full range of discharges available the effects of weir length and crest height, channel slope and regulation of the flow by the channel control structures were investigated. For each reading the measured discharges were compared with values obtained by the appropriate mathematical model, and for selected readings measured and computed surface profiles were also compared.

5.2 Description of the Apparatus

5.2.1 An existing 102mm wide x 204mm deep rectangular flume was modified so that any of five different side weirs could be fitted. This was achieved by replacing the central section with a specially constructed unit in which 915mm of the channel wall had been removed. The edges of the opening were flanged and accurately drilled so that a weir could easily be bolted into place with its crest parallel to the bed of the channel and the inside surface of the weir plate flush with the face of the perspex channel wall (Figs. 5.1, 5.2 and 5.3).

5.2.2 The flume was supplied by a centrifugal pump which pumped water from a sump tank through a 100mm delivery pipe to a specially shaped inlet section designed to still the flow on entry to the flume. An expanded polystyrene float was loosely connected to the flume at entry to reduce surface disturbances (Fig. 5.3).

The delivery pipe was fitted with a Venturi meter which was connected to two differential manometers, an air/water manometer used for low flows, and a water/mercury manometer, used for higher flows (Fig. 5.4). The Venturi meter and manometers were calibrated by weighing, for the full range of flows, prior to the start of the main series of tests.

The flow in the delivery pipe was regulated by a 76mm sluice valve and a 38mm sluice valve fitted on a short by-pass pipe (Fig. 5.3).

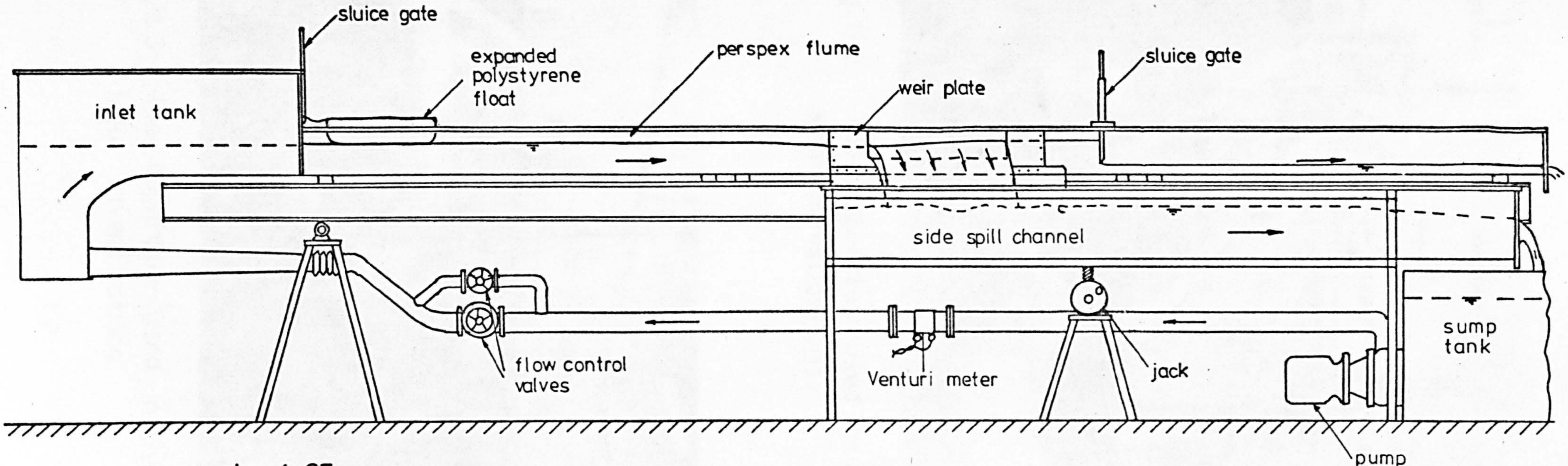

scale 1:25

fig. 5.1

General Arrangement of the Main Apparatus,
(manometers and depth gauges omitted).

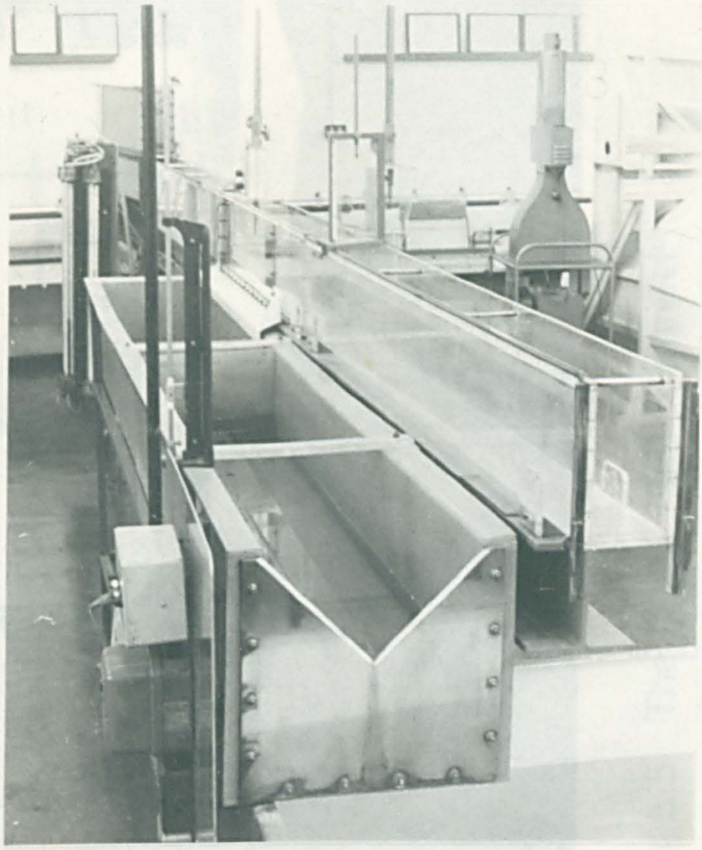

fig. 5.2 The Apparatus used in the Main Investigations.

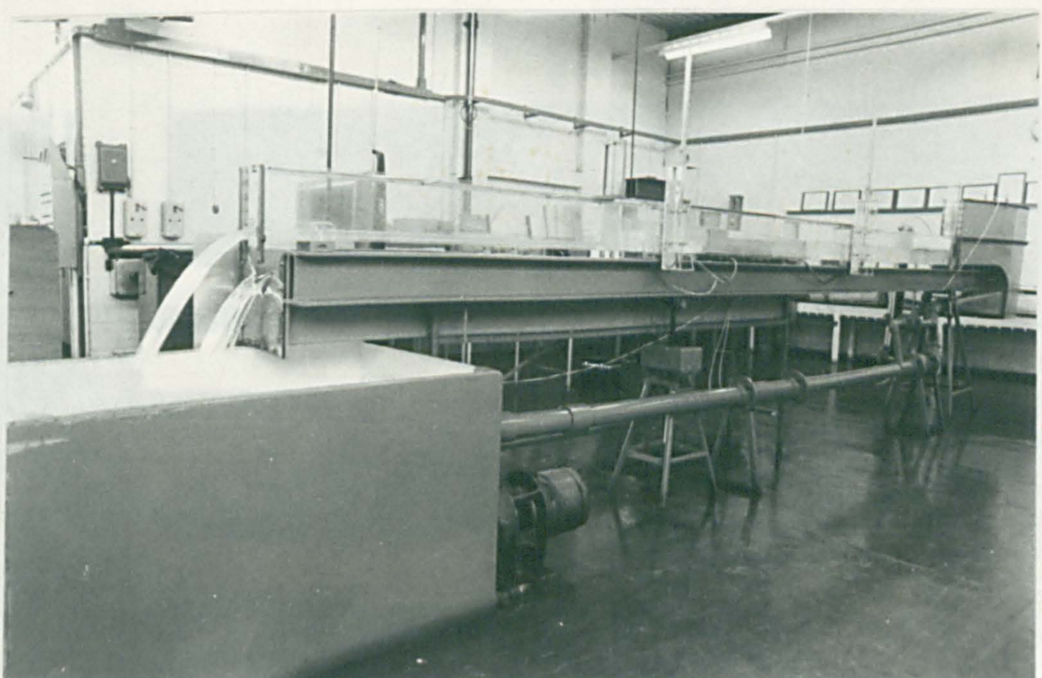

fig. 5.3 The Apparatus used in the Main Investigations.

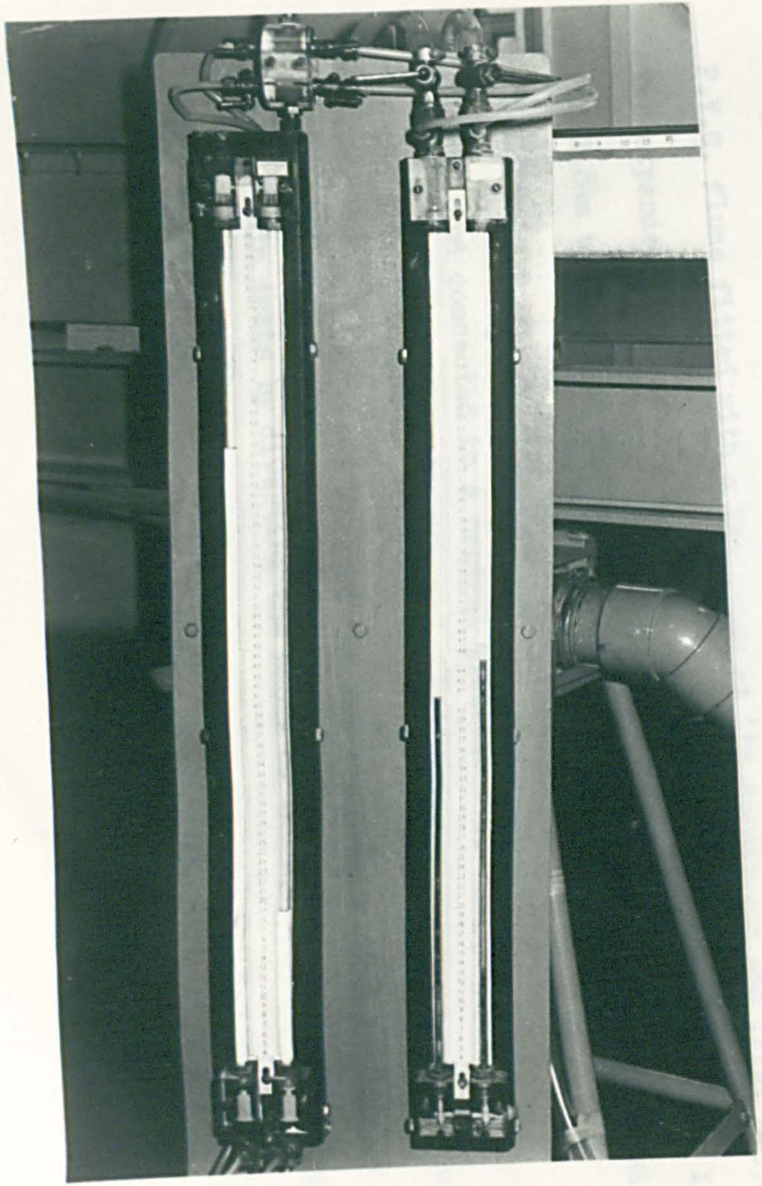

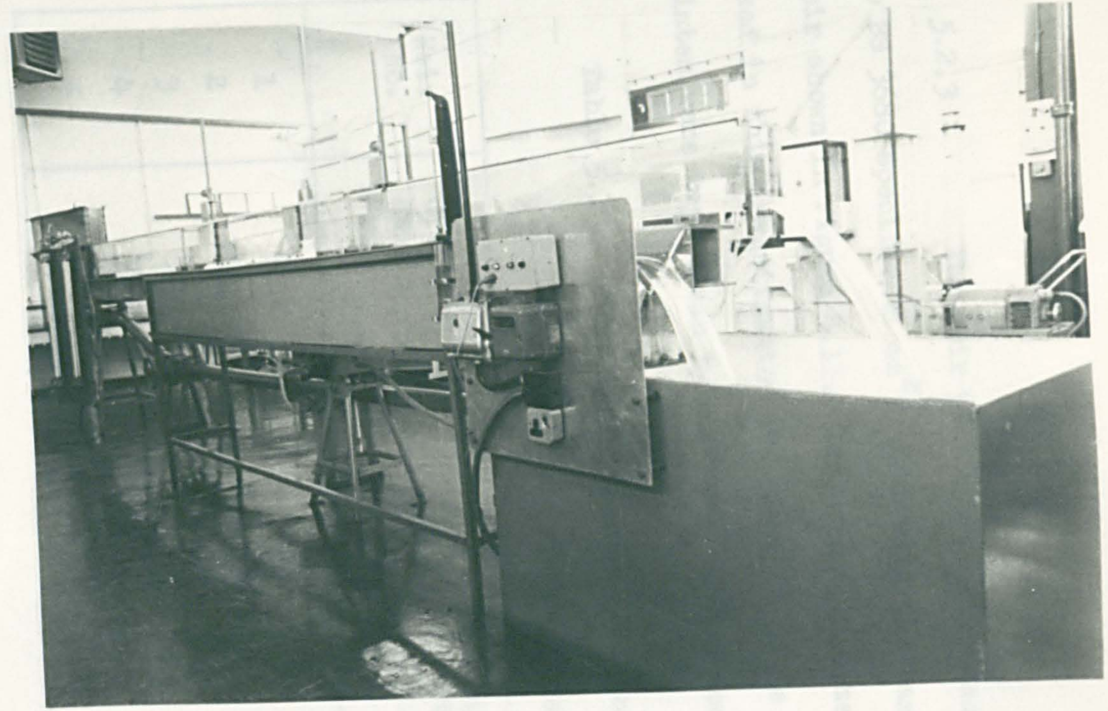

△ fig. 5.5 The Side Spill Channel Showing the Vee Notch and the Stilling Tube.

◁ fig. 5.4 The Differential Manometers.

5.2.3 The weir plates were each machined from 5mm sheet brass to BS 3680 specifications[23], i.e. with the same crest geometry as the weir shown in Figure 4.11. The principal dimensions of the five weirs used in this investigation are given in Table 5.1 below. The weir plates were kept clean by polishing with a non-abrasive polish.

Table 5.1 Principal Dimensions of the Side Weirs used in the Main Investigation.

Weir No.	Crest Height mm	Length m	Chainage at Upstream End inches	Chainage at Downstream End inches
1	80.0	0.6096	96	120
2	118.0	0.6096	96	120
3	36.0	0.6096	96	120
4	79.5	0.4572	99	117
5	80.5	0.7620	93	123

5.2.4 The side spill flow was collected in a 305mm x 305mm P.V.C. flume fitted with a Vee notch at its downstream end (Fig. 5.5). Two expanded metal meshes were placed transversely across the flume 1.67m and 1.84m upstream of the Vee notch to still the flow, and a vertical stilling tube and pointer gauge were fastened to the side of the channel and connected to a central pressure tapping, 530mm upstream of the notch, to enable accurate recordings of the water level in the channel to be made. The channel and Vee notch were calibrated prior to the main tests by diverting the whole of the upstream flow over the side weir and then passing the outflow through the Vee notch into a weigh tank.

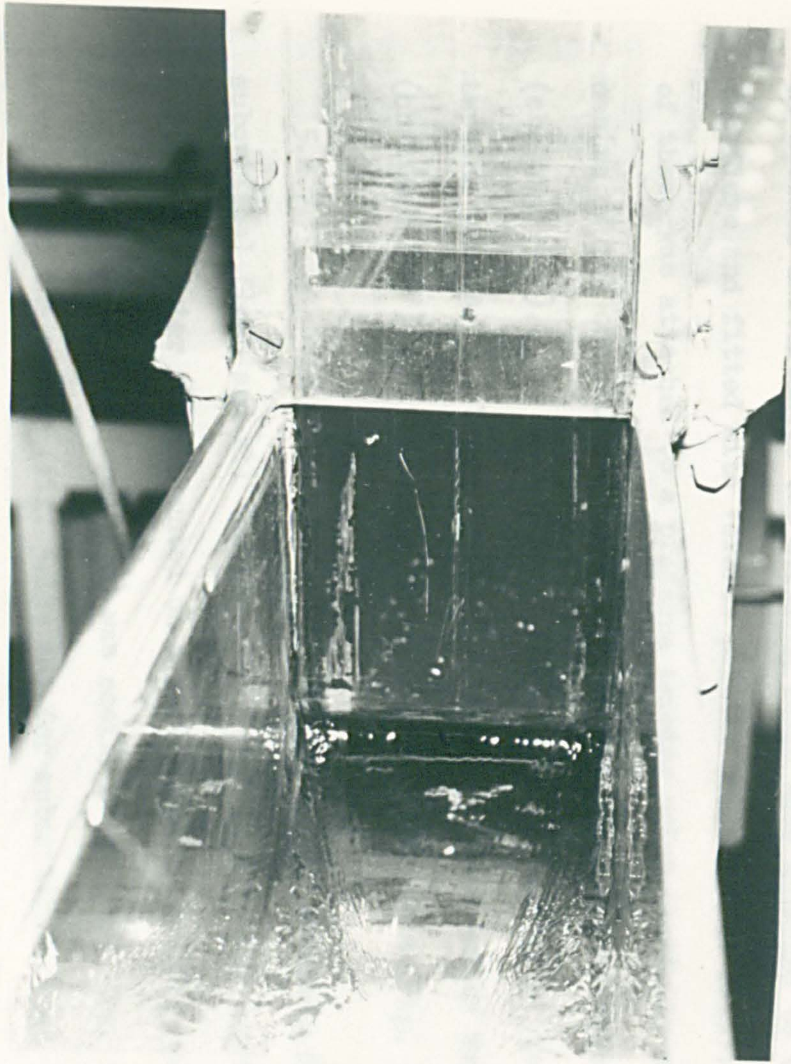

fig. 5.6 The Upstream Sluice Gate.

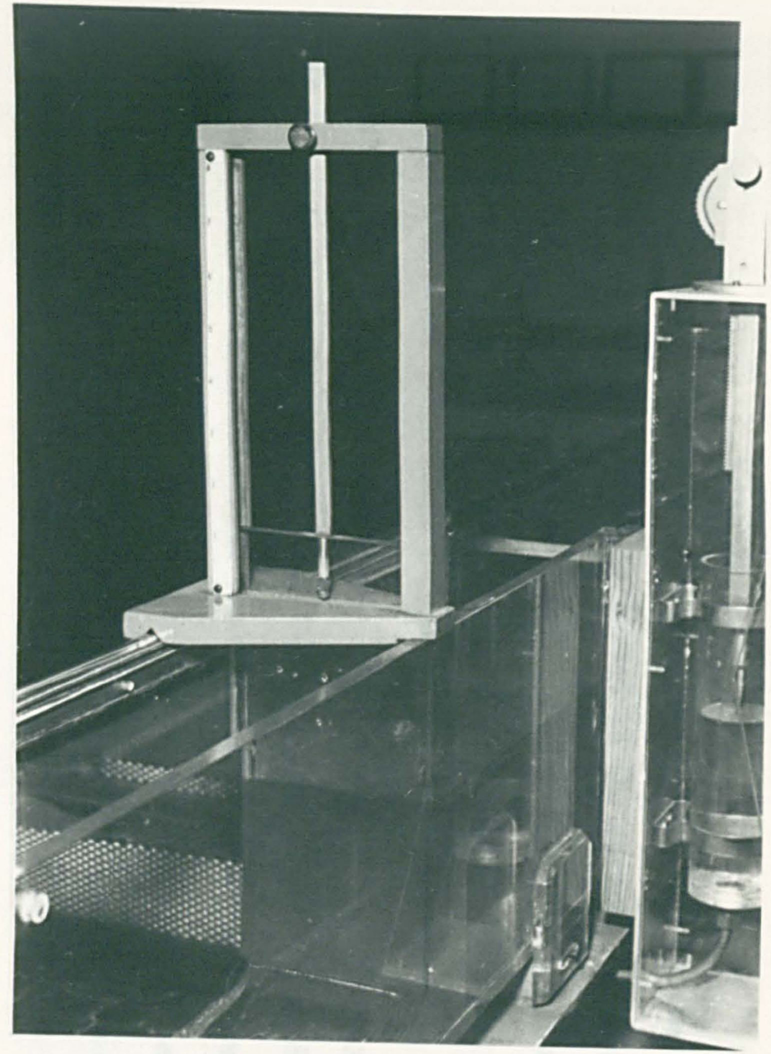

fig. 5.7 The Downstream Sluice Gate.

5.2.5 A sluice gate was installed at entry to the flume so that supercritical flow could be formed in the channel upstream of the weir (Case IV). The sluice gate was adjustable enabling a range of Froude Numbers to be attained in the upstream flow. A second sluice gate was installed downstream of the side weirs (Fig. 5.7) to regulate the flow in the downstream channel. Thus the flow immediately downstream of the weir could be free flowing supercritical flow (Fig. 5.8) or regulated subcritical flow with the downstream sluice gate lowered (Fig. 5.9). In addition the flow in the downstream channel could be regulated using an adjustable rectangular weir clamped to the downstream end of the flume. (Fig. 5.10)

5.2.6 For all readings measurements of the depth of flow upstream and downstream of the weir were required. To reduce the effect of surface disturbances two stilling wells were attached to the wall of the flume and fitted with Vernier pointer gauges (Fig. 5.11). The first of these was attached to a pressure tapping point carefully set in the centre of the channel bed level with the upstream end of Weir 1 (chainage 96"). The second could be attached to either of two such tapping points, one being level with the downstream end of Weir 1 (chainage 120") and the other 398mm further downstream (Fig. 5.12).

5.2.7 In addition surface profiles were measured for selected subcritical flows and all supercritical flows. This was achieved using a Vernier pointer gauge mounted on a perspex carriage (Fig. 5.13). Its longitudinal position (chainage) was easily determined from the scale attached to the runner (Fig. 5.13) and for subcritical flow profiles the surface elevation was readily determined by carefully lowering the pointer until it just touched the water surface.

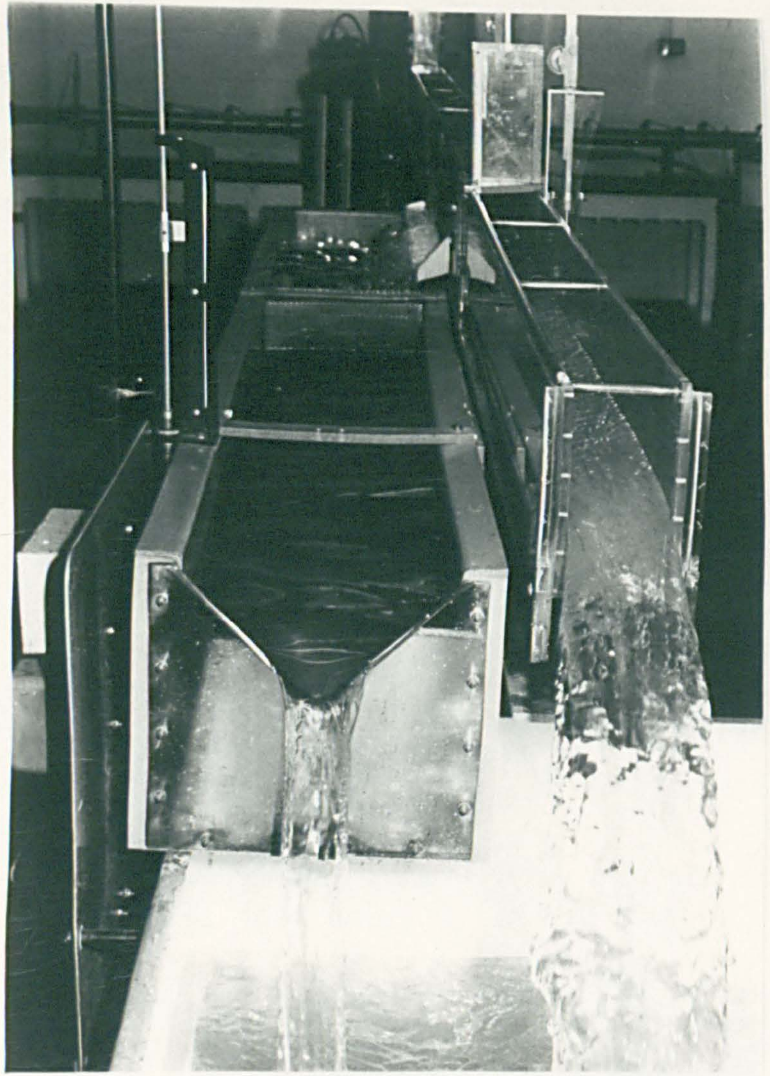

fig. 5.8 Downstream Sluice Gate Raised.

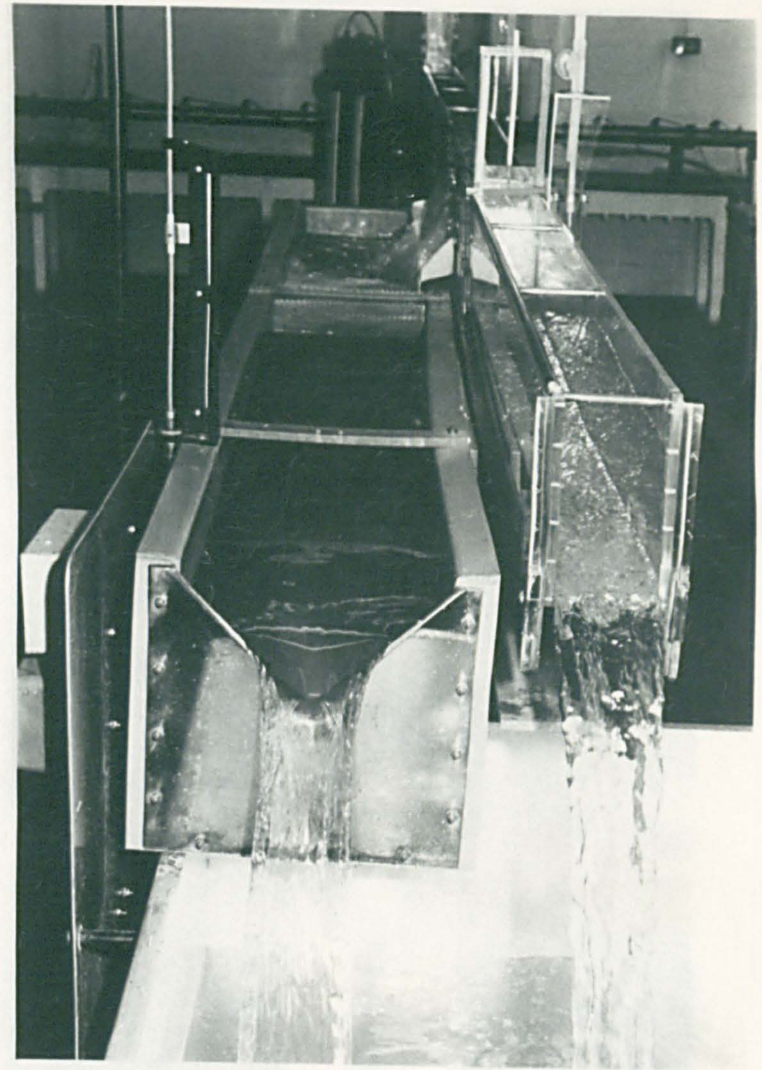

fig. 5.9 Downstream Sluice Gate Lowered.

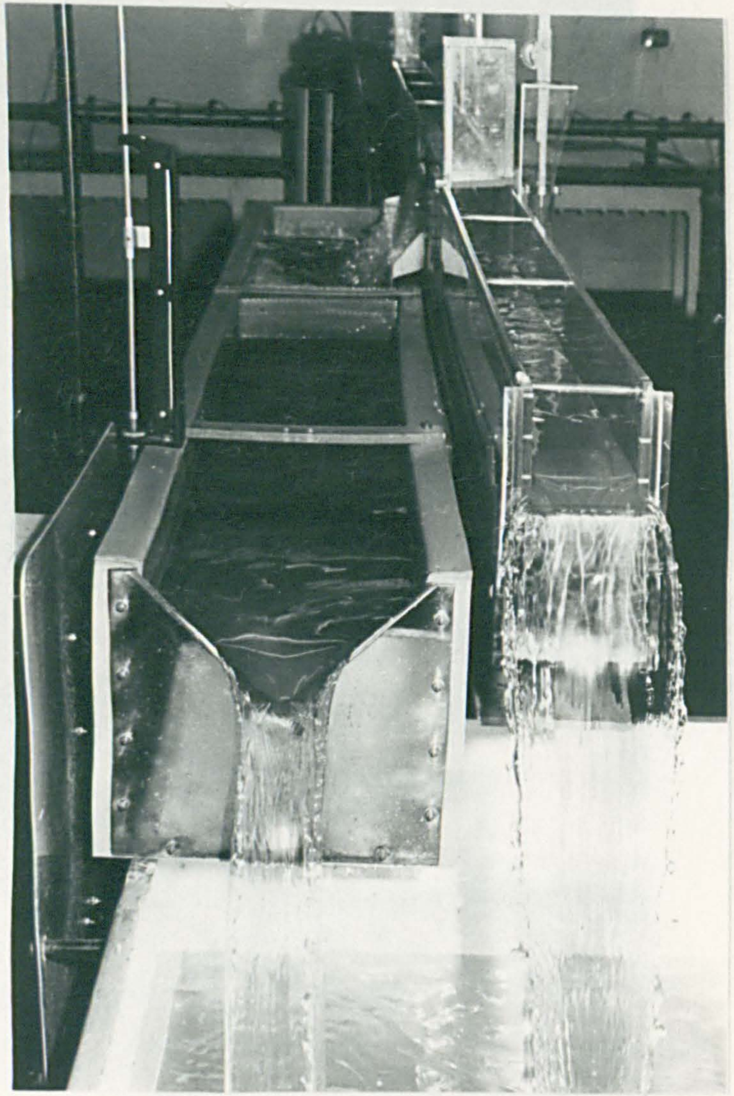

fig. 5.10 Downstream Weir Fitted

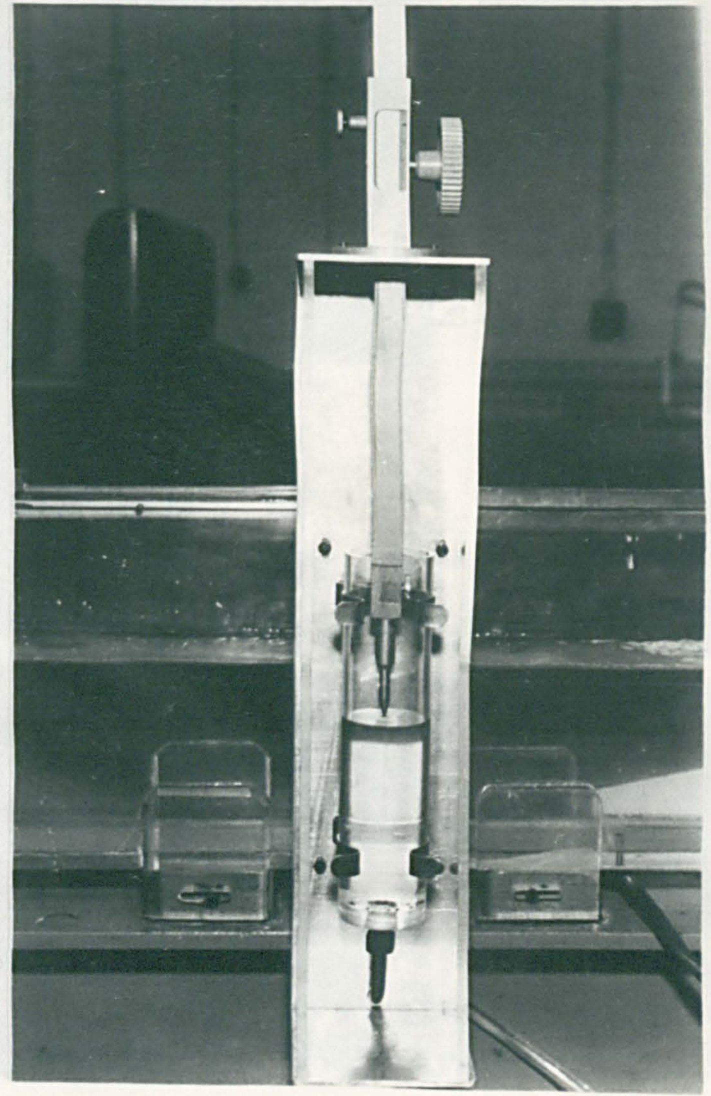

fig. 5.11 Stilling Well and Pointer Gauge.

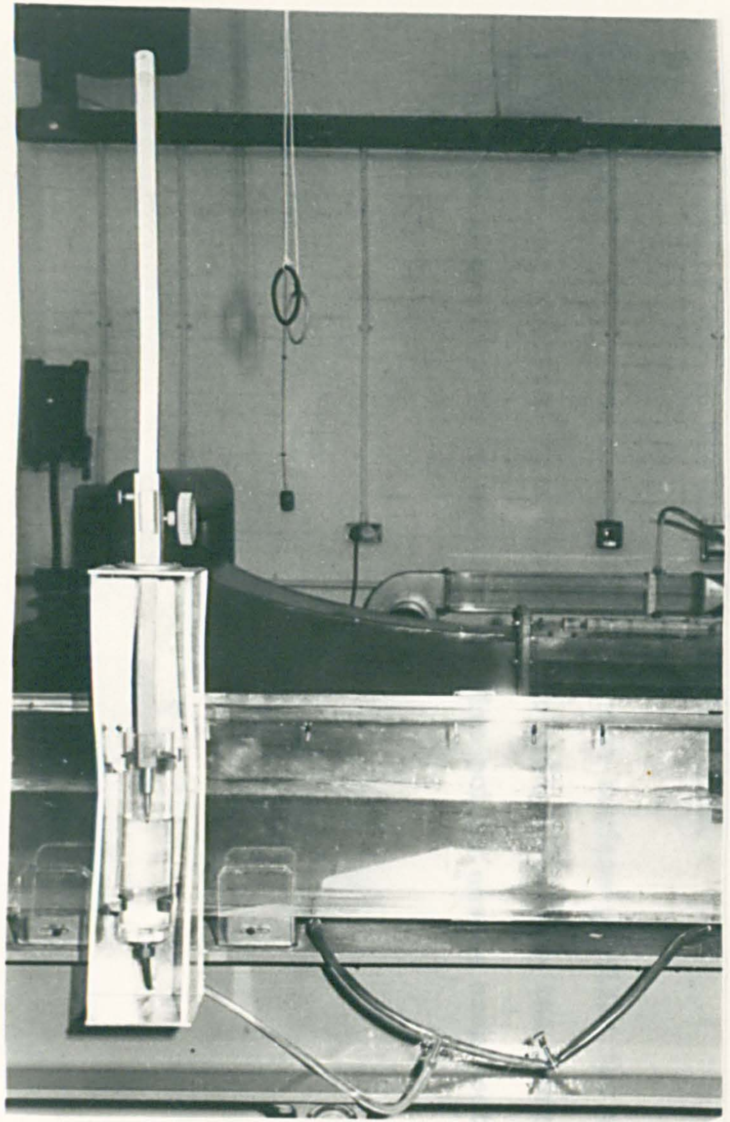

fig. 5.12 Alternative Downstream Pressure Tappings

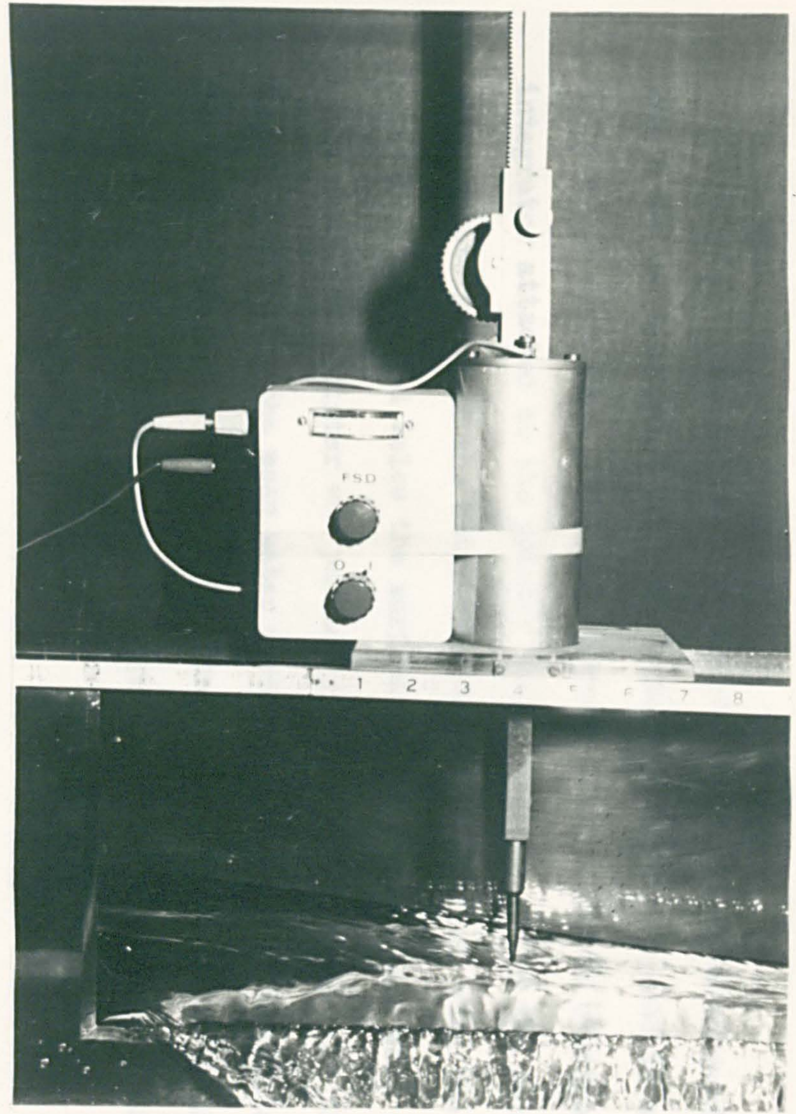

fig. 5.13 Depth Gauge, Carriage and Electronic Integrator

For supercritical flow, however, the water surface was disturbed by small waves and difficulty was experienced in measuring the surface elevation. This was overcome using a simple electronic integrator attached to the pointer gauge carriage. When the pointer was completely out of the water the scale read zero and when the pointer was immersed below the surface the scale read 10. When the scale read 5 the pointer was partially immersed for 50% of the time, thereby indicating the mean water surface level. Some fluctuation of the scale reading was observed but provided the reading was within the range 4 to 6 the pointer accurately gave the mean elevation of the water surface.

5.2.8 For cases where the surface curvature was appreciable the depths at the beginning and end of the side weir were taken from the readings of the moveable pointer gauge in preference to the stilling well recordings as the latter were subject to the effects of vertical acceleration due to the curvature of the flow.

5.2.9 For measuring transverse surface profiles the single pointer was replaced by a five pointer bridge enabling the water surface elevation to be measured at five points across each section (Fig. 5.14).

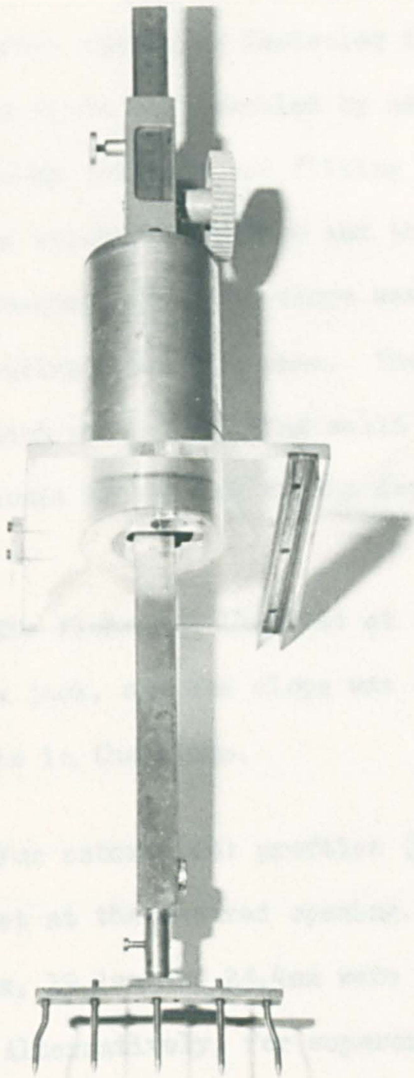

fig.5.14 The Five Point Depth Gauge.

5.3 Experimental Procedure

5.3.1 After carefully fastening the weir in place and sealing with plasticene the flume was levelled by sealing the downstream sluice gate in a fully closed position and filling the flume with about 50mm of water. This was allowed to settle and the depth measured at three points along the channel. The bed slope was then slowly adjusted until all three depth readings were the same. The water surface level was then measured in each of the stilling wells so that readings taken during each test could be related to the depth at the pressure tapping points.

The flume was then set at the desired slope using the scale on the screw jack, and the slope was checked by recording the depth at two points in the flume.

5.3.2 For subcritical profiles (Case II) the downstream sluice gate was set at the desired opening. During the main investigation openings of 12.7mm, 19.1mm and 25.4mm were used.

Alternatively, for supercritical profiles (Case IV) the upstream sluice gate was set, or for supercritical flow Case I both sluice gates were fully raised clear of the flow.

5.3.3 For each configuration a series of 9 readings was generally taken, for a full range of flows. The upstream discharge was set by carefully adjusting the control valves on the delivery pipe until the desired reading on the appropriate manometer was obtained. The flow was then allowed to settle for a few minutes before the upstream discharge was recorded. The side spill discharge was also recorded using the stilling tube and pointer gauge attached to the side spill channel.

5.3.4 The depths upstream and downstream of the weir were then measured using the stilling wells described in 5.2.6, or where appropriate the travelling pointer gauge. The surface profile was then obtained by traversing the carriage along the runners and recording the water surface level and bed elevation every 2" between chainage 76" and chainage 138". For supercritical flow profiles the electronic integrator was used to position the pointer, as described in 5.2.7.

5.3.5 The temperature of the water flowing over the side weir was recorded using a thermometer installed at the upstream end of the side spill channel.

5.3.6 The upstream and side spill discharges were measured again at the end of the test to ensure that the flow had remained steady throughout. Provided that sufficient time had been allowed to establish steady flow before readings commenced, the flow was found to remain steady during each test run. The test results were found to be fully repeatable.

5.4 Computation of the Results

5.4.1 The downstream discharge was obtained by subtracting the side spill discharge from the upstream discharge. The viscosity of the water flowing was computed from the recorded temperature using standard tables.

5.4.2 For subcritical flow conditions the depth downstream of the weir and the downstream discharge are used as input data to the Mathematical Model. For each configuration these values of depth and discharge were checked by plotting a depth-discharge rating curve for the downstream channel.

5.4.3 For supercritical flow the upstream depth and discharge are required as input data. Because of curvature effects the former was obtained from the travelling pointer gauge recordings.

5.4.4 The appropriate Mathematical Model was then used to compute theoretical profiles and discharges and the results are fully discussed in Chapter 6.

CHAPTER 6 DISCUSSION OF THE EXPERIMENTAL RESULTS

6.1 The Coefficient of Discharge

6.1.1 The results of the preliminary investigations are contained in Appendix V. The head above the crest of the side weir was found to be virtually constant over the whole of the tapering section except the region immediately behind the weir where draw-down of the water surface was observed, and the region immediately adjacent to the channel wall. Values for the 200mm, 300mm and 400mm longitudinal sections, used to compute the mean head, showed little variation.

6.1.2 Values of the coefficient of discharge obtained from the preliminary investigations are given in Table 6.1 and Figure 6.1. The latter also contains a plot of C_D values obtained from the Rehbock equation[19].

$$C_D = (0.602 + 0.083\frac{h}{c})(1 + \frac{0.0012}{h})^{1.5} \qquad \text{.........(6.1)}$$

and the experimental results generally fall within ± 1% of the values given by this equation. An error analysis (Appendix VI) revealed a possible error due to the scale divisions on the apparatus of ± 0.5% which would account for a substantial part of the deviations shown. There is no systematic error in the results nor any trends to indicate that the coefficient of discharge is affected by the longitudinal velocity, as suggested by Collinge[14]. The results of the supplementary tests in which the weir was tested transversely also gave C_D values within ± 1% of the Rehbock values, and they were indistinguishable from the side weir results. The Rehbock equation was therefore used to compute values of the coefficient of discharge in the mathematical model, and in the other methods tested.

Table 6.1

Coefficients of Discharge - Side Weir with Constant Head.

Reading No.	Mean Head h mm	$\frac{h}{c}$	C_D Measured	C_D Rehbock	Longitudinal Velocity m/s	Remarks
1	23.95	0.0670	0.652	0.654	0.098	
2	29.19	0.0817	0.658	0.647	0.102	
3	33.55	0.0938	0.641	0.643	0.117	1st Series
4	34.11	0.0954	0.642	0.642	0.133	
5	38.78	0.1085	0.632	0.640	0.148	Channel taper
6	40.72	0.1139	0.638	0.639	0.158	= 0.245m/m
7	37.28	0.1043	0.640	0.640	0.136	
8	25.24	0.0706	0.656	0.652	0.077	
9	21.01	0.0588	0.656	0.660	0.057	
10	25.15	0.0703	0.655	0.652	0.065	
11	27.52	0.0770	0.646	0.649	0.076	
12	29.93	0.0837	0.642	0.646	0.087	2nd Series
13	32.38	0.0906	0.649	0.644	0.097	
14	34.96	0.0978	0.640	0.642	0.108	Channel taper
15	39.95	0.1117	0.646	0.639	0.130	= 0.292m/m
16	37.46	0.1048	0.638	0.640	0.120	
17	42.51	0.1189	0.636	0.638	0.143	
18	45.14	0.1263	0.644	0.637	0.153	
19	22.42	0.0627	0.658	0.657	0.081	
20	24.98	0.0699	0.650	0.652	0.092	
21	26.48	0.0741	0.649	0.650	0.103	3rd Series
22	28.67	0.0802	0.646	0.647	0.114	
23	30.56	0.0855	0.646	0.645	0.126	Channel taper
24	33.29	0.0931	0.641	0.643	0.141	= 0.204m/m
25	35.97	0.1006	0.638	0.641	0.160	
26	37.90	0.1060	0.633	0.640	-	
27	39.09	0.1093	0.633	0.639	0.179	
28	41.31	0.1156	0.630	0.638	0.196	

FIG. 6.1 RELATIONSHIP BETWEEN C_D AND h/c.

Sharp Crested Side Weir, length = 1107.2 mm
crest height = 357.5 mm

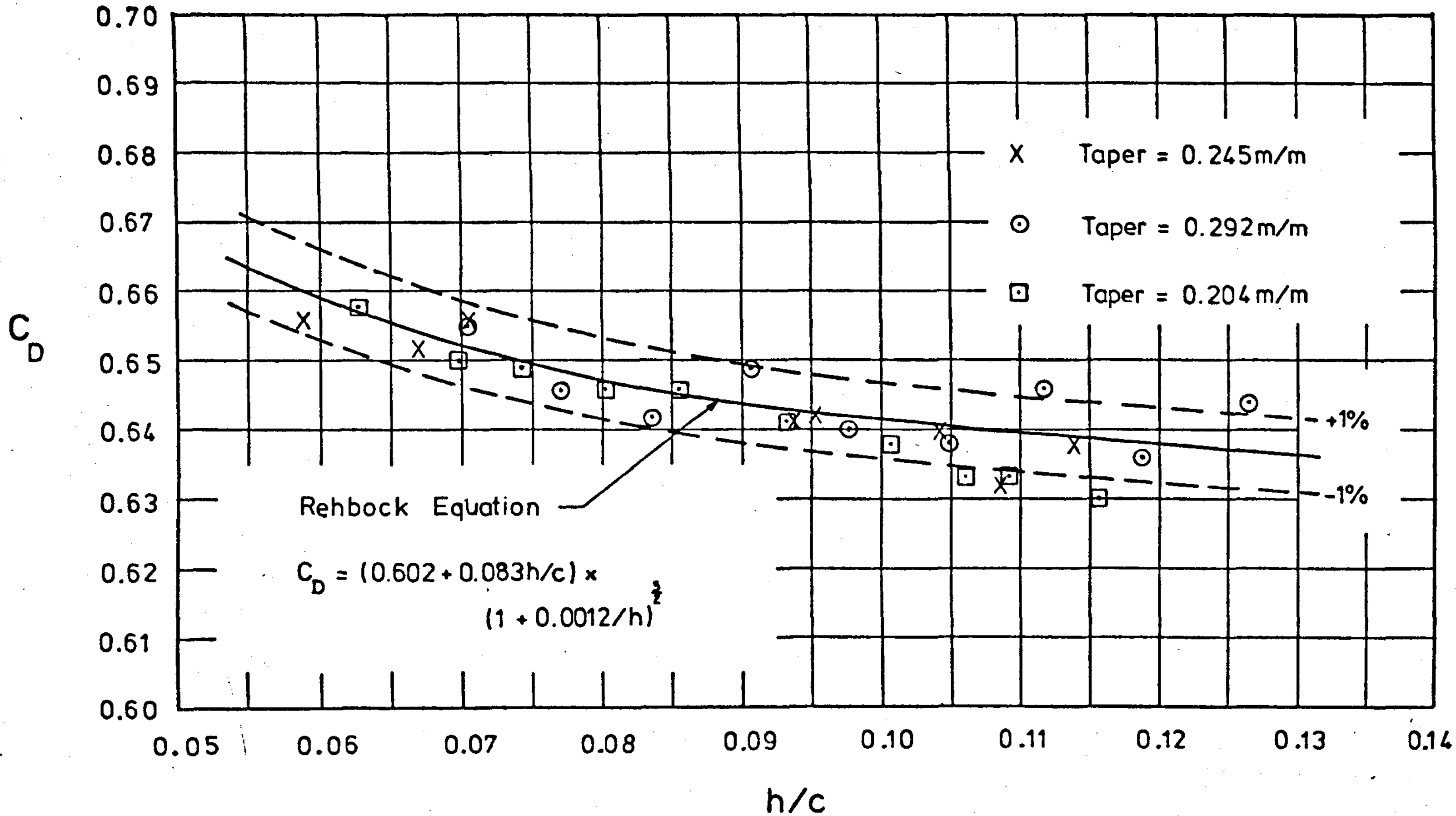

FIG.6.2 VELOCITY PROFILE: Reading 16

Cross Section 200mm, 100mm behind weir.

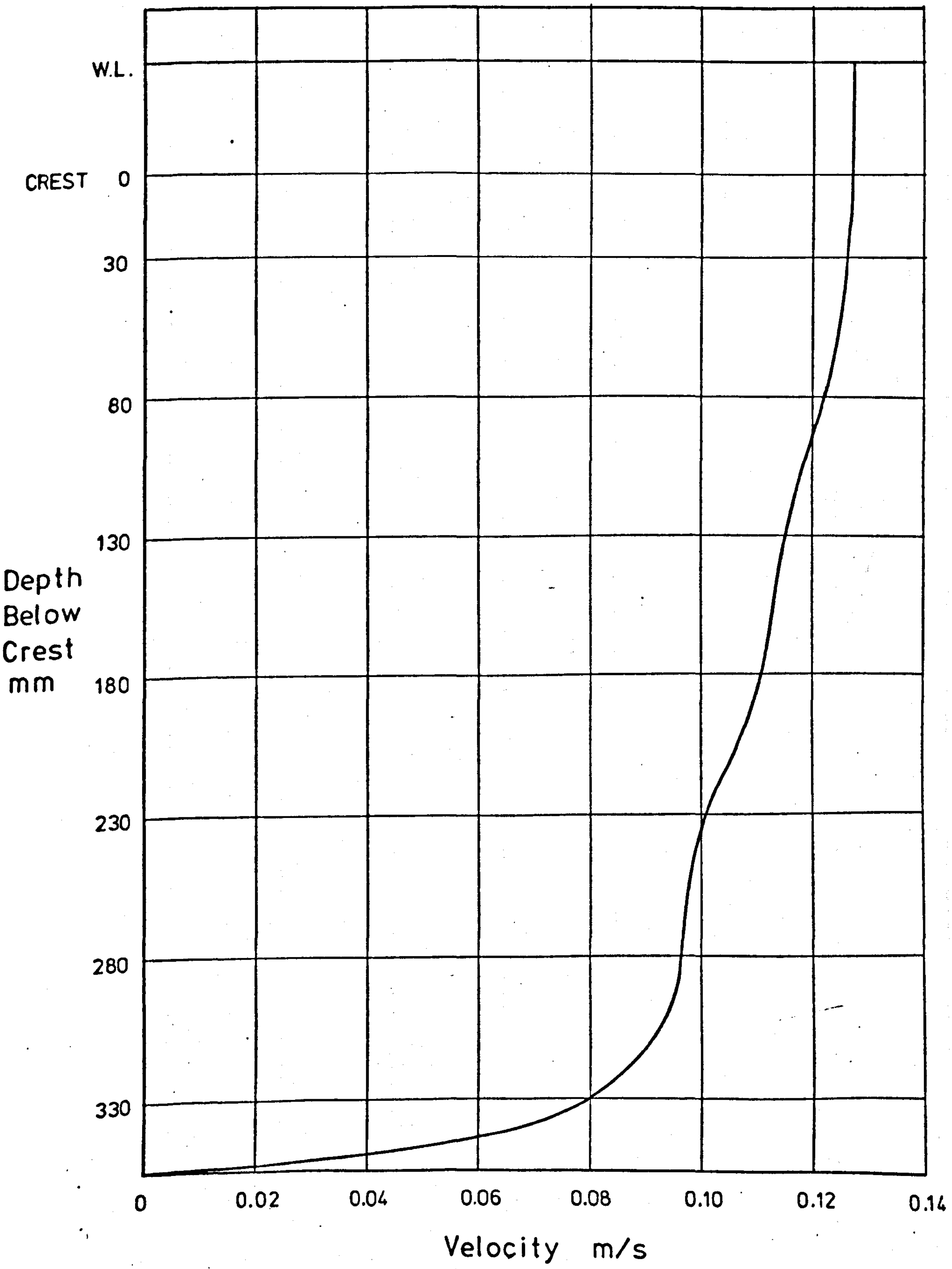

FIG. 6.3 VELOCITY PROFILE: Reading 16

Cross Section 200mm, 200mm behind weir.

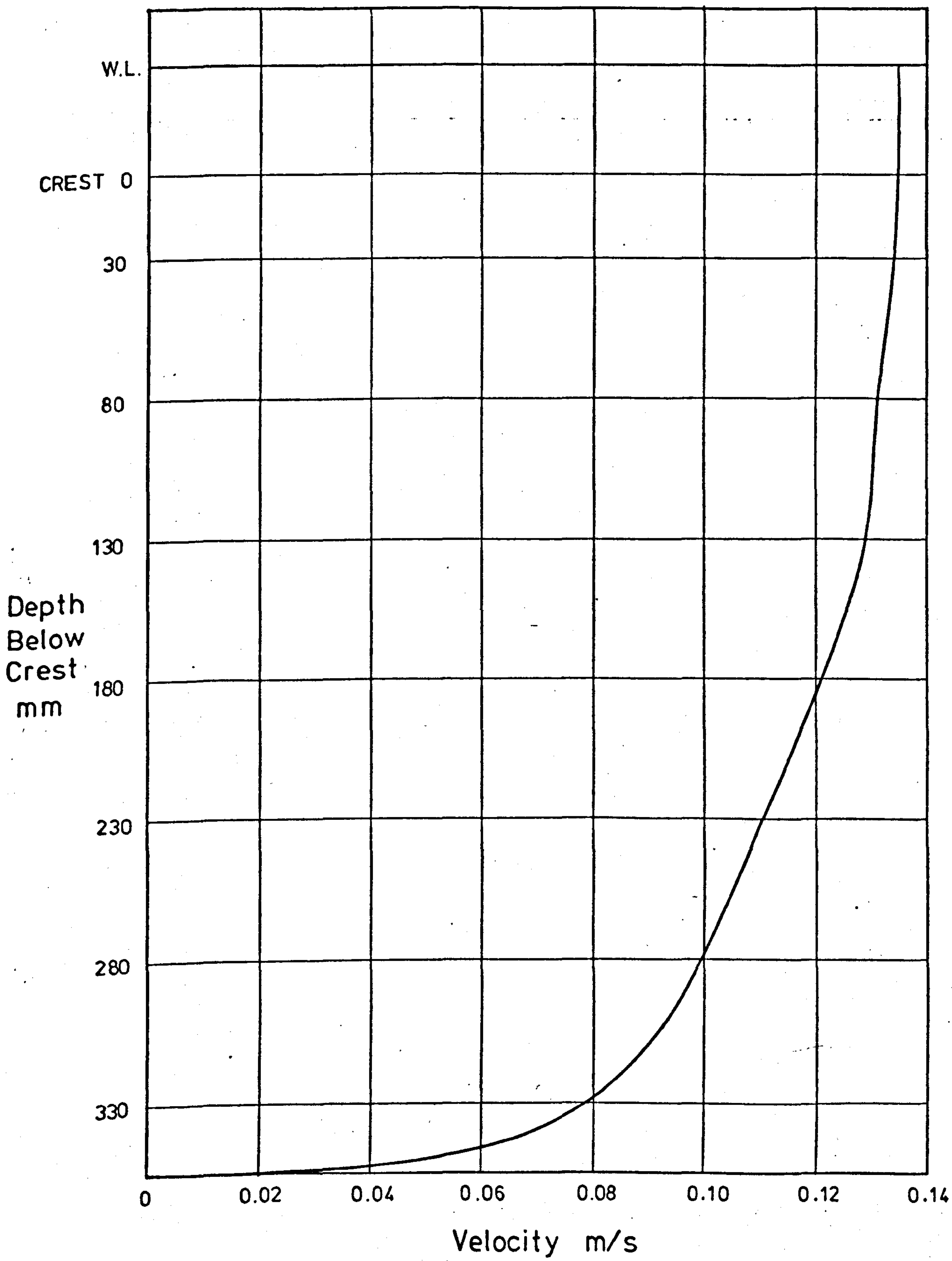

FIG.6.4 VELOCITY PROFILE: Reading 16

Cross Section 200 mm, 400 mm behind weir.

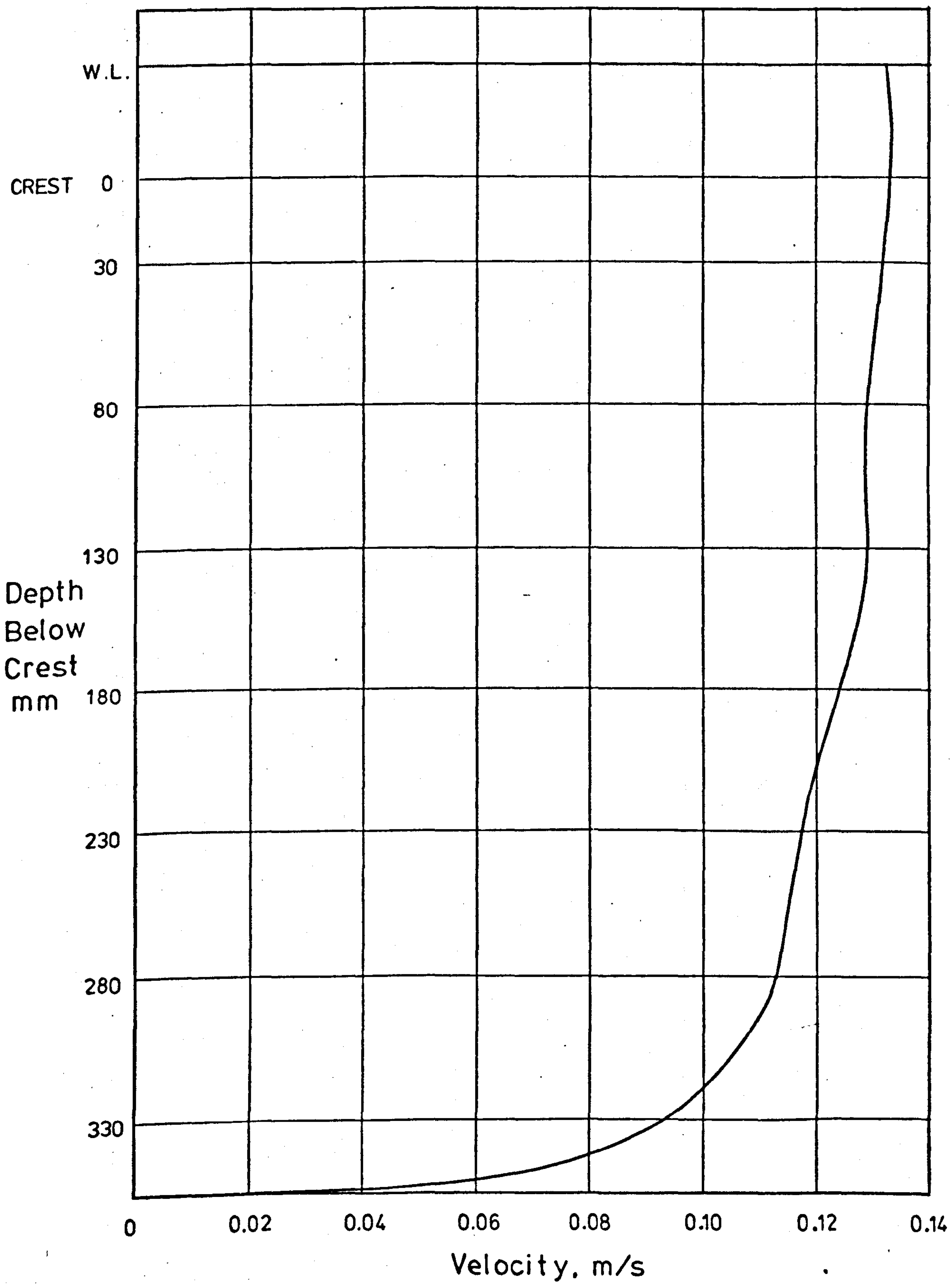

FIG. 6.5 VELOCITY PROFILE: Reading 16

Cross Section 200 mm, 500 mm behind weir.

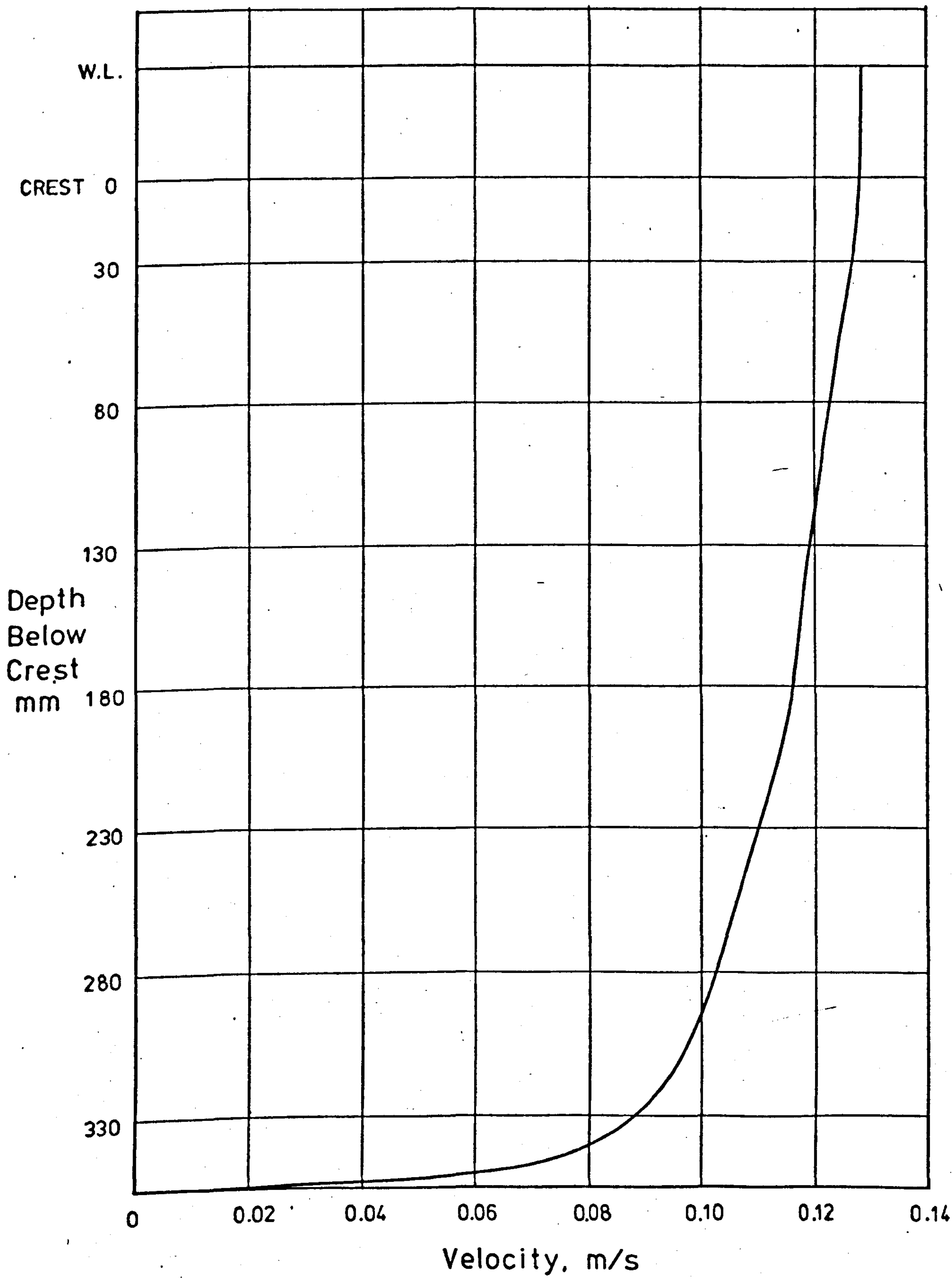

FIG. 6.6 VELOCITY PROFILE: Reading 16

Cross Section 200mm, 600mm behind weir.

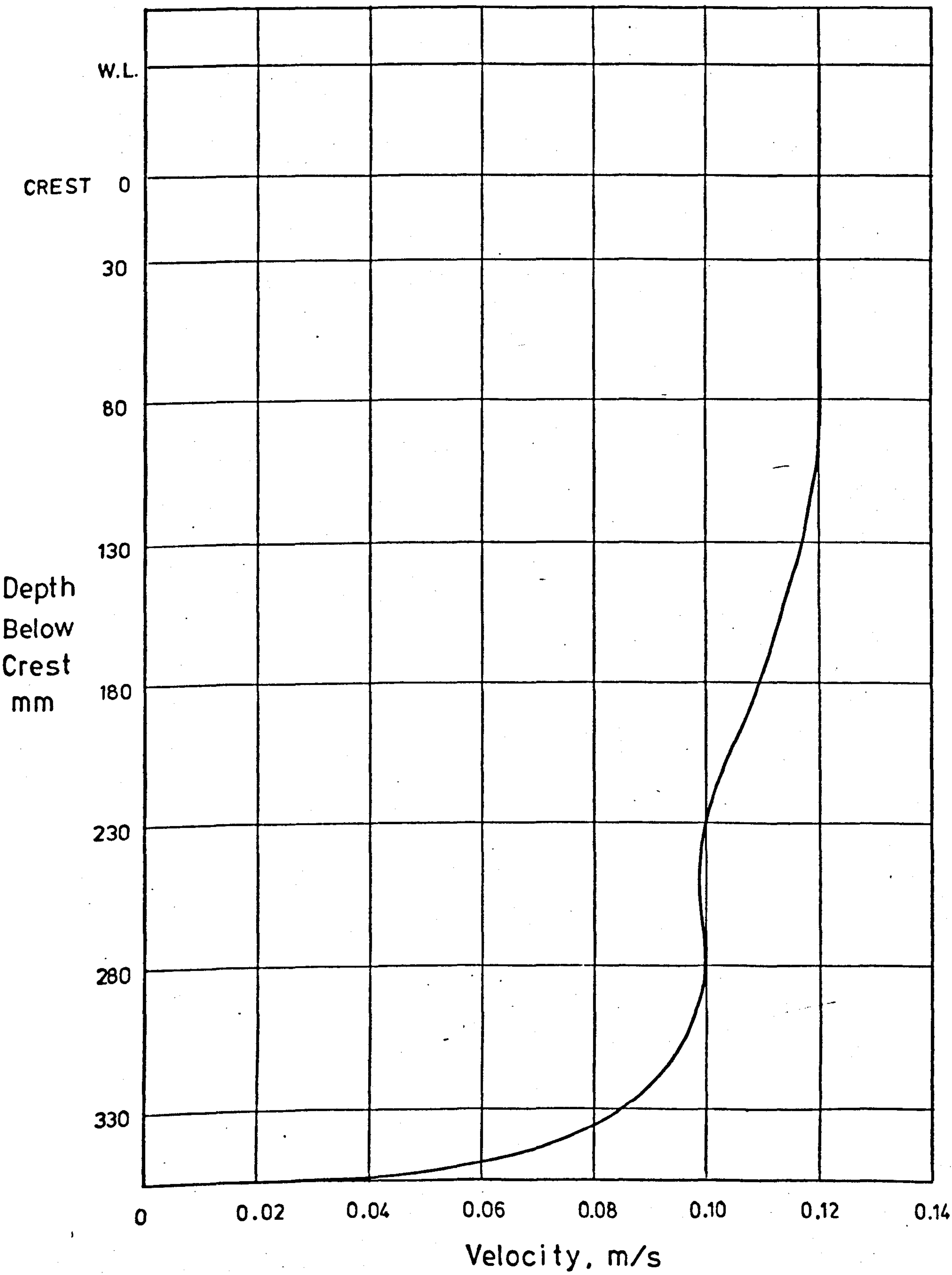

6.2 The Energy and Momentum Coefficients

6.2.1 Appendix V also contains the results of the velocity traverses undertaken with the current meter in the tapering channel, and typical velocity distributions, for test No. 16, are plotted in Figures 6.2 to 6.6. Velocity energy coefficients and momentum coefficients were calculated at each cross-section numerically, using the method described by Chow[24] and outlined in Appendix V. The results are summarised in Table 6.2, which shows that the mean velocity and α and β all remain sensibly constant along the length of the weir in each case.

6.2.2 The values of α and β obtained compare favourably with those quoted by Chow[24], and although neither α nor β vary a great deal over the whole series of tests, there is some indication that they decrease in magnitude with increasing longitudinal velocity, as shown in Figure 6.7. A least squares regression analysis gave the following expressions for α and β with correlation coefficients of about 0.83.

$$\alpha = 1.14 - 0.28v \qquad \text{..........(6.2)}$$

$$\beta = 1.06 - 0.10v \qquad \text{..........(6.3)}$$

Equation (6.3) was used to obtain values of β in the mathematical model for values of v not exceeding 0.6m/s.

Table 6.2

Velocity Energy Coefficients and Momentum Flux Correction Factors.

Reading No.	v m/s	α	β	Reading No.	v m/s	α	β
	0.0855	1.1176	1.0490		0.1163	1.0955	1.0413
	0.0864	1.1215	1.0508		0.1136	1.0896	1.0396
2	0.0844	1.1613	1.0635	3	0.1164	1.1048	1.0450
	0.0828	1.2723	1.1050		0.1141	1.1273	1.0528
	0.0843	1.1864	1.0716		0.1140	1.1197	1.0497
	0.0876	1.2083	1.0796		0.1161	1.1334	1.0541
Mean	0.0852	1.1779	1.0699	Mean	0.1151	1.1117	1.0471
Reading No.	v m/s	α	β	Reading No.	v m/s	α	β
	0.1519	1.0995	1.0424		0.0729	1.0849	1.0381
	0.1530	1.0846	1.0379		0.0704	1.0944	1.0414
6	0.1545	1.0730	1.0339	8	0.0699	1.1173	1.0497
	0.1499	1.0965	1.0417		0.0698	1.1459	1.0595
	0.1508	1.1139	1.0474		0.0700	1.1096	1.0464
	0.1580	1.1370	1.0551		0.0720	1.1321	1.0540
Mean	0.1530	1.1008	1.0431	Mean	0.0708	1.1140	1.0482
Reading No.	v m/s	α	β	Reading No.	v m/s	α	β
	0.0809	1.1220	1.0517		0.0913	1.1292	1.0536
	0.0799	1.0893	1.0398		0.0902	1.0914	1.0403
12	0.0782	1.0978	1.0427	13	0.0892	1.1032	1.0446
	0.0770	1.1321	1.0551		0.0897	1.1060	1.0454
	0.0793	1.1050	1.0450		0.0908	1.0995	1.0430
	0.0796	1.1435	1.0576		0.0930	1.1010	1.0433
Mean	0.0792	1.1150	1.0487	Mean	0.0907	1.1051	1.0450

Table 6.2 continued

Reading No.	v m/s	α	β	Reading No.	v m/s	α	β
16	0.1116	1.1546	1.0625	17	0.1348	1.1559	1.0641
	0.1140	1.0905	1.0397		0.1366	1.0790	1.0358
	0.1111	1.1033	1.0440		0.1338	1.0933	1.0409
	0.1108	1.1134	1.0478		0.1330	1.1064	1.0453
	0.1121	1.1038	1.0441		0.1376	1.0852	1.0379
	0.1158	1.1041	1.0441		0.1415	1.0830	1.0370
Mean	0.1126	1.1116	1.0470	Mean	0.1362	1.1005	1.0435
Reading No.	v m/s	α	β	Reading No.	v m/s	α	β
21	0.1021	1.1237	1.0506	23	0.1220	1.1324	1.0552
	0.1018	1.0834	1.0378		0.1247	1.0853	1.0383
	0.0987	1.0941	1.0415		0.1227	1.0915	1.0403
	0.0984	1.1163	1.0492		0.1234	1.1056	1.0454
	0.0978	1.1286	1.0535		0.1215	1.1281	1.0530
	0.0980	1.1561	1.0623		0.1238	1.1285	1.0530
Mean	0.0995	1.1170	1.0492	Mean	0.1230	1.1119	1.0475
Reading No.	v m/s	α	β	Reading No.	v m/s	α	β
25	0.1546	1.1087	1.0467	27	0.1718	1.1153	1.0485
	0.1600	1.0756	1.0350		0.1760	1.0776	1.0354
	0.1579	1.0784	1.0358		0.1737	1.0743	1.0344
	0.1557	1.0931	1.0407		0.1739	1.0758	1.0348
	0.1556	1.1038	1.0443		0.1724	1.0909	1.0400
	0.1537	1.1543	1.0613		0.1720	1.1203	1.0496
Mean	0.1563	1.1023	1.0440	Mean	0.1733	1.0924	1.0405

FIG. 6.7 VELOCITY ENERGY AND MOMENTUM COEFFICIENTS.

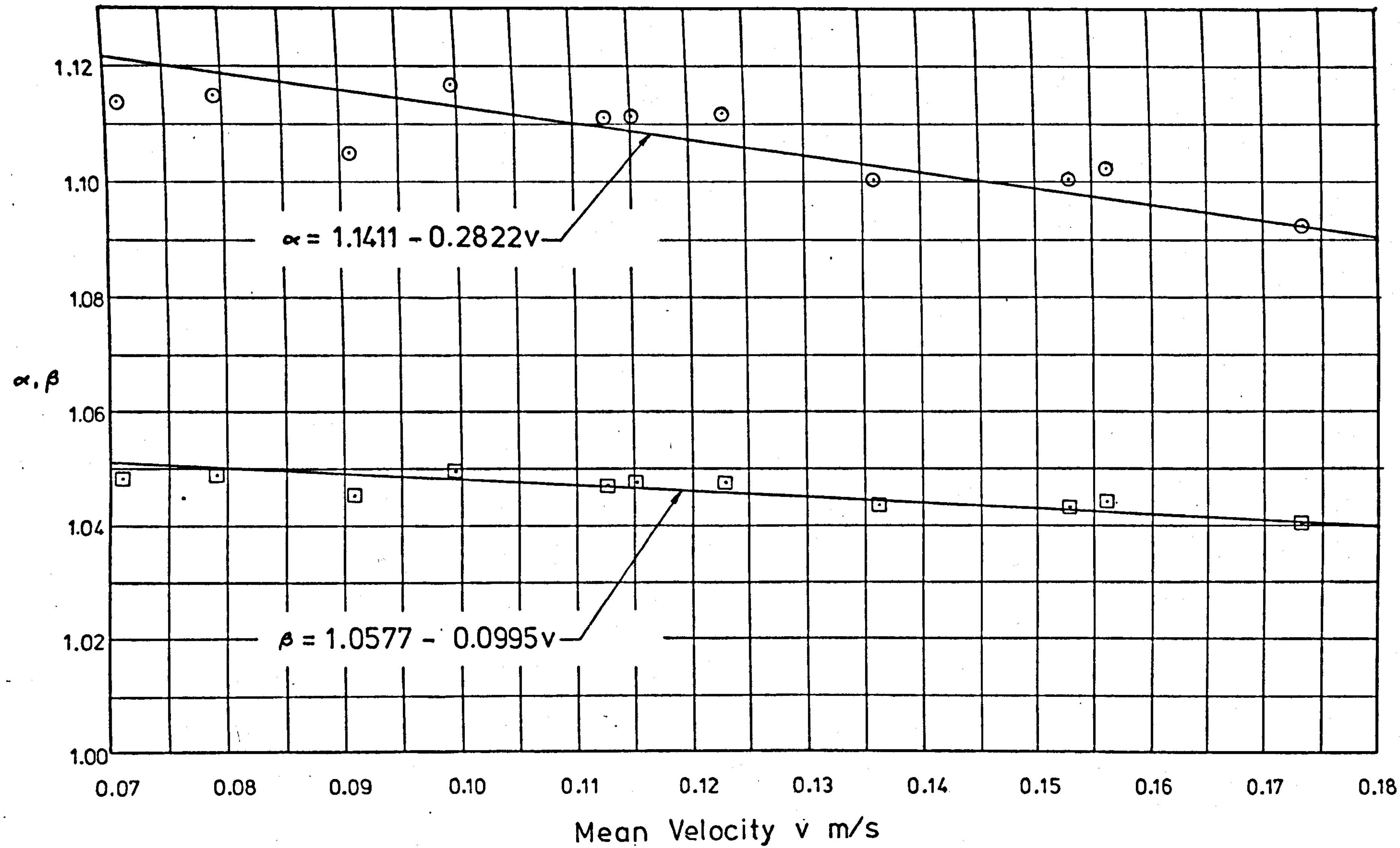

6.3 A Qualitative Discussion of Side Weir Flow

6.3.1 Using the apparatus described in Chapter 5 it was possible to produce all the five flow cases identified by Frazer[15] and described in section 2.1, although it was not possible to achieve all the flow cases on each weir independently. The full range of conditions achieved is shown in Figures 6.8 to 6.37.

6.3.2 Figures 6.8 to 6.12 show Weir I (whose dimensions are given in Table 5.1) with the downstream sluice gate lowered and controlling the flow. The discharge progressively increases from Figure 6.8, which shows the first spill condition for a Case II subcritical profile, to Figure 6.11 where the upstream flow has been sufficiently drawn down to form supercritical flow along the upstream section of the weir, with an undular hydraulic jump forming on the weir (Case III).

6.3.3 A further increase in the flow rate produced a broken jump on the weir (Figure 6.12). Although Case III (and Case V) profiles were observed during the tests readings were not taken when a hydraulic jump formed on the weir as this condition was beyond the scope of the current investigation.

6.3.4 Similar results were obtained when the transverse weir was used instead of the sluice gate as the downstream control. With the downstream control removed a supercritical flow profile formed (Case I) (Figure 6.13).

6.3.5 Figures 6.14 to 6.18 show a similar set of conditions occurring on Weir 2, but because of the increased crest height the subcritical profiles existed up to a much greater discharge. Also, when the downstream control was removed it was only just possible to produce a falling supercritical profile at the maximum channel discharge (Fig. 6.18). Figures 6.17 and 6.18 clearly show the importance of a downstream throttle. In both cases the upstream discharge is about the same, but in the former case the downstream flow is throttled by the sluice gate which substantially increases the discharge over the weir.

6.3.6 With the lower crest height of Weir 3, however, it was only possible to produce a subcritical profile at low discharges, and with a severe downstream throttle (Fig. 6.19). Any significant increase in the flow lead to a hydraulic jump forming on the weir (Figs. 6.20 to 6.22) and quite strong jumps could be achieved. The stronger jumps were observed to be unstable and oscillated up and down the weir by up to 0.3m. Although moving the sluice gate further downstream tended to reduce the magnitude of the oscillations the effect could not be entirely eliminated.

Fig. 6.23 shows the same upstream conditions as Fig. 6.22, but with the downstream throttle removed, forming a supercritical flow profile. Again the side spill discharge is reduced but the effect is not as dramatic as with Weir 2.

6.3.7 The effect of changing the length of the weir is shown in Figs. 6.25 to 6.30 with Weir 4, a shorter version of Weir 1, and in Figs. 6.31 to 6.36 with Weir 5, a longer version of Weir 1. In each case the flow profiles follow the same pattern as the Weir 1 profiles, but with shorter Weir 4 a greater range of subcritical profiles is possible, whereas with Weir 5 the range is reduced.

6.3.8 The effect of changing the weir length is clearly less significant than varying the crest height, and this conclusion is supported by the discharge characteristics and depth-discharge relationships discussed in section 6.4.

6.3.9 Finally the effect of lowering the upstream sluice gate was observed on Weir 3. This produced supercritical flow both along the weir and in the upstream channel (Case IV). The longitudinal velocities along the weir increased and the upstream depth and side spill discharge decreased (Figs. 6.37 and 6.38).

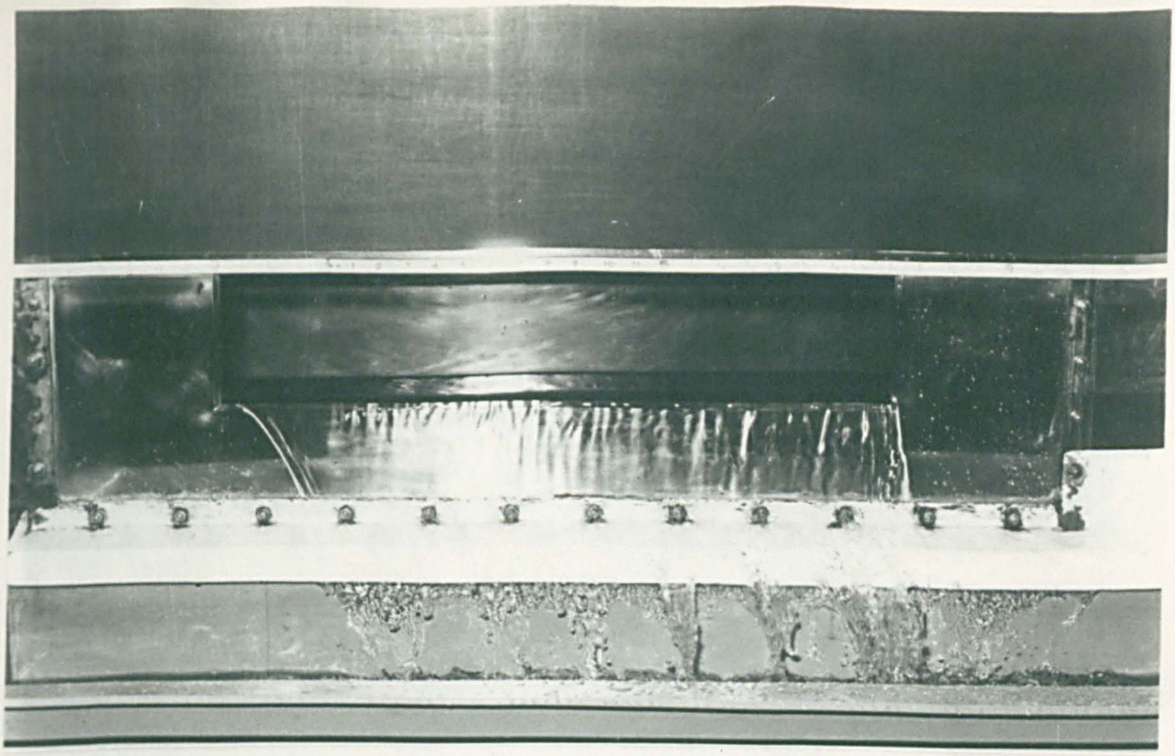

fig. 6.8 Weir 1, First Spill, Case II Flow, Clinging Nappe.

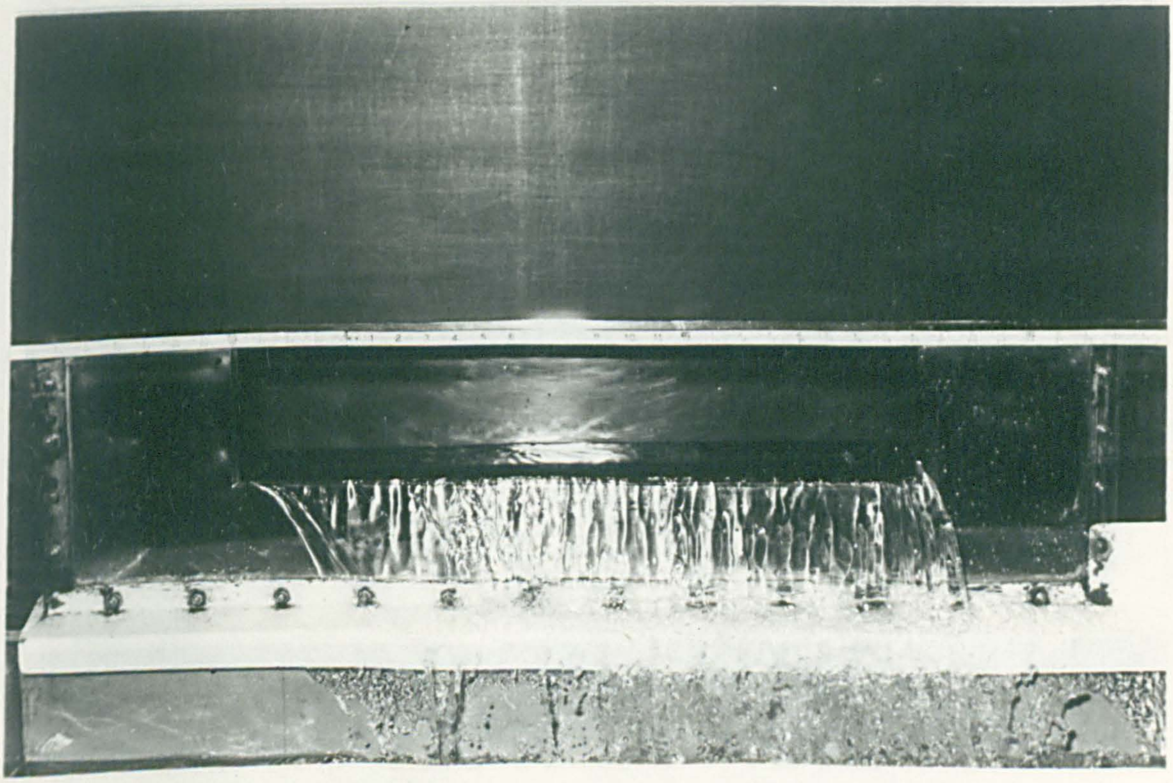

fig. 6.9 Weir 1, Low Flow Case II, Free Nappe.

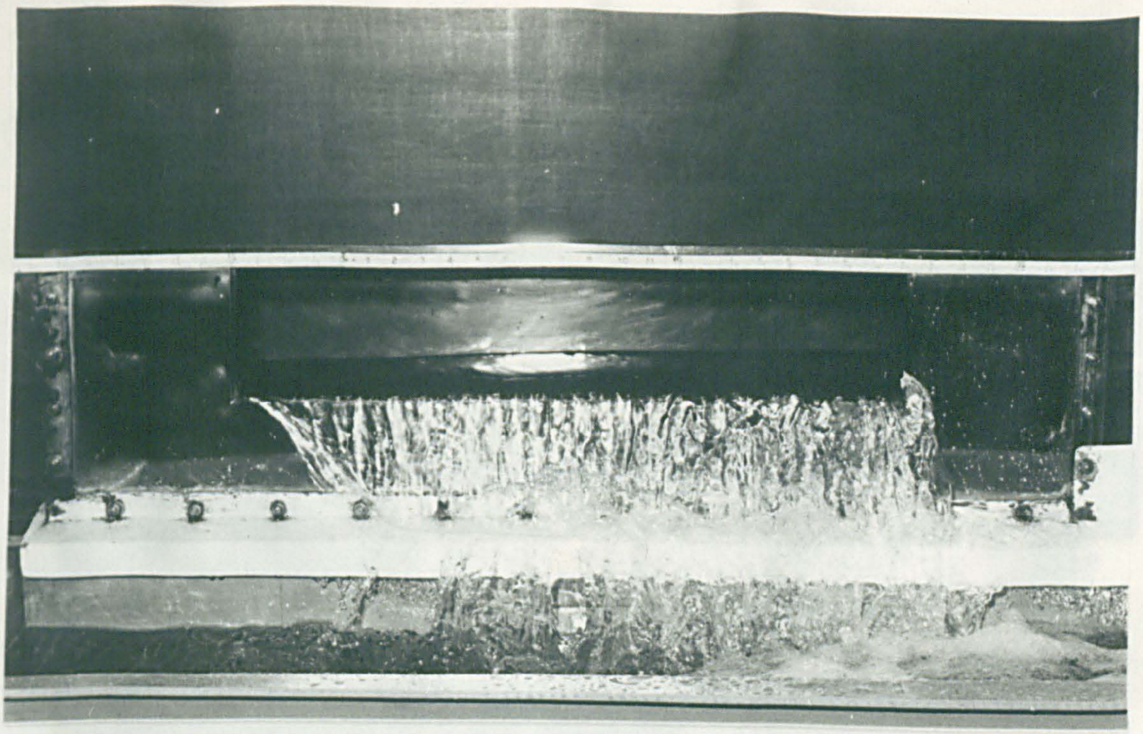

fig. 6.10 Weir 1, Intermediate Flow, Case II.

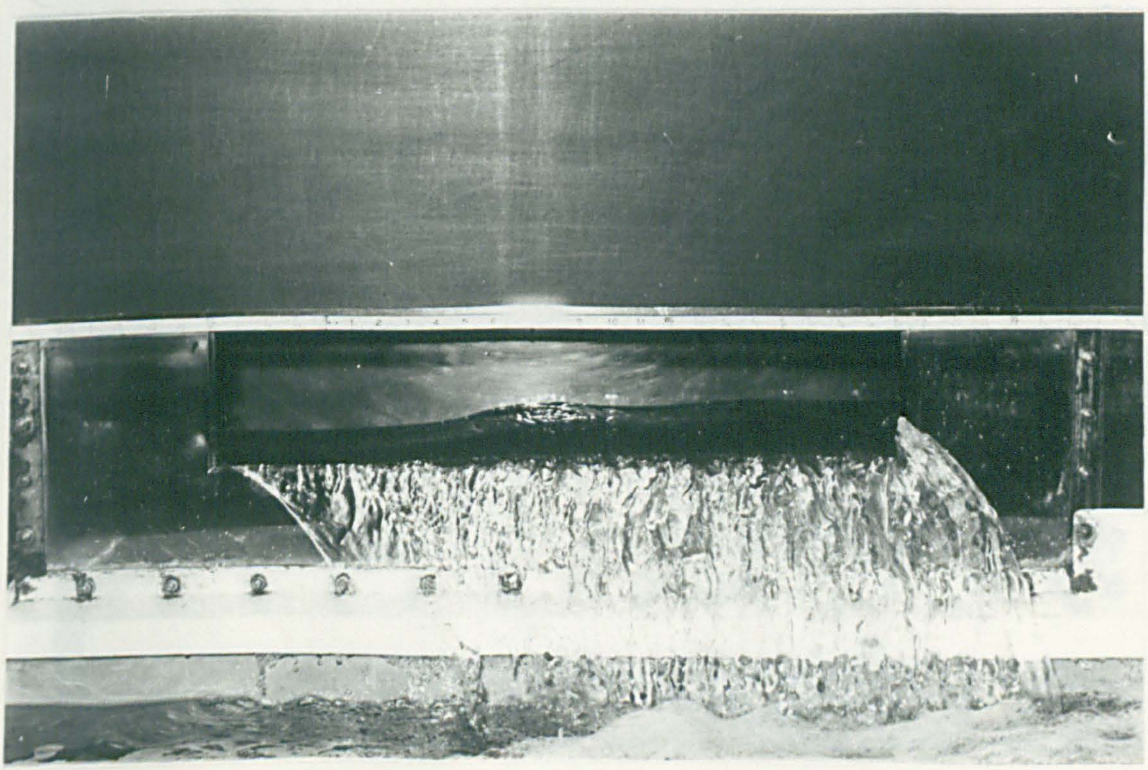

fig. 6.11 Weir 1, Undular Jump, Case III.

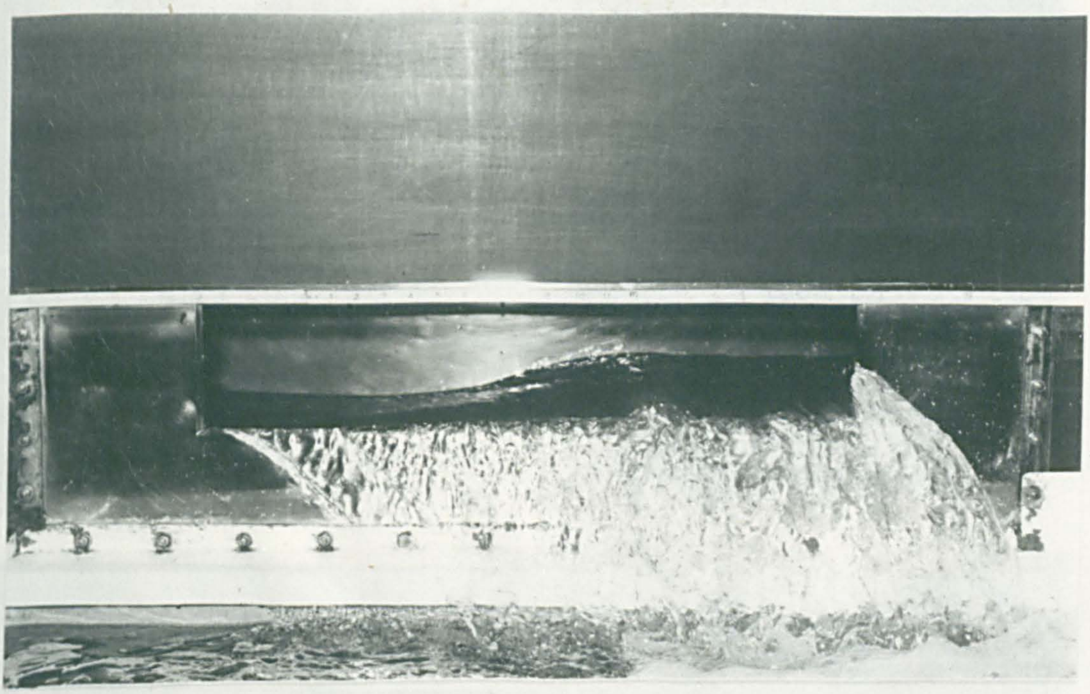

fig. 6.12 Weir 1, Broken Jump, Case III.

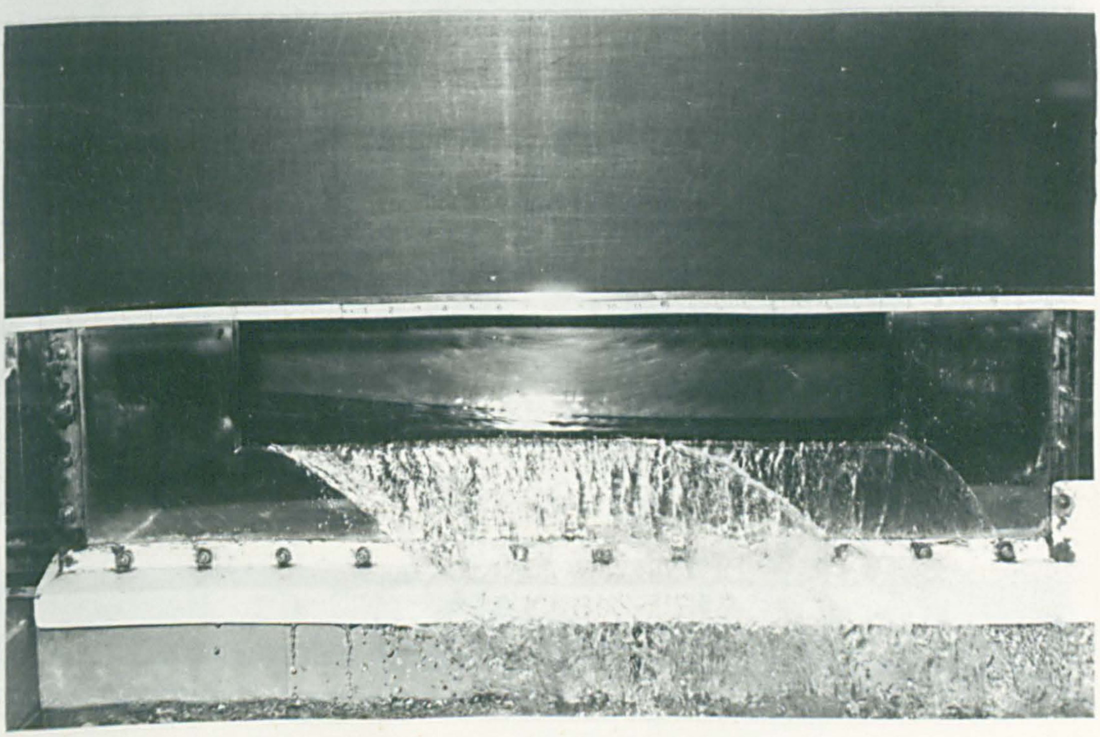

fig. 6.13 Weir 1, Case I Flow.

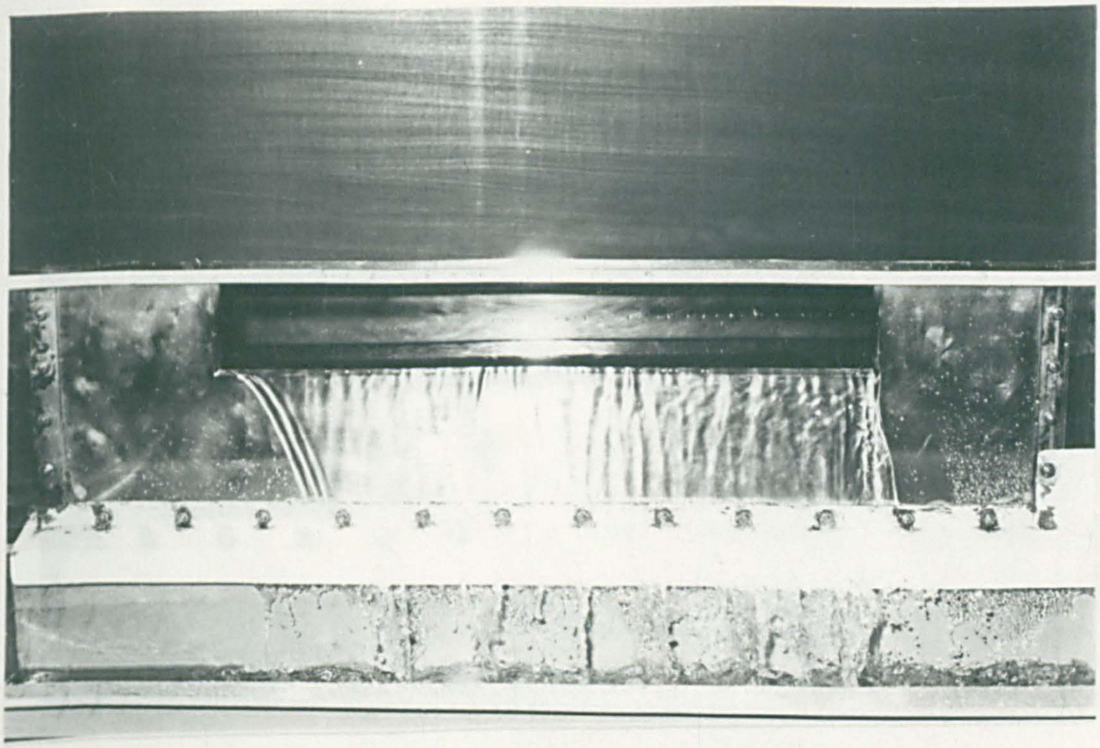

fig. 6.14 Weir 2, First Spill, Case II Flow, Clinging Nappe.

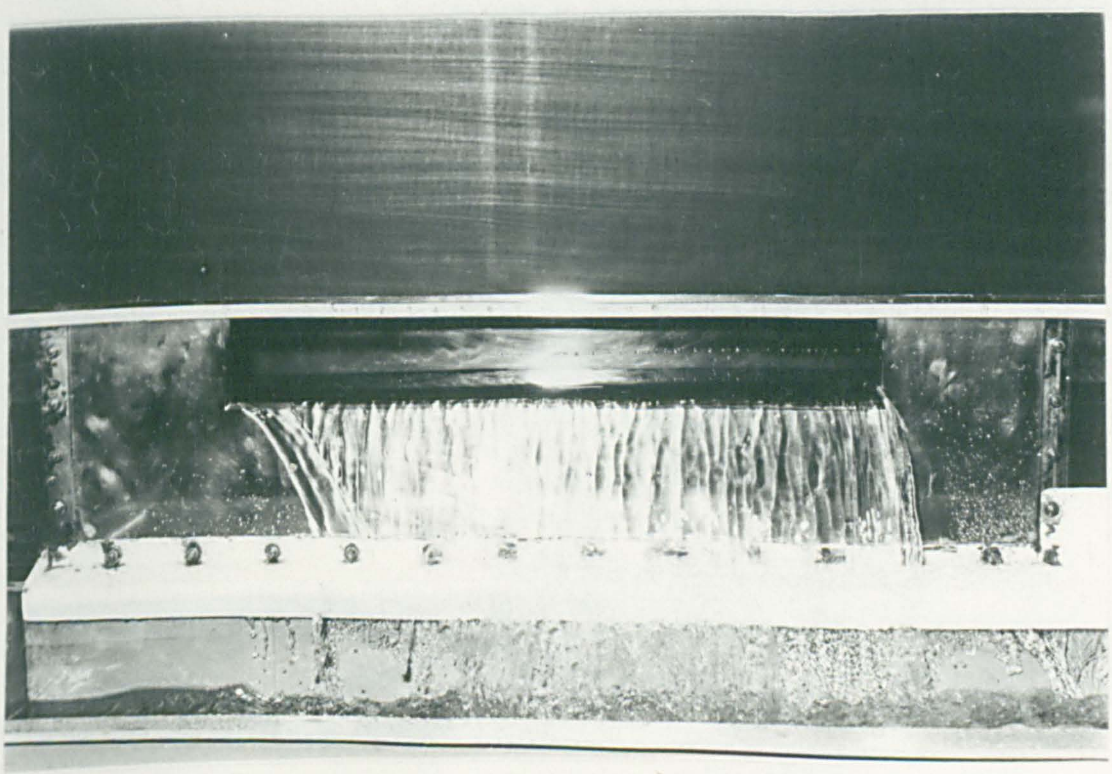

fig. 6.15 Weir 2, Intermediate Flow Case II.

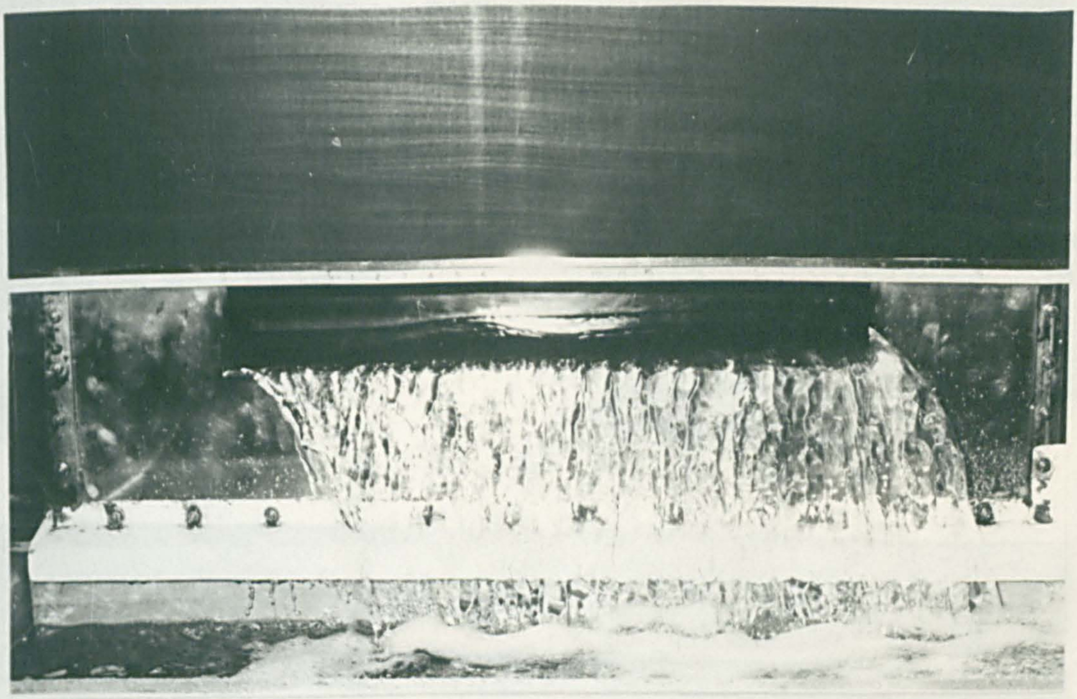

fig. 6.16 Weir 2, High Flow Case II.

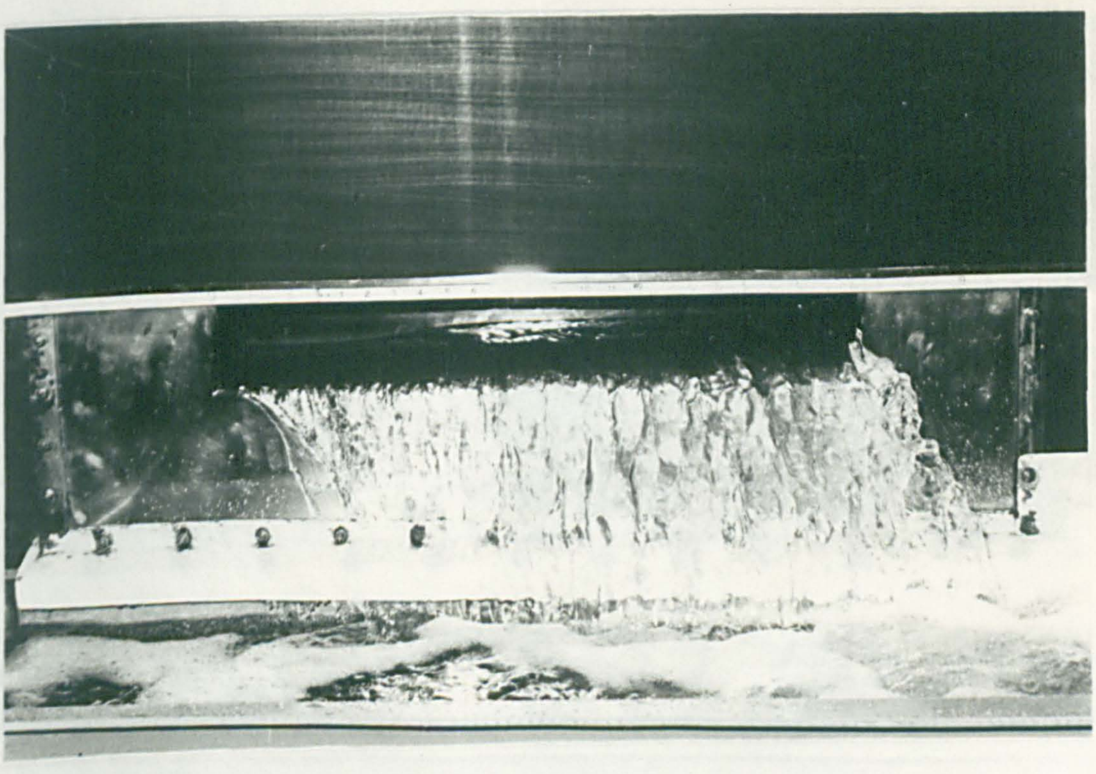

fig. 6.17 Weir 2, Maximum Flow Case II.

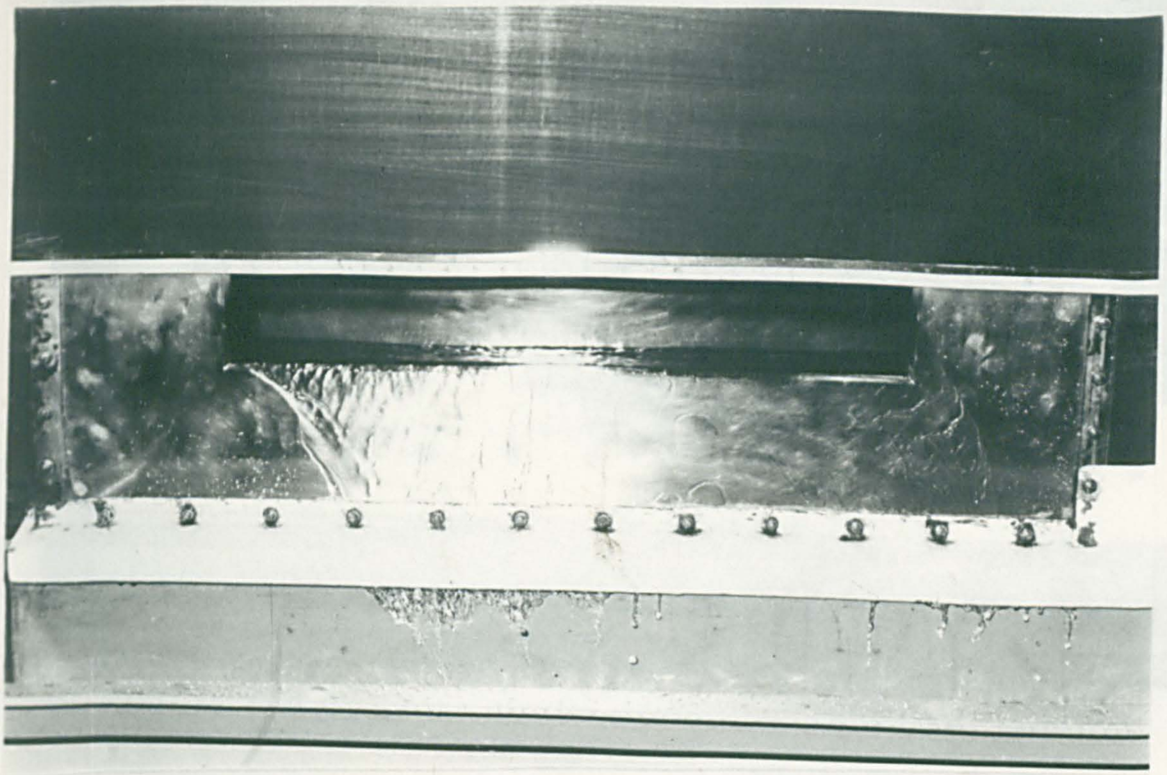

fig. 6.18 Weir 2, Maximum Flow Case I

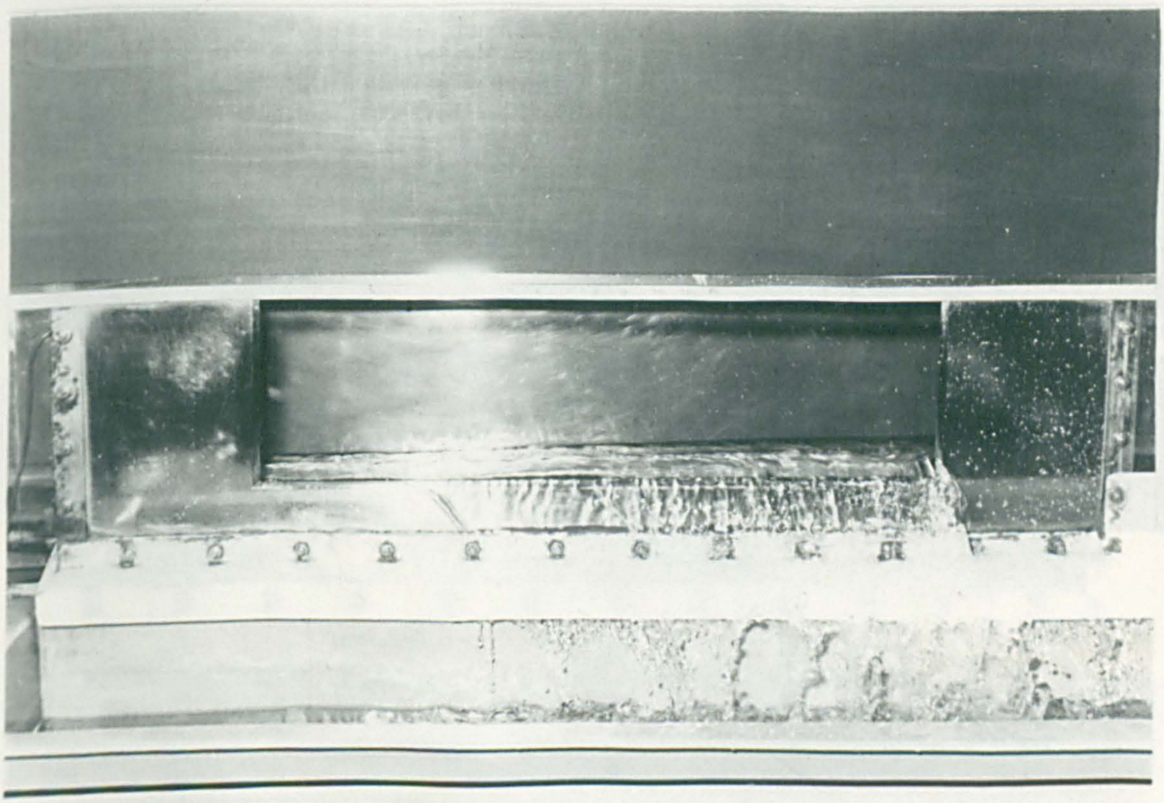

fig. 6.19 Weir 3, Case II Flow with Severe Downstream Throttle (part of nappe clinging)

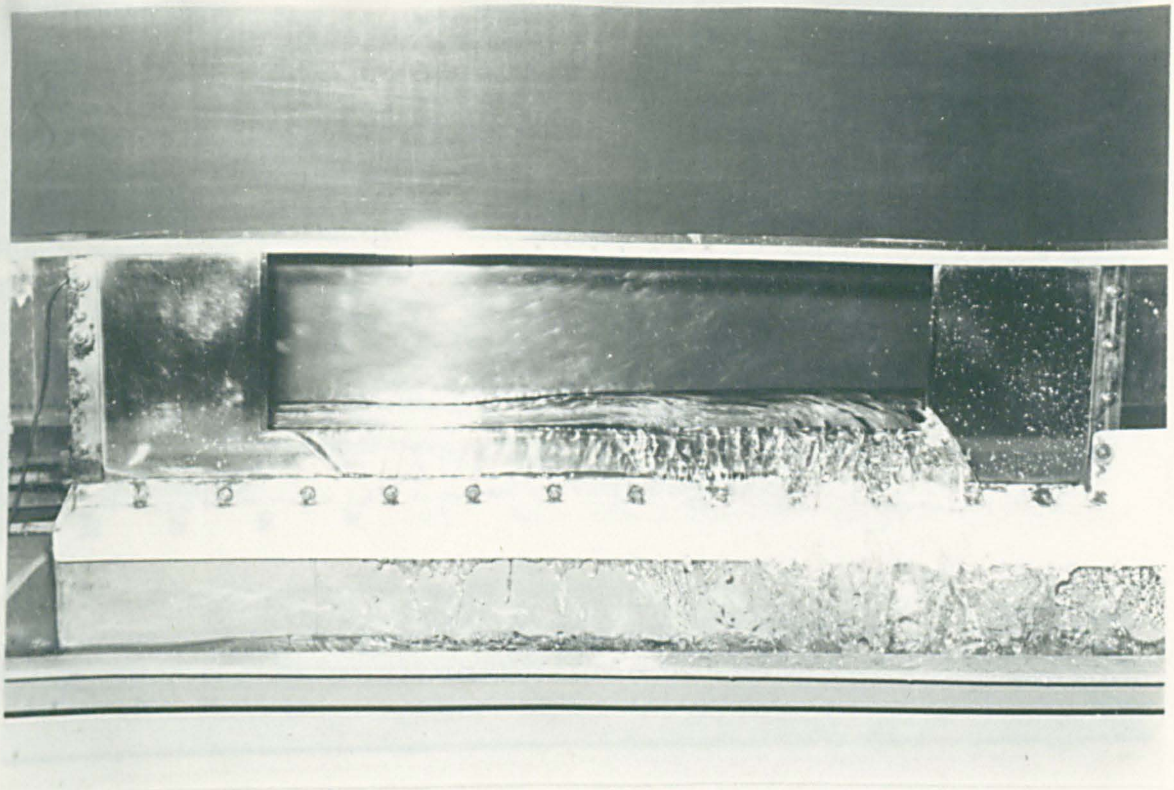

fig. 6.20 Weir 3, Weak Jump Forming, Case III.

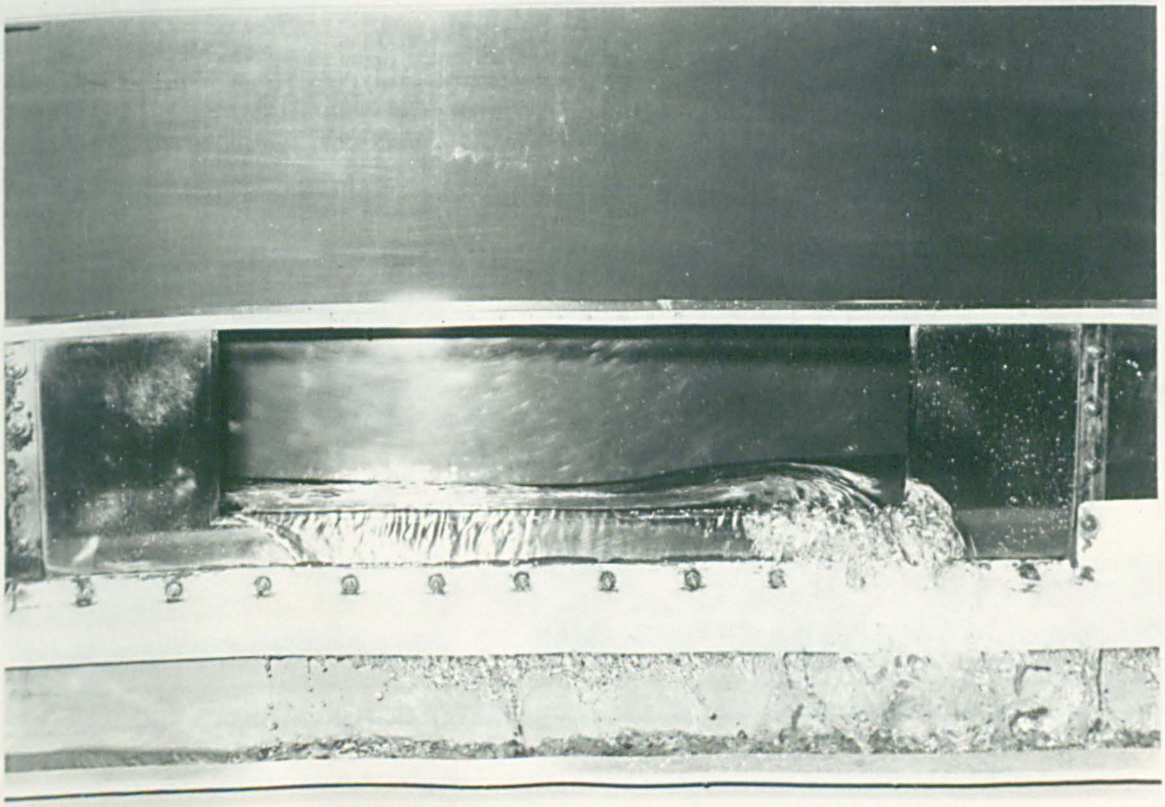

fig. 6.21 Weir 3, Increased Flow, Stronger Jump Case III.

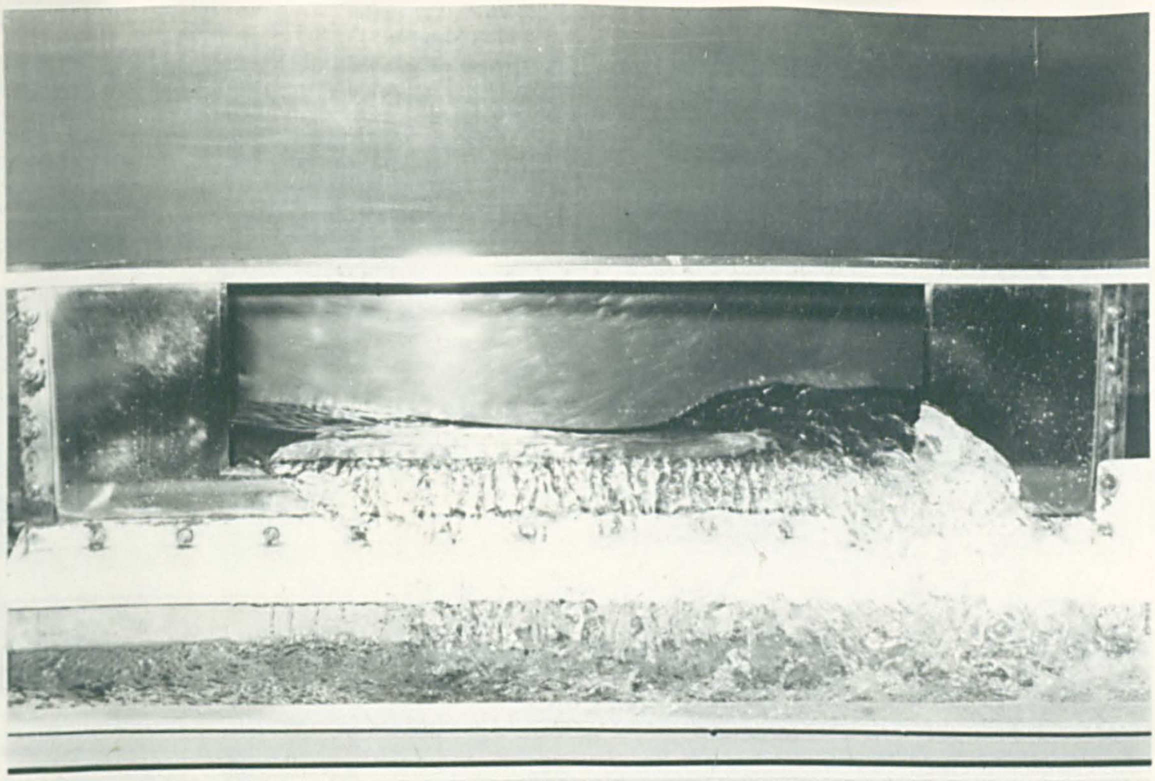

fig. 6.22 Weir 3, Strong Broken Jump, Case III (some instability)

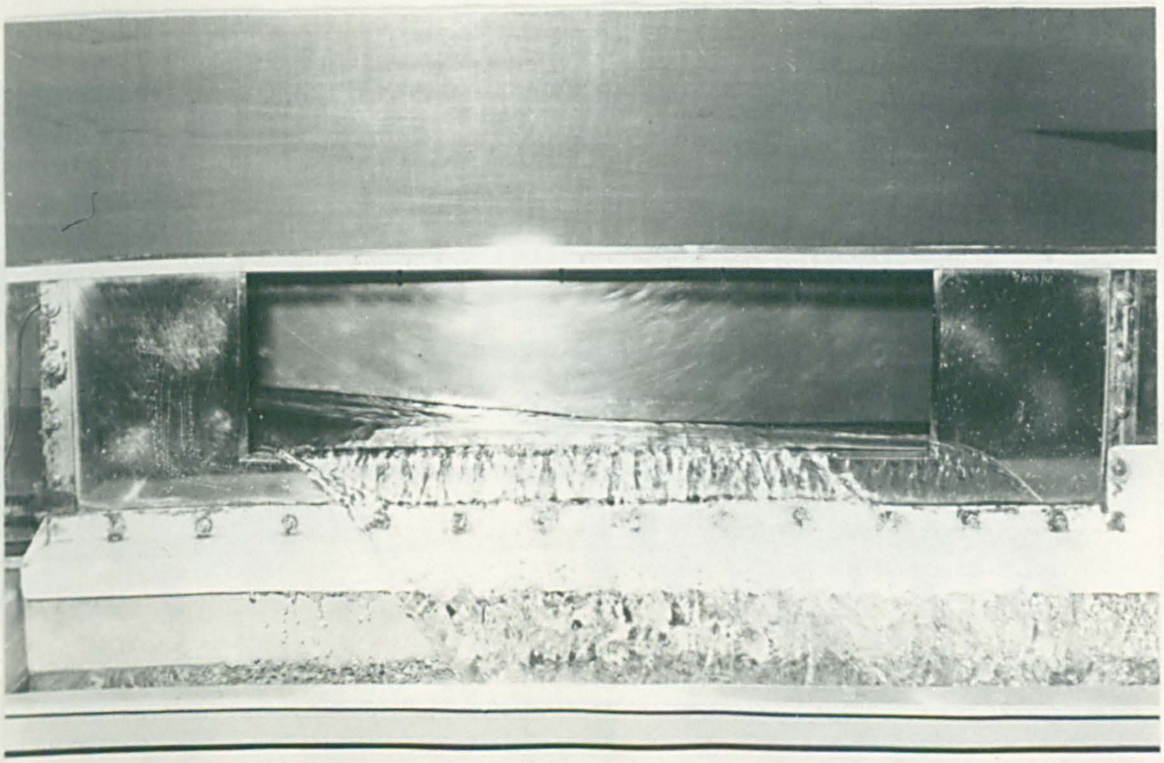

fig. 6.23 Weir 3, as fig. 6.22 but with downstream throttle removed, Case I.

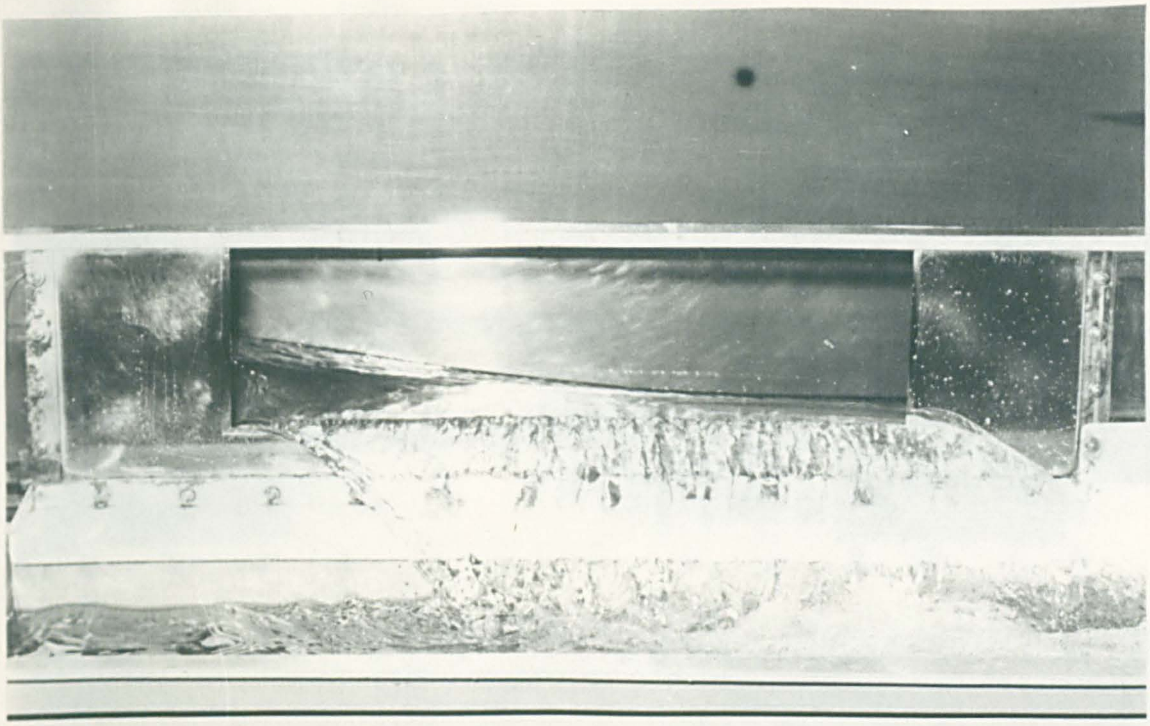

fig. 6.24 Weir 3, High Flow Case I.

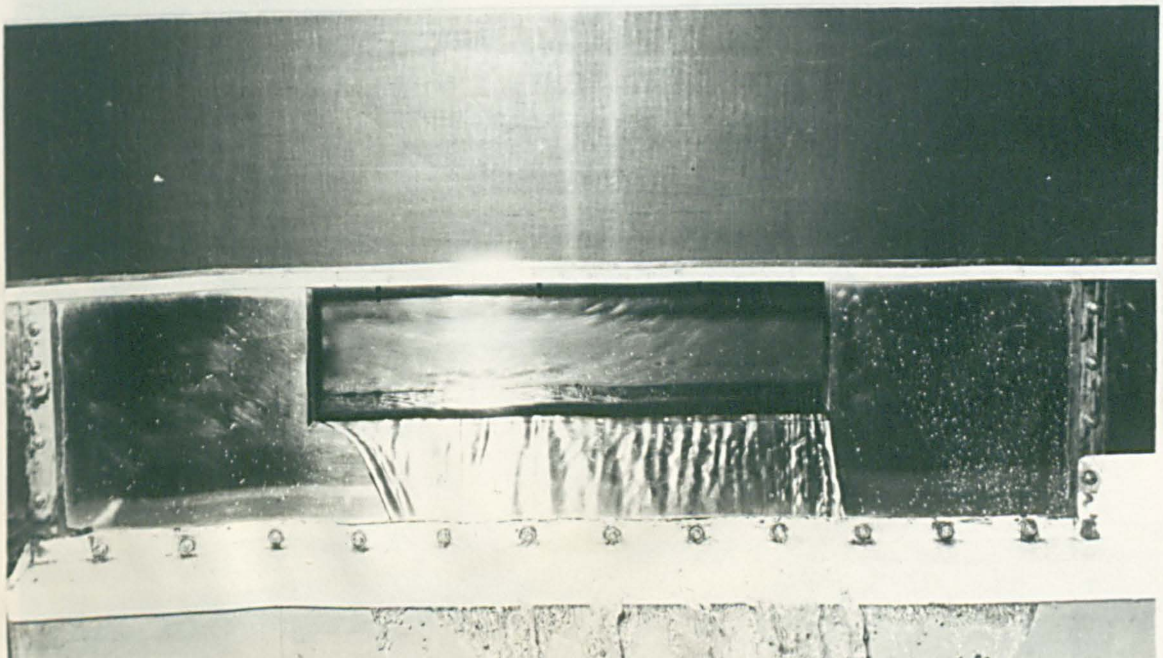

fig. 6.25 Weir 4, Low Flow Case II.

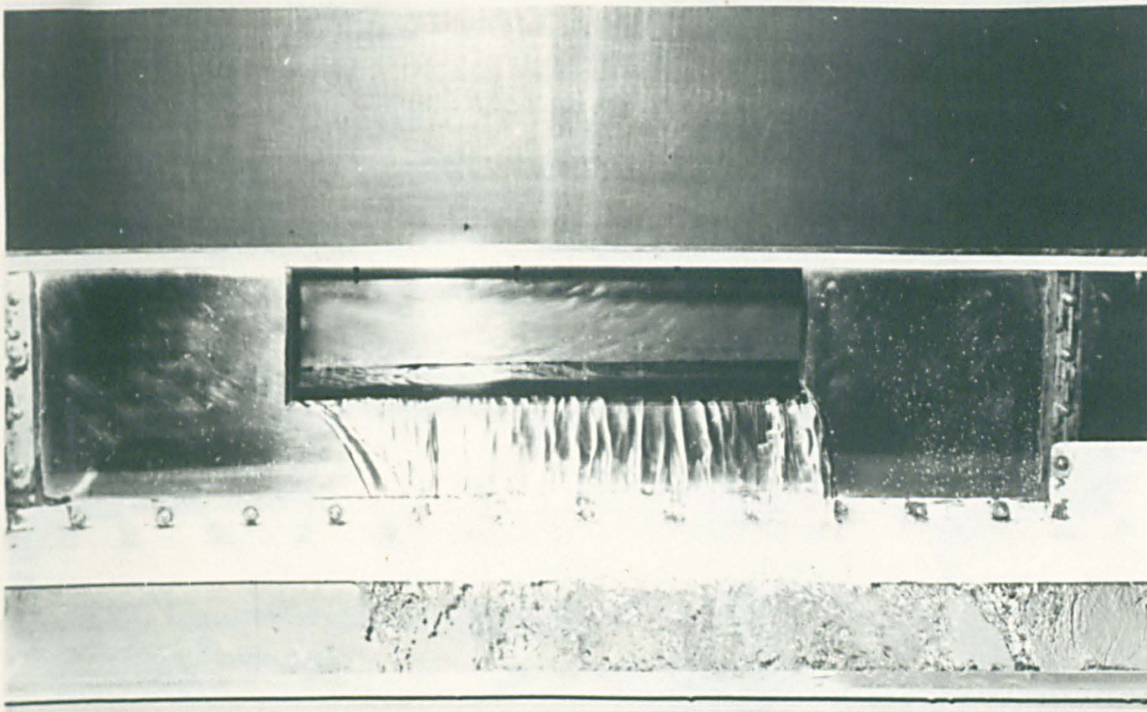

fig. 6.26 Weir 4, Intermediate Flow Case II.

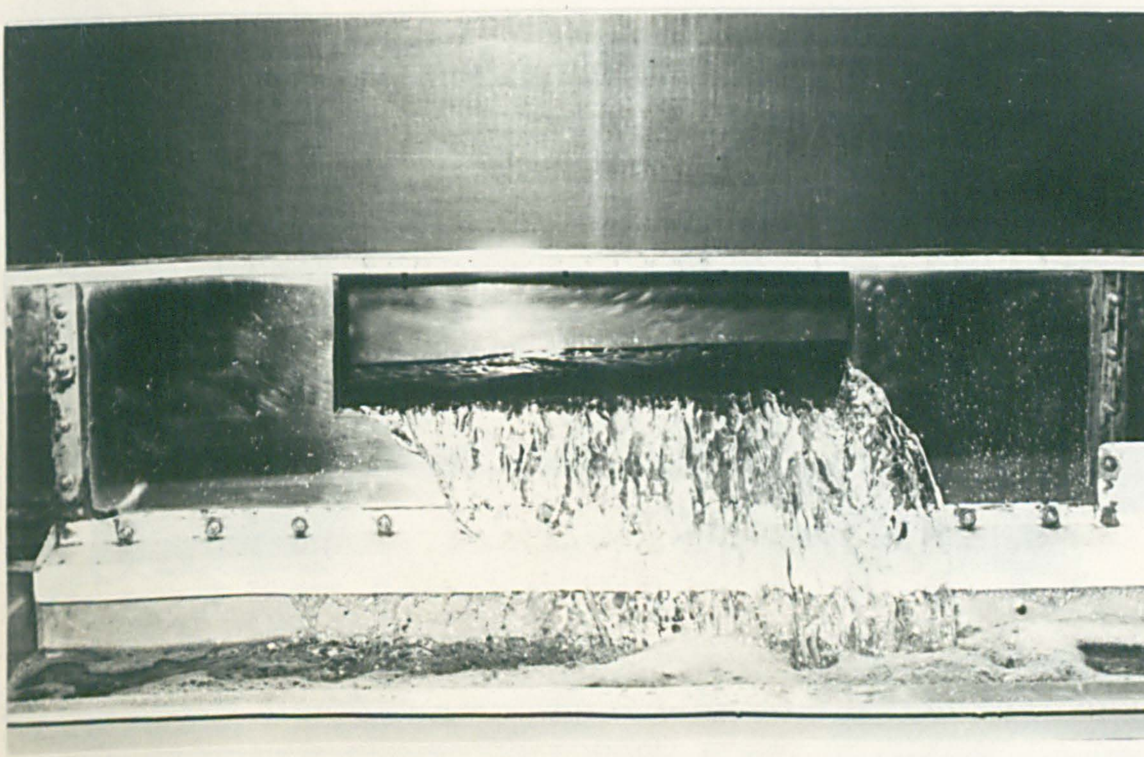

fig. 6.27 Weir 4, as fig. 6.26 but with increased flow, Case II.

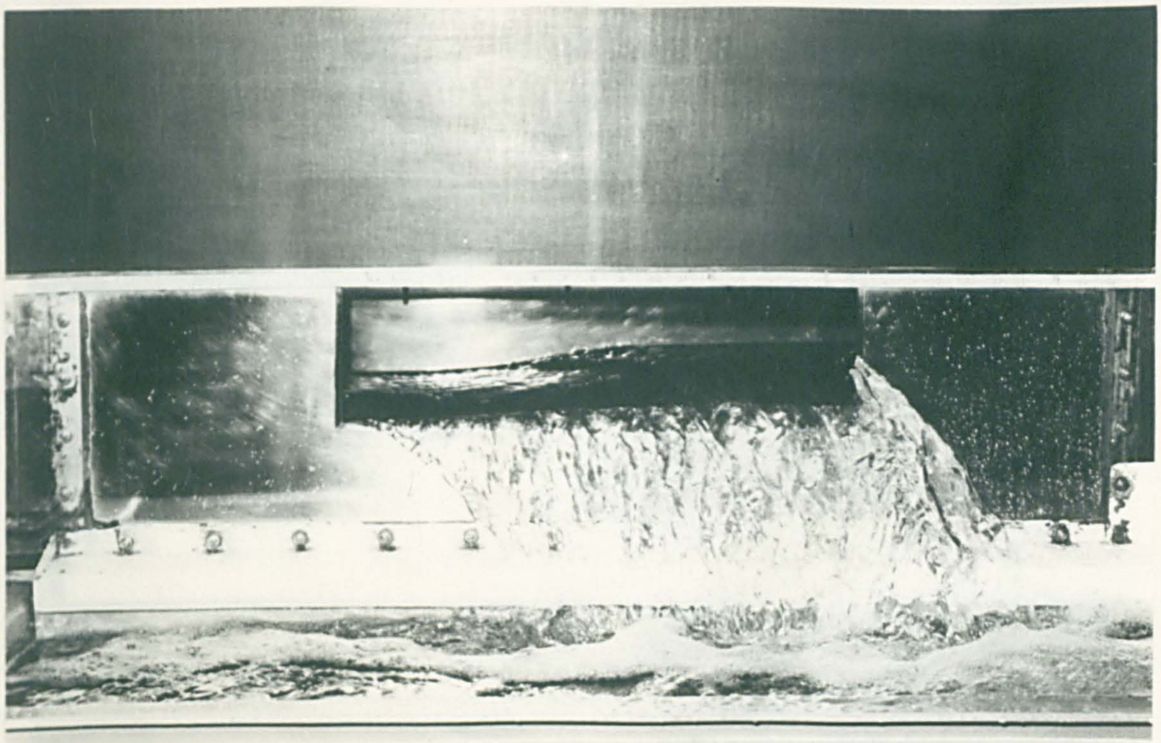

fig. 6.28 Weir 4, Broken Jump, Case III.

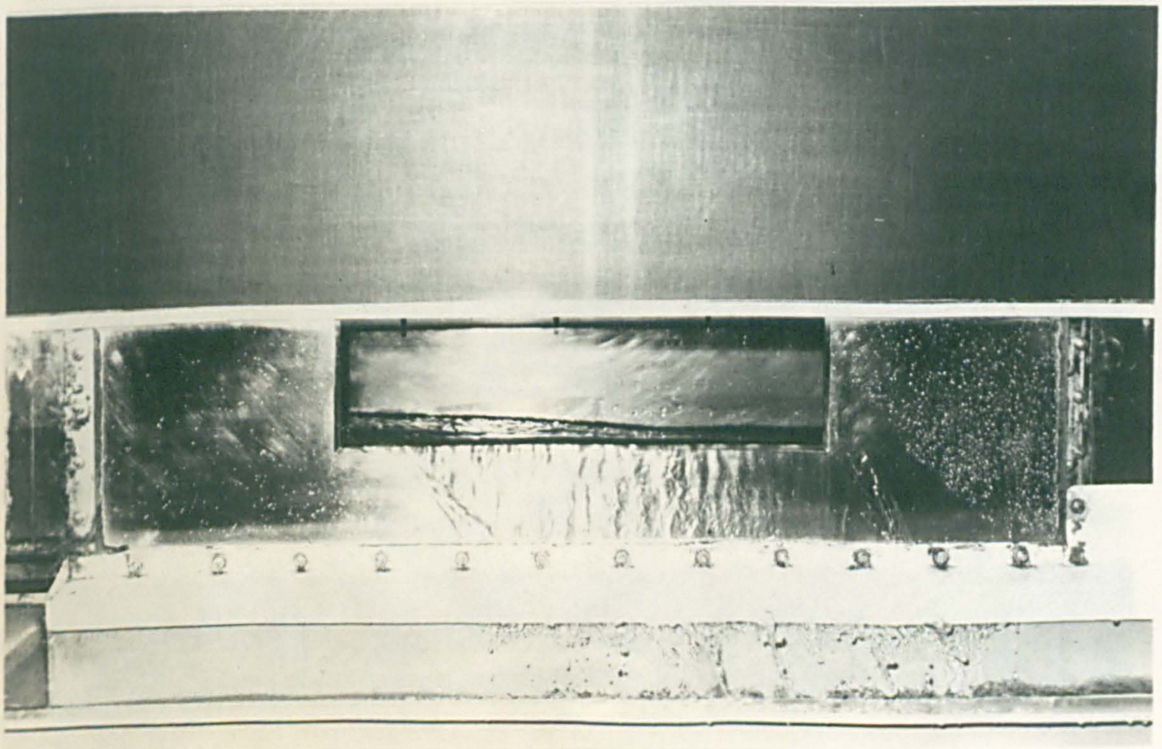

fig. 6.29 Weir4, Intermediate Flow CaseI

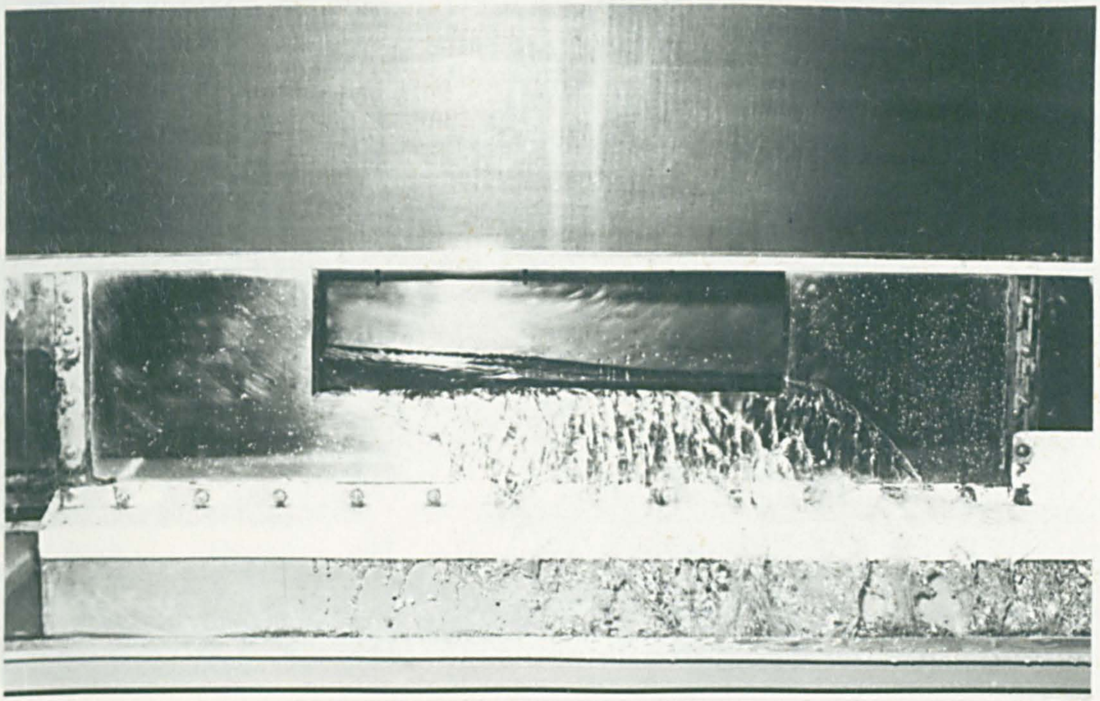

fig. 6.30 Weir 4, High Flow Case I

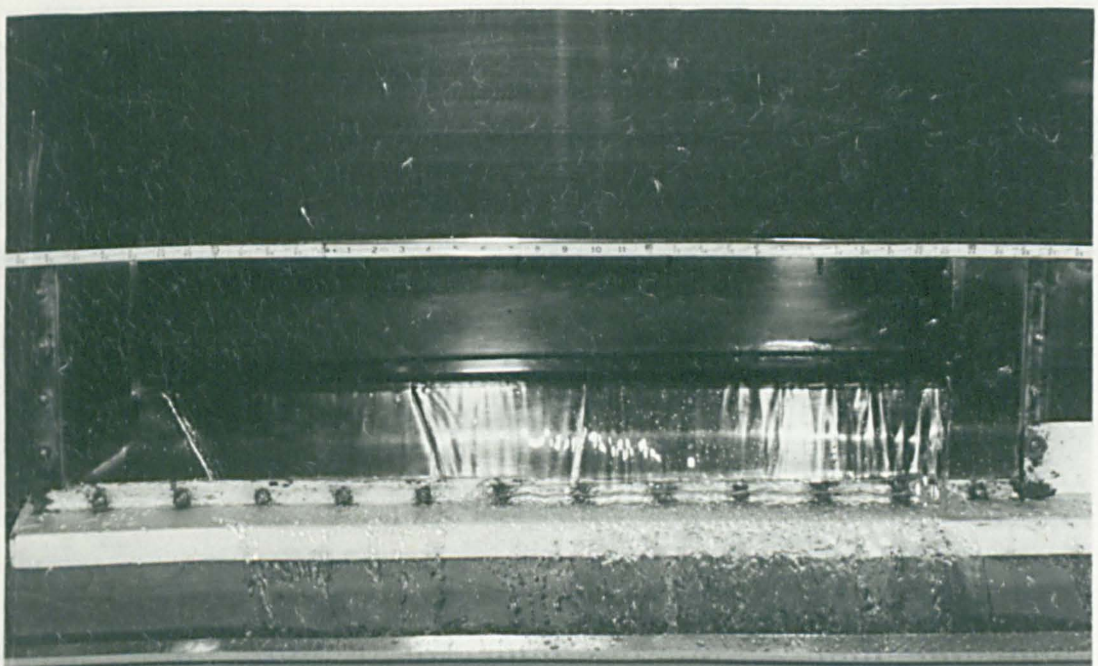

fig. 6.31 Weir 5, Low Flow Case II.

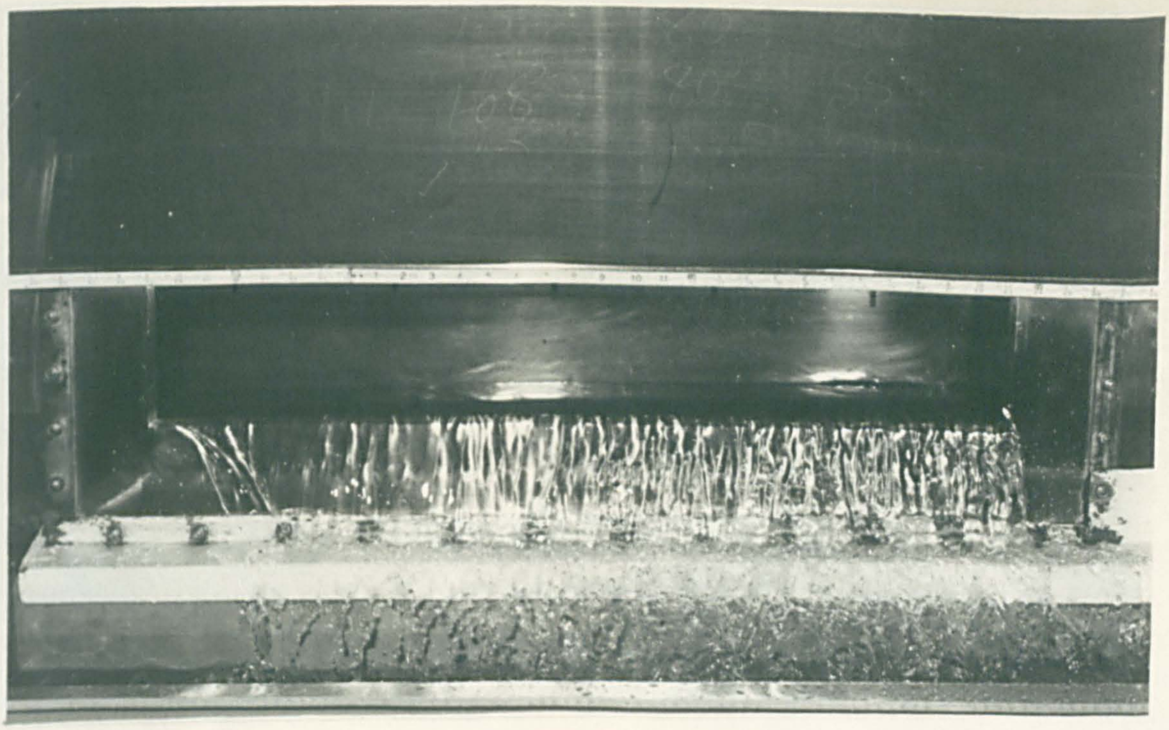

fig.6.32 Weir 5, Intermediate Flow Case II

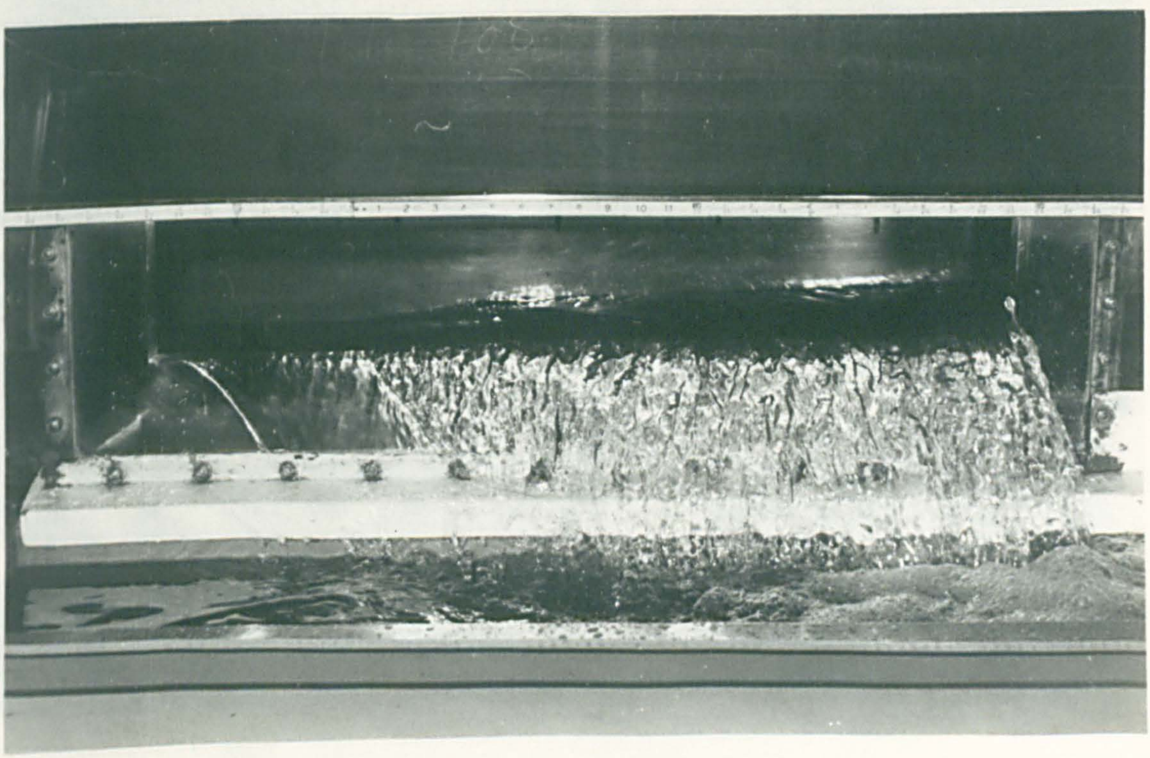

fig.6.33 Weir 5, High Flow Case II.

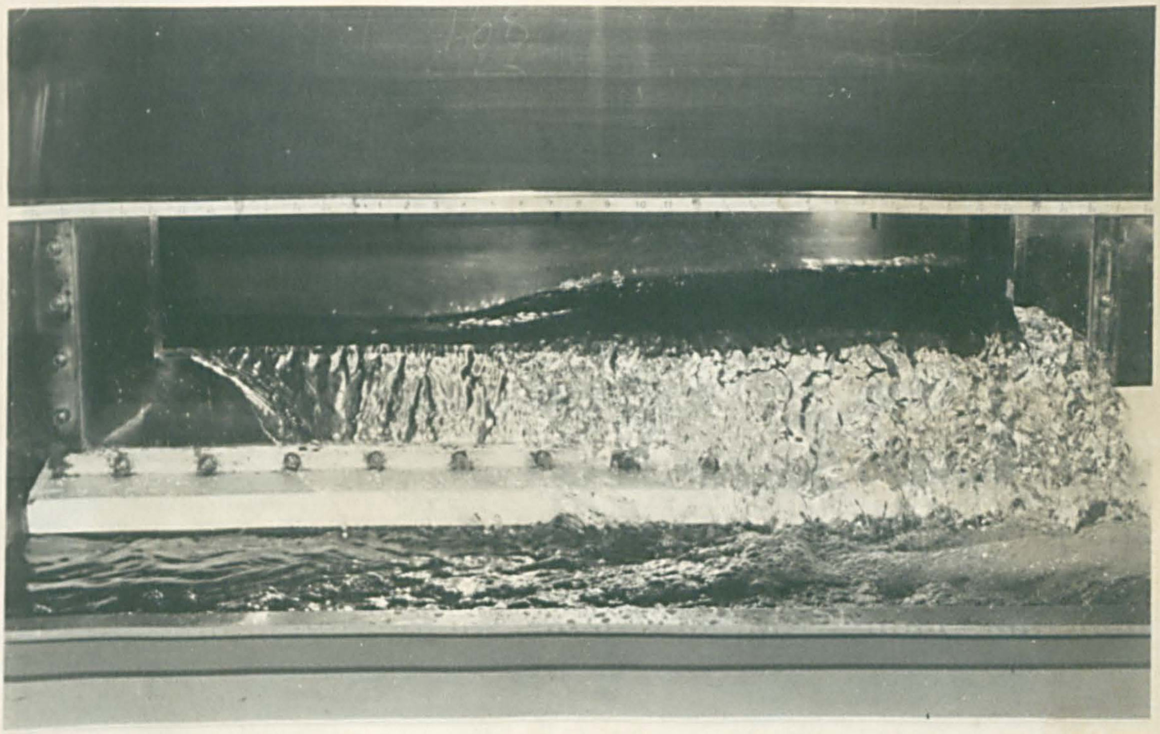

fig. 6.34 Weir 5, Broken Jump, Case III.

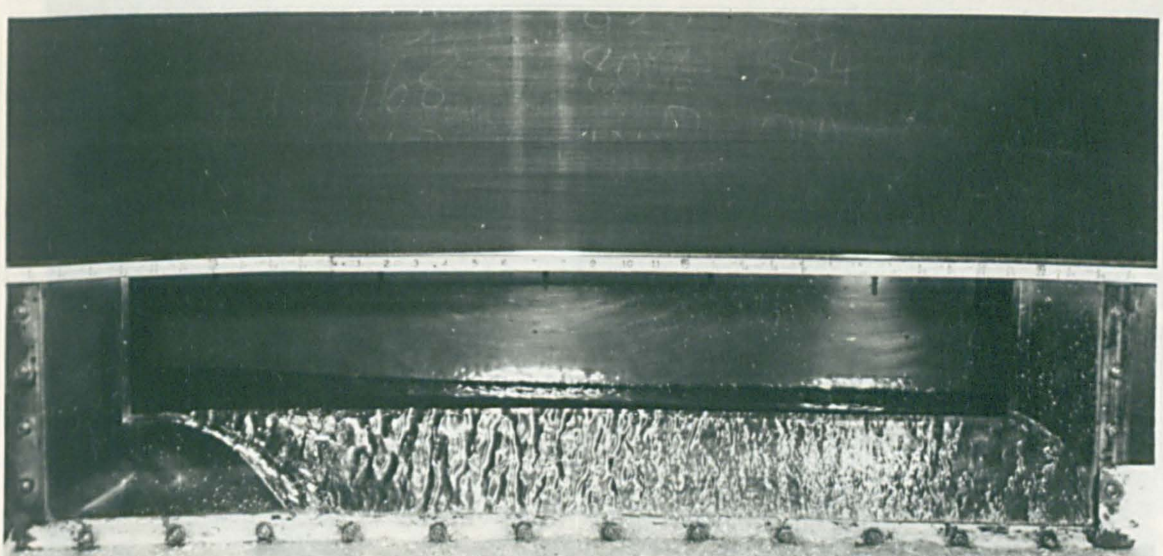

fig. 6.35 Weir 5, Intermediate Flow Case I.

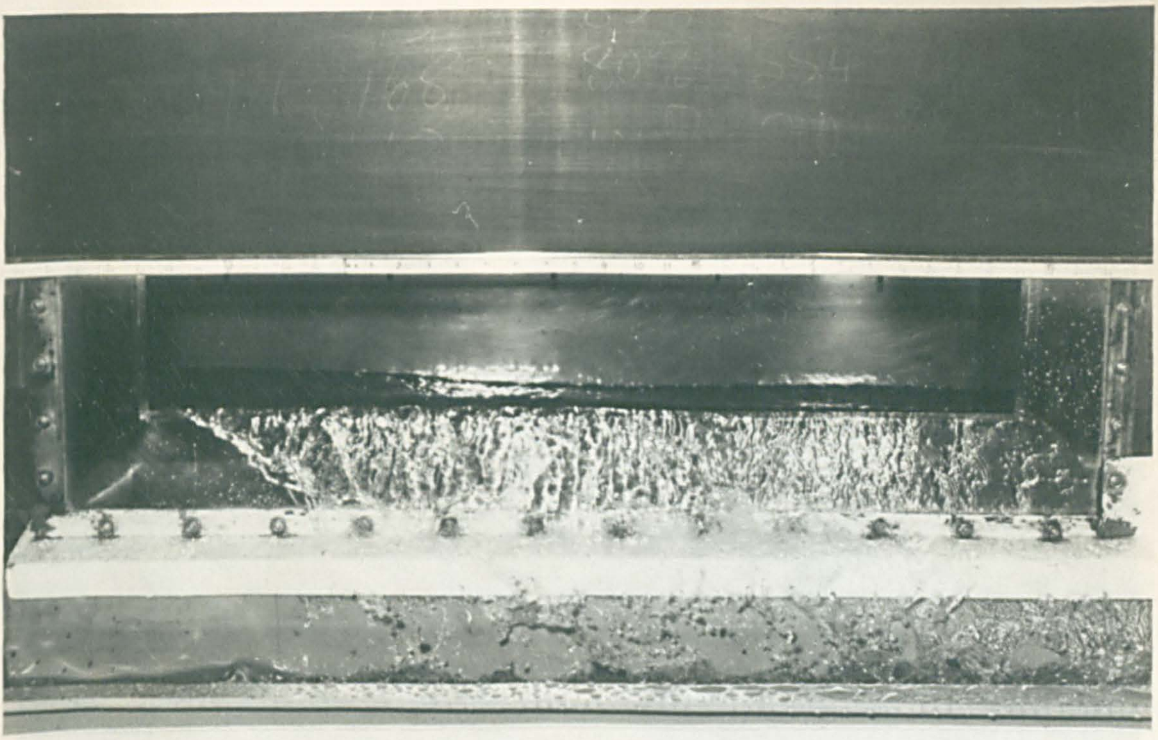

fig. 6.36 Weir5, High Flow, Case I.

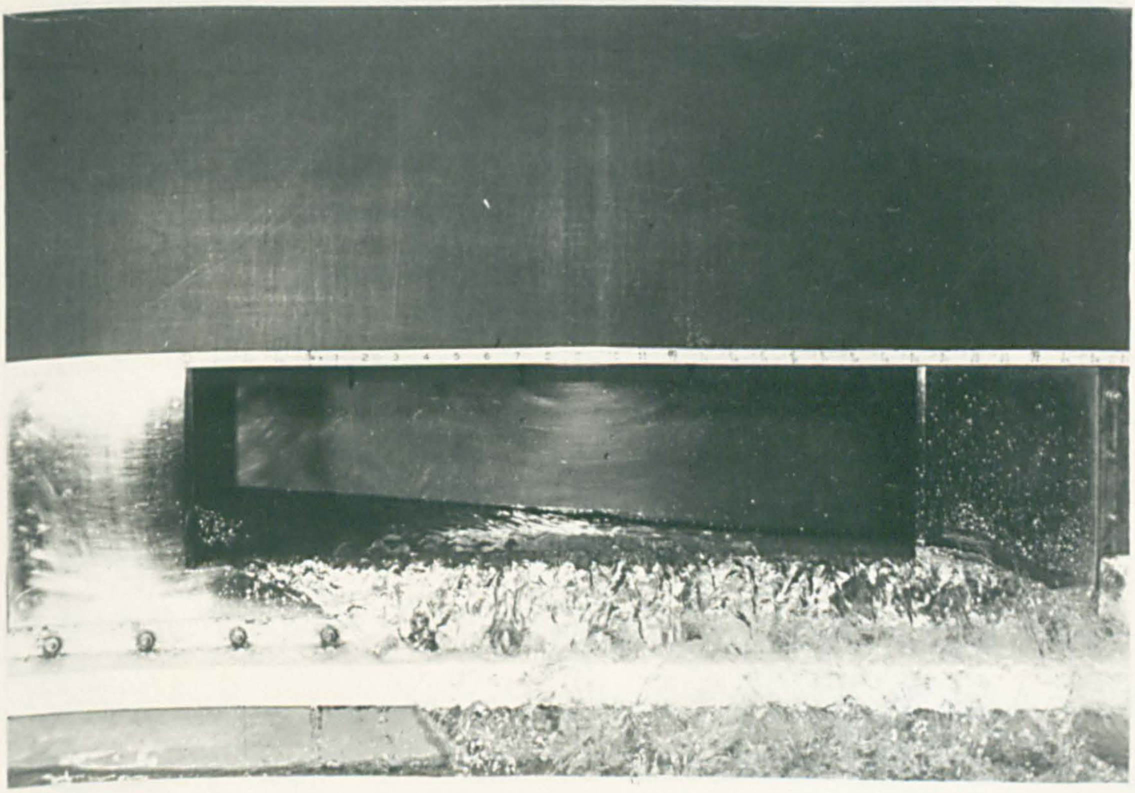

fig. 6.37 Weir 3, High Flow Case IV, (upstream sluice gate controlling flow)

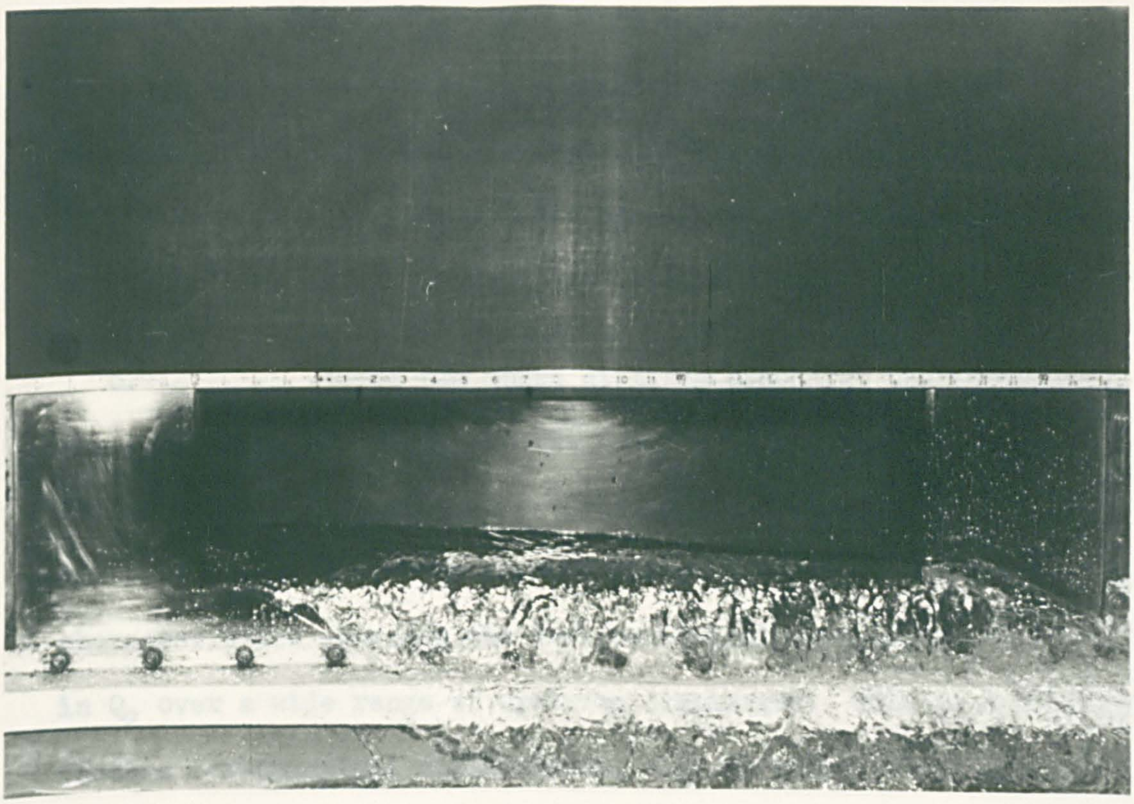

fig. 6.38 Weir 3, as fig. 6.37 but with the upstream sluice gate set lower, Case IV.

6.4 A Quantitative Discussion of Side Weir Flow

6.4.1 The hydraulic performance of the side weirs tested is shown graphically in Figures 6.39 to 6.55. The former half, Figs. 6.39 to 6.46, show the discharge characteristics whilst the remainder show the relationship between the depths at the upstream and downstream ends of the weir and the upstream discharge. The experimental data used in plotting these graphs is included in Appendix VII.

6.4.2 There are three distinct discharge characteristics that can be identified. With subcritical flow along the weir, controlled by the downstream sluice gate (Figs. 6.39, 6.40 and 6.42 to 6.45), the discharge characteristics form a family of straight lines. The Q_2/Q_1 characteristics approach the horizontal indicating only small changes in Q_2 over a wide range of upstream discharges. This is a desirable feature for practical applications, e.g. as storm sewage overflows, and similar results would be obtained with an orifice plate or throttle pipe as the downstream control.

6.4.3 When the sluice gate is replaced by a transverse weir, however, the discharge characteristics become curved (Fig. 6.41) and in this case pass through the origin as the transverse weir crest was set level with that of the side weir. Values of Q_2 at the upper end of the range increase significantly with increasing Q_1, with is generally undesirable.

6.4.4 For supercritical flow (Fig. 6.46) the characteristics are also straight but in this case the residual mainstream discharge Q_2 is greater than the side spill discharge Q_w in every case due to the higher longitudinal velocities and smaller depths resulting from the absence of the downstream throttle.

6.4.5 In every case the Q_w/Q_1 characteristic has been extrapolated to give the first spill discharge. Thus for Weir 1 with a horizontal bed and the downstream sluice gate open 19.1mm first spill occurs at 1.50 l/s (Fig. 6.39). The Q_2/Q_1 characteristics have also been extended to the first spill values, where $Q_2 = Q_1$. Below this point Q_2 is always equal to Q_1 and the characteristics form a 45° straight line. A further property of all the discharge characteristics is their symmetrical placing about the line $Q_w = \frac{1}{2}Q_1$.

6.4.6 The discharge characteristics clearly indicate the effects of variations in the bed slope, weir length, crest height, and downstream control. The latter has the most significant effect on both discharge over the weir and drawdown in the upstream channel for subcritical flow profiles. Reference to Figure 6.57 (the depth-discharge rating curve for the downstream sluice gate) shows that lowering of the sluice gate substantially increases the downstream depth. This leads to an increase in depth along the weir and, therefore, an increase in the side spill discharge. The shift in the characteristics in Figures 6.39 and 6.40 clearly reflects this. The effect is also shown in the depth-discharge relationships in Figures 6.48 and 6.49. Note that in the former the y_1/Q_1 curve tends to level off at the higher discharges so that any increase in Q_1 leads to a corresponding increase in v_1 and the Froude number rapidly increases until it exceeds one and supercritical flow occurs. This feature is not evident with Weir 2 as the slope of the y_1/Q_1 curve is steeper, and increases in Q_1 are offset by corresponding increases in y_1, leading to only small changes in v_1.

6.4.7 Figures 6.41, 6.42 and 6.43 show that the channel's slope has little effect on the subcritical discharge relationships. This effect can be explained by Figures 6.51 and 6.52. An increase in the channel slope has the effect of decreasing y_1 and increasing y_2. Thus the side spill discharge over the first part of the weir is reduced whilst over the latter part of the weir the discharge is increased. The net result is that the total side spill discharge remains virtually unchanged.

6.4.8 The effect of varying the crest height is shown in Figure 6.44 and is the second most important variable to affect the discharge. An increase in crest height clearly reduces the side spill discharge Q_w, all other variables remaining constant. Figure 6.53 shows that the surface profile is also affected by crest height. The depth-discharge curves are not merely shifted by the change in crest elevation, but the gradients and first spill points also differ, as shown when the Weir 2 results are reduced to Weir 1 level, as denoted by the broken line.

6.4.9 For subcritical profiles Figure 6.45 shows that variation in the weir length produces surprisingly little variation in the discharge characteristic, despite changes in length of $\pm$ 25%. This phenomenon can be explained to some extent by Figure 6.54. For a given upstream discharge a decrease in weir length leads to an increase in both y_1 and y_2. This gives a greater discharge per unit length of weir, thus compensating for the reduction in the length. The converse is true for the longer weir.

6.4.10 The discharge characteristics for supercritical profiles shown in Figure 6.46 clearly show the channel slope to be significant in this case. An increase in the bed slope leads to a reduction in the upstream depth (Fig. 6.55) which in turn reduces the side spill discharge. Q_2 is substantially greater than corresponding values for subcritical flow and generally exceeds Q_w in practical cases. Figure 6.56 shows the depth-discharge relationship in dimensionless form. Extrapolation of the curve to the point where supercritical flow is just formed at the upstream end of the weir, i.e. $y_1 = y_c$, gives a value of $\frac{c}{y_c} = 0.75$. Since $y_c = \frac{2}{3}E_c$ then $E_c = 2c$. Thus, as first stated by Ackers[5], the condition for formation of supercritical flow at the upstream end of the weir is that the specific energy of the upstream flow exceeds twice the crest height.

6.4.11 Lowering of the upstream sluice gate to produce Case IV profiles has the effect of reducing both the upstream depth and the side spill discharge. The depth at the upstream end of the weir is now governed by the gradually varied flow profile in the upstream channel. A relationship was found between the percentage reduction in y_1 and the percentage reduction in Q_w from their respective values for Case I profiles at the same upstream discharge. This relationship is shown graphically in Figure 6.47 and is unaffected by the channel slope.

6.4.12 In all cases the first spill conditions shown on the depth-discharge relationships indicate a first spill depth 1 to 2mm greater than the crest height. This was observed during the experiments and is due to surface tension effects.

FIG. 6.39 DISCHARGE CHARACTERISTIC : Effect of Varying Downstream Control : Weir 1, Slope Horizontal : Case II Flow.

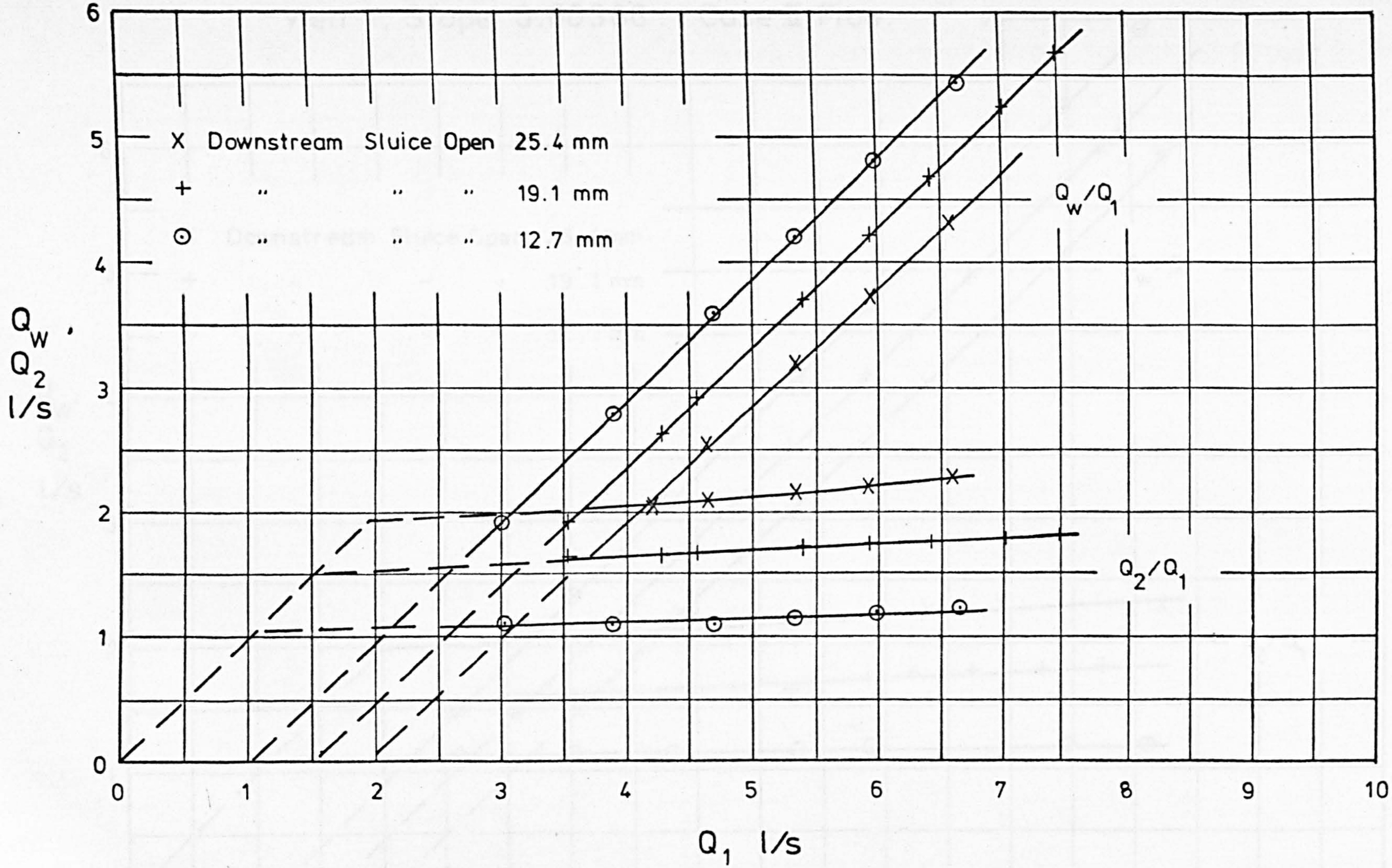

FIG. 6.40 DISCHARGE CHARACTERISTIC: Effect of Varying Downstream Control: Weir 4, Slope 0.00366: Case II Flow.

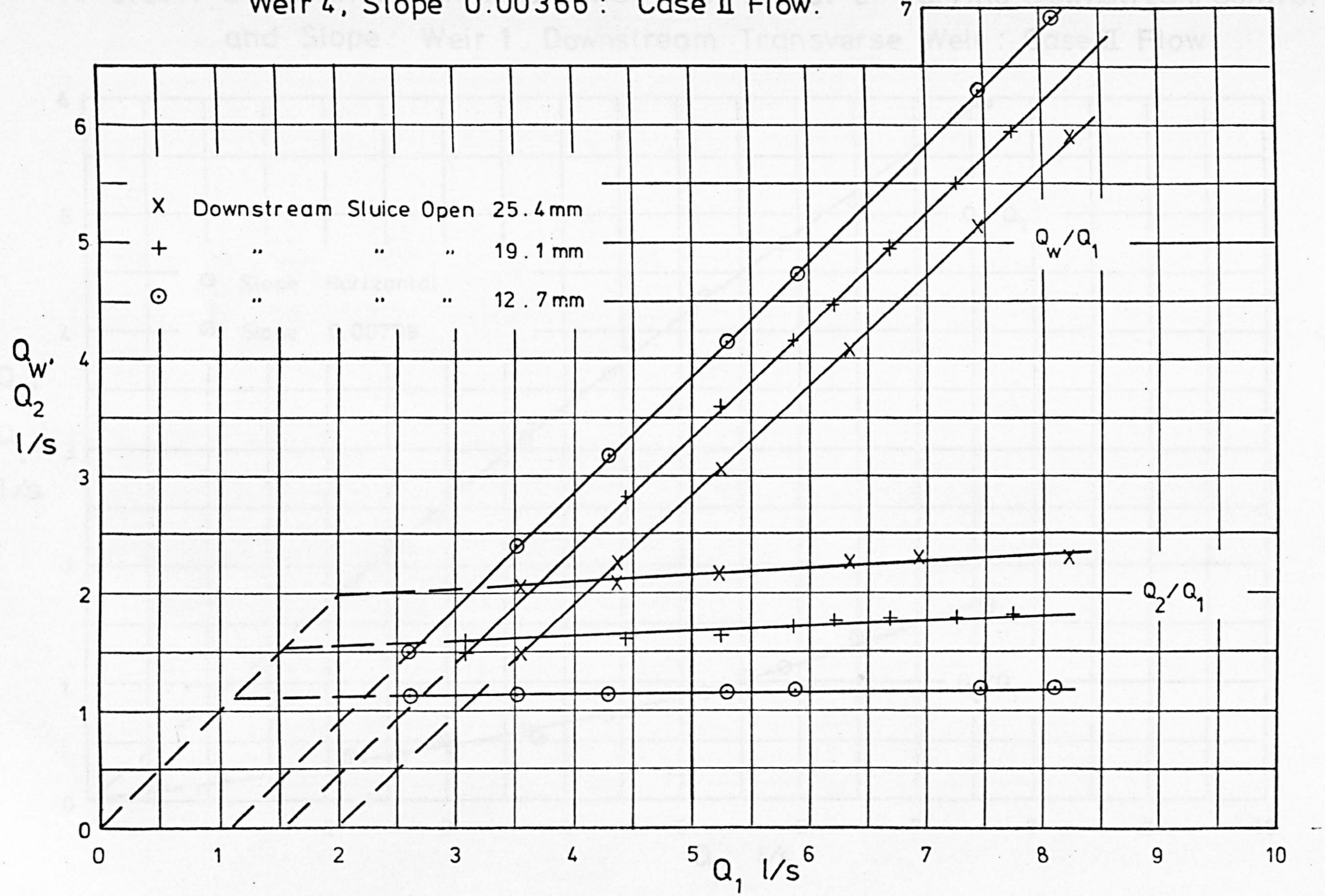

FIG.6.41 DISCHARGE CHARACTERISTIC : Effect of Varying Downstream Control and Slope : Weir 1, Downstream Transverse Weir : Case II Flow.

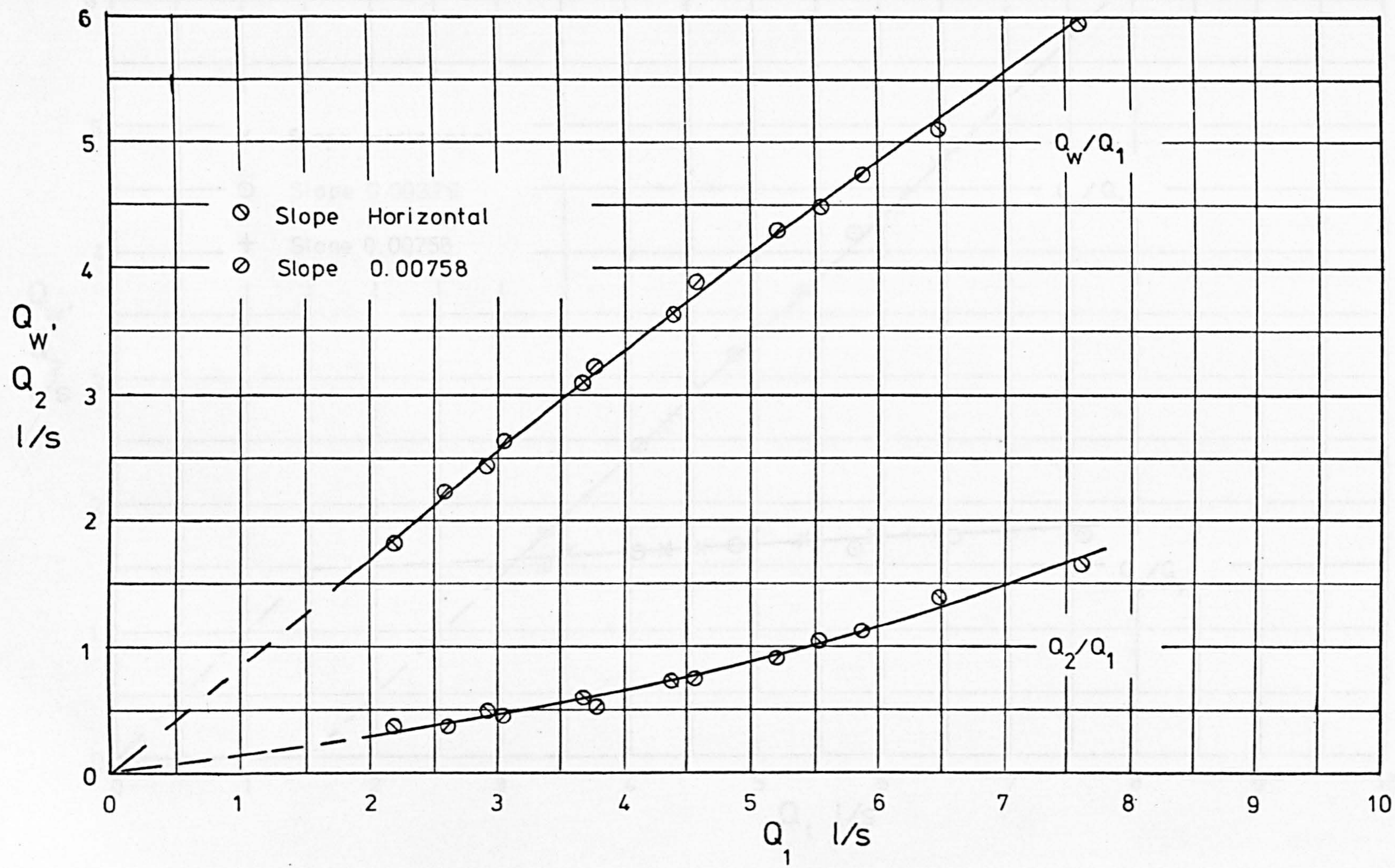

FIG. 6.42 DISCHARGE CHARACTERISTIC: Effect of Varying Bed Slope: Weir 1, Downstream Sluice Open 19.1mm: Case II Flow.

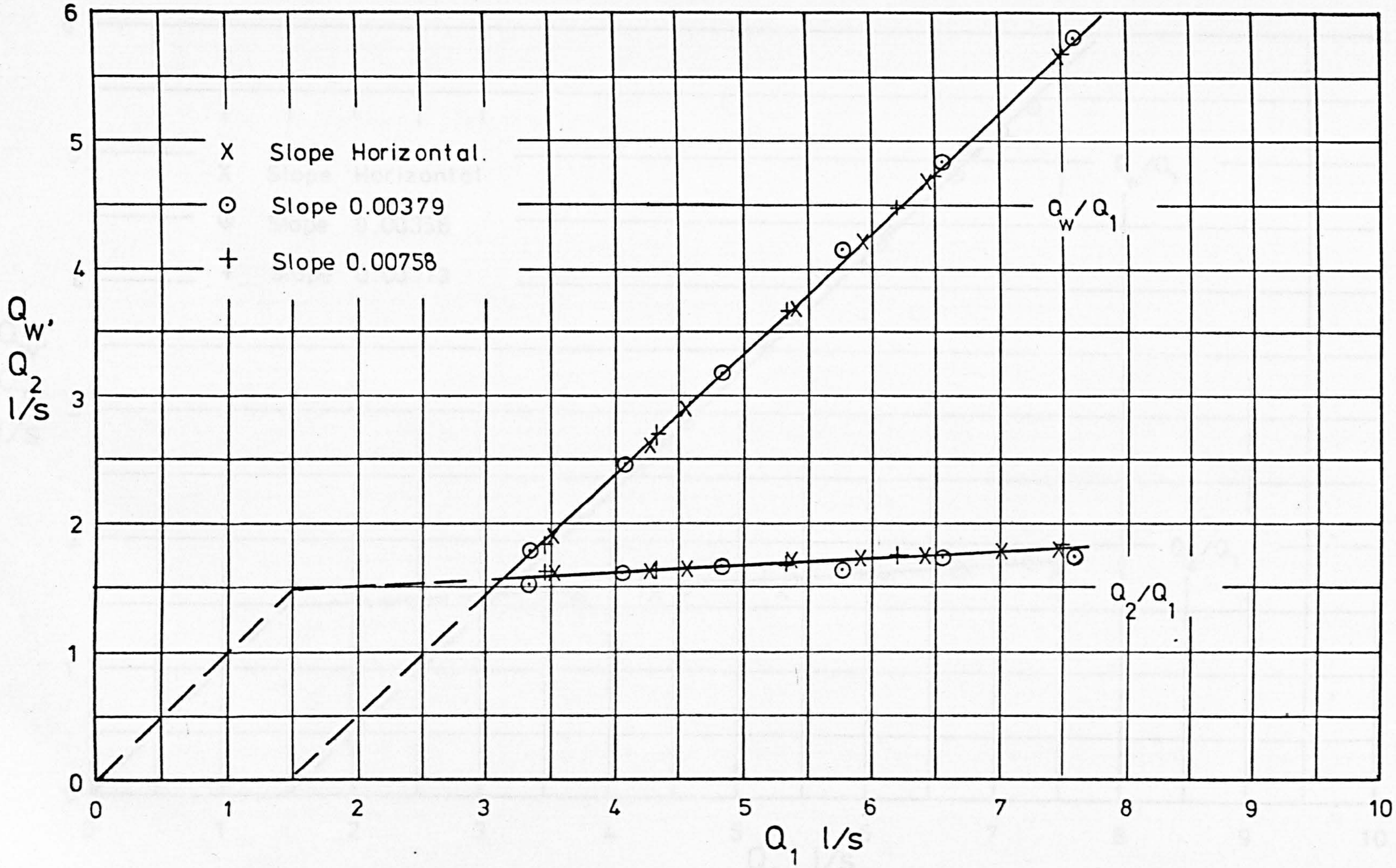

FIG. 6.43 DISCHARGE CHARACTERISTIC: Effect of Varying Channel Bed Slope: Weir 5, Downstream Sluice Open 19.1mm : Case II Flow.

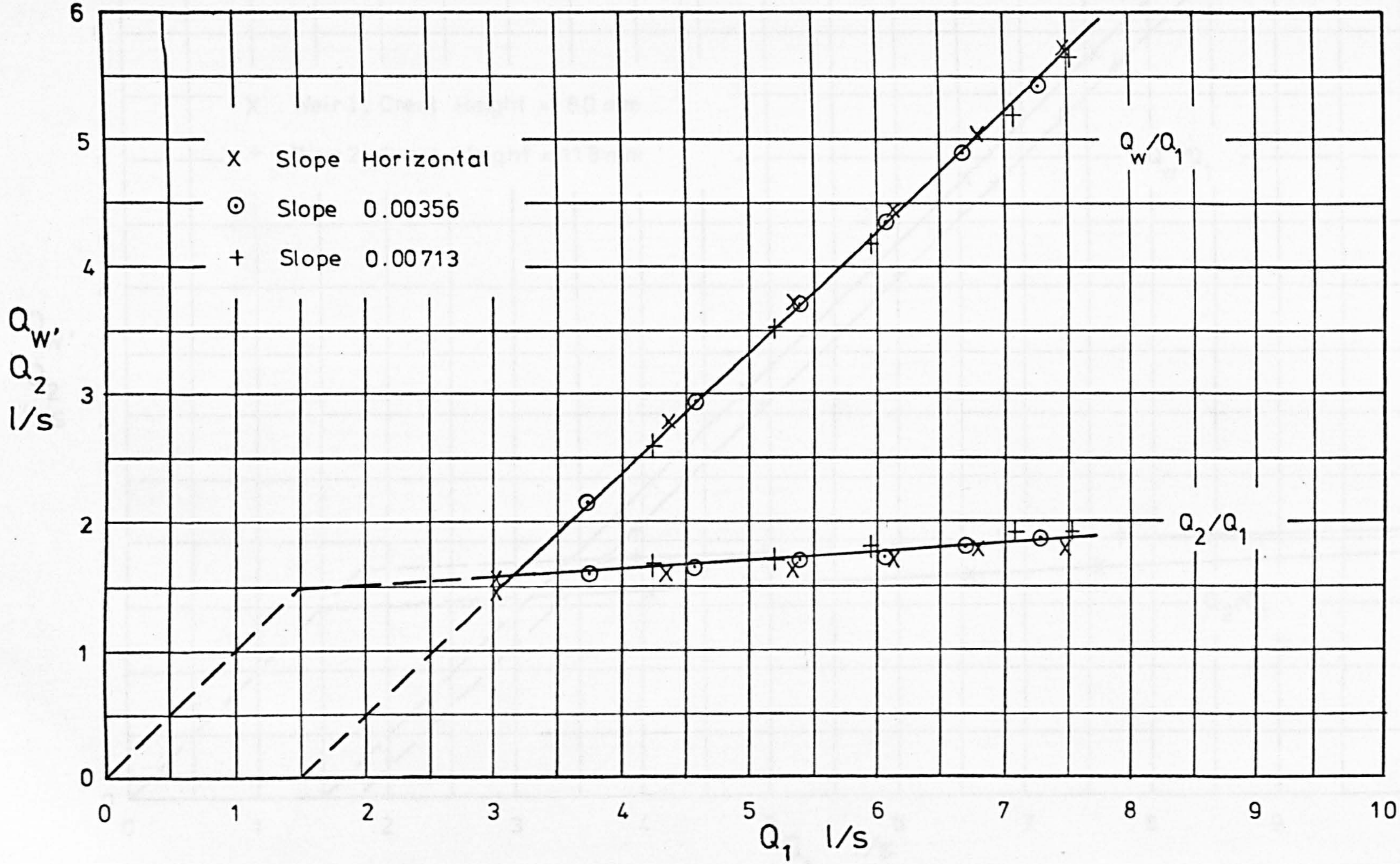

FIG. 6.44 DISCHARGE CHARACTERISTIC: Effect of Varying Crest Height: Weir Length = 0.6096m, Downstream Sluice Open 19.1mm : Case II Flow.

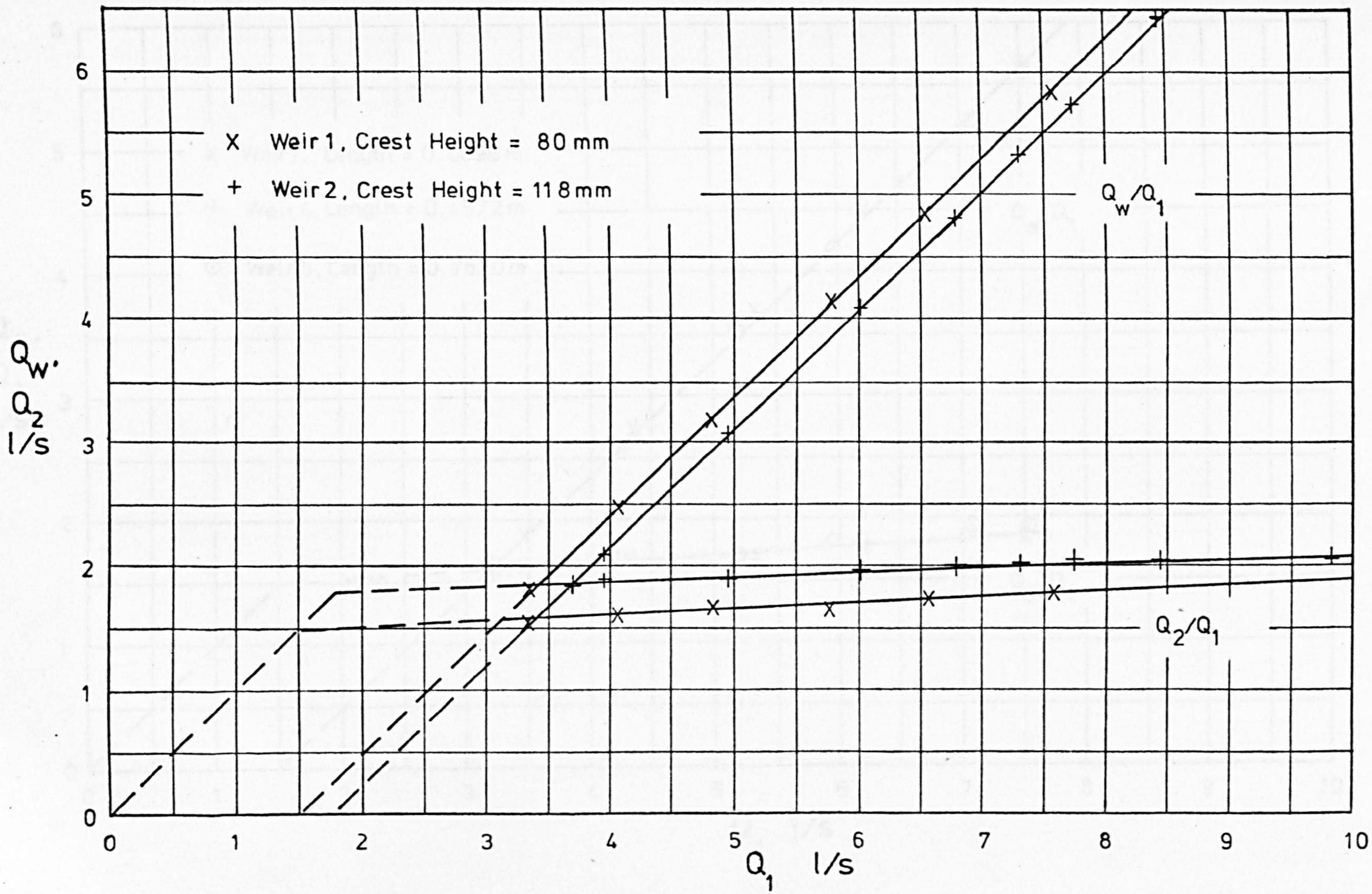

FIG. 6.45 DISCHARGE CHARACTERISTIC: Effect of Varying Weir Length: Crest Height 80 mm approx., Downstream Sluice Open 19.1 mm: Case II Flow.

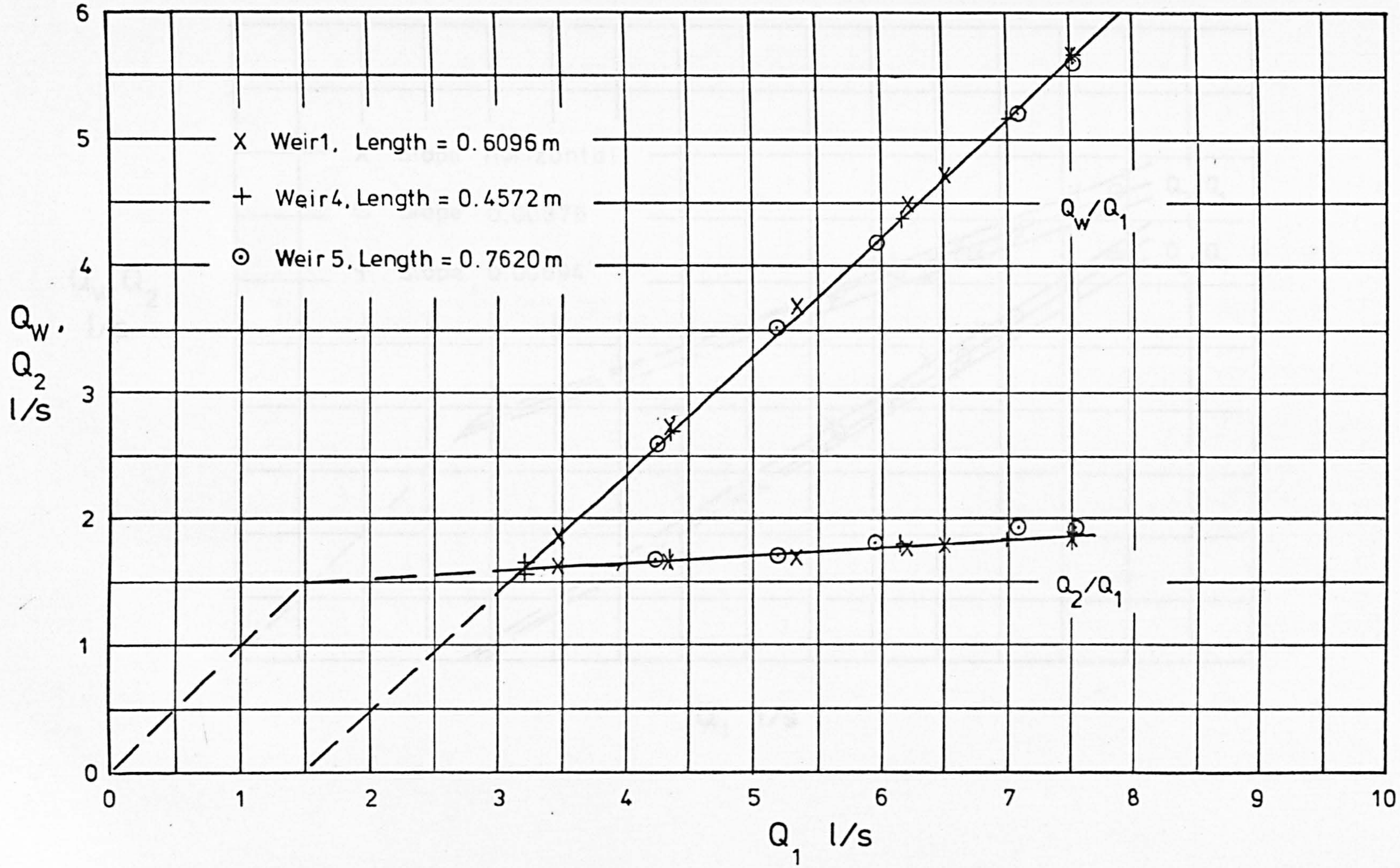

FIG. 6.46 DISCHARGE CHARACTERISTIC : Effect of Varying Channel Bed Slope: Weir 3: Case I Flow.

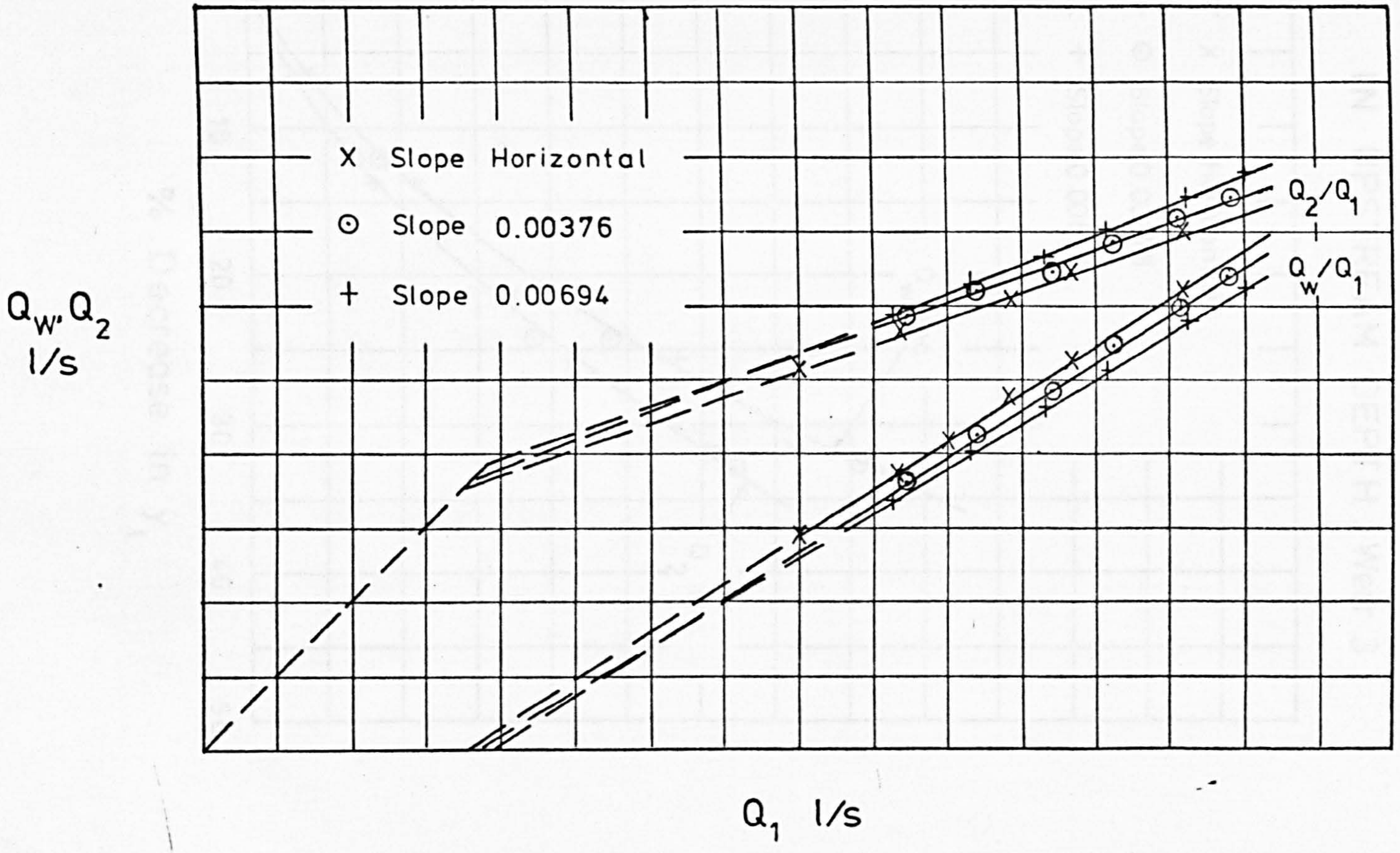

FIG. 6.47 CASE IV FLOW: REDUCTION IN SIDE SPILL DISCHARGE FROM CASE I FLOW DUE TO REDUCTION IN UPSTREAM DEPTH : Weir 3.

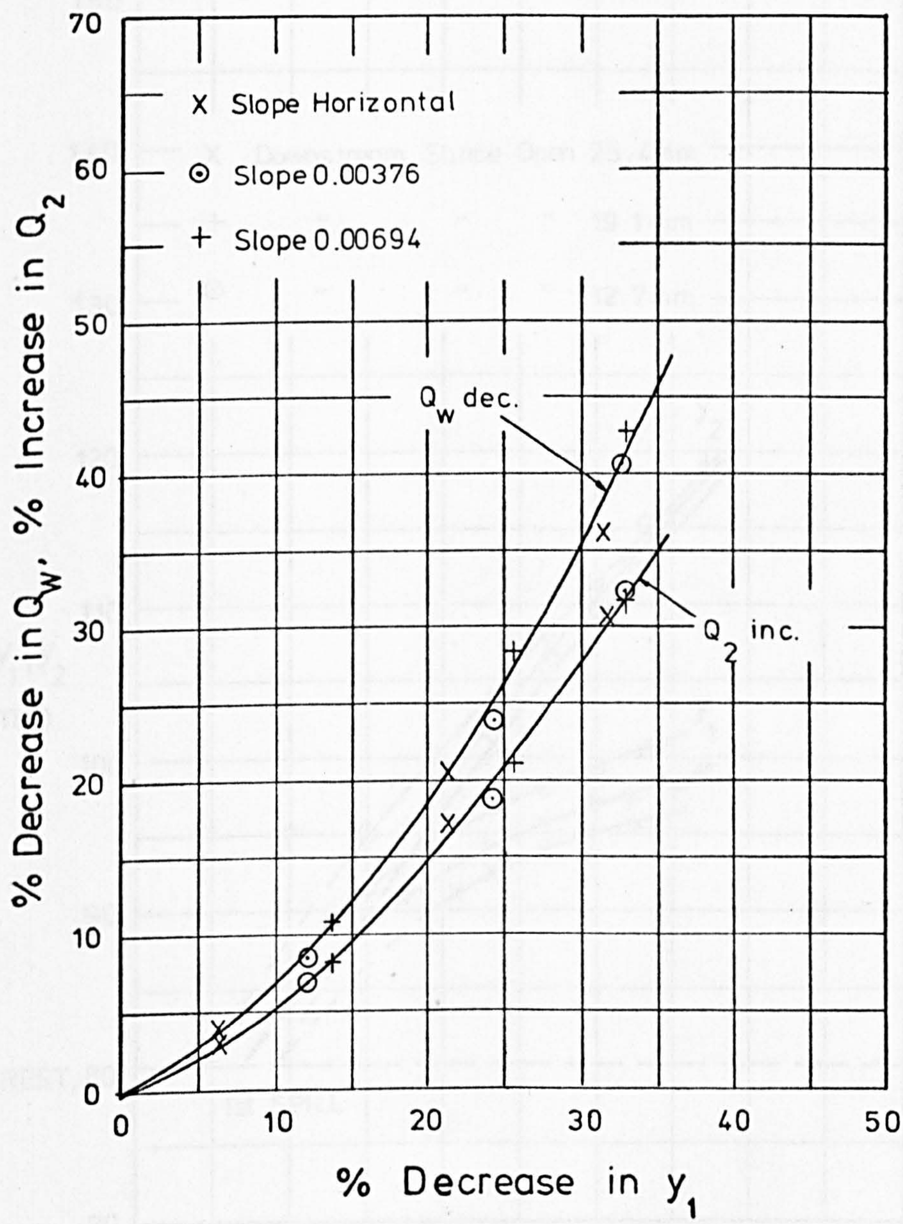

FIG. 6.48 DEPTH - DISCHARGE RELATIONSHIP: Effect of Varying Downstream Control: Weir 1, Slope Horizontal: Case II Flow.

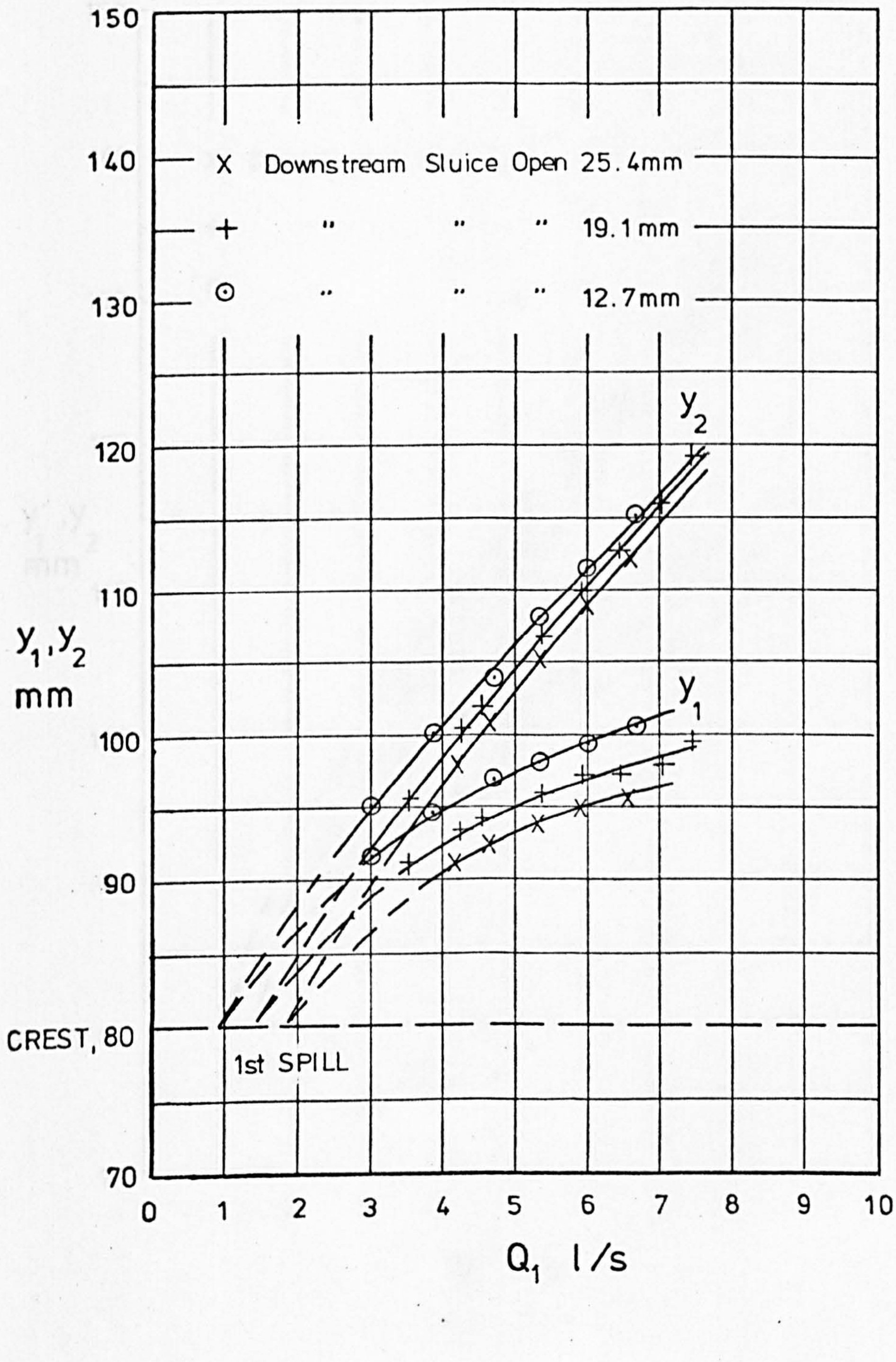

FIG. 6.49 DEPTH - DISCHARGE RELATIONSHIP : Effect of Varying Downstream Control: Weir 4, Slope 0.00366 : Case II Flow.

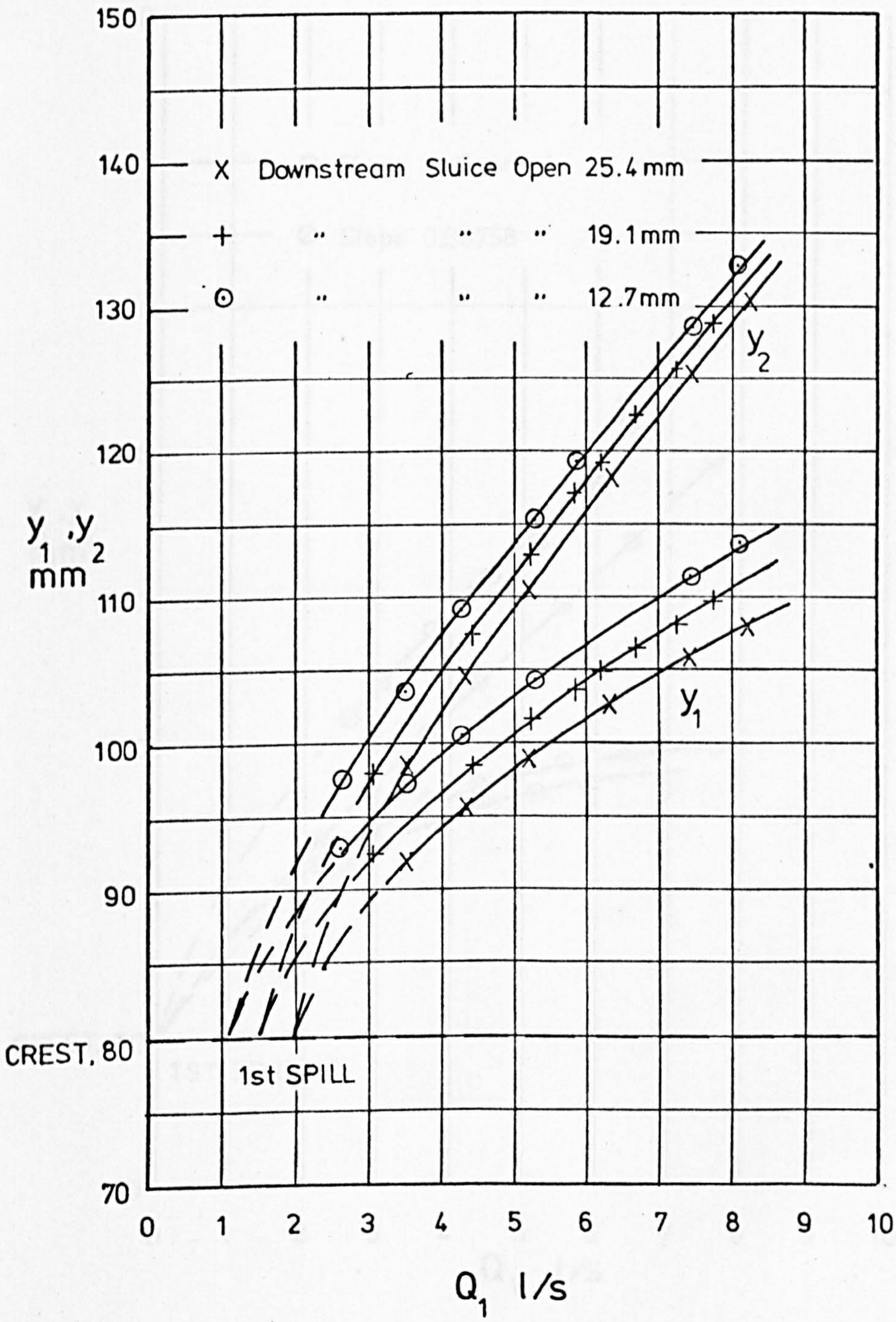

FIG.6.50 DEPTH-DISCHARGE RELATIONSHIP: Effect of Varying Downstream Control and Slope: Weir 1, Downstream Transverse Weir: Case II Flow.

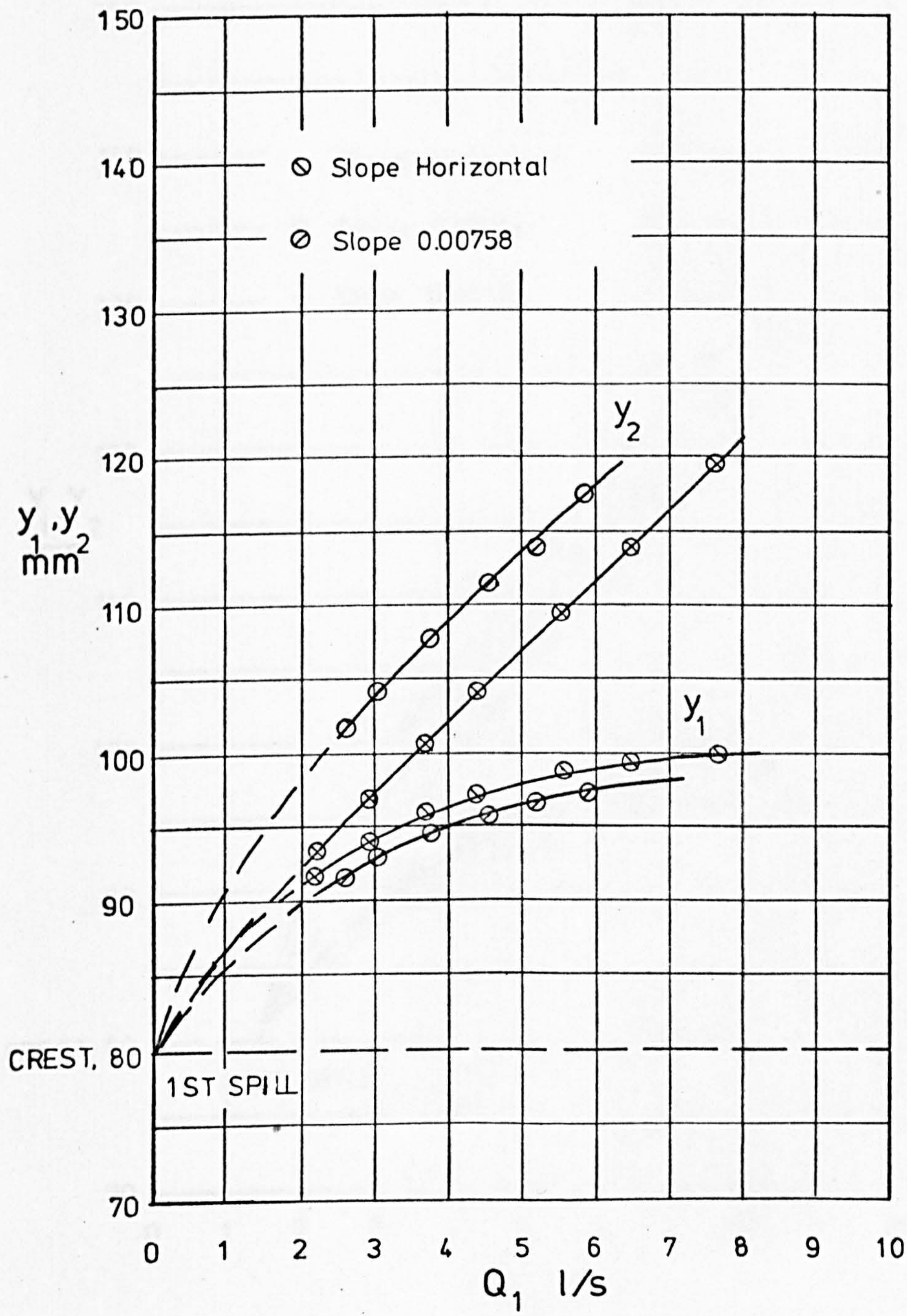

FIG. 6.51 DEPTH - DISCHARGE RELATIONSHIP: Effect of Varying Channel Slope: Weir 1, Downstream Sluice Open 19.1 mm: Case II Flow.

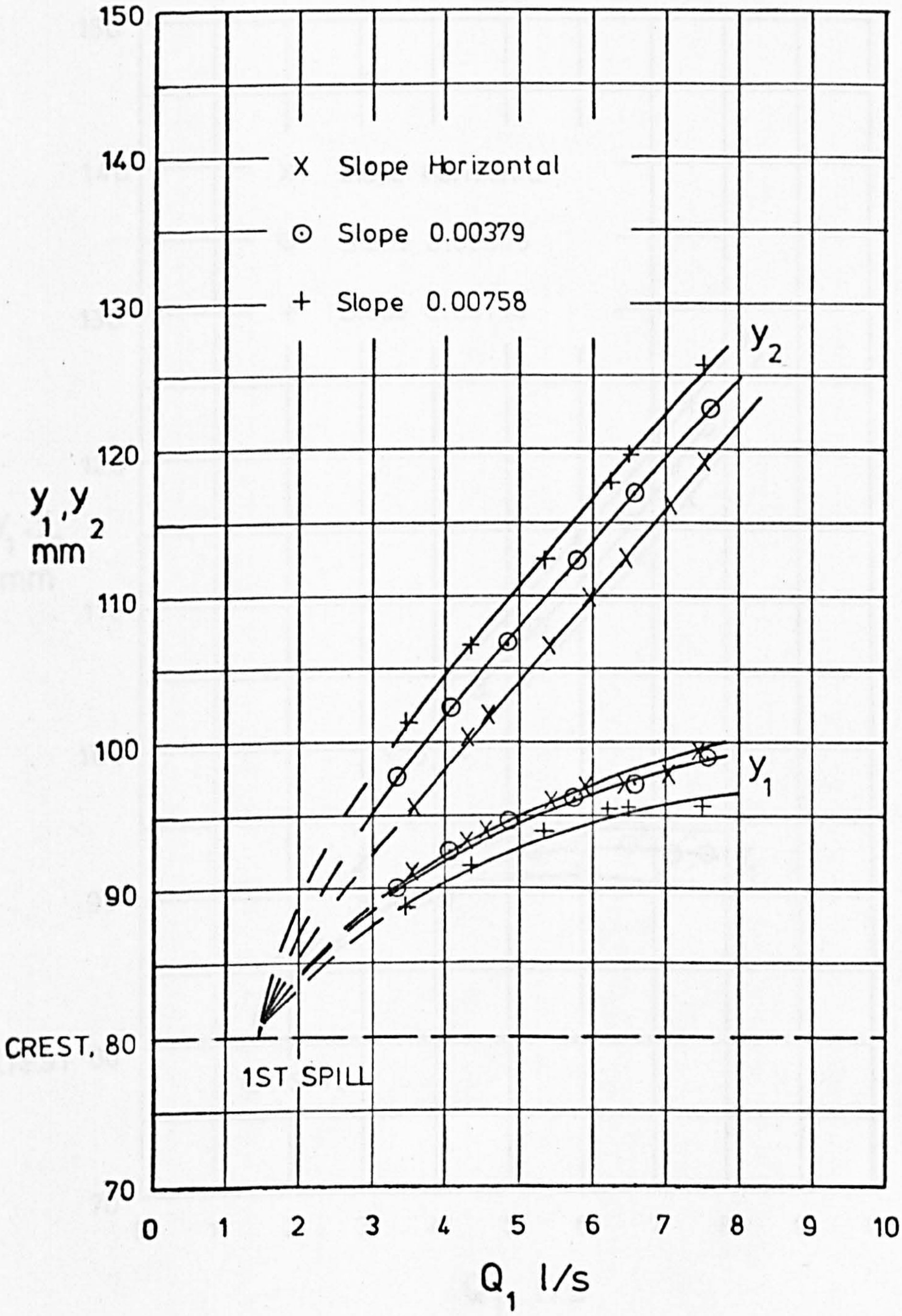

FIG. 6.52 DEPTH - DISCHARGE RELATIONSHIP: Effect of Varying Channel Slope: Weir 5, Downstream Sluice Open 19.1 mm: Case II Flow.

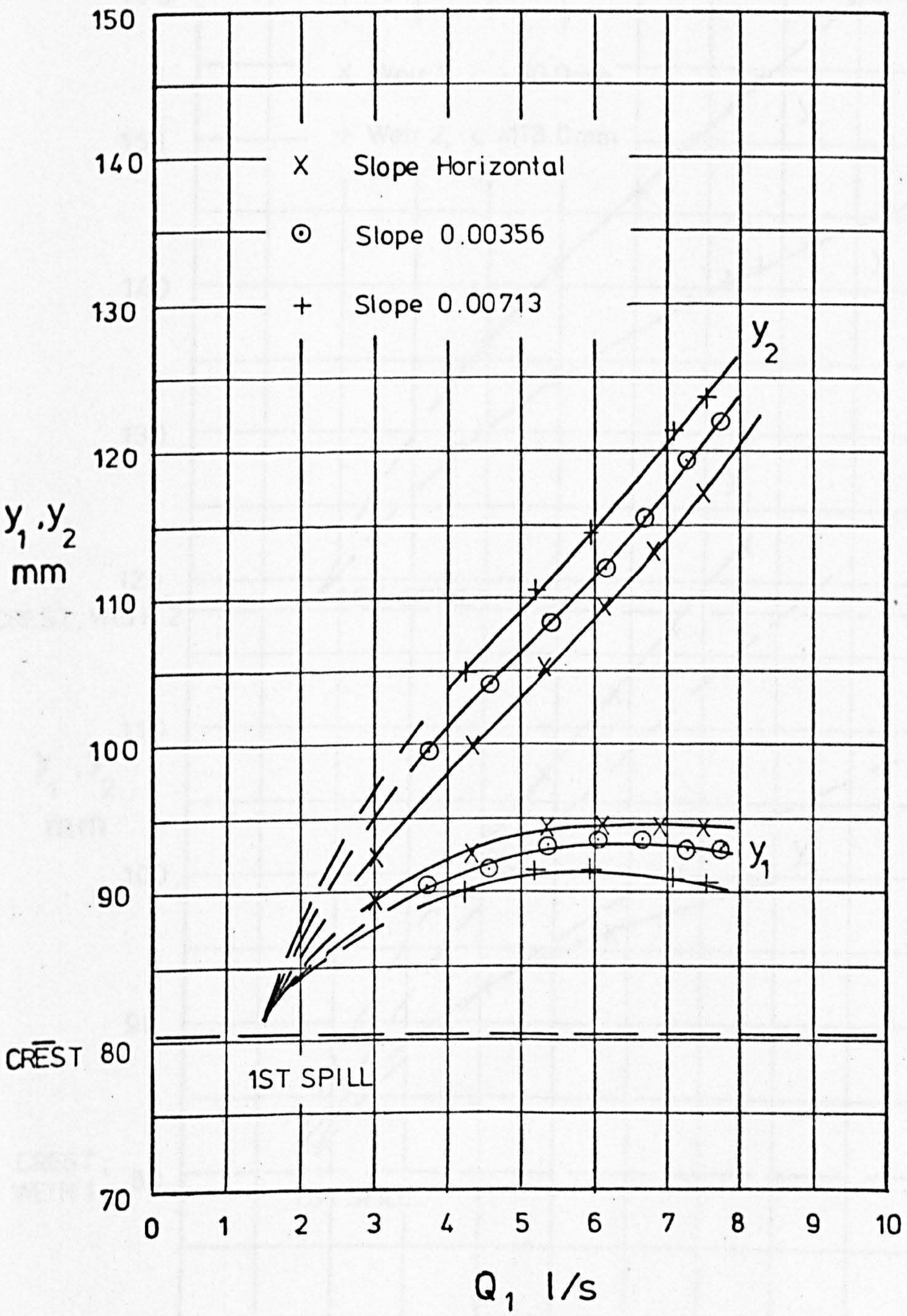

FIG.6.53 DEPTH-DISCHARGE RELATIONSHIP: Effect of Varying Crest Height: Weir Length = 0.6096 m ; Case II Flow

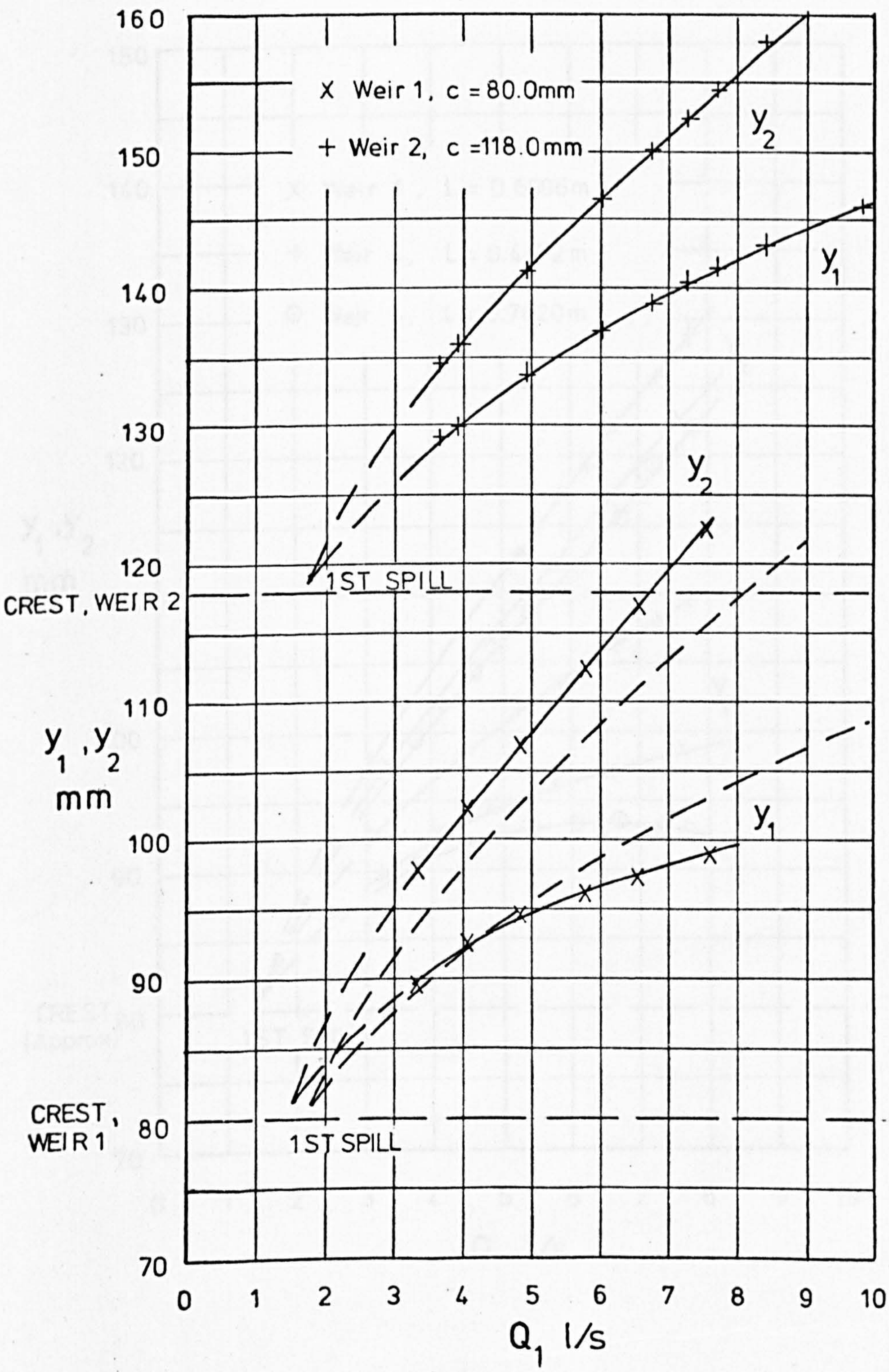

FIG. 6.54 DEPTH - DISCHARGE RELATIONSHIP: Effect of Varying Weir Length: Crest Height = 80 mm approx.: Case II Flow.

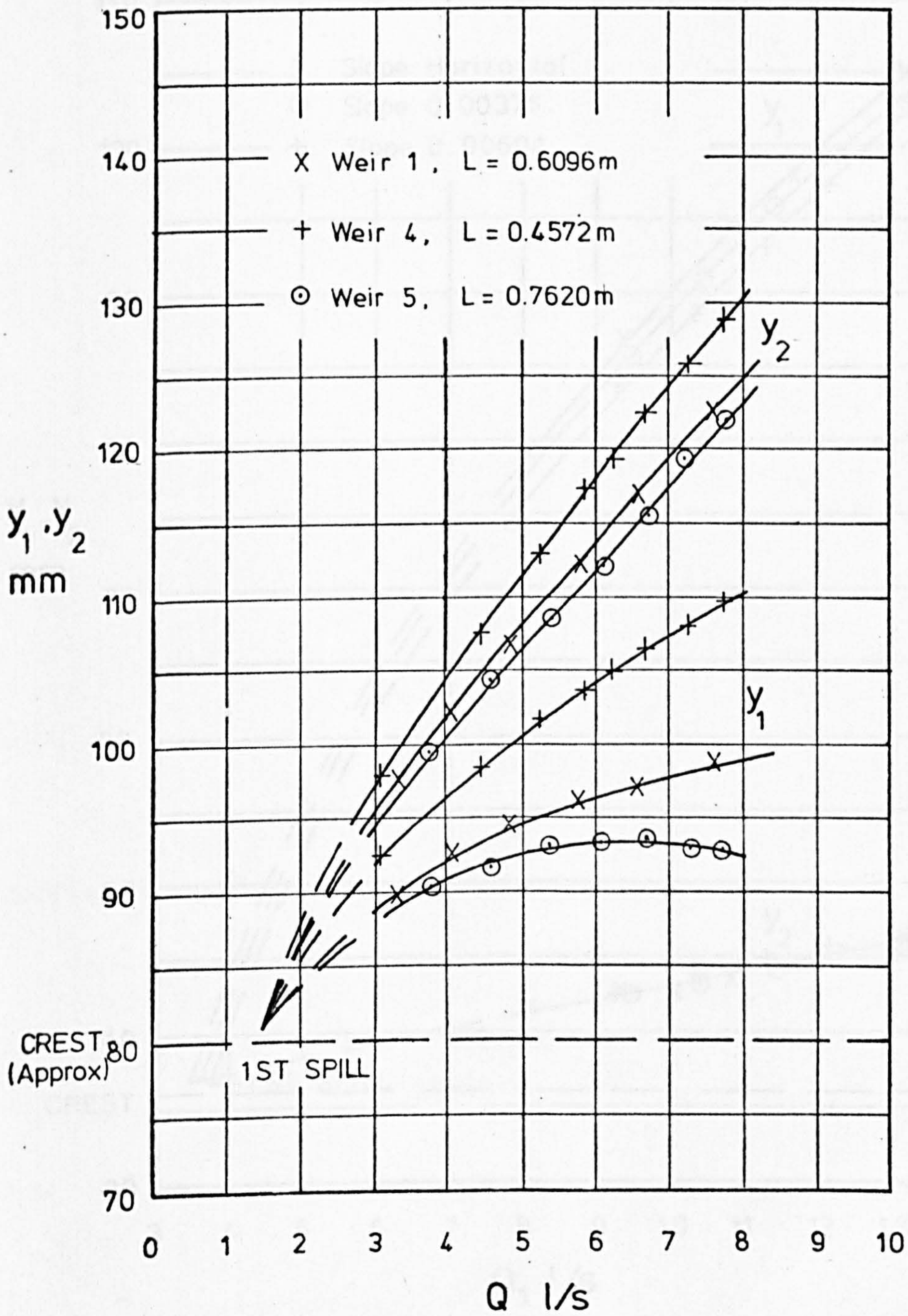

FIG. 6.55 DEPTH - DISCHARGE RELATIONSHIP: Effect of Varying Channel Slope: Weir 3 : Case I Flow.

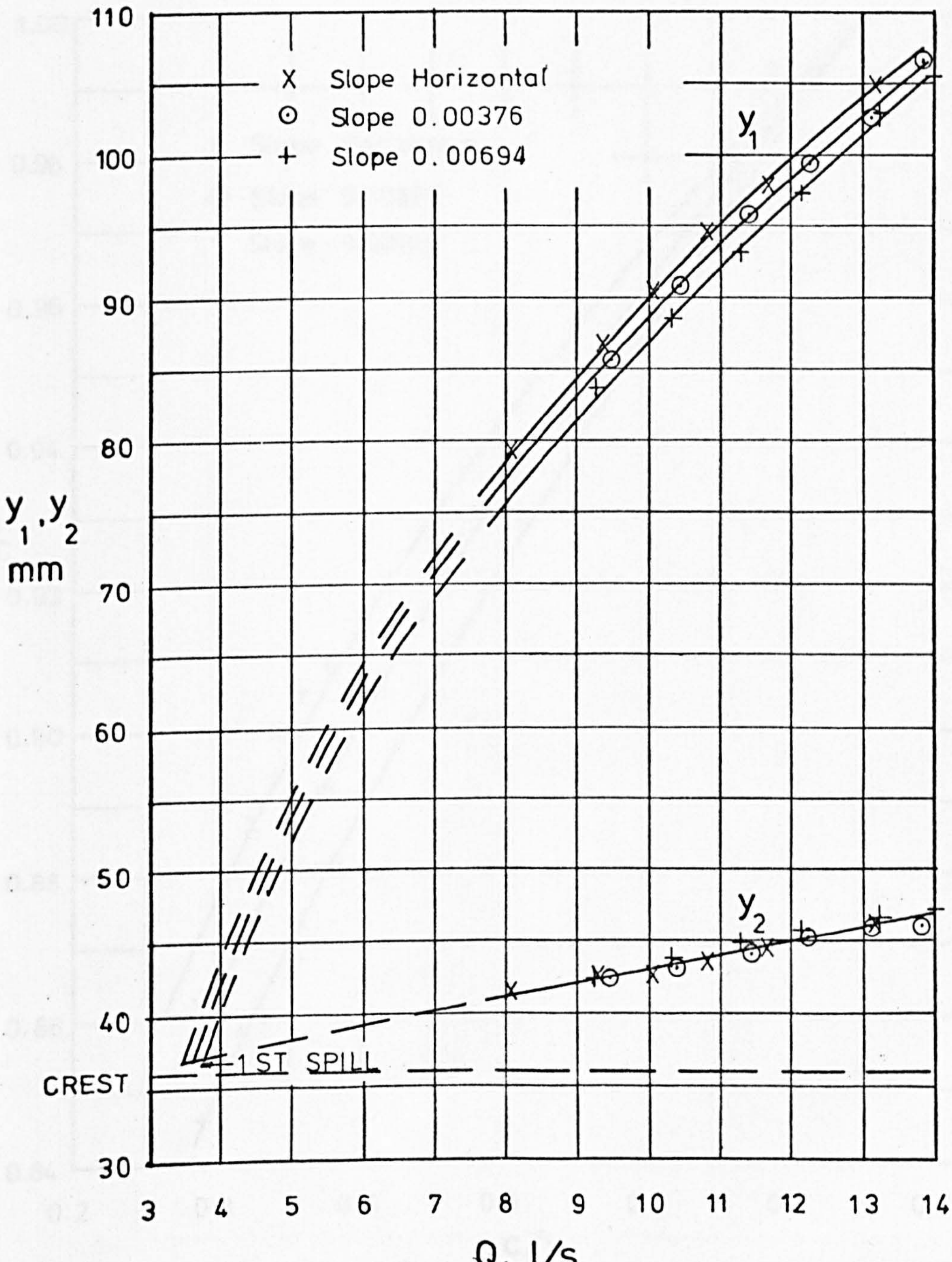

FIG. 6.56 DIMENSIONLESS DEPTH - DISCHARGE RELATIONSHIP FOR SUPERCRITICAL CASE I FLOW: Weir 3.

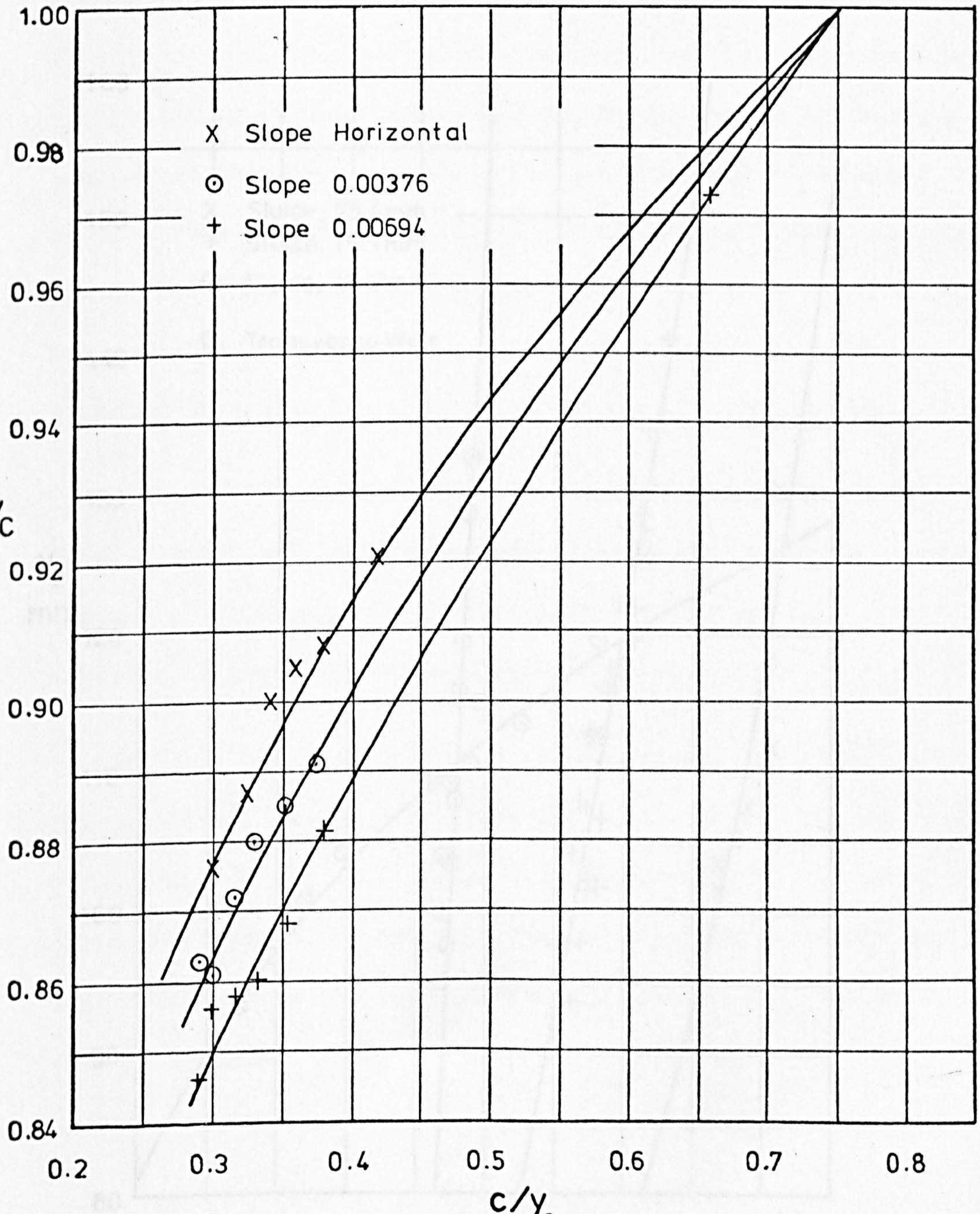

FIG. 6.57 DOWNSTREAM CONTROL DEPTH - DISCHARGE RATING CURVES:
Results for Weirs 1,2,4,&5, all slopes.

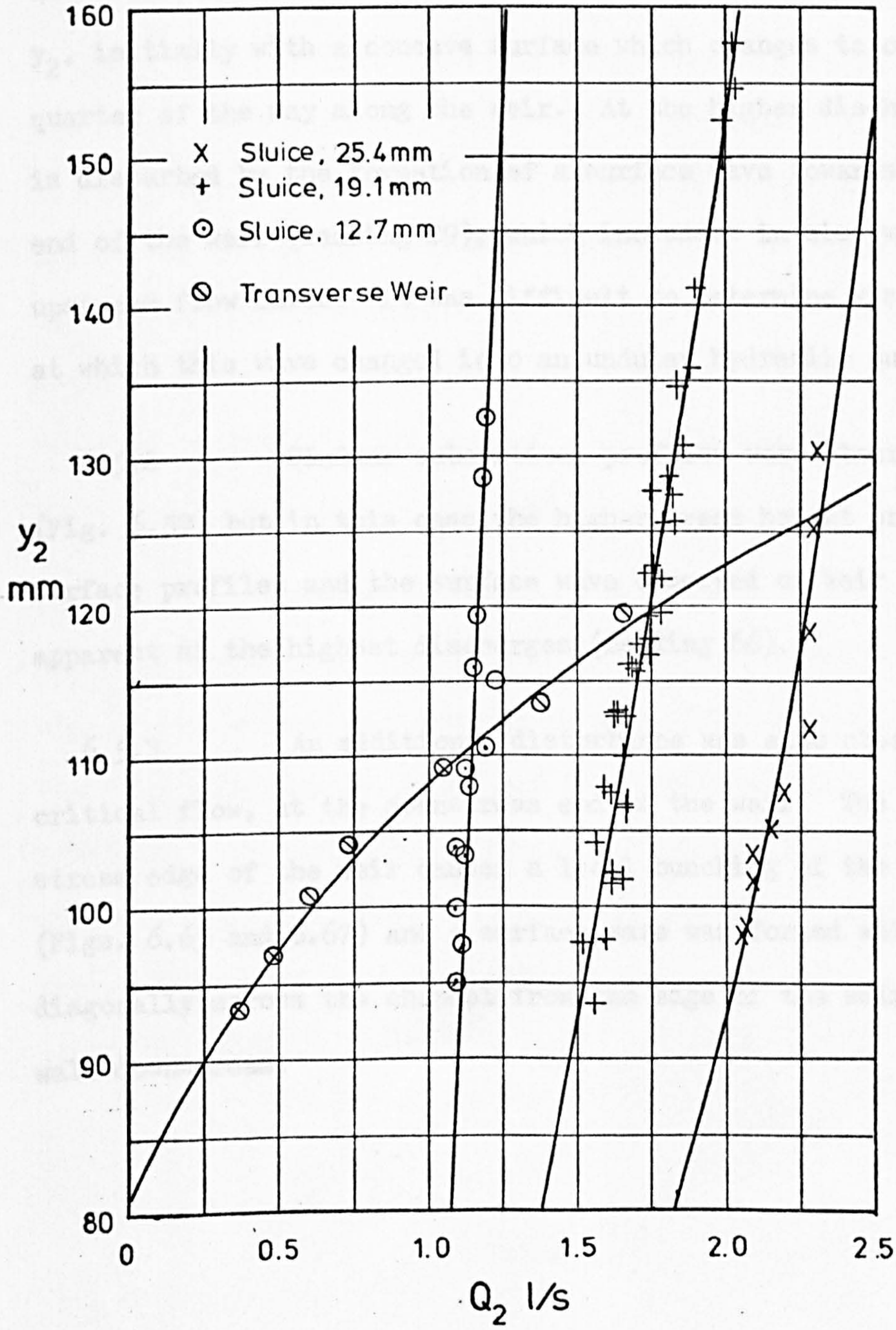

6.5 Longitudinal Surface Profiles

6.5.1 Longitudinal surface profiles were measured along the centreline of the channel for a number of the subcritical flow readings and the profile coordinates are tabulated in Appendix VII. The shape of the surface profile is not appreciably affected by the slope of the channel and Figure 6.58 shows typical profiles, for readings 19 and 29. At the lower discharges subcritical profiles rise smoothly from y_1 to y_2, initially with a concave surface which changes to convex about a quarter of the way along the weir. At the higher discharges the profile is disturbed by the formation of a surface wave towards the upstream end of the weir (reading 29), which increases in size with increasing upstream flow rates. It was difficult to determine visually the point at which this wave changed into an undular hydraulic jump.

6.5.2 Similar subcritical profiles were observed on Weir 2 (Fig. 6.59) but in this case the higher crest height produced smoother surface profiles and the surface wave observed on Weir 1 only became apparent at the highest discharges (reading 66).

6.5.3 An additional disturbance was also observed in subcritical flow, at the downstream end of the weir. The vertical downstream edge of the weir caused a local bunching of the water surface (Figs. 6.65 and 6.67) and a surface wave was formed which passed diagonally across the channel from the edge of the weir to the opposite wall downstream.

6.5.4 Supercritical surface profiles were measured for each supercritical reading, the results also being tabulated in Appendix VII. On Weir 1, Case I profiles only could be produced with a clinging nappe formed over most of the length of the weir (Fig. 6.60). With Weir 3 however it was possible to achieve a range of profiles (with free nappes) of both the Case I and Case IV types, the latter being achieved by lowering the upstream sluice gate.

6.5.5 Figures 6.61 and 6.62 show two typical Case I profiles. The water surface falls rapidly as it approaches the weir with appreciable curvature of the flow. This curvature is sufficient to affect the hydrostatic pressure distribution, as shown in Table 6.3, so that the incorporation of curvature effects in the mathematical model is justified. The 'S-shaped' surface profile is similar to that observed by Frazer[15] and its shape is unaffected by the length of the weir.

6.5.6 Figure 6.64 shows the shape of the surface profiles for the Case I condition upstream of the weir. The profiles are in dimensionless form and upstream of the critical depth ($y/y_c = 1.0$) the flow is gradually varied and the dimensionless profiles are virtually identical. On approaching the critical depth, however, the profiles diverge slightly to give unique conditions at the upstream end of the weir. The position of the critical depth varies between 0.8 and 1.1 times the critical depth upstream of the weir.

TABLE 6.3				
Reading No.	Flow Case	y_1 mm	$\frac{p_1}{\rho g}$ measured mm	$\frac{p_1}{\rho g}$ computed + mm
132	I	106.7	97.4	98.6
133	I	102.8	93.7	95.6
134	I	99.4	91.3	93.6
135	I	95.7	88.2	90.8
136	I	90.5	85.6	87.2
137	I	85.5	81.2	82.7
138	IV	89.0	81.7	84.7
139	IV	76.2	69.6	72.3
140	IV	68.0	61.1	62.3
141	I	105.5	96.0	98.5
142	I	103.0	93.3	96.3
143	I	97.4	89.1	92.1
144	I	93.1	85.7	88.6
145	I	88.4	81.6	85.3
146	I	83.5	77.4	80.9
147	IV	85.2	76.4	80.1
148	IV	73.5	63.7	69.8
149	IV	66.2	55.2	62.6

\+ These values are computed from the theory used to formulate the mathematical model with curvature.

6.5.7 The Case IV profiles (Fig. 6.63) show the same 'S-shaped curve but with less pronounced curvature. Upstream of the weir the supercritical flow is gradually varied, being controlled by the upstream sluice gate, and this determines the value of the depth at the start of the weir.

6.5.8 The supercritical profile coordinates were used to compute values of curvature and slope which helped to formulate the mathematical model described in section 3.4. The method of computation is described in Appendix III.

FIG. 6.58 LONGITUDINAL SURFACE PROFILES:
Weir 1 : Case II Flow.

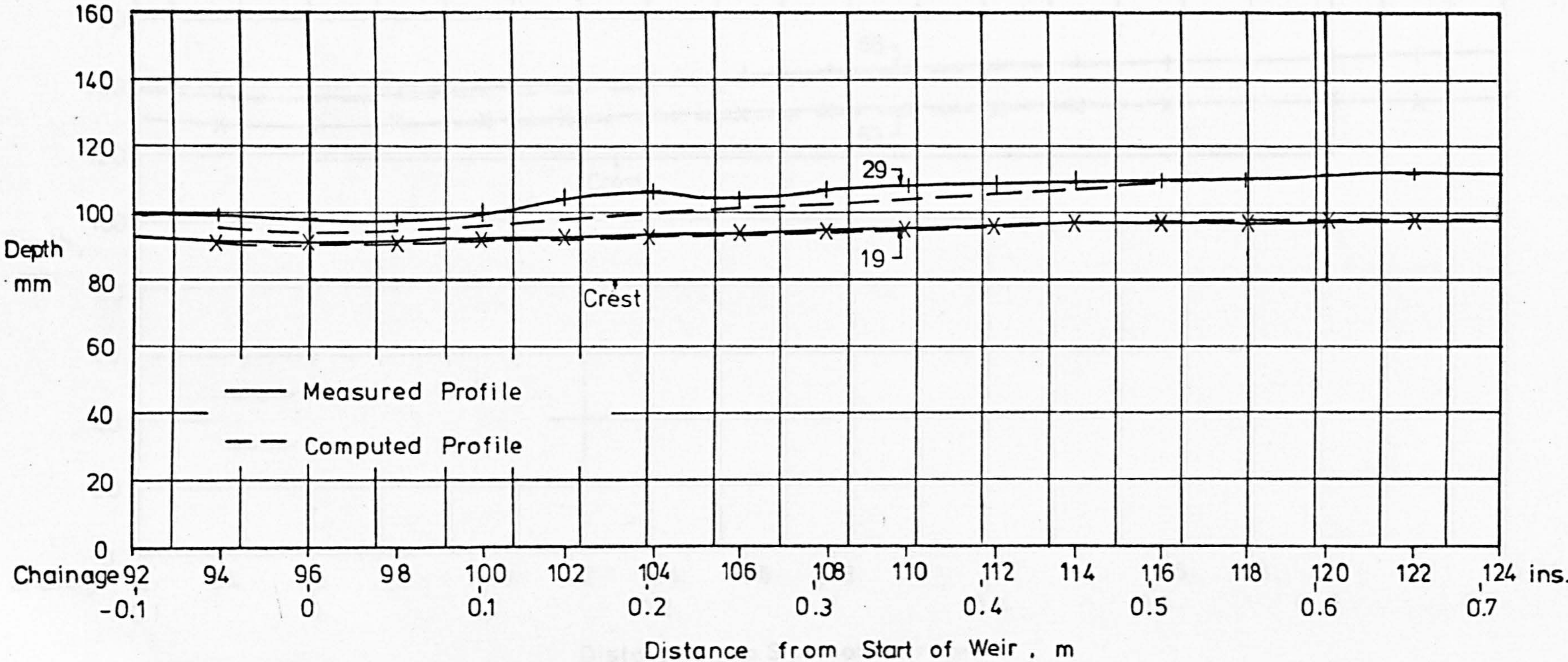

FIG. 6.59 LONGITUDINAL SURFACE PROFILES:
Weir 2: Case II Flow.

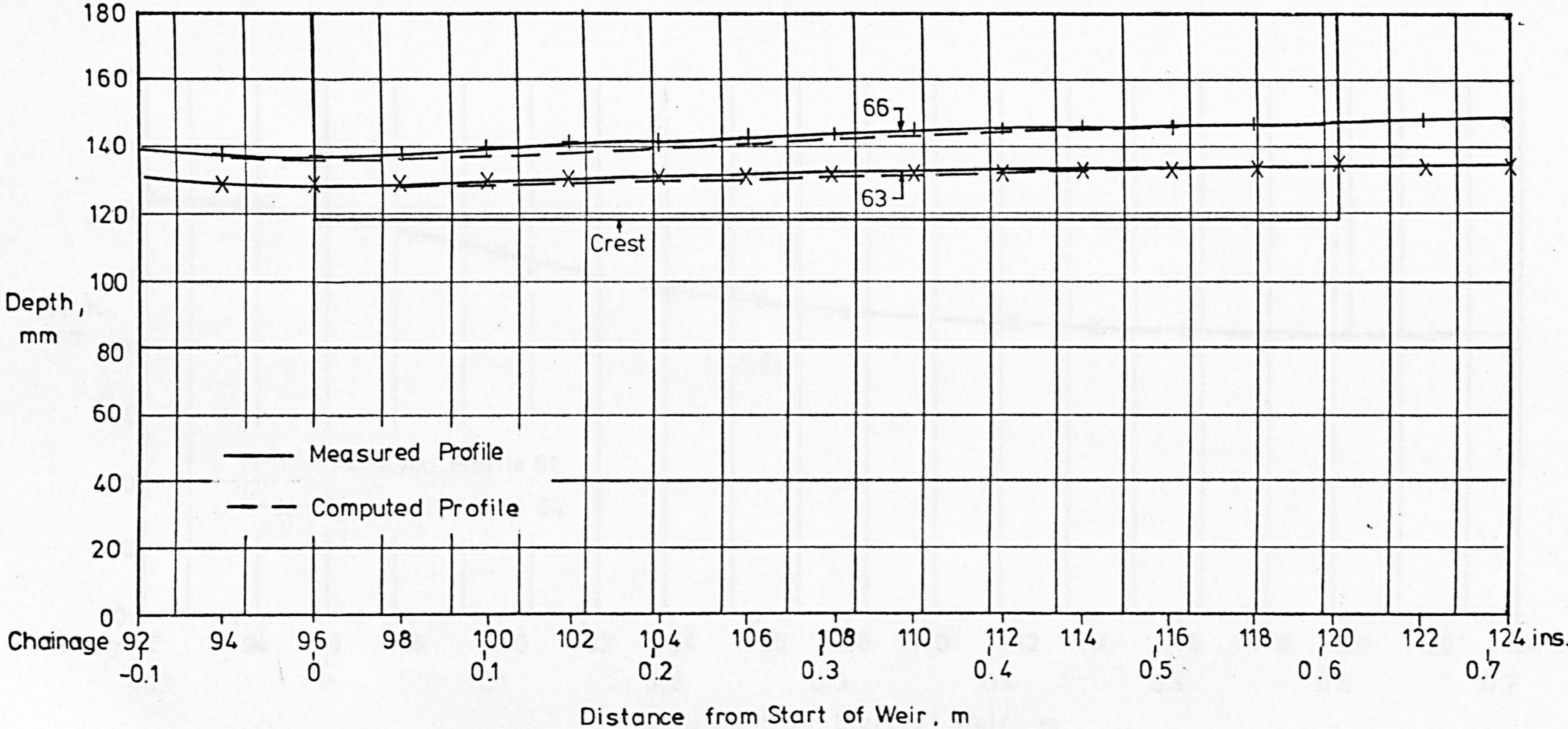

FIG. 6.60 LONGITUDINAL SURFACE PROFILES:
Weir 1: Case I Flow.

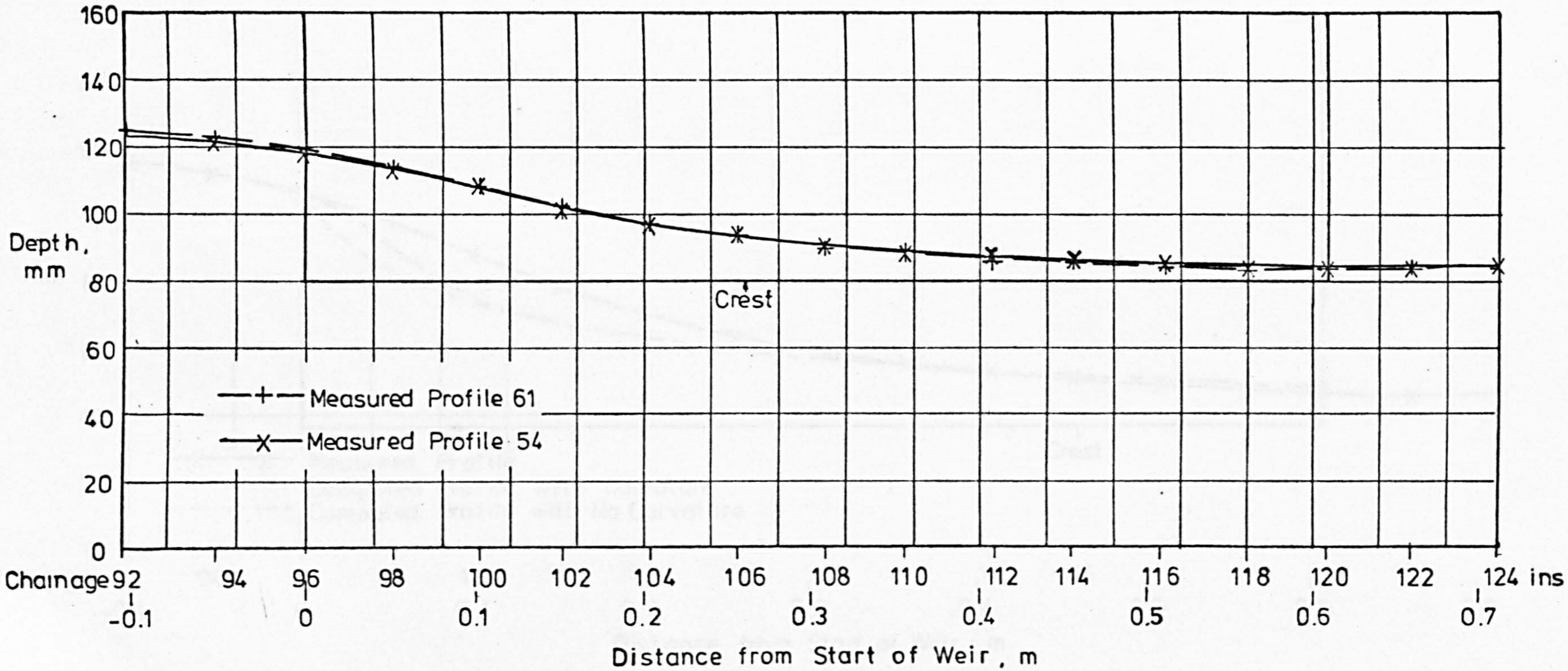

FIG. 6.61 LONGITUDINAL SURFACE PROFILES:
Weir 3: Case I Flow: Reading No. 132.

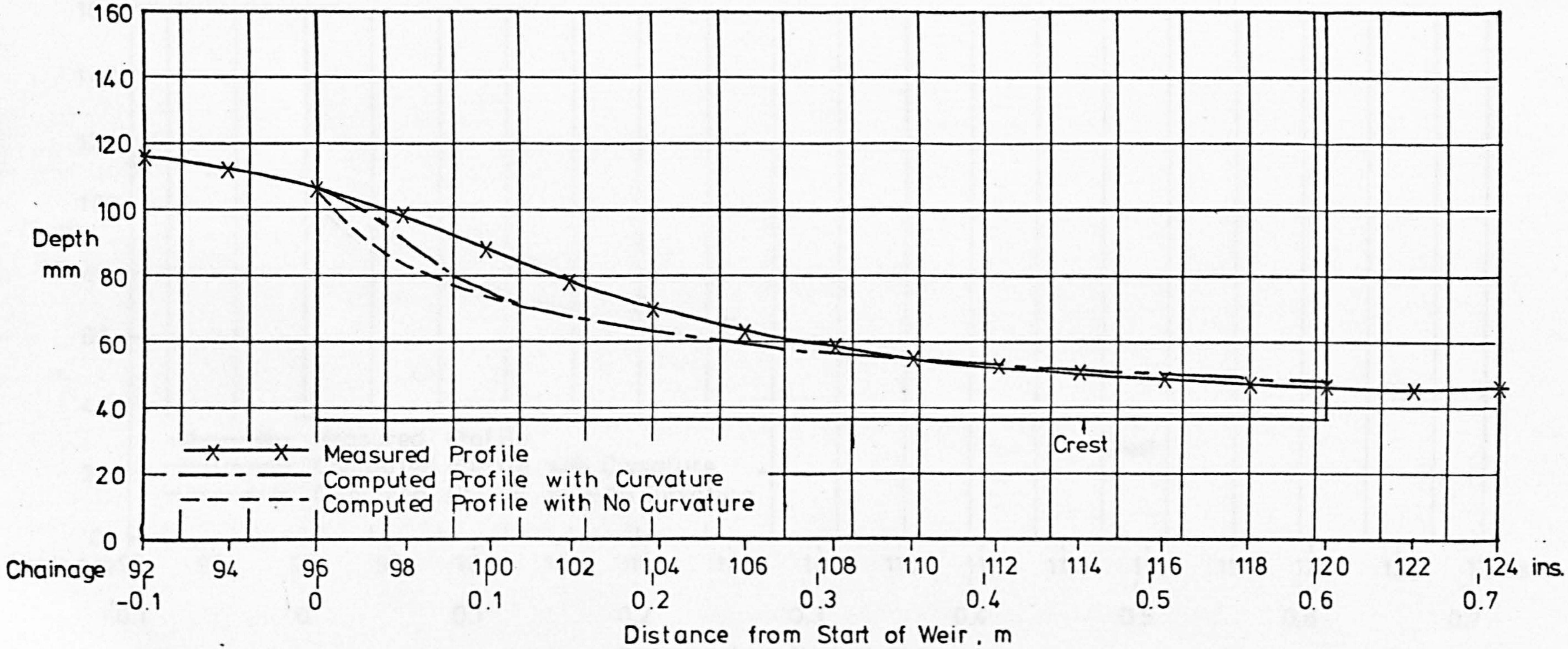

FIG. 6.62 LONGITUDINAL SURFACE PROFILES :
Weir 3 : Case I Flow : Reading No. 141 .

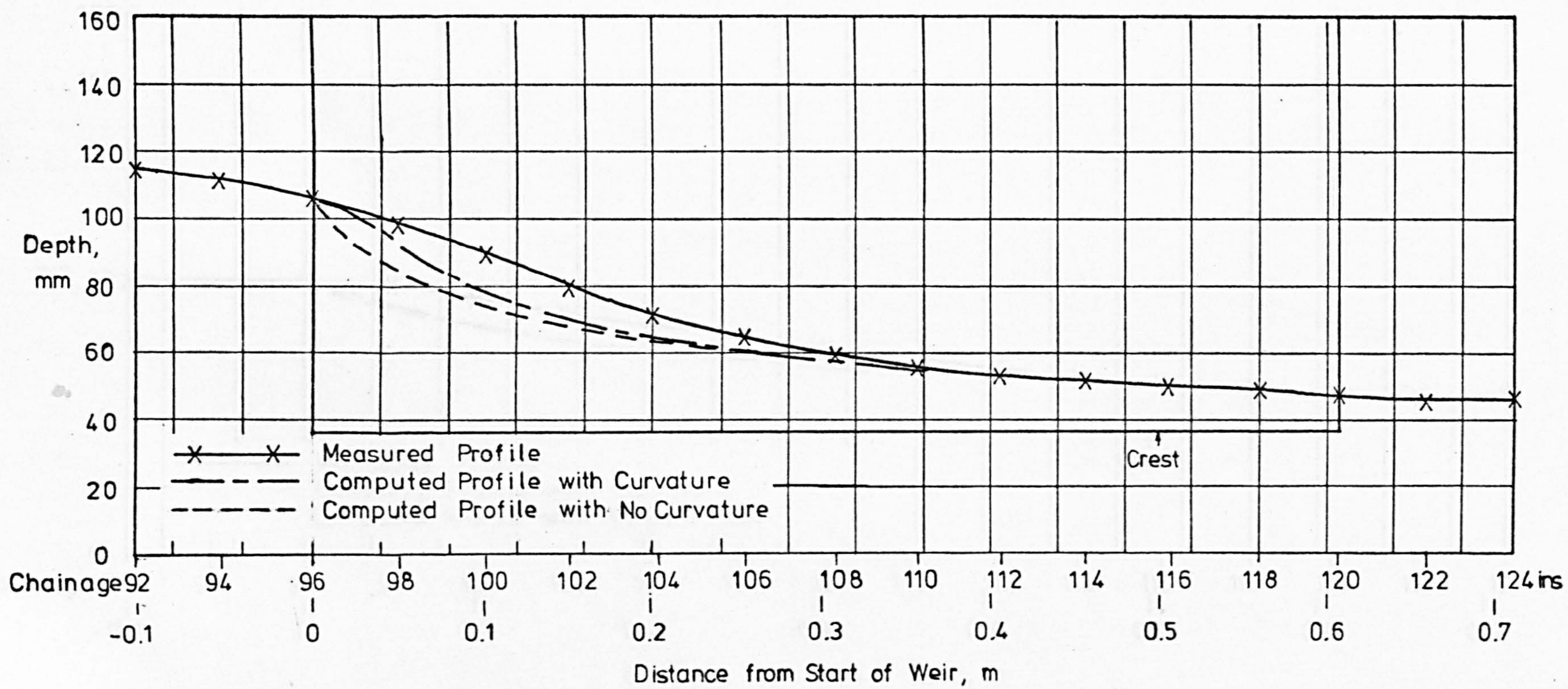

FIG. 6.63 LONGITUDINAL SURFACE PROFILES:
Weir 3: Case IV Flow: Reading No. 78.

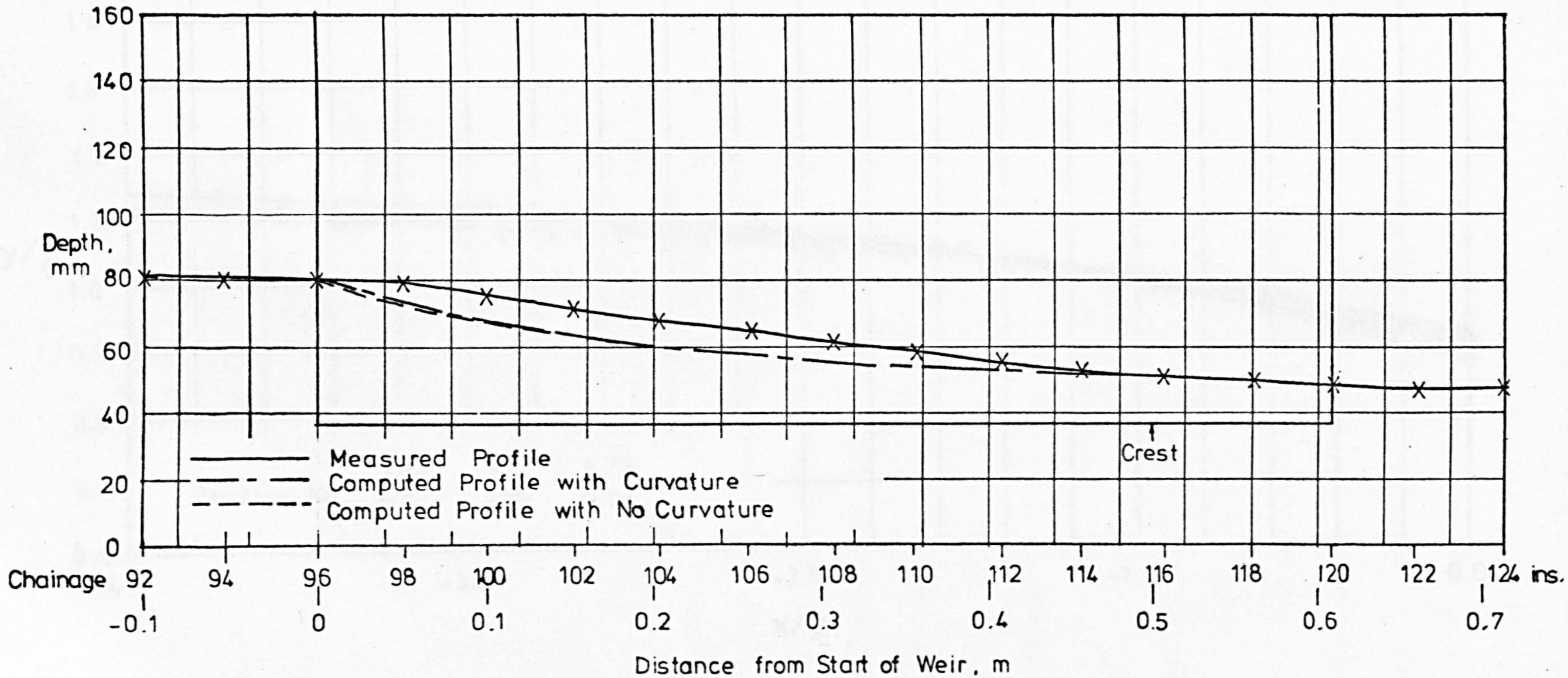

FIG. 6.64 DIMENSIONLESS SURFACE PROFILES UPSTREAM OF WEIR3: Case I Flow.

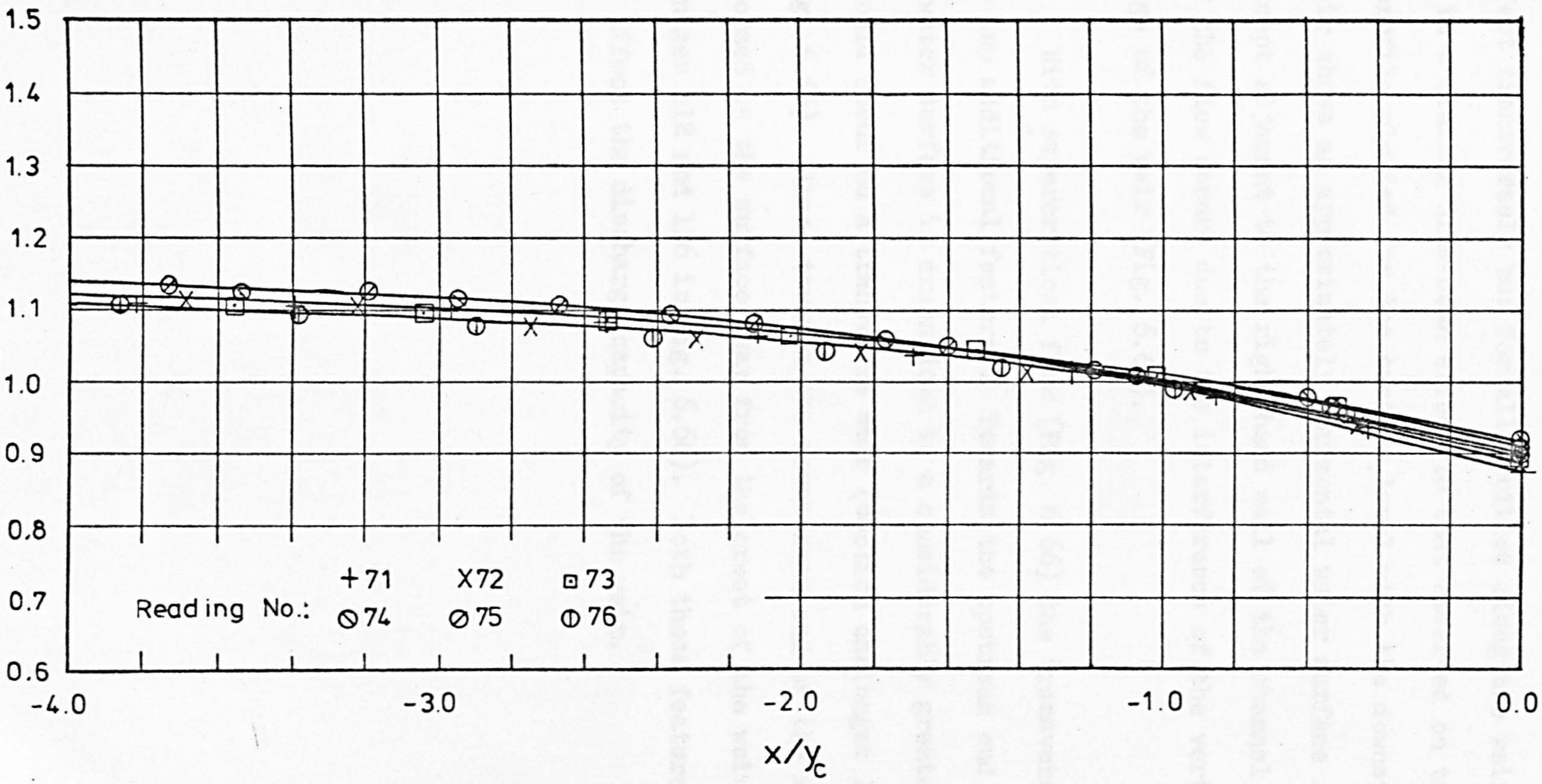

6.6 Transverse Surface Profiles

6.6.1 Figure 6.65 shows typical transverse surface profiles for subcritical flow. At the upstream end of the weir there is no draw-down effect transversely but for all profiles along the weir itself there is a similar draw-down effect to that observed on transverse weirs. The profile plotted for the section level with the downstream end of the weir shows an approximately horizontal water surface at this point except adjacent to the right hand wall of the channel where a bunching of the flow occurs due to the interference of the vertical downstream edge of the weir (Fig. 6.67).

6.6.2 With supercritical flow (Fig. 6.66) the transverse profiles show two additional features. Towards the upstream end of the weir the water surface is drawn down to a considerably greater extent than would occur on a transverse weir (section chainages 100 and 104 in Fig. 6.66). Also, towards the downstream end of the weir a trough is formed in the surface away from the crest of the weir (section chainages 112 and 116 in Fig. 6.66). Both these features are likely to affect the discharge capacity of the weir.

FIG. 6.65 TYPICAL TRANSVERSE SURFACE PROFILES : Case II Flow.

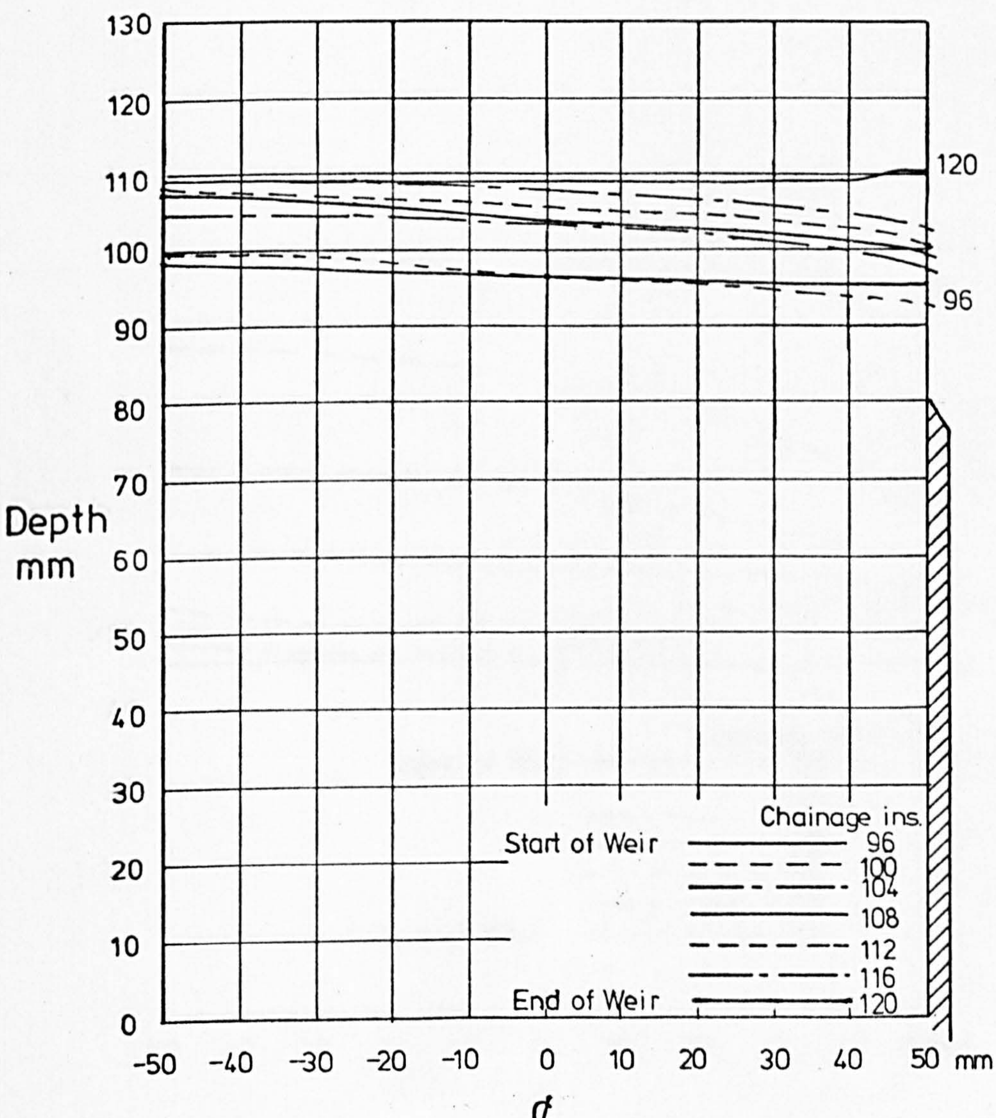

FIG. 6.66 TYPICAL TRANSVERSE SURFACE PROFILES: Case I Flow.

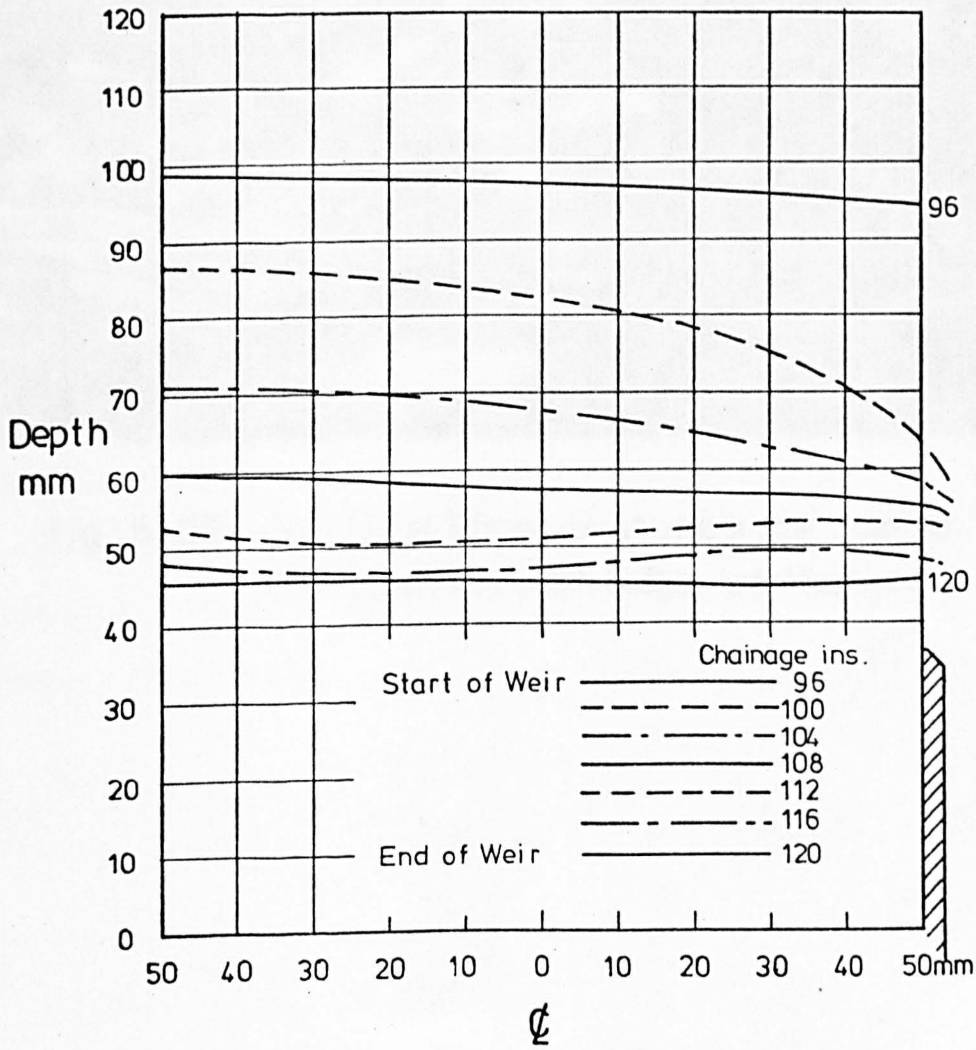

fig. 6. 67 Surface Wave Disturbance due to the Downstream Edge of the Weir.

6.7 Performance of the Mathematical Model for Subcritical Flow

6.7.1 In assessing the performance of the mathematical model described in Chapter 3 the computed upstream discharge, side spill discharge, and upstream depth were compared with measured values for all subcritical readings on Weirs 1, 2, 4 and 5. The results of this comparison are contained in Appendix VIII.

6.7.2 The mean and standard deviation of the percentage errors in Q_1, Q_w and y_1 were computed for each weir. The largest mean errors in Q_1 and Q_w were recorded on Weir 2 (-4.26% and -6.37%) but this weir showed the smallest standard deviation (0.90% and 0.87%). Conversely, Weir 5 showed the smallest mean (-2.18% and -2.71%) and the largest standard deviation (3.15% and 4.82%). Errors in the computed upstream depth did not follow the same pattern. The largest mean and standard deviation were recorded on Weir 4 (-5.94% and 4.24%) and the smallest on Weir 2 (-2.56% and 1.39%). The variation in the mean and standard deviation of errors followed a random pattern and there were no trends that indicated a relationship between the magnitude of error and the dimensions of the weir.

6.7.3 The overall means and standard deviations of errors for all the subcritical results are given in Table 6.4 below.

TABLE 6.4
Means and Standard Deviations of Error, Subcritical Flow

	Mean % Error	S.D. % Error	No. of Readings
Upstream Discharge Q_1	- 2.54	2.46	
Side Spill Discharge Q_n	- 3.39	3.52	104
Upstream Depth y_1	- 4.80	3.26	

Both the mean and standard deviation are small in each case showing that the mathematical model performs well. Furthermore, a comparison between measured and computed surface profiles showed excellent agreement (Figs. 6.58 and 6.59) although the model did not simulate the surface wave that formed at the higher flow rates on Weir 1.

6.7.4 The inclusion of an allowance for curvature made virtually no difference to the computed values confirming that curvature effects are negligible for subcritical flow.

6.8 Performance of the Mathematical Model for Supercritical Flow

6.8.1 In assessing the performance of the mathematical model for supercritical flow the computed downstream discharge, side spill discharge, and downstream depth were compared with measured values, for both Case I and Case IV profiles, and the results are also contained in Appendix VIII. The overall mean and standard deviation of errors are tabulated below.

TABLE 6.5
Mean and Standard Deviations of Error. Supercritical Flow.

	No Curvature Allowance		With Curvature Allowance		No. of Readings
Case I Profiles	Mean % Error	S.D. % Error	Mean % Error	S.D. % Error	
Downstream Discharge Q_2	6.39	1.80	3.64	1.71	18
Side Spill Discharge Q_W	- 8.76	2.27	- 5.03	2.30	
Downstream Depth y_2	4.13	1.12	2.88	1.18	
Case IV Profiles					
Downstream Discharge Q_2	1.18	3.21	0.71	2.47	9
Side Spill Discharge Q_W	- 0.77	5.73	- 0.14	4.97	
Downstream Depth y_2	0.29	1.30	- 0.39	1.13	

6.8.2 When no allowance is made for curvature effects the model shows reasonably good correlation for Case IV profiles but for the Case I results the mean errors are larger. This additional error is further illustrated by the comparison of computed and measured surface profiles shown in Figures 6.61 and 6.62. The slope of the computed profile at the upstream end of the weir is too great when the model does not allow for curvature. This leads to a profile substantially lower than is actually the case and the side spill discharge is therefore underestimated.

6.9 Effect of Modifying the Model to Allow for Curvature.

6.9.1 In order to improve the simulation of supercritical flow the mathematical model was modified to incorporate an allowance for curvature, as described in Chapter 2. The effect was to considerably improve the computations for all the Case I results, as shown in Table 6.5, giving mean and standard deviation of errors of a similar order to those achieved for subcritical flow. An improvement to the computed longitudinal profiles was also observed (Figs. 6.61 and 6.62), the computed curve now following the same shape as the measured profile but still with significantly smaller depths at the upstream end of the weir.

6.9.2 For Case IV profiles, once the Froude Number at the upstream end of the weir exceeds 1.5, curvature effects become negligible and the modified model gives virtually the same profile and computed values of Q_2, Q_w and y_2 as the model not modified for curvature (Fig. 6.63). Thus the modified model was only used for simulating Case IV profiles where the Froude Number was less than 1.5 at the upstream end of the weir, but this still significantly improved the overall accuracy of computation, as shown in Table 6.5.

6.9.3 As an independent check of the theory on which the curvature analysis is based the modified pressure head at the upstream end of the weir was computed for readings 132 to 149 using equation (2.30.3). The computed values are compared with measured values (using the stilling well), and measured depths, in Table 6.3. The curvature analysis significantly modifies the pressure head from its hydrostatic value (equal to the depth) and there is good correlation with measured values for Case I profiles. The theory does, however, underestimate the effects of curvature to some extent which would account for the deviation of the measured and computed profiles shown in Figures 6.61 to 6.63.

6.9.4 In order to verify the distribution of curvature obtained by theoretical analysis (Section 2.6) an attempt was made to measure the curvature of the streamlines directly in the test flume. Streaks of permanganate dye were injected into the flow at various depths a short distance upstream of the weir. Although the curvature effects could be seen to extend below the level of the weir crest, the magnitude of turbulent and secondary currents was sufficient to cause rapid dispersal of the dye and prevent any direct measurements being made.

6.9.5 Specimen velocity traverses were performed in the test flume using a miniature propellor current meter. There was no variation in the velocity over the depth that could be attributed to curvature effects.

6.10 Starting Values

6.10.1 When the mathematical model was initially tested against measured data for subcritical flow the depth at the downstream end of the weir was used as a starting value. The agreement between the measured and computed surface profiles was not as good as had been expected, but inspection of the water surface in the vicinity of the downstream end of the weir revealed the presence of a surface wave (described earlier in section 6.5) and this was found to be affecting the depth measurements locally.

6.10.2 The performance of the mathematical model was significantly improved by starting the computations some distance downstream of the weir, where the depth could be measured without being affected by surface disturbances. The model was modified to compute the gradually varied flow profile back as far as the weir in addition to computing the spatially varied flow profile along the weir itself.

6.10.3 When taking readings on Weir No. 4, depth recordings were made at 76mm and 505mm downstream of the weir so that the effect of the position of the starting depth could be established. A comparison of the two sets of computations is given in Appendix IX. Despite a substantial shift in the position of the starting station of 429mm the mean and standard deviation of errors are only changed slightly, the 76mm values giving errors a little larger than those for the 505mm results.

6.10.4 For supercritical flow computations the depth and discharge at the upstream end of the weir were used as starting values. The starting slope of the water surface was fixed at -0.12 for computations involving an allowance for curvature, and to test the effect of this duplicate computations were performed for readings 71 to 79 using the actual slope at the start of the weir. The actual surface slope was obtained from measured longitudinal surface profiles using a standard finite difference technique as described in Appendix III. The results (Appendix IX) show the effects of this approximation to be negligible.

6.10.5 In practical applications the starting depth at the upstream end of the weir would be obtained from Figure 6.56 for Case I supercritical flow computations.

6.11 Assessment of Possible Errors

6.11.1 The effect of possible errors in readings, due to the scale divisions of the apparatus, on the measured value of C_D has been assessed by conventional error analysis, details of which are given in Appendix VI. A similar analysis for the main results and computations is not possible, however, due to the complex nature of the mathematical model.

6.11.2 In order to assess the possible error in computed values a typical reading was chosen (No. 23) and the possible range of error for each piece of input data was assessed in the usual way. A separate computation was then performed to assess the effects of possible errors in each piece of data in turn on the computed values Q_1 and y_1. The results of those computations are given in Table 6.6 below.

TABLE 6.6
Error Analysis - Mathematical Model

Measured Value	Possible Error	Input Data Affected	Possible Error	Resultant+ Error in Q_1	Resultant + Error in d_1
U-tube Manometer	$\pm$ 1mm	Upstream Discharge	$\pm$0.063 l/s		
Vee Notch Stage	$\pm$ 0.05mm	Side Spill Discharge	$\pm$0.005 l/s		
		Downstream Discharge	$\pm$0.068 l/s	$\pm$0.041 l/s	$\pm$0.172mm
Depth of Flow	$\pm$ 0.05mm	Downstream Depth	$\pm$0.05mm	$\pm$0.008 l/s	$\pm$0.005mm
Temperature	$\pm$ 0.05°C	Viscosity	$\pm 0.002 \times 10^{-6}$ kg/ms	Zero	Zero

+ See overleaf.

+ The resultant error in Q_1 and y_1 is equal to the difference between the computed value of Q_1 (or y_1) with the input data as measured, and the computed value with the input data $\pm$ the possible error.

6.11.3 In addition to the possible errors in the computed values in Table 6.6 the possible errors in the measured upstream discharge and depth must also be considered when assessing the performance of the mathematical model.

If the total possible errors between measured and computed values of Q_1 and y_1 are denoted as dQ_1 and dy_1 respectively then

$$\frac{dQ_1}{Q_1} = \pm \left\{ \underbrace{\left(\frac{0.063}{5.400}\right)^2}_{\text{Possible Error in Measured Value}} + \underbrace{\left(\frac{0.041}{5.193}\right)^2 + \left(\frac{0.008}{5.193}\right)^2}_{\text{Possible Errors in Computed Value}} \right\}^{\frac{1}{2}}$$

$$= \pm\ 0.0142 \quad \text{or} \quad \pm\ \underline{1.42\%}$$

and $$\frac{dy_1}{y_1} = \pm \left\{ \underbrace{\left(\frac{0.05}{95.90}\right)^2}_{\text{Possible Error in Measured Value}} + \underbrace{\left(\frac{0.172}{92.58}\right)^2 + \left(\frac{0.005}{92.58}\right)^2}_{\text{Possible Errors in Computed Value}} \right\}^{\frac{1}{2}}$$

$$= \pm\ 0.0019 \quad \text{or} \quad \pm\ \underline{0.19\%}$$

Thus 1.42% of the observed errors in computed values of Q_1 and 0.19% of the observed errors in computed values of y_1 could be attributed to errors in the readings taken from the experimental apparatus.

6.11.4 It is arguable that the Blasius and Darcy-Weisbach formulae for computing the friction gradient s_f are generally applicable. In view of the smooth surface of the experimental flume and the range of Reynolds' numbers encountered the use of the Blasius equation can be justified in this case, but in practical applications another method of assessing s_f, such as the Manning equation, might be appropriate. Further computations were therefore performed, for readings 15 to 40, using the Manning equation with an appropriate roughness value, instead of the Blasius and Darcy-Weisbach equations, and the results are tabulated in Appendix IX. Table 6.7 summarises the effect of using the Manning equation, and the differences between both the means and the standard deviations is seen to be negligible.

TABLE 6.7

Comparison between Methods of Computing the Friction Gradient s_f

	s_f from Blasius & Darcy-Weisbach		s_f from Manning		No. of Readings
	Mean % Error	S.D. % Error	Mean % Error	S.D. % Error	
Upstream Discharge Q_1	- 4.20	1.85	- 4.15	1.91	
Side Spill Discharge Q_w	- 5.65	2.11	- 5.51	2.14	26
Upstream Depth y_1	- 3.69	2.22	- 3.34	1.97	

6.11.5 Chow[24] recommends an additional term in the computation of the energy gradient to allow for increased eddy effects in diverging or converging flow. Also, it may be argued that the transverse components of the flow alter the velocity distributions and thus affect the value of s_f, but it should be remembered that the magnitude of s_f has only a small effect on the computed values obtained from the mathematical model.

An attempt was made, however, to improve the performance of the mathematical model by applying multiplying factors to s_f to account for any possible increase in its value due to secondary current effects. The result was that the mean errors in the computed values were reduced slightly in certain cases whilst there was a significant overall increase in the standard deviations of the errors.

Attempts to improve the computations in this way were therefore abandoned.

6.12 Performance of the Mathematical Model with Engel's[8] and Gentilini's[11] Data

6.12.1 The performance of the mathematical model, when applied to side weir installations with substantially different dimensions from those used in this investigation, was assessed using the experimental data of Engels[8] and Gentilini[11].

6.12.2 Engels tested single side weirs ranging from 0.5m to 10.0m in length in prismatic rectangular channels with widths varying between 205mm and 2m. His experiments were conducted for subcritical flow and a comparison between his measured values, and corresponding values computed by the mathematical model, is given in Appendix X. Table 6.8 below gives the means and standard deviations of the computed values. There is excellent agreement between computed and measured values of depth and discharge at the upstream end of the weir. The agreement between the measured and computed side spill discharge is not so good, however, the mean error exceeding 20%. Inspection of the actual values of the side spill discharge reveals the reason for this. In all the tests the side spill discharge is very small in comparison with the upstream flow. For reading E 19, for example, the upstream discharge is 103.7 l/s whereas only 8.2 l/s of that passes over the weir. The error in the computed value of Q_1 of 1.543 l/s is small in comparison with Q_1, but it also appears in the computed value of Qw since $Q_w = Q_1 - Q_2$, and as Q_w is only 8.2 l/s the percentage error is appreciable.

TABLE 6.8
Performance of the Model with Engels Data

	Mean % Error	S.D. % Error	No. of Readings
Upstream Discharge Q_1	3.17	5.53	
Side Spill Discharge Q_w	20.23	28.68	19
Upstream Depth y_1	0.24	1.74	

6.12.3 Differences in crest geometry will also affect the value of the coefficient of discharge and this will be reflected in the accuracy of computation.

6.12.4 Using Gentilini's[11] data, results for both subcritical and supercritical flow were available for weirs in a 214mm wide prismatic rectangular channel, with weir lengths of 499mm and 1068mm, and crest heights ranging from 50.9mm to 252.3mm.

6.12.5 A table comparing measured values with those computed from the model appears in Appendix X and the means and standard deviations of errors are given in Table 6.9 below. The computed supercritical values were calculated using upstream depths obtained from Figure 6.56, which would be the method used in practice. Values were also computed, however, using the measured upstream depths, and these also appear in Appendix X. There is little difference between the two sets of computed values.

The mathematical model gives excellent results in this case.

TABLE 6.9
Performance of the Mathematical Model with Gentilini's Data

Subcritical Flow	Mean % Error	S.D. % Error	No. of Readings
Upstream Discharge Q_1	- 1.40	1.76	8
Side Spill Discharge Q_w	- 2.01	2.70	
Upstream Depth y_1	- 0.86	1.03	

Supercritical Flow+	Mean % Error	S.D. % Error	No. of Readings
Downstream Discharge Q_2	2.48	0.69	4
Side Spill Discharge Q_w	- 7.60	2.00	
Downstream Depth y_2	- 1.47	3.99	

+ Upstream depths obtained from Fig. 6.56.

6.13 Performance of De Marchi's[4] Method and Chow's Numerical Integration Method

6.13.1 De Marchi's graphical method has been widely used for analysing side weir flow, and it is appropriate that its accuracy is established and compared with that of the mathematical model. The De Marchi Method was therefore tested against the experimental data obtained during this investigation and the results are given in Appendix XI and summarised below in Table 6.10. In computing the results tabulated in the Appendix, the values of the coefficient of discharge were computed from the Rehbock equation (6.1).

TABLE 6.10
Performance of De Marchi's Method

Subcritical Flow	Mean % Error	S.D. % Error	No. of Readings
Upstream Discharge Q_1	4.95	9.17	103
Side Spill Discharge Q_w	7.57	13.51	
Upstream Depth y_1	- 3.63	4.55	
Supercritical Flow	**Mean % Error**	**S.D. % Error**	**No. of Readings**
Downstream Discharge Q_2	6.00	3.48	27
Side Spill Discharge Q_w	- 8.42	4.87	
Downstream Depth y_2	0.11	2.00	

6.13.2 Comparison between Table 6.10 and Tables 6.4 and 6.5 show De Marchi's method to be substantially worse than the mathematical model and in particular errors in Q_w as high as 43% were recorded for subcritical flow, and 15% for supercritical flow. This is not surprising since the method does not account for the slope of the channel or for friction. In addition it was not possible to compute values for five of the results.

6.13.3 However, De Marchi's method does in general give errors less than 10% so it could prove useful for establishing approximate weir dimensions in design.

6.13.4 Chow's Numerical Integration method[6] was found to give fairly good results for subcritical flow, somewhat worse than the mathematical model but significantly better than De Marchi's method. The accuracy is summarised in Table 6.11 and the detailed results are given in Appendix XI. Values of the coefficient of discharge were again computed from the Rehbock equation (6.1).

TABLE 6.11
Performance of Chow's Numerical Integration Method

Subcritical Flow	Mean % Error	S.D. % Error	No. of Readings
Upstream Discharge Q_1	2.34	5.86	
Side Spill Discharge Q_w	3.87	8.88	103
Upstream Depth y_1	- 4.71	3.94	
Supercritical Flow	**Mean % Error**	**S.D. % Error**	**No. of Readings**
Downstream Discharge Q_2	5.00	3.27	
Side Spill Discharge Q_w	- 6.69	4.88	27
Downstream Depth y_2	2.81	2.18	

6.13.5 The method can be easily arranged into tabular form and is recommended for the computation of side weir flow when access to a digital computer is not available.

CHAPTER 7. CONCLUSIONS

7.1.1 Whatever method of analysis is used to determine the discharge over a side weir reliable values of the coefficient of discharge are required. It has been shown conclusively that the coefficient of discharge is unaffected by longitudinal velocity components and that it takes the same value as if the weir were a full width transverse weir. Thus, for the sharp crested weir used in this investigation, the Rehbock equation would be appropriate for computing C_D. If a different crest geometry were to be used then an expression for C_D under transverse conditions would have to be established prior to any computations.

7.1.2 The values of the velocity energy coefficient α and momentum flux correction factor β were found to be within the range of values normally applicable to open channel flow, although some reduction in their values was observed with increasing longitudinal velocity.

7.1.3 The formula proposed by Ackers[5], that defines the uniform taper of a rectangular channel which produces a constant head along a side weir, performed well, and only minor adjustments to the downstream discharge were required to achieve a constant head and constant longitudinal velocity in practice.

7.1.4 When subcritical flow occurs along a side weir with a downstream orifice or sluice control the relationship between the upstream and side spill discharge is linear. The increase in downstream discharge is only small for large increases in upstream discharge. A downstream weir does not give such good control to the flow and the downstream discharge rises appreciably with increasing upstream flow.

7.1.5 Subcritical flow conditions will exist along a side weir until the upstream discharge rises to a value where the upstream specific energy exceeds twicethe crest height whereupon the subcritical flow changes to supercritical flow and the surface profile falls. If the downstream flow is throttled a hydraulic jump will form on the weir, but otherwise the flow will generally be supercritical over the whole length of the weir.

7.1.6 When subcritical flow in the upstream channel is drawn down to form supercritical flow along the weir there is a relationship between the depth at the upstream end of the weir, the crest height, and the critical depth in the upstream flow. This relatinnship is dependent upon the slope of the channel and is shown in dimensionless form in Figure 6.56. Both the side spill and downstream discharges increase linearly with increasing upstream discharge, the downstream discharge always exceeding the side spill flow. Towards the upstream end of the weir there is an appreciable curvature of the flow which affects the distribution of pressure with depth.

7.1.7 A mathematical model has been developed capable of simulating both subcritical and supercritical flow to a high degree of accuracy (both mean and standard deviations of errors being less than 5%). The model incorporates an allowance for curvature which is used for supercritical flows where the Froude Number at the upstream end of the weir does not exceed 1.5.

7.1.8 The theory on which the mathematical model is based follows well established analytical techniques which agree with the work of previous investigations. Standard integration techniques have been used and the model only requires empirical values of the coefficient of discharge and momentum flux correction factor, both of which have been thoroughly investigated and found to agree with well established values.

7.1.9 The mathematical model gives significantly better results than methods previously available and has been shown to perform well using data from previous investigations not undertaken by the author. The model may therefore be applied with confidence to any size of side weir installation in a prismatic rectangular channel.

7.1.10 Since the theory is based on a generalised momentum analysis of the flow it may readily be extended to cover non-prismatic and non-rectangular channels.

REFERENCES

1. Parmley W.C., "The Walworth Sewer, Cleveland, Ohio", Transactions of the American Society of Civil Engineers, Paper No. 1011, 1905.

2. Nimmo W.H.R., "Side Spillways for Regulating Diversion Canals", Transactions of the American Society of Civil Engineers, Paper No. 1694, 1928.

3. De Marchi G., "Saggio di teoria del funzionamento degli stramazzi laterali", L'Energia Elettrica, Vol XI, Nov. 1934.

4. De Marchi G, "Des Formes de la Surface Libre de Courants Permanents avee Debit Progressivement Croissant ou Progressivement Decroissant daus un Canal de Section Constante", Revue Generale de l'Hydraulique, March/ April 1947.

5. Ackers P., "A Theoretical Consideration of Side Weirs as Storm Water Overflows", Proceedings of the Institution of Civil Engineers, Vol. 6, Feb. 1957.

6. Chow V.T., Discussion of "Flood Protection of Canals by Lateral Spillways", by H. Tults, Proceedings of the American Society of Civil Engineers, Journal of the Hydraulics Division, Vol. HY2, pp 47 to 49, April 1957.

7. Smith K.V., "Computer Programming for Flow Over Side Weirs", Proceedings of the American Society of Civil Engineers, Journal of the Hydraulics Division, Vol. HY3, March 1973.

8. Engels H., "Mitteilungen ausdem Dresdener Flußbau-Laboratorium", Forschungsarbeiten auf dem Gebiete des Ingenieurwesens, Dec. 1917.

9. Coleman S. and Smith D., "The Discharging Capacities of Side Weirs", Proceedings of the Institution of Civil Engineers, 1923.

10. Favre H. and Braendle F., "Expériences sur le Mouvement Permanent de l'Eau daus les Canaux Découverts, avec Apport ou Prélèvement le long du Courant", Bulletin Technique de la Suisse Romande, No. 8, April 1937.

11. Gentilini B., "Ricerche Sperimentali Sugli Sfioratori Longitudinali", L'Energia Elettrica, Vol. 15, Sept. 1938.

12. Schmidt M., "Zur Frage des Abflusses uber Streichwehre", Institut fur Wasserbau, Universitat Berlin - Charlottenburg, 1954.

13. Allen J.W., "The Discharge of Water over Side Weirs in Circular Pipes", Proceedings of the Institution of Civil Engineers, Vol. 6, Feb. 1957.

14. Collinge V.K., "The Discharge Capacity of Side Weirs", Proceedings of the Institution of Civil Engineers, Vol. 6, Feb. 1957.

15. Frazer W., "The Behaviour of Side Weirs in Prismatic Rectangular Channels", Proceedings of the Institution of Civil Engineers, Vol. 6, Feb. 1957.

16. El-Khashab A. and Smith K.V.H., "Experimental Investigation of Flow over Side Weirs", Proceedings of the American Society of Civil Engineers, Journal of the Hydraulics Division, Vol. HY9, Paper No. 12402, September 1976.

17. Balmforth D.J. and Sarginson E.J., Discussion of "Experimental Investigation of Flow over Side Weirs", by El-Khashab and Smith, Proceedings of the American Society of Civil Engineers, Journal of the Hydraulics Division, Vol. HY8, pp 941 to 943, August 1977.

18. Yen B.C. and Wenzel H.G., "Dynamic Equations for Steady Spatially Varied Flow", Proceedings of the American Society of Civil Engineers, Journal of the Hydraulics Division, Vol. HY3, Paper No. 7179, March 1970.

19. Rehbock T., "Wassermessung mit Scharf Kautigen uber fallwehren, Z. Ver. dt Ing, 1929, Vol. 73, pp 817-823.

20. Jaeger C., "Engineering Fluid Mechanics", Trans. by P.O. Wolf, Blackie, 1961.

21. Humpidge H.B. and Moss W.D., "The Development of a Comprehensive Computer Program for the Calculation of Flow Profiles in Open Channels", Proceedings of The Institution of Civil Engineers, Paper 7406, September 1971.

22. Ralston A., "A First Course in Numerical Analysis", McGraw-Hill Ltd., London, 1965.

23. British Standard BS3680 Part 4A "Methods of Measurement of Liquid Flow in Open Channels", H.M.S.O. 1965.

24. Chow V.T., "Open Channel Hydraulics", McGraw-Hill Ltd., London, 1959, page 267.

APPENDICES

APPENDIX I

Balmforth, D.J. and Sarginson, E.J. Discussion of "Experimental Investigation of Flow over Side Weirs", by El-Khashab, A. and Smith, K.V.H., Proceedings of the American Society of Civil Engineers, Journal of the Hydraulics Division, Vol HY8, pp 941 to 943, August 1977.

Experimental Investigation of Flow over Side Weirs[a]

Discussion by David J. Balmforth[4] and Edward J. Sarginson[5]

The authors have developed an interesting method of analyzing side weir flows; the writers would like to compare the authors' findings with the results of similar investigations carried out in Sheffield, England. The authors' use of a longitudinal velocity component of the side spill flow, u, involves the use of empirical correlations that cannot be extrapolated with certainty beyond the range of the authors' tests. Also, for subcritical flow, a preliminary computation is required to estimate u. The computational method suggested (6) involves a step procedure requiring an iterative solution at each step. The writers suggest the following method that overcomes these drawbacks.

In the momentum analysis, if d is the depth at the center line, it may be assumed that the longitudinal velocity with which the side spill flow initially deviates from the mainstream is equal to the mean velocity of the mainstream. Eq. 14 then becomes

$$\frac{dd}{dx} = \frac{S_o - S_f + \dfrac{Vq}{gA}(2\beta - 1)}{1 - \beta\dfrac{Q^2 T}{gA^3}} \qquad (17)$$

The assumption inherent in Eq. 17 is compatible with the authors' findings, since at any cross section the value of u corresponds to the mean velocity some distance upstream. This is generally greater than the mean velocity at the section under consideration.

For a rectangular section:

$$V = \frac{Q_x}{Bd} = \frac{Q_1 - \int_0^x q\,dx}{Bd} \qquad (18)$$

$$\text{Let} \quad w = Vd = \frac{Q_1 - \int_0^x q\,dx}{B} \qquad (19)$$

$$\text{Differentiating:} \quad \frac{dw}{dx} = -\frac{q}{B} = -\frac{C_w}{B}\sqrt{g}\,(d - c)^{1.5} \qquad (20)$$

---

[a] September, 1976, by Ahmed El-Khashab and Kenneth V. H. Smith (Proc. Paper 12402).

[4] Sr. Lect. in Civ. Engrg., Sheffield City Polytechnic, Sheffield, England.

[5] Sr. Lect. in Civ. Engrg., Univ. of Sheffield, Sheffield, England.

Eq. 17 becomes

$$\frac{dd}{dx} = \frac{S_o - S_f + \dfrac{qw}{gBd^2}(2\beta - 1)}{1 - \dfrac{\beta w^2}{gd^3}} \qquad (21)$$

The friction slope, S_f, is determined by a suitable channel flow formula (e.g., Manning). The writers used a fourth-order Runge-Kutta method for the simultaneous solution of Eqs. 20 and 21. It was necessary to find the coefficients, C_w and β, experimentally before the method could be used. The former was found by measuring the discharge over a sharp-edged side weir. A constant head was achieved by tapering the channel over the length of the weir, and C_w was found to be unaffected by longitudinal velocity components, and came within $\pm 1\%$ of Rehbock's values for a transverse sharp-edged weir. Values of β were found from velocity traverses to vary between 1.04 and 1.05.

TABLE 1.—Accuracy of Writers' Method of Computation

Upstream flow (1)	Flow along weir section (2)	Number of tests (3)	Computed channel flow (4)	Error in Computed Flow, as a percentage: Mean value (5)	Error in Computed Flow, as a percentage: Standard deviation (6)
Subcritical	Subcritical	105	Upstream	−2.8	2.3
Supercritical	Supercritical	9	Downstream	+1.4	3.2
Subcritical	Supercritical	18	Downstream	+6.6	1.8

TABLE 2.—Values of d_1/d_c

S_o (1)	c/d_1: 0.3 (2)	0.35 (3)	0.4 (4)	0.6 (5)
0	0.877	0.898	0.915	—
0.0038	0.864	0.886	0.905	—
0.0069	0.849	0.871	0.892	0.957

Tests were made over a wide range of weir lengths and heights, and the results are summarized in Table 1. In the third case the mean error is significantly larger, and this was attributed to streamline curvature at the upstream end of the weir. Also in this case, the writers found that the ratio d_1/d_c depended on the weir height and channel bed slope, as summarized in Table 2. These values gave more accurate flow computations than the authors' recommended value of 0.93 (see Fig. 10).

The writers' method gives good correlation with measured values. Since the only empirically derived values used in the computation are C_w and β, which were found to correspond with well established values, the method is applicable to any side weir installation in a rectangular channel. The method can also be adapted to suit nonrectangular sections.

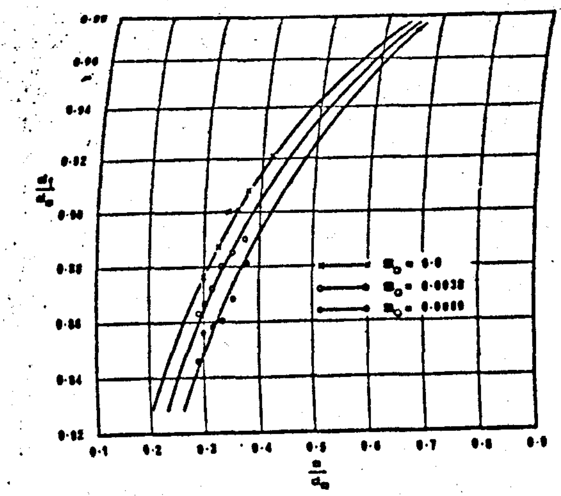

FIG. 10.—Relationship for d_1, Upstream Channel Flow Subcritical, Weir Channel Flow Supercritical

Appendix.—Notation

The following symbols are used in this discussion:

Q_x = mainstream discharge at section x; and
w = $V \times d$.

Exact Solution of Gradually Varied Flow[a]

Discussion by John Allen[4] and Keith J. Enever[5]

The writers wish to compliment the author on producing such a versatile method for solving the problem of calculating water surface profiles in open channels of complex cross-sectional shape. In his introduction, the author suggests that nothing significant has been achieved in the derivation of exact solutions

[a]September, 1976, by Mohammad Akram Gill (Proc. Paper 12406).
[4]Sr. Lect. in Civ. Engrg., Queen Mary Coll., Univ. of London, London, England.
[5]Lect. in Civ. Engrg., The City Univ., London, England.

APPENDIX II

(a) Details of the Computer Program used to obtain the Theoretical Distributions of Curvature and Velocity.

(b) Computed Curvature and Velocity Distributions.

(a) Details of the Computer Program used to obtain the Theoretical Distributions of Curvature and Velocity.

II.1 Two computer programs were used to obtain theoretical distributions of velocity and curvature. For positive surface curvatures the programme DISTN was used, whilst for negative surface curvatures RDISTN was used. Both programs follow the same logical progression as shown in the flow chart below (Fig. II.1), and only differ in the form of the mathematical expressions used, after the theory given in Chapter 2. The principal mathematical equations used are tabulated in Table II.1.

TABLE II.1. Principal Equations used in DISTN and RDISTN

Variable Computed	Equation used in DISTN	Equation used in RDISTN
K_s	$\sqrt{yt/(1+yt)}$	$\sqrt{-yt/(1+yt)}$
ψ_n	$\cos^{-1}(n\ K_s)$	$\sinh^{-1}(n\ K_s)$
Curvature	$\dfrac{n\ K_s^{\ 2}}{y(1 - n^2 K_s^{\ 2})}$	$-\dfrac{n\ K_s^{\ 2}}{y(1 + n^2 K_s^{\ 2})}$
Velocity	$\dfrac{\psi_n - \psi_{n-1}}{y_n - y_{n-1}}$	$\dfrac{\psi_n - \psi_{n-1}}{y_n - y_{n-1}}$

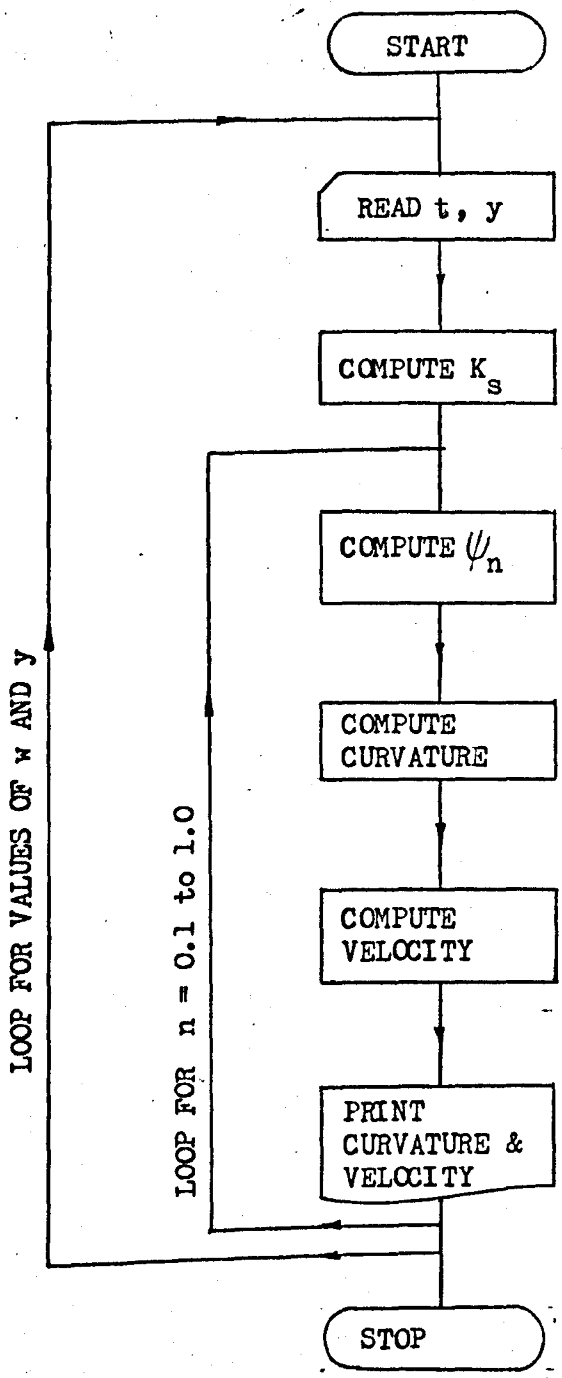

Fig. II.1

Flow Chart for Programs DISTN and RDISTN

A listing and specimen printout for programs DISTN and RDISTN are given overleaf.

Tables of velocity and curvature distributions are contained in part (b).

```
/ID D.J.PALMFORTH                  010 050                                        10H07M    MON MAR 06, 1978
/ETC            729 MUSIC JOB                                          2
/LOAD FORTG1

 FORTRAN IV G1  RELEASE 2.0                MAIN                DATE = MON MAR 06, 1978                    PAGE 0001

                      DIMENSION Z(10),CURV(10),U(10)
                      WRITE(6,3)
                    3 FORMAT(5X,'PROGRAM DISTN'//)
                    5 READ(5,10)D2YDX,Y
                   10 FORMAT(2F10.0)
                      IF(D2YDX.LT.0.0)GOTO100
                      WRITE(6,12)
                   12 FORMAT(11X,'Y',10X,'U',10X,'CURV',8X,'N',5X,'PROP CURV'/)
                      A=D2YDX*Y
                      AKS=SQRT(A/(1.+A))
                      CUM=0.0
                      DO50 N=1,10
                      EN=N/10.
                      IF(N.GT.1)EM=(N-1)/10.
                      Z(N)=EN*Y
                      CURV(N)=EN*AKS*AKS/(Y*(1.-EN*EN*AKS*AKS))
                      IF(N.EQ.1)U(N)=10.*(1.5709-ARCOS(EN*AKS))/Y
                      IF(N.GT.1)U(N)=10.*(ARCOS(EM*AKS)-ARCOS(EN*AKS))/Y
                      PROP=CURV(N)/D2YDX
                      WRITE(6,22)U(N)
                      WRITE(6,20)Z(N),CURV(N),EN,PROP
                   20 FORMAT(10X,F10.7,10X,3F10.7)
                   22 FORMAT(20X,F10.7)
                      CUM=CUM+U(N)
                   50 CONTINUE
                      AMEAN=CUM/10.0
                      WRITE(6,55)AMEAN
                   55 FORMAT(10X,'MEAN VELOCITY= ',F10.7///)
                      GOTO5
                  100 CALL EXIT
                      END

   *OPTIONS IN EFFECT*  NOTERM,ID,EBCDIC,SOURCE,NOLIST,NODECK,LOAD,NOMAP,NOTEST
   *OPTIONS IN EFFECT*  NAME = MAIN    , LINECNT =       56
   *STATISTICS*    SOURCE STATEMENTS =       31,PROGRAM SIZE = 0004F2
   *STATISTICS*  NO DIAGNOSTICS GENERATED
 /DATA                                                                                    3.4S
 003880 BYTES USED
 EXECUTION BEGINS      3.9S
     PROGRAM DISTN


           Y          U          CURV        N     PROP CURV

                     2.1927824
           0.0100000           0.0476417 0.1000000 0.0952834
                     2.1833410
           0.0200000           0.0954198 0.2000000 0.1908396
                     2.1855345
           0.0300000           0.1434720 0.3000000 0.2869439
                     2.1885862
           0.0400000           0.1919385 0.4000000 0.3838770
                     2.1927824
           0.0500000           0.2409639 0.5000000 0.4819279
                     2.1981230
           0.0600000           0.2906976 0.6000000 0.5813953
```

245

```
0.0700000      2.2045126      0.3412970 0.7000000 0.6825939
0.0800000      2.2120466      0.3929274 0.8000000 0.7858548
0.0900000      2.2208204      0.4457655 0.9000000 0.8915310
0.1000000      2.2306433      0.5000003 1.0000000 1.0000000
MEAN VELOCITY=  2.2009153
```



```
END OF JOB D.J.BALMFORT          AT 10H07M MON MAR 06, 1978 EXECUTE TIME      0.07 MINS.
        6 CARDS READ        72 LINES PRINTED        0 CARDS PUNCHED 0 TAPE MOUNTS 0 DISK MOUNTS
```

```
      DIMENSION Z(10),CURV(10),U(10)
      REAL*8 X1,X2,EM,EN,AKS
      COMMON EM,EN,AKS
      EXTERNAL FUN1,FUN2
      WRITE(6,3)
    3 FORMAT(5X,'PROGRAM RCISTN'//)
    5 READ(5,10)D2YDX,Y
   10 FORMAT(2F10.0)
      IF(Y.LT.0.0)GOTO100
      WRITE(6,12)
   12 FORMAT(6X,'Y',10X,'U',10X,'CURV',8X,'N',5X,'PROP CURV'/)
      A=D2YDX*Y
      AKS=SQRT(-A/(1.+A))
      CUM=0.0
      DO50 N=1,10
      EN=N
      EN=EN/10.
      IF(N.GT.1)EM=EN-0.1
      Z(N)=EN*Y
      CURV(N)=-EN*AKS*AKS/(Y*(1.+EN*EN*AKS*AKS))
      CALL C05 AAF(-10.0D0,10.0D0,0.0000010D0,0.0000010D0,FUN1,X1,1)
      CALL C05 AAF(-10.0D0,10.0D0,0.0000010D0,0.0000010D0,FUN2,X2,1)
      IF(IFAIL.GT.0)WRITE(6,15)
   15 FORMAT(5X,'FUNCTION HAS SAME SIGN AT INTERVAL LIMITS'/)
      IF(N.EQ.1)U(N)=10.*X1/Y
      IF(N.GT.1)U(N)=10.*(X1-X2)/Y
      PROP=CURV(N)/D2YDX
      WRITE(6,22)U(N)
      WRITE(6,20)Z(N),CURV(N),EN,PROP
   20 FORMAT(5X,F10.7,10X,3F10.7)
   22 FORMAT(15X,F10.7)
      CUM=CUM+U(N)
   50 CONTINUE
      AMEAN=CUM/10.0
      WRITE(6,55)AMEAN
   55 FORMAT(5X,'MEAN VELOCITY =',F10.7///)
      GOTO5
  100 CALL EXIT
      END
```



```
*OPTIONS IN EFFECT*  NOTERM,ID,EBCDIC,SOURCE,NOLIST,NODECK,LOAD,NOMAP,NOTEST
*OPTIONS IN EFFECT*  NAME = MAIN     , LINECNT =       56
*STATISTICS*     SOURCE STATEMENTS =        39,PROGRAM SIZE = 000586
*STATISTICS*  NO DIAGNOSTICS GENERATED
```



```
      DOUBLE PRECISION FUNCTION FUN1(X)
      REAL*8 EM,EN,AKS,X
      COMMON EM,EN,AKS
      FUN1=DSINH(X)-EN*AKS
      RETURN
      END
```

```
*OPTIONS IN EFFECT*  NOTERM,ID,EBCDIC,SOURCE,NOLIST,NODECK,LOAD,NOMAP,NOTEST
*OPTIONS IN EFFECT*  NAME = FUN1     , LINECNT =       56
```

```
*STATISTICS*    SOURCE STATEMENTS =        6,PROGRAM SIZE = 000152
*STATISTICS*  NO DIAGNOSTICS GENERATED
```



```
      DOUBLE PRECISION FUNCTION FUN2(X)
      REAL*8 EM,EN,AKS,X
      COMMON EM,EN,AKS
      FUN2=DSINH(X)-EM*AKS
      RETURN
      END
```

```
*OPTIONS IN EFFECT*  NOTERM,ID,EBCDIC,SOURCE,NOLIST,NODECK,LOAD,NOMAP,NOTEST
*OPTIONS IN EFFECT*  NAME = FUN2    , LINECNT =       56
*STATISTICS*    SOURCE STATEMENTS =        6,PROGRAM SIZE = 000152
*STATISTICS*  NO DIAGNOSTICS GENERATED

*STATISTICS*  NO DIAGNOSTICS THIS STEP
/DATA                                                                6.2S
004920 BYTES USED
EXECUTION BEGINS      8.8S
    PROGRAM RDISTN


   Y            U            CURV          N       PROP CURV

             2.2939358
  0.0100000               -0.0526039 0.1000000 0.1052077
             2.2929535
  0.0200000               -0.1050420 0.2000000 0.2100840
             2.2909355
  0.0300000               -0.1571503 0.3000000 0.3143007
             2.2868271
  0.0400000               -0.2087682 0.4000000 0.4175365
             2.2821083
  0.0500000               -0.2597402 0.5000000 0.5194805
             2.2762518
  0.0600000               -0.3099173 0.6000000 0.6198347
             2.2692871
  0.0700000               -0.3591586 0.7000000 0.7183172
             2.2612448
  0.0800000               -0.4073320 0.8000000 0.8146640
             2.2521620
  0.0900000               -0.4543160 0.9000000 0.9086320
             2.2420797
  0.1000000               -0.5000000 1.0000000 1.0000000
  MEAN VELOCITY = 2.2747784
```



```
END OF JOB D.J.BALMFORT          AT 10H07M MON MAR 06, 1978 EXECUTE TIME       0.16 MINS.
        6 CARDS READ      105 LINES PRINTED        0 CARDS PUNCHED 0 TAPE MOUNTS 0 DISK MOUNTS
```

(b) Computed Curvature and Velocity Distributions.

TABLE II.2. Theoretical Velocity and Curvature Distributions Positive Curvature.

y m	u m/s	Curv. m^{-1}	N	Prop Curv
0.010	1.005	0.0099	0.1	0.099
0.020	0.995	0.0198	0.2	0.198
0.030	0.995	0.0297	0.3	0.297
0.040	0.996	0.0397	0.4	0.397
0.050	0.996	0.0496	0.5	0.496
0.060	0.997	0.0596	0.6	0.596
0.070	0.997	0.0696	0.7	0.696
0.080	0.998	0.0797	0.8	0.797
0.090	0.999	0.0898	0.9	0.898
0.100	0.999	0.1000	1.0	1.000

MEAN VELOCITY = 0.998 m/s

y m	u m/s	Curv. m^{-1}	N	Prop Curv
0.010	1.411	0.0196	0.1	0.098
0.020	1.401	0.0392	0.2	0.196
0.030	1.401	0.0589	0.3	0.295
0.040	1.402	0.0787	0.4	0.393
0.050	1.403	0.0985	0.5	0.493
0.060	1.404	0.1185	0.6	0.592
0.070	1.406	0.1386	0.7	0.693
0.080	1.408	0.1589	0.8	0.794
0.090	1.410	0.1793	0.9	0.897
0.100	1.413	0.2000	1.0	1.000

MEAN VELOCITY = 1.406 m/s

TABLE II.2. continued

y m	u m/s	Curv. m^{-1}	N	Prop Curv
	1.717			
0.010		0.0291	0.1	0.097
	1.707			
0.020		0.058	0.2	0.194
	1.708			
0.030		0.0876	0.3	0.292
	1.710			
0.040		0.1170	0.4	0.390
	1.712			
0.050		0.1466	0.5	0.489
	1.714			
0.060		0.1766	0.6	0.589
	1.717			
0.070		0.2068	0.7	0.689
	1.721			
0.080		0.2374	0.8	0.791
	1.725			
0.090		0.2684	0.9	0.895
	1.730			
0.100		0.3000	1.0	1.000
MEAN VELOCITY = 1.716 m/s				
y m	**u m/s**	**Curv. m^{-1}**	**N**	**Prop Curv**
	1.972			
0.010		0.0384	0.1	0.096
	1.962			
0.020		0.0770	0.2	0.193
	1.963			
0.030		0.1157	0.3	0.289
	1.966			
0.040		0.1548	0.4	0.387
	1.969			
0.050		0.1942	0.5	0.485
	1.973			
0.060		0.2340	0.6	0.585
	1.977			
0.070		0.2744	0.7	0.686
	1.983			
0.080		0.3155	0.8	0.789
	1.989			
0.090		0.3573	0.9	0.893
	1.996			
0.100		0.4000	1.0	1.000
MEAN VELOCITY = 1.975 m/s				

TABLE II.2. continued

y m	u m/s	Curv. m^{-1}	N	Prop Curv
0.010	2.193	0.0477	0.1	0.095
0.020	2.183	0.0954	0.2	0.191
0.030	2.186	0.1435	0.3	0.287
0.040	2.189	0.1919	0.4	0.384
0.050	2.193	0.2410	0.5	0.482
0.060	2.198	0.2907	0.6	0.581
0.070	2.205	0.3413	0.7	0.683
0.080	2.212	0.3929	0.8	0.786
0.090	2.221	0.4458	0.9	0.891
0.100	2.231	0.5000	1.0	1.000
MEAN VELOCITY = 2.201 m/s				

y m	u m/s	Curv. m^{-1}	N	Prop Curv
0.010	2.390	0.0566	0.1	0.094
0.020	2.381	0.1135	0.2	0.189
0.030	2.384	0.1707	0.3	0.284
0.040	2.387	0.2285	0.4	0.381
0.050	2.393	0.2871	0.5	0.478
0.060	2.400	0.3467	0.6	0.578
0.070	2.408	0.4075	0.7	0.679
0.080	2.418	0.4699	0.8	0.783
0.090	2.429	0.5339	0.9	0.890
0.100	2.442	0.6000	1.0	1.000
MEAN VELOCITY = 2.403 m/s				

TABLE II.2. continued

y m	u m/s	Curv. m^{-1}	N	Prop Curv
	2.569			
0.010		0.0655	0.1	0.094
	2.560			
0.020		0.1312	0.2	0.187
	2.563			
0.030		0.1974	0.3	0.282
	2.568			
0.040		0.2645	0.4	0.378
	2.575			
0.050		0.3325	0.5	0.475
	2.584			
0.060		0.4020	0.6	0.574
	2.594			
0.070		0.4731	0.7	0.676
	2.606			
0.080		0.5462	0.8	0.780
	2.621			
0.090		0.6217	0.9	0.888
	2.637			
0.100		0.7000	1.0	1.000
MEAN VELOCITY = 2.588 m/s				

y m	u m/s	Curv. m^{-1}	N	Prop Curv
	2.732			
0.010		0.0741	0.1	0.093
	2.724			
0.020		0.1486	0.2	0.186
	2.728			
0.030		0.2237	0.3	0.280
	2.734			
0.040		0.2998	0.4	0.375
	2.742			
0.050		0.3774	0.5	0.472
	2.753			
0.060		0.4566	0.6	0.571
	2.765			
0.070		0.5380	0.7	0.673
	2.780			
0.080		0.6221	0.8	0.778
	2.798			
0.090		0.7092	0.9	0.887
	2.818			
0.100		0.8000	1.0	1.000
MEAN VELOCITY = 2.757 m/s				

TABLE II.2. continued

y m	u m/s	Curv. m^{-1}	N	Prop Curv
0.010	2.884	0.0826	0.1	0.092
0.020	2.876	0.1657	0.2	0.184
0.030	2.881	0.2496	0.3	0.277
0.040	2.888	0.3347	0.4	0.372
0.050	2.898	0.4215	0.5	0.468
0.060	2.910	0.5106	0.6	0.567
0.070	2.925	0.6024	0.7	0.669
0.080	2.943	0.6974	0.8	0.775
0.090	2.963	0.7964	0.9	0.885
0.100	2.987	0.9000	1.0	1.000

MEAN VELOCITY = 2.916 m/s

y m	u m/s	Curv. m^{-1}	N	Prop Curv
0.010	3.026	0.0910	0.1	0.091
0.020	3.018	0.1825	0.2	0.182
0.030	3.024	0.2750	0.3	0.275
0.040	3.032	0.3690	0.4	0.369
0.050	3.043	0.4651	0.5	0.465
0.060	3.058	0.5639	0.6	0.564
0.070	3.075	0.6660	0.7	0.666
0.080	3.095	0.7722	0.8	0.772
0.090	3.119	0.8832	0.9	0.883
0.100	3.147	1.0000	1.0	1.000

MEAN VELOCITY = 3.064 m/s

TABLE II.3 Theoretical Velocity and Curvature Distributions Negative Curvature.

y m	u m/s	Curv. m^{-1}	N	Prop Curv
0.010		-0.0101	0.1	0.101
	1.005			
0.020		-0.0202	0.2	0.202
	1.005			
0.030		-0.0303	0.3	0.303
	1.005			
0.040		-0.0403	0.4	0.403
	1.005			
0.050		-0.0504	0.5	0.504
	1.004			
0.060		-0.0604	0.6	0.604
	1.004			
0.070		-0.0704	0.7	0.704
	1.002			
0.080		-0.0803	0.8	0.803
	1.002			
0.090		-0.0902	0.9	0.902
	1.001			
0.100		-0.1000	1.0	1.000

MEAN VELOCITY = 1.104 m/s

y m	u m/s	Curv. m^{-1}	N	Prop Curv
	1.429			
0.010		-0.0204	0.1	0.102
	1.428			
0.020		-0.0408	0.2	0.204
	1.428			
0.030		-0.0611	0.3	0.306
	1.427			
0.040		-0.0814	0.4	0.407
	1.426			
0.050		-0.1015	0.5	0.508
	1.424			
0.060		-0.1216	0.6	0.608
	1.423			
0.070		-0.1414	0.7	0.707
	1.421			
0.080		-0.1612	0.8	0.806
	1.418			
0.090		-0.1807	0.9	0.903
	1.416			
0.100		-0.2000	1.0	1.000

MEAN VELOCITY = 1.424 m/s

TABLE II.3. continued

y m	u m/s	Curv. m^{-1}	N	Prop Curv
	1.759			
0.010		-0.0310	0.1	0.103
	1.758			
0.020		-0.0618	0.2	0.206
	1.757			
0.030		-0.0925	0.3	0.308
	1.756			
0.040		-0.1231	0.4	0.410
	1.753			
0.050		-0.1535	0.5	0.512
	1.751			
0.060		-0.1835	0.6	0.612
	1.747			
0.070		-0.2133	0.7	0.711
	1.744			
0.080		-0.2426	0.8	0.809
	1.740			
0.090		-0.2715	0.9	0.905
	1.735			
0.100		-0.3000	1.0	1.000
MEAN VELOCITY = 1.750 m/s				

y m	u m/s	Curv. m^{-1}	N	Prop Curv
	2.041			
0.010		-0.0416	0.1	0.104
	2.040			
0.020		-0.0832	0.2	0.208
	2.039			
0.030		-0.1245	0.3	0.311
	2.037			
0.040		-0.1656	0.4	0.414
	2.033			
0.050		-0.2062	0.5	0.515
	2.029			
0.060		-0.2463	0.6	0.616
	2.024			
0.070		-0.2858	0.7	0.715
	2.018			
0.080		-0.3247	0.8	0.812
	2.012			
0.090		-0.3628	0.9	0.907
	2.004			
0.100		-0.4000	1.0	1.000
MEAN VELOCITY = 2.028 m/s				

TABLE II.3 continued

y m	u m/s	Curv. m-1	N	Prop Curv
	2.294			
0.010	2.293	-0.0526	0.1	0.105
0.020	2.291	-0.1050	0.2	0.210
0.030	2.287	-0.1572	0.3	0.314
0.040	2.282	-0.2088	0.4	0.418
0.050	2.276	-0.2597	0.5	0.519
0.060	2.269	-0.3099	0.6	0.620
0.070	2.261	-0.3592	0.7	0.718
0.080	2.252	-0.4073	0.8	0.815
0.090	2.242	-0.4543	0.9	0.909
0.100		-0.5000	1.0	1.000

MEAN VELOCITY = 2.275 m/s

y m	u m/s	Curv. m-1	N	Prop Curv
	2.526			
0.010	2.525	-0.0638	0.1	0.106
0.020	2.522	-0.1273	0.2	0.212
0.030	2.517	-0.1904	0.3	0.317
0.040	2.510	-0.2527	0.4	0.421
0.050	2.503	-0.3141	0.5	0.524
0.060	2.493	-0.3744	0.6	0.624
0.070	2.483	-0.4333	0.7	0.722
0.080	2.471	-0.4906	0.8	0.818
0.090	2.457	-0.5462	0.9	0.910
0.100		-0.6000	1.0	1.000

MEAN VELOCITY = 2.501 m/s

TABLE II.3 continued

y m	u m/s	Curv. m^{-1}	N	Prop Curv
	2.743			
0.010		-0.0752	0.1	0.107
	2.741			
0.020		-0.1501	0.2	0.214
	2.738			
0.030		-0.2243	0.3	0.320
	2.731			
0.040		-0.2975	0.4	0.425
	2.723			
0.050		-0.3694	0.5	0.528
	2.713			
0.060		-0.4397	0.6	0.628
	2.701			
0.070		-0.5081	0.7	0.726
	2.688			
0.080		-0.5745	0.8	0.821
	2.673			
0.090		-0.6385	0.9	0.912
	2.656			
0.100		-0.7000	1.0	1.000
MEAN VELOCITY = 2.711 m/s				

y m	u m/s	Curv. m^{-1}	N	Prop Curv
	2.948			
0.010		-0.0869	0.1	0.109
	2.946			
0.020		-0.1733	0.2	0.217
	2.942			
0.030		-0.2588	0.3	0.324
	2.933			
0.040		-0.3431	0.4	0.429
	2.923			
0.050		-0.4255	0.5	0.532
	2.911			
0.060		-0.5059	0.6	0.632
	2.896			
0.070		-0.5838	0.7	0.730
	2.880			
0.080		-0.6590	0.8	0.824
	2.861			
0.090		-0.7311	0.9	0.914
	2.841			
0.100		-0.8000	1.0	1.000
MEAN VELOCITY = 2.908 m/s				

TABLE II.3 continued

y m	u m/s	Curv. m^{-1}	N	Prop Curv
	3.144			
0.010	3.142	-0.0988	0.1	0.110
0.020	3.136	-0.1970	0.2	0.219
0.030	3.126	-0.2941	0.3	0.327
0.040	3.114	-0.3894	0.4	0.433
0.050	3.099	-0.4826	0.5	0.536
0.060	3.082	-0.5730	0.6	0.637
0.070	3.062	-0.6603	0.7	0.734
0.080	3.039	-0.7441	0.8	0.827
0.090	3.013	-0.8241	0.9	0.916
0.100		-0.9000	1.0	1.000

MEAN VELOCITY = 3.096 m/s

y m	u m/s	Curv. m^{-1}	N	Prop Curv
	3.333			
0.010	3.329	-0.1110	0.1	0.111
0.020	3.322	-0.2212	0.2	0.221
0.030	3.311	-0.3300	0.3	0.330
0.040	3.297	-0.4367	0.4	0.437
0.050	3.280	-0.5405	0.5	0.541
0.060	3.258	-0.6410	0.6	0.641
0.070	3.235	-0.7376	0.7	0.738
0.080	3.208	-0.8299	0.8	0.830
0.090	3.178	-0.9174	0.9	0.917
0.100		-1.0000	1.0	1.000

MEAN VELOCITY = 3.275 m/s

APPENDIX III

Details of the Computer Program used to calculate Surface Slope and Curvature from the Measured Longitudinal Surface Profiles.

III.1 The computer program, SLP1, makes use of a standard scientific subroutine, DET5, available on the program library file. This subroutine computes values of $^{dy}/_{dx}$ at each point along a curve specified by co-ordinate values of x and y. Measured values of y in metres at equal intervals of x of 0.0508m are read from data cards by the main program, SLP1, and stored as a one-dimensional array. The subroutine DET5 is then called and values of $^{dy}/_{dx}$ are computed at each co-ordinate point and stored in a second one-dimensional array. Subroutine DET5 is called a second time, but now the array in y is replaced by the array in $^{dy}/_{dx}$ so that second derivative values $^{d^2y}/_{dx^2}$ are computed. A third array is used to store these values. The main program then prints a table of x, y, $^{dy}/_{dx}$ and $^{d^2y}/_{dx^2}$ values.

III.2 The subroutine DET5 uses a standard five point finite difference method for computing derivative values. Values of $^{d^2y}/_{dx^2}$ are particularly sensitive to variations in y and occasional large values of curvature were computed due to local disturbances of the water surface.

A flow chart for the main program is shown in Fig. III.1 followed by a listing of the program and a specimen printout.

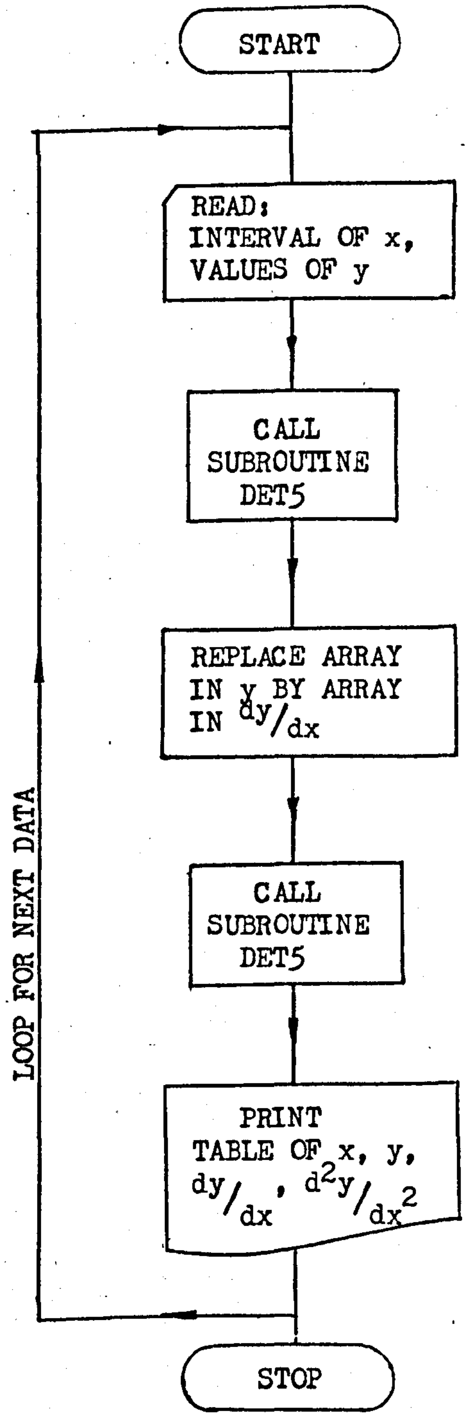

FIG. III.1. FLOW CHART FOR PROGRAM SLP1.

```
      DIMENSIONX(33),Y(32),DYDX(32),D2YDX(32)
      READ(5,9)H
    9 FORMAT(F10.0)
    8 READ(5,11)N
      IF(N.LT.0.0)GOTO100
      WRITE(6,12)N
      READ(5,10)(Y(J),J=1,32)
   10 FORMAT(7F10.0)
   11 FORMAT(I3)
   12 FORMAT(5X,'READING NO.',I4//)
      CALL DET5(H,Y,DYDX,32,E1)
      CALL DET5(H,DYDX,D2YDX,32,E2)
      WRITE(6,60)
      X(1)=0.0
      DO50K=1,32
      X(K+1)=X(K)+H
      WRITE(6,70)X(K),Y(K),DYDX(K),D2YDX(K)
   50 CONTINUE
      WRITE(6,71)E1
      WRITE(6,72)E2
   60 FORMAT(10X,'X',15X,'Y',13X,'DYDX',11X,'D2YDX2'//)
   70 FORMAT(5X,F11.9,5X,F11.9,5X,F11.9,5X,F11.9/)
   71 FORMAT(5X,'ERROR IN DYDX COMPUTATION =',I3/)
   72 FORMAT(5X,'ERROR IN D2YDX2 COMPUTATION =',I3///)
      GOTO8
  100 CONTINUE
      END
```



```
*OPTIONS IN EFFECT*  NOTERM,ID,EBCDIC,SOURCE,NOLIST,NODECK,LOAD,NOMAP,NOTEST
*OPTIONS IN EFFECT*  NAME = MAIN , LINECNT = 56
*STATISTICS*   SOURCE STATEMENTS =      27,PROGRAM SIZE = 0005AC
*STATISTICS*  NO DIAGNOSTICS GENERATED
/DATA                                                          3.1S
003CD8 BYTES USED
EXECUTION BEGINS    4.8S
 READING NO. 132
```

X	Y	DYDX	D2YDX2
0.0	0.136200011	-.289205849	***********
0.050799999	0.129700005	-.027066220	1.53410339
0.101599991	0.129100025	-.021817867	-.550852656
0.152399957	0.126699984	-.036745418	-.078834057
0.203199923	0.125500023	-.030839421	-.167112470
0.253999889	0.123300016	-.051191350	-.063518107
0.304799855	0.120700002	-.035433453	0.277710915
0.355599821	0.119499981	-.034776982	-.364886105

[illegible]	[illegible]	[illegible]	[illegible]
0.457199752	0.112500012	-.096496468	-.694919212
0.507999718	0.106700003	-.140256166	-.913053036
0.558799684	0.098299980	-.182086766	-.605730534
0.609599650	0.088599980	-.197342098	0.001087471
0.660399616	0.078700006	-.183890343	0.423285663
0.711199582	0.070200026	-.155347705	0.851414561
0.761999547	0.063199997	-.104166746	0.817789912
0.812799513	0.059300002	-.078575969	0.287397265
0.863599479	0.055000000	-.068241477	0.352516174
0.914399445	0.052499998	-.043143008	0.353056669
0.965199411	0.050400000	-.035597082	0.072655976
1.01599884	0.048799999	-.032644339	0.048975755
1.06679821	0.047100000	-.028543279	0.165764153
1.11759758	0.046000000	-.016568217	0.196709931
1.16839695	0.045400001	-.008038059	0.298159540
1.21919632	0.045299999	0.011482913	0.191328049
1.26999569	0.046399999	0.014107589	0.342830241
1.32079506	0.046999998	0.043963231	0.441589475
1.37159443	0.050400000	0.042814974	-.862187326
1.42239380	0.050500002	-.028051142	-.960139811
1.47319317	0.048300002	-.036417324	0.414138615
1.52399254	0.047300000	-.004593346	0.545457840
1.57479191	0.046999998	-.021981742	***********

ERROR IN DYDX COMPUTATION = 0

ERROR IN D2YDX2 COMPUTATION = 0

STOP 0

END OF JOB D.J.BALMFORT AT 10H07M MON MAR 06, 1978 EXECUTE TIME 0.09 MINS.
12 CARDS READ 116 LINES PRINTED 0 CARDS PUNCHED 0 TAPE MOUNTS 0 DISK MOUNTS

APPENDIX IV

Listing of the Computer Programs for the Mathematical Model and Specimen Printouts.

```
                C
                C     SIDE WEIRS IN PRISMATIC RECTANGULAR CHANNELS
                C
                C     THIS PROGRAM USES S.I. UNITS ONLY
                C
                C     L IS THE OVERALL LENGTH OF CHANNEL.
                C     THE SHARP CRESTED SIDE WEIR CCCUPIES THE SECTION
                C     BETWEEN XCON1 ANDXCON2.
                C
 0001                 REAL L
 0002                 DIMENSIONX(3000),Y(3000),V(3000)
 0003              10 READ(5,50)NUM,I
 0004                 IF(NUM.LT.0)GOTO100
 0005                 READ(5,52)B,SO,EN
 0006                 READ(5,52)C2,XCON1,XCON2
 0007                 READ(5,54)XST,XEN
 0008                 READ(5,52)Y1,Q1,H
 0009              50 FORMAT(2I5)
 0010              52 FORMAT(3F10.0)
 0011              54 FORMAT(2F10.0)
                C
                C     THE NEXT SECTICN PRINTS DATA AND HEADINGS
                C
 0012                 WRITE(6,60)
 0013              60 FORMAT(5X,'SURFACE PROFILES FOR RECTANGULAR PRISMATIC OPEN CHANNEL
                     CS'/)
 0014                 WRITE(6,61)I
 0015              61 FORMAT(5X,'TEST RUN ',I6/)
 0016                 IF(XCON1.LT.XCON2)WRITE(6,62)XCON1,XCON2
 0017              62 FORMAT(5X,'SIDE WEIR BETWEEN ',F11.4,'M, AND ',F11.4,'M'//)
 0018                 WRITE(6,63)B,SO,EN
 0019              63 FORMAT(5X,'CHANNEL WIDTH =',F11.6,'M, SLOPE = ',F11.8,'   VISCOCIT
                     CY =',F11.9,'KG/MS'/)
 0020                 WRITE(6,64)C2
 0021              64 FORMAT(5X,'CREST HEIGHT =',F11.6,'M'/)
 0022                 WRITE(6,65)Q1,H
 0023              65 FORMAT(5X,'INITIAL DISCHARGE =',F11.6,' CUBIC METRES PER SEC.,   ST
                     CEP LENGTH =',F11.8,'M'//)
 0024                 WRITE(6,66)XST,Y1
 0025              66 FORMAT(5X,'INITIAL STATION ',F11.6,'M, INITIAL DEPTH =',F11.6,'M'/
                     C)
 0026                 WRITE(6,68)
 0027              68 FORMAT(13X,'X METRES',13X,'Y METRES',13X,'V M/S',14X,'FROUDE NO.'/
                     C)
 0028                 V1=Q1/B/Y1
 0029                 L=ABS(XEN-XST)
 0030                 N=ABS(L/H)+0.5
                C
 0031                 CALL PROFL(C2,B,SO,EN,H,XST,Y1,V1,N,XCON1,XCON2,X,Y,V,DN1,DN2)
                C
                C     THE NEXT SECTICN PRINTS PROFILE CC-ORDINATES
                C
 0032                 M=N+1
 0033                 DO87K=1,M,2
```


FORTRAN IV G1 RELEASE 2.0 MAIN DATE = MON MAR 06, 1978 PAGE 0002

```
                 [illegible]
                 WRITE(6,70)X(K),Y(K),V(K),W
              70 FORMAT(10X,F9.4,10X,F11.6,10X,F11.6,10X,F11.6/)
                 ST=X(K)+2.*H
                 IF(H.LT.0.)GOTO77
                 IF(X(K).GE.XCON1)GOTO75
                 IF(ST.GE.XCON1)WRITE(6,72)DN1
              72 FORMAT(10X,'START OF SIDE WEIR, DEPTH = ',F11.6,'M'/)
              75 IF(X(K).GE.XCON2)GOTO77
                 IF(ST.GE.XCON2)WRITE(6,76)DN2
              76 FORMAT(10X,'END OF SIDE WEIR, DEPTH = ',F11.6,'M'/)
              77 IF(H.GT.0.)GOTO87
                 IF(X(K).LE.XCON2)GOTO85
                 IF(ST.LE.XCON2)WRITE(6,82)DN2
              82 FORMAT(10X,'END OF SIDE WEIR, DEPTH = ',F11.6,'M'/)
              85 IF(X(K).LE.XCON1)GOTO87
                 IF(ST.LE.XCON1)WRITE(6,86)DN1
              86 FORMAT(10X,'START OF SIDE WEIR, DEPTH = ',F11.6,'M'/)
              87 CONTINUE
                 Q2=V(M)*Y(M)*B
                 WRITE(6,95)Q2
              95 FORMAT(5X,'FINAL DISCHARGE = ',F11.6,' CUBIC METRES PER SECOND'/)
                 WRITE(6,96)Y(M)
              96 FORMAT(5X,'FINAL DEPTH = ',F11.6,'M'///)
                 GOTO10
             100 CONTINUE
                 CALL EXIT
                 END

 *OPTIONS IN EFFECT*  NOTERM,ID,EBCDIC,SOURCE,NOLIST,NODECK,LOAD,NOMAP,NOTEST
 *OPTIONS IN EFFECT*  NAME = MAIN     , LINECNT =       56
 *STATISTICS*  SOURCE STATEMENTS =       62,PROGRAM SIZE = 00960A
 *STATISTICS*  NO DIAGNOSTICS GENERATED
```

```
FORTRAN IV G1  RELEASE 2.0            PROFL              DATE = MON MAR 06, 1978              PAGE 0001

                 SUBROUTINE PROFL(C2,B,S0,FN,H,XST,Y1,V1,N,XCON1,XCON2,X,Y,V,DN1,DN
                C2)
                 REAL K0,M0,K1,M1,K2,M2,K3,M3
                 DIMENSIONX(3000),Y(3000),V(3000),W(3000)
      C
      C          STARTING VALUES FED INTO ARRAY
      C
                 X(1)=XST
                 Y(1)=Y1
                 V(1)=V1
                 W(1)=V(1)*Y(1)
      C
      C          CALCULATES NEXT VALUES OF X, Y, V, AND W
      C
                 DO40J=1,N
      C
                 XL1=XCON1-ABS(H/2.)
                 XL2=XCON1+ABS(H/2.)
                 IF(X(J)-XL2)15,20,20
              15 IF(X(J).GE.XL1)DN1=Y(J)
              20 CONTINUE
                 XL3=XCON2-ABS(H/2.)
                 XL4=XCON2+ABS(H/2.)
                 IF(X(J)-XL4)30,35,35
              30 IF(X(J).GE.XL3)DN2=Y(J)
```

```
0020                BETA=1.0977-0.0995*W(J)/Y(J)
0021                IF(BETA.LT.1.00)BETA=1.00
0022                IF(X(J).LT.XCON1)C1=0.
0023                IF(X(J).GT.XCON2)C1=0.
0024                KO=H*FUN1(C1,C2,B,SO,EN,BETA,Y(J),W(J))
0025                MO=H*FUN2(C1,C2,B,Y(J))
0026                YY=Y(J)+KO/2.
0027                WW=W(J)+MO/2.
0028                K1=H*FUN1(C1,C2,B,SO,EN,BETA,YY,WW)
0029                M1=H*FUN2(C1,C2,B,YY)
0030                YY=Y(J)+K1/2.
0031                WW=W(J)+M1/2.
0032                K2=H*FUN1(C1,C2,B,SO,EN,BETA,YY,WW)
0033                M2=H*FUN2(C1,C2,B,YY)
0034                YY=Y(J)+K2
0035                WW=W(J)+M2
0036                K3=H*FUN1(C1,C2,B,SO,EN,BETA,YY,WW)
0037                M3=H*FUN2(C1,C2,B,YY)
0038                Y(J+1)=Y(J)+(KO+2.*K1+2.*K2+K3)/6.
0039                W(J+1)=W(J)+(MO+2.*M1+2.*M2+M3)/6.
0040                V(J+1)=W(J+1)/Y(J+1)
0041                X(J+1)=X(J)+H
0042             40 CONTINUE
0043                RETURN
0044                END

  *OPTIONS IN EFFECT*  NOTERM,ID,EBCDIC,SOURCE,NOLIST,NODECK,LOAD,NOMAP,NOTEST

FORTRAN IV G1  RELEASE 2.0          PROFL          DATE = MON MAR 06, 1978          PAGE 0002

  *OPTIONS IN EFFECT*  NAME = PROFL   , LINECNT =     56
  *STATISTICS*    SOURCE STATEMENTS =        44,PROGRAM SIZE = 003634
  *STATISTICS*  NO DIAGNOSTICS GENERATED

FORTRAN IV G1  RELEASE 2.0          FUN1           DATE = MON MAR 06, 1978          PAGE 0001

0001                FUNCTION FUN1(C1,C2,B,SO,EN,BETA,Y,W)
              C
              C     THE VALUE OF SF IS COMPUTED FROM THE DARCY EQUATION WITH THE
              C     THE FRICTION FACTOR GOVERNED BY THE BLASIUS FORMULA.
              C     THIS IS A LITTLE MORE ACCURATE THAN MANNING FOR SMOOTH CHANNELS.
              C
0002                IF(C1.LE.0.000001)GOTO1
0003                R=B*Y/(B+Y+C2)
0004                GOTO2
0005              1 R=B*Y/(B+2.*Y)
0006              2 RE=4.*W*R/(EN*Y)
0007                SF=W*W*0.3164/(RE**0.25*Y*Y*R*78.48)
0008                Q=2.95296*C1*(Y-C2)**1.5
0009                FUN1=(SO-SF+(2.*BETA-1.)*Q*W/(9.81*B*Y*Y))/(COS(ATAN(SO))-BETA*W*W
               C/(9.81*Y*Y*Y))
0010                RETURN
0011                END

  *OPTIONS IN EFFECT*  NOTERM,ID,EBCDIC,SOURCE,NOLIST,NODECK,LOAD,NOMAP,NOTEST
  *OPTIONS IN EFFECT*  NAME = FUN1   , LINECNT =        56
  *STATISTICS*    SOURCE STATEMENTS =        11,PROGRAM SIZE = 000382
  *STATISTICS*  NO DIAGNOSTICS GENERATED

FORTRAN IV G1  RELEASE 2.0          FUN2           DATE = MON MAR 06, 1978          PAGE 0001
```

```
0004                    END

*OPTIONS IN EFFECT*  NOTERM,ID,EBCDIC,SOURCE,NOLIST,NODECK,LOAD,NOMAP,NOTEST
*OPTIONS IN EFFECT*    NAME = FUN2        , LINECNT =        56
*STATISTICS*      SOURCE STATEMENTS =             4,PROGRAM SIZE = 000186
*STATISTICS*   NO DIAGNOSTICS GENERATED

*STATISTICS*   NO DIAGNOSTICS THIS STEP
/DATA                                                                    15.4S
010F58 BYTES USED
EXECUTION BEGINS     16.7S
```

SURFACE PROFILES FOR RECTANGULAR PRISMATIC OPEN CHANNELS

TEST RUN 19

SIDE WEIR BETWEEN 0.0500M, AND 0.6596M

CHANNEL WIDTH = 0.101600M, SLOPE = 0.0 VISCOCITY =0.000000951KG/MS

CREST HEIGHT = 0.080000M

INITIAL DISCHARGE = 0.002060 CUBIC METRES PER SEC., STEP LENGTH =-0.01000000M

INITIAL STATION 1.088000M, INITIAL DEPTH = 0.098100M

X METRES	Y METRES	V M/S	FROUDE NO.
1.0880	0.098100	0.206683	0.210686
1.0680	0.098108	0.206666	0.210659
1.0480	0.098116	0.206648	0.210633
1.0280	0.098125	0.206631	0.210606
1.0080	0.098133	0.206614	0.210580
0.9880	0.098141	0.206596	0.210553
0.9680	0.098149	0.206579	0.210527
0.9480	0.098158	0.206562	0.210500
0.9280	0.098166	0.206544	0.210474
0.9080	0.098174	0.206527	0.210448
0.8880	0.098182	0.206510	0.210421
0.8680	0.098190	0.206492	0.210395
0.8480	0.098199	0.206475	0.210368
0.8280	0.098207	0.206458	0.210342
0.8080	0.098215	0.206441	0.210315

0.7680	0.098232	0.206406	0.210263
0.7480	0.098240	0.206389	0.210236
0.7280	0.098248	0.206371	0.210210
0.7080	0.098256	0.206354	0.210183
0.6880	0.098265	0.206337	0.210157
0.6680	0.098273	0.206320	0.210131

END OF SIDE WEIR, DEPTH = 0.098277M

0.6480	0.098161	0.211528	0.215557
0.6280	0.097925	0.221873	0.226373
0.6080	0.097680	0.232099	0.237102
0.5880	0.097429	0.242199	0.247739
0.5680	0.097172	0.252171	0.258280
0.5480	0.096908	0.262011	0.268723
0.5280	0.096640	0.271715	0.279061
0.5080	0.096367	0.281279	0.289294
0.4880	0.096090	0.290701	0.299415
0.4680	0.095809	0.299978	0.309423
0.4480	0.095525	0.309108	0.319313
0.4280	0.095239	0.318088	0.329082
0.4080	0.094951	0.326915	0.338728
0.3880	0.094661	0.335590	0.348247
0.3680	0.094371	0.344108	0.357636
0.3480	0.094080	0.352470	0.366893
0.3280	0.093789	0.360674	0.376015
0.3080	0.093498	0.368719	0.385000
0.2880	0.093208	0.376605	0.393845
0.2680	0.092919	0.384331	0.402548
0.2480	0.092632	0.391897	0.411108
0.2280	0.092347	0.399303	0.419523
0.2080	0.092065	0.406549	0.427792

0.1680	0.091504	0.420964	0.443883
0.1480	0.091234	0.427333	0.451704
0.1280	0.090964	0.433946	0.459374
0.1080	0.090697	0.440402	0.466894
0.0880	0.090435	0.446704	0.474261
0.0680	0.090177	0.452853	0.481477

START OF SIDE WEIR, DEPTH = 0.089923M

0.0480	0.089923	0.458850	0.488541
0.0280	0.089966	0.458628	0.488186
0.0080	0.090010	0.458407	0.487833

FINAL DISCHARGE = 0.004192 CUBIC METRES PER SECOND

FINAL DEPTH = 0.090032M

END OF JOB BALMFORTH D AT 10H09M MON MAR 06, 1978 EXECUTE TIME 0.35 MINS.
10 CARDS READ 327 LINES PRINTED 0 CARDS PUNCHED 0 TAPE MOUNTS 0 DISK MOUNTS

```
C
C PROGRAM NAME CHECK2
C
C S.I.UNITS ONLY
C
      DIMENSION PRMT(5),Y(3),DERY(3),AUX(16,3)
      COMMON/COM1/B,S0,EN,Q1,D3YDX3,C2,AJ,AK,SF,Q,BETA,FAC,TRY,AJ1
      EXTERNAL FCT,OUTP,XCT,XUTP
   10 READ(5,50)NUM,I
      AJ=0.0
      IF(NUM.LT.0)GOTO100
      READ(5,52)B,S0,EN
      READ(5,52)C2,XST,XFN
      READ(5,52)Y1,Q1,H
      DYD1=-0.12
   50 FORMAT(2I5)
   52 FORMAT(3F10.0)
   54 FORMAT(2F10.0)
C
C THE NEXT SECTION PRINTS HEADINGS AND DATA
C
      WRITE(6,60)I
   60 FORMAT(5X,'PROGRAM CHECK2, TEST RUN ',I6//)
      WRITE(6,61)
   61 FORMAT(5X,'ALL VALUES PRINTED IN BASIC S.I. UNITS'//)
      WRITE(6,62)
   62 FORMAT(3X,'WIDTH',5X,'SLOPE',4X,'VISCOCITY',3X,'XST',7X,'XFN',6X,'
     CDEPTH1  DISCHARGE      STEP          C2'/)
      WRITE(6,63)B,S0,EN,XST,XFN,Y1,Q1,H,C2
   63 FORMAT(9F10.6//)
      WRITE(6,64)
   64 FORMAT(5X,'X',10X,'Y',8X,'DYDX',5X,'D2YDX2',4X,'D3YDX3  VELOCITY
     CFROUDE NO.',3X,'FACTOR'/)
      PRMT(1)=XST
      V1=Q1/B/Y1
      Y(1)=Y1
      Y(2)=Q1/B
      IF(V1/SQRT(9.81*Y1).GE.1.5)GOTO65
      PRMT(2)=XFN
      PRMT(3)=H
      Y(2)=DYD1
      Y(3)=Q1/B
      DERY(1)=0.17
      DERY(2)=0.50
      DERY(3)=0.33
      NDIM=3
      DC=((Q1/B)*(Q1/B)/9.81)**0.333333
      D3YDX3=0.0716/DC/DC
      PRMT(4)=0.05*DC
C
      CALL HPCG(PRMT,Y,DERY,NDIM,IHLF,FCT,OUTP,AUX)
C
      PRMT(1)=AJ
      Y(2)=Y(3)
```

272

```
                 PRMT(4)=0.01
                 DERY(1)=0.34
                 DERY(2)=0.66
                 NDIM=2
      C
                 CALL HPCG(PRMT,Y,DERY,NDIM,IHLF,FCT,XOUTP,AUX)
      C
                 WRITE(6,300)AJ,AK
             300 FORMAT(5X,'FINAL DEPTH =',F10.6,' M,  FINAL DISCHARGE =',
                CF10.6,' CU.M. PER SEC.'///)
                 GOTO10
             100 CONTINUE
                 CALL EXIT
                 END

 *OPTIONS IN EFFECT*  NOTERM,ID,EBCDIC,SOURCE,NOLIST,NODECK,LOAD,NOMAP,NOTEST
 *OPTIONS IN EFFECT*  NAME = MAIN     , LINECNT =        56
 *STATISTICS*    SOURCE STATEMENTS =         55,PROGRAM SIZE = 00072E
 *STATISTICS*  NO DIAGNOSTICS GENERATED

FORTRAN IV G1  RELEASE 2.0          FCT                  DATE = MON MAR 06, 1978                    PAGE 0001

                 SUBROUTINE FCT(X,Y,DERY)
                 DIMENSION Y(3),DERY(3)
                 COMMON/COM1/B,SO,EN,Q1,D3YDX3,C2,AJ,AK,SF,Q,BETA,FAC,TRY,AJ1
                 FAC=0.0
                 R=B*Y(1)/(B+Y(1)+C2)
                 V=Y(3)/Y(1)
                 RE=4.*R*V/EN
                 SF=0.3164*V*V/(78.48*R*RE**0.25)
                 C1=(0.602+0.083*(Y(1)-C2)/C2)*(1.+0.0012/(Y(1)-C2))**1.5
                 IF(ABS(AJ).LT.0.01)GOTO68
                 EH=Y(1)-C2
                 AK1=COS(ATAN(SO))+V*V/9.81*AJ
                 IF(AJ.GT.0.0)GOTO67
                 AK2=-0.5*V*V/Y(1)/9.81*AJ
                 Q=2.21472*C1*SQRT(AK2)*((EH+AK1/2./AK2)*SQRT(EH*EH+AK1*EH
                C/AK2)-(AK1/2./AK2)**2.*ALOG((2.*AK2*EH/AK1+1.)
                C+2.*AK2/AK1*SQRT(EH*EH+AK1*EH/AK2)))
                 FAC=1.0
                 GOTO68
              67 AK2=0.5*V*V/Y(1)/9.81*AJ
                 Q=2.21472*C1*SQRT(AK2)*((AK1/2./AK2)**2.
                C*(1.5708+ARSIN(2.*AK2*EH/AK1-1.))+(EH-AK1/2./AK2)*
                CSQRT(AK1*EH/AK2-EH*EH))
                 FAC=1.0
              68 CONTINUE
                 IF(FAC.LT.0.9)Q=2.95296*C1*(Y(1)-C2)**1.5
                 FAC=Q/(2.95296*C1*(Y(1)-C2)**1.5)
                 BETA=1.0577-0.0995*V
                 IF(BETA.LT.1.0)BETA=1.0
                 AK=1./3.
                 CE=COS(ATAN(SO))
                 DERY(1)=Y(2)
                 DERY(2)=V*Y(1)*B/2./Q*D3YDX3+4.905*B/Q/AK/V*(CE-BETA
                C*V*V/9.81/Y(1))*Y(2)+0.5/AK/Y(1)*(1.-2.*BETA)
                C-4.905*B/Q/AK/V*(SO-SF)
                 DERY(3)=-Q/B
                 AJ=AJ1+0.5*(DERY(2)-AJ1)
                 IF(AJ.LT.-1.0)AJ=-1.0
```

```
0034            CONTINUE
0035            RETURN
0036            END

*OPTIONS IN EFFECT*  NOTERM,ID,EBCDIC,SOURCE,NOLIST,NODECK,LOAD,NOMAP,NOTEST
*OPTIONS IN EFFECT*  NAME = FCT      , LINECNT =       56
*STATISTICS*    SOURCE STATEMENTS =        36,PROGRAM SIZE = 00078C
*STATISTICS*  NO DIAGNOSTICS GENERATED

FORTRAN IV G1  RELEASE 2.0        OUTP              DATE = MON MAR 06, 1978                    PAGE 0001

0001               SUBROUTINE OUTP(X,Y,DERY,IHLF,NDIM,PRMT)
0002               DIMENSION Y(3),DERY(3),PRMT(5)
0003               COMMON/COM1/B,SO,EN,Q1,D3YDX3,C2,AJ,AK,SF,Q,BETA,FAC,TRY,AJ1
0004               V=Y(3)/Y(1)
0005               F=V/SQRT(9.81*Y(1))
0006               WRITE(6,70)X,Y(1),DERY(1),DERY(2),D3YDX3,V,F,FAC
0007            70 FORMAT(8F10.6/)
0008               AJ1=DERY(2)
0009               IF(AJ1.LT.-1.0)AJ1=-1.0
0010               IF(AJ1.GT.1.0)AJ1=1.0
0011               AJ=AJ1
0012               IF(F.GE.1.2)GOTO199
0013               GOTO210
0014           199 IF(DERY(2).GT.0.0)GOTO200
0015               GOTO210
0016           200 CE=COS(ATAN(SO))
0017               C1=(0.602+0.083*(Y(1)-C2)/C2)*(1.+0.0012/(Y(1)-C2))**1.5
0018               Q=2.95296*C1*(Y(1)-C2)**1.5
0019               SLOPE=(SO-SF-Q*V/9.81/B/Y(1)*(1.-2.*BETA))/
                  C(CE-BETA*V*V/9.81/Y(1))
0020               DIFF=ABS(DERY(1)-SLOPE)
0021               TEST=0.1*ABS(DERY(1))
0022               IF(DIFF.LE.TEST)GOTO203
0023               GOTO210
0024           203 IF(DERY(2).LT.TRY)GOTO205
0025               GOTO210
0026           205 PRMT(5)=1.0
0027               AJ=X
0028           210 TRY=DERY(2)
0029               RETURN
0030               END

*OPTIONS IN EFFECT*  NOTERM,ID,EBCDIC,SOURCE,NOLIST,NODECK,LOAD,NOMAP,NOTEST
*OPTIONS IN EFFECT*  NAME = OUTP     , LINECNT =       56
*STATISTICS*    SOURCE STATEMENTS =        30,PROGRAM SIZE = 0004A6
*STATISTICS*  NO DIAGNOSTICS GENERATED

FORTRAN IV G1  RELEASE 2.0        XCT               DATE = MON MAR 06, 1978                    PAGE 0001

0001               SUBROUTINE XCT(X,Y,DERY)
0002               DIMENSION Y(2),DERY(2)
0003               COMMON/COM1/B,SO,EN,Q1,D3YDX3,C2,AJ,AK,SF,Q,BETA,FAC,TRY,AJ1
0004               R=B*Y(1)/(B+Y(1)+C2)
0005               V=Y(2)/Y(1)
0006               RE=4.*R*V/EN
0007               SF=0.3164*V*V/(78.48*R*RE**0.25)
0008               C1=(0.602+0.083*(Y(1)-C2)/C2)*(1.+0.0012/(Y(1)-C2))**1.5
0009               Q=2.95296*C1*(Y(1)-C2)**1.5
0010               BETA=1.0577-0.0995*V
0011               IF(BETA.LT.1.0)BETA=1.0
```

```
      [illegible]
      C/(CB-BETA*V*V/9.81/Y(1))
      DERY(2)=-C/B
      RETURN
      END
```

```
*OPTIONS IN EFFECT*  NOTERM,ID,EBCDIC,SOURCE,NOLIST,NODECK,LOAD,NOMAP,NOTEST
*OPTIONS IN EFFECT*  NAME = XCT     , LINECNT =       56
*STATISTICS*    SOURCE STATEMENTS =          16,PROGRAM SIZE = 00035A
*STATISTICS*  NO DIAGNOSTICS GENERATED
```

FORTRAN IV G1 RELEASE 2.0 XUTP DATE = MON MAR 06, 1978 PAGE 0001

```
      SUBROUTINE XUTP(X,Y,DERY,IHLF,NDIM,PRMT)
      DIMENSION Y(2),DERY(2),PRMT(5)
      COMMON/COM1/B,SO,EN,Q1,D3YDX3,C2,AJ,AK,SF,Q,BETA,FAC,TRY,AJ1
      V=Y(2)/Y(1)
      F=V/SQRT(9.81*Y(1))
      CN=0.0
      WRITE(6,270)X,Y(1),DERY(1),CN,CN,V,F
  270 FORMAT(7F10.6/)
      AK=Y(1)*B*V
      AJ=Y(1)
      RETURN
      END
```

```
*OPTIONS IN EFFECT*  NOTERM,ID,EBCDIC,SOURCE,NOLIST,NODECK,LOAD,NOMAP,NOTEST
*OPTIONS IN EFFECT*  NAME = XUTP    , LINECNT =       56
*STATISTICS*    SOURCE STATEMENTS =          12,PROGRAM SIZE = 000248
*STATISTICS*  NO DIAGNOSTICS GENERATED

*STATISTICS*  NO DIAGNOSTICS THIS STEP
/DATA                                                         19.0S
007198 BYTES USED
EXECUTION BEGINS      22.3S
PROGRAM CHECK2, TEST RUN      132
```

ALL VALUES PRINTED IN BASIC S.I. UNITS

WIDTH	SLOPE	VISCOCITY	XST	XFN	DEPTH1	DISCHARGE	STEP	C2
0.101600	0.003760	0.000001	0.0	0.609600	0.106700	0.013820	0.020000	0.036000

X	Y	DYDX	D2YDX2	D3YDX3	VELOCITY	FROUDE NO.	FACTOR
0.0	0.106700	-0.120000	-11.447030	4.690338	1.274822	1.246043	1.000000
0.010000	0.104962	-0.225565	-9.707077	4.690338	1.257509	1.239254	0.933023
0.020000	0.102247	-0.313863	-7.886063	4.690338	1.254661	1.252753	0.933102
0.030000	0.098755	-0.380967	-5.368194	4.690339	1.264156	1.284362	0.931721
0.040000	0.094733	-0.418258	-1.966059	4.690338	1.285218	1.333186	0.928918
0.050000	0.090518	-0.418882	0.063381	4.690338	1.314721	1.395185	1.029774
0.051250	0.089965	-0.416795	-0.130373	4.690338	1.319006	1.404026	1.070313

0.052500	0.089434	-0.415959	0.662117	4.690338	1.322847	1.412287	1.050354
0.053125	0.089176	-0.415587	0.775046	4.690338	1.324693	1.416307	1.057883
0.053750	0.088917	-0.415085	0.917010	4.690338	1.326560	1.420363	1.063608
0.054375	0.088658	-0.414469	1.021968	4.690338	1.328453	1.424467	1.071425
0.055000	0.088399	-0.413768	1.253573	4.690338	1.330358	1.428596	1.071662
0.056250	0.087883	-0.411945	1.711826	4.690338	1.334225	1.436952	1.072124
0.057500	0.087369	-0.409504	2.158341	4.690338	1.338167	1.445428	1.072594
0.058750	0.086859	-0.406534	2.593065	4.690338	1.342160	1.453993	1.073072
0.060000	0.086353	-0.403026	3.012239	4.690338	1.346199	1.462636	1.073565
0.062500	0.085356	-0.394521	3.795437	4.690338	1.354358	1.480069	1.074550
0.065000	0.084382	-0.384157	4.487689	4.690338	1.362570	1.497608	1.075564
0.067500	0.083437	-0.372184	5.072849	4.690338	1.370749	1.515112	1.076555
0.070000	0.082523	-0.358893	5.537325	4.690338	1.378808	1.532438	1.077559
0.075000	0.080801	-0.329661	6.083292	4.690338	1.394277	1.566054	1.079496
0.080000	0.079229	-0.298915	6.132408	4.690338	1.408537	1.597687	1.081318
0.085000	0.077810	-0.268995	5.779958	4.690338	1.421296	1.626794	1.082981
0.090000	0.076535	-0.241562	5.166968	4.690338	1.432470	1.653185	1.084453
0.100000	0.074360	-0.197987	3.784552	4.690338	1.450297	1.698053	1.086897
0.110000	0.072560	-0.168554	2.749703	4.690338	1.463513	1.734656	1.088778
0.120000	0.070998	-0.146899	1.928212	4.690338	1.474011	1.766212	1.090350
0.120000	0.070998	-0.132591	0.0	0.0	1.474011	1.766212	
0.130000	0.069724	-0.122538	0.0	0.0	1.481918	1.791842	
0.140000	0.068543	-0.113741	0.0	0.0	1.489145	1.816019	
0.150000	0.067445	-0.105979	0.0	0.0	1.495778	1.838894	
0.160000	0.066421	-0.099079	0.0	0.0	1.501885	1.860590	
0.170000	0.065461	-0.092905	0.0	0.0	1.507527	1.881215	
0.180000	0.064560	-0.087349	0.0	0.0	1.512753	1.900862	
0.200000	0.062912	-0.077760	0.0	0.0	1.522115	1.937514	
0.220000	0.061439	-0.069782	0.0	0.0	1.530241	1.971069	
0.240000	0.060113	-0.063048	0.0	0.0	1.537336	2.001937	

0.280000	0.057816	-0.052328	0.0	0.0	1.549038	2.056954
0.300000	0.056814	-0.048002	0.0	0.0	1.553868	2.081389
C.320000	0.055892	-0.044207	0.0	0.0	1.558134	2.104235
0.340000	0.055042	-0.040852	0.0	0.0	1.561902	2.125546
C.360000	0.054256	-0.037871	0.0	0.0	1.565228	2.145459
0.380000	0.053525	-0.035206	0.0	0.0	1.568162	2.164094
0.400000	0.052846	-0.032813	0.0	0.0	1.570744	2.181554
0.420000	0.052211	-0.030654	0.0	0.0	1.573008	2.197929
0.440000	0.051618	-0.028698	0.0	0.0	1.574984	2.213300
0.460000	0.051062	-0.026921	0.0	0.0	1.576699	2.227739
0.480000	0.050540	-0.025299	0.0	0.0	1.578176	2.241310
0.500000	0.050049	-0.023816	0.0	0.0	1.579434	2.254073
0.520000	0.049587	-0.022455	0.0	0.0	1.580494	2.266080
0.539999	0.049150	-0.021203	0.0	0.0	1.581369	2.277379
0.559999	0.048738	-0.020049	0.0	0.0	1.582074	2.288013
0.579999	0.048348	-0.018981	0.0	0.0	1.582623	2.298023
0.599999	0.047978	-0.017993	0.0	0.0	1.583024	2.307444
0.619999	0.047628	-0.017075	C.C	0.0	1.583290	2.316309

FINAL DEPTH = 0.047628 M, FINAL DISCHARGE = 0.007661 CU.M. PER SEC.

END OF JOB D.J.BALMFORT AT 10H08M MON MAR 06, 1978 EXECUTE TIME 0.42 MINS.
9 CARDS READ 341 LINES PRINTED 0 CARDS PUNCHED 0 TAPE MOUNTS 0 DISK MOUNTS

APPENDIX V

Results of the Preliminary Experimental Investigation.

(a) Head, Discharge and Coefficient of Discharge Values.

(b) Velocity Traverse Readings.

(c) Details of the Method of Computing α and β Values.

(a) Head, Discharge and Coefficient of Discharge Values.

Test No. 1.

Dahl tube manometer reading:	1.05	Q_1	=	$0.02612 m^3/s$
Side spill stage :	6.62cm	Q_w	=	$0.007866 m^3/s$
Weir length L :	110.72cm	Q_2	=	$0.01824 m^3/s$
Crest height C :	35.75cm	V_1	=	0.093m/s
B_1 :	73.50cm	V_2	=	0.103m/s
B_2 :	46.32cm	V_{mean}	=	0.098m/s
Mean head above crest h* :	2.387cm	C_D (measured)	=	0.652
Mean depth* :	38.137cm	C_D (Rehbock)	=	0.654

Surface Profiles

X-Section (Distance from start of weir) mm	HEAD ABOVE CREST mm								
	LONG SECTION (DISTANCE BEHIND WEIR) mm								
	0	50	100	200	300	400	500	605	700
0 (50)→	19.6	23.1	23.7	23.7	23.7	23.6	23.6	23.3	23.4
100	19.6	23.1	23.7	23.7	23.7	23.6	23.5	23.3	
200	19.6	23.3	23.8	23.8	23.8	23.7	23.6	23.1	
300	19.7	23.5	23.8	23.9	23.8	23.7	23.6	23.2	
400	19.8	23.5	23.8	24.1	23.8	23.7	23.6		
500	19.7	23.5	23.8	24.1	23.8	23.8	23.6		
600	19.8	23.6	23.9	24.1	23.9	23.8	23.4		
700	19.9	23.8	24.1	24.2	23.8	23.7	23.4		
800	20.0	23.8	24.1	24.3	23.9	23.8	23.4		
900	20.0	23.9	24.2	24.2	23.9	23.8			
1000	20.3	24.1	24.4	24.3	23.9	23.8			
1050	20.5	24.4	24.5	24.4	23.9	23.6			

* Averaged over 200mm, 300m and 400mm, long sections.

Test No. 2.

Dahl tube manometer reading:	1.30	Q_1	=	$0.02894 m^3/s$
Side spill stage :	8.02cm	Q_W	=	$0.01072 m^3/s$
Weir length L :	110.72cm	Q_2	=	$0.01824 m^3/s$
Crest height C :	35.75cm	V_1	=	0.102m/s
B_1 :	73.50cm	V_2	=	0.102m/s
B_2 :	46.32cm	V_{mean}	=	0.102m/s
Mean head above crest h* :	2.919cm	C_D (measured)	=	0.658
Mean depth* :	38.664cm	C_D (Rehbock)	=	0.647

Surface Profiles

X-Section (Distance from start of weir) mm	HEAD ABOVE CREST mm								
	LONG SECTION (DISTANCE BEHIND WEIR) mm								
	0	50	100	200	300	400	500	605	700
0 (50)→	23.8	28.1	28.6	28.8	28.9	28.9	29.0	28.5	28.7
100	23.9	28.1	28.7	28.9	29.0	29.0	28.9	28.7	
200	23.8	28.2	28.8	29.0	29.0	29.0	28.9	28.5	
300	23.9	28.4	28.8	29.1	29.0	29.0	28.8	28.5	
400	23.9	28.5	28.9	29.2	29.0	29.0	28.9	28.5	
500	24.1	28.5	29.1	29.2	29.1	29.1	28.9		
600	23.9	28.7	29.2	29.3	29.2	29.1	29.0		
700	24.0	28.7	29.3	29.4	29.3	29.2	28.9		
800	24.1	28.8	29.4	29.5	29.3	29.2	28.9		
900	24.3	28.9	29.5	29.6	29.4	29.2			
1000	24.5	29.3	29.8	29.6	29.5	29.2			
1050	24.9	29.6	29.9	29.8	29.6	29.1			

* Averaged over 200mm, 300m and 400mm, long sections.

Test No. 3.

Dahl tube manometer reading:	1.785	Q_1	=	$0.03389 m^3/s$
Side spill stage :	8.99cm	Q_w	=	$0.01288 m^3/s$
Weir length L :	110.72cm	Q_2	=	$0.02101 m^3/s$
Crest height C :	35.75cm	V_1	=	0.118m/s
B_1 :	73.50cm	V_2	=	0.116m/s
B_2 :	46.32cm	V_{mean}	=	0.117m/s
Mean head above crest h* :	3.355cm	C_D (measured)	=	0.641
Mean depth* :	39.105cm	C_D (Rehbock)	=	0.643

Surface Profiles

X-Section (Distance from start of weir) mm	HEAD ABOVE CREST mm								
	LONG SECTION (DISTANCE BEHIND WEIR) mm								
	0	50	100	200	300	400	500	605	700
0 (50)→	27.0	32.2	33.0	33.4	33.4	33.3	33.2	32.8	32.8
100	27.3	32.2	33.0	33.4	33.4	33.4	33.1	32.6	
200	27.4	32.4	33.1	33.4	33.5	33.4	33.3	32.6	
300	27.5	32.5	33.2	33.5	33.4	33.4	33.2	32.7	
400	27.5	32.6	33.3	33.5	33.5	33.3	33.2	32.7	
500	27.5	32.6	33.4	33.6	33.6	33.3	33.2		
600	27.6	32.8	33.4	33.7	33.6	33.3	33.2		
700	27.7	32.8	33.4	33.8	33.6	33.3	33.1		
800	27.8	32.9	33.5	33.9	33.6	33.6	33.2		
900	27.9	32.9	33.5	33.9	33.7	33.4			
1000	28.1	33.1	33.9	34.0	33.8	33.5			
1050	28.3	33.7	34.1	34.1	33.7	33.6			

* Averaged over 200mm, 300m and 400mm, long sections.

Test No. 4.

Dahl tube manometer reading:		2.22	Q_1	=	$0.03774 m^3/s$
Side spill stage	:	9.14cm	Q_w	=	$0.01323 m^3/s$
Weir length L	:	110.72cm	Q_2	=	$0.02451 m^3/s$
Crest height C	:	35.75cm	V_1	=	0.131m/s
B_1	:	73.50cm	V_2	=	0.135m/s
B_2	:	46.32cm	V_{mean}	=	0.133m/s
Mean head above crest h*	:	3.413cm	C_D (measured)	=	0.642
Mean depth*	:	39.163cm	C_D (Rehbock)	=	0.642

Surface Profiles

X-Section (Distance from start of weir) mm	HEAD ABOVE CREST mm								
	LONG SECTION (DISTANCE BEHIND WEIR) mm								
	0	50	100	200	300	400	500	605	700
0 (50)→	27.0		33.5	34.0	34.2	34.0	34.0	33.8	33.9
100	27.8		33.5	33.9	34.2	34.1	34.1	33.7	
200	28.1		33.5	34.0	34.0	33.9	33.9	33.5	
300	28.2		33.7	34.0	34.0	34.0	33.9	33.4	
400	28.2		33.8	34.1	34.1	34.1	33.9	33.5	
500	28.2		33.9	34.3	34.1	34.1	33.8		
600	28.2		34.0	34.3	34.1	34.1	33.8		
700	28.2		34.1	34.3	34.2	34.0	33.9		
800	28.4		34.2	34.3	34.1	34.0	33.7		
900	28.5		34.2	34.5	34.1	34.2			
1000	28.9		34.5	34.6	34.2	33.8			
1050	29.9		34.8	34.6	34.1	33.9			

* Averaged over 200mm, 300m and 400mm, long sections.

Test No. 5.

Dahl tube manometer reading:	2.89	Q_I	=	$0.04294 m^3/s$
Side spill stage :	10.21cm	Q_w	=	$0.01581 m^3/s$
Weir length L :	110.72cm	Q_2	=	$0.02713 m^3/s$
Crest height C :	35.75cm	V_1	=	0.148m/s
B_1 :	73.50cm	V_2	=	0.148m/s
B_2 :	46.32cm	V_{mean}	=	0.148m/s
Mean head above crest h* :	3.884cm	C_D (measured)	=	0.632
Mean depth* :	39.634cm	C_D (Rehbock)	=	0.640

Surface Profiles

X-Section (Distance from start of weir) mm	HEAD ABOVE CREST mm								
	LONG SECTION (DISTANCE BEHIND WEIR) mm								
	0	50	100	200	300	400	500	605	700
0 (50)→	29.5		38.2	38.5	38.8	38.6	38.9	38.3	38.3
100	31.3		38.2	38.5	38.8	38.5	38.7	38.3	
200	31.5		38.3	38.6	38.9	38.5	38.5	38.3	
300	31.8		38.3	38.7	38.8	38.6	38.7	38.1	
400	31.8		38.3	38.8	38.8	38.7	38.7	38.2	
500	32.2		38.5	38.8	38.9	38.8	38.6		
600	32.3		38.5	38.8	38.9	38.8	38.6		
700	32.5		38.5	38.9	38.9	38.9	38.5		
800	32.6		38.8	39.0	38.9	38.9	38.5		
900	32.5		38.9	39.2	28.9	38.8			
1000	32.4		39.1	39.3	39.0	38.9			
1050	33.8		39.4	39.4	39.1	38.9			

* Averaged over 200mm, 300m and 400mm, long sections.

Test No. 6.

Dahl tube manometer reading:	3.355	Q_1 =	$0.04618 m^3/s$
Side spill stage :	10.73cm	Q_w =	$0.01713 m^3/s$
Weir length L :	110.72cm	Q_2 =	$0.2905 m^3/s$
Crest height C :	35.75cm	V_1 =	0.158m/s
B_1 :	73.50cm	V_2 =	0.157m/s
B_2 :	46.32cm	V_{mean} =	0.158m/s
Mean head above crest h* :	4.072cm	C_D (measured) =	0.638
Mean depth* :	39.822cm	C_D (Rehbock) =	0.639

Surface Profiles

X-Section (Distance from start of weir) mm	HEAD ABOVE CREST mm								
	LONG SECTION (DISTANCE BEHIND WEIR) mm								
	0	50	100	200	300	400	500	605	700
0 (50)	31.2		39.9	40.6	40.7	40.8	40.7	40.7	40.5
100	32.9		40.0	40.5	40.6	40.6	40.6	40.5	
200	32.2		40.0	40.7	40.5	40.6	40.5	40.3	
300	33.2		40.1	40.7	40.6	40.6	40.5	40.3	
400	33.5		40.1	40.7	40.5	40.7	40.3	40.2	
500	33.7		40.3	40.6	40.7	40.6	40.5		
600	33.8		40.4	40.7	40.8	40.6	40.4		
700	33.8		40.4	40.9	40.8	40.7	40.4		
800	33.9		40.5	41.0	40.8	40.6	40.4		
900	34.0		40.8	41.0	40.9	40.5			
1000	34.5		41.0	41.2	40.9	40.4			
1050	35.0		41.4	41.4	40.9	40.4			

* Averaged over 200mm, 300m and 400mm, long sections.

Test No. 7.

Dahl tube manometer reading:	2.47	Q_1	=	$0.03975 m^3/s$
Side spill stage :	9.90cm	Q_w	=	$0.01505 m^3/s$
Weir length L :	110.72cm	Q_2	=	$0.02470 m^3/s$
Crest height C :	35.75cm	V_1	=	0.137m/s
B_1 :	73.50cm	V_2	=	0.135m/s
B_2 :	46.32cm	V_{mean}	=	0.136m/s
Mean head above crest h* :	3.728cm	C_D (measured)	=	0.640
Mean depth* :	39.478cm	C_D (Rehbock)	=	0.640

Surface Profiles

X-Section (Distance from start of weir) mm	HEAD ABOVE CREST mm								
	LONG SECTION (DISTANCE BEHIND WEIR) mm								
	0	50	100	200	300	400	500	605	700
0 (50)→	28.5		36.5	36.9	37.2	37.2	37.2	37.0	37.0
100	29.8		36.5	36.9	37.2	37.2	37.2	36.9	
200	30.5		36.8	37.1	37.3	37.2	37.1	36.9	
300	30.9		36.8	37.2	37.3	37.2	37.1	36.8	
400	30.8		36.9	37.2	37.3	37.2	37.2	36.7	
500	30.8		36.9	37.3	37.3	37.3	37.1		
600	30.8		37.0	37.4	37.3	37.2	37.2		
700	30.8		37.1	37.5	37.3	37.2	37.1		
800	30.9		37.2	37.6	37.3	37.2	37.1		
900	31.1		37.4	37.7	37.3	37.1	36.9		
1000	31.3		37.6	37.8	37.4	37.1			
1050	31.7		37.8	37.8	37.4	37.0			

* Averaged over 200mm, 300m and 400mm, long sections.

Test No. 8.

Dahl tube manometer reading:	0.74	Q_1	=	$0.02200 m^3/s$
Side spill stage :	7.00cm	Q_w	=	$0.00861 m^3/s$
Weir length L :	110.72cm	Q_2	=	$0.01339 m^3/s$
Crest height C :	35.75cm	V_1	=	0.078m/s
B_1 :	73.50cm	V_2	=	0.076m/s
B_2 :	46.32cm	V_{mean}	=	0.077m/s
Mean head above crest h* :	2.524cm	C_D (measured)	=	0.656
Mean depth* :	38.274cm	C_D (Rehbock)	=	0.652

Surface Profiles

X-Section (Distance from start of weir) mm	HEAD ABOVE CREST mm								
	LONG SECTION (DISTANCE BEHIND WEIR) mm								
	0	50	100	200	300	400	500	605	700
0 (50)→	20.4		24.9	25.0	25.0	25.0	25.0	24.9	24.9
100	20.5		24.9	25.1	25.0	25.0	24.9	24.8	
200	20.5		25.0	25.1	25.1	24.9	25.0	24.8	
300	20.5		25.1	25.2	25.2	25.0	24.9	24.6	
400	20.6		25.1	25.2	25.3	24.9	24.9	24.7	
500	20.7		25.2	25.3	25.3	25.0	24.9		
600	20.6		25.3	25.4	25.3	25.1	25.0		
700	20.7		25.3	25.5	25.4	25.1	25.0		
800	20.7		25.4	25.5	25.4	25.2	25.2		
900	20.9		25.5	25.5	25.5	25.3			
1000	21.1		25.7	25.6	25.5	25.3			
1050	21.2		25.8	25.7	25.5	25.1			

* Averaged over 200mm, 300m and 400mm, long sections.

Test No. 9.

Dahl tube manometer reading:	0.40	Q_1	= 0.01627m^3/s
Side spill stage :	5.90cm	Q_w	= 0.00653m^3/s
Weir length L :	110.72cm	Q_2	= 0.00974m^3/s
Crest height C :	35.75cm	V_1	= 0.058m/s
B_1 :	73.50cm	V_2	= 0.056m/s
B_2 :	46.32cm	V_{mean}	= 0.057m/s
Mean head above crest h* :	2.101cm	C_D (measured)	= 0.656
Mean depth* :	37.851cm	C_D (Rehbock)	= 0.660

Surface Profiles

X-Section (Distance from start of weir) mm	HEAD ABOVE CREST mm								
	LONG SECTION (DISTANCE BEHIND WEIR) mm								
	0	50	100	200	300	400	500	605	700
0 (50)→	16.8		20.5	20.9	20.9	20.9	20.9	20.5	20.3
100	16.7		20.6	20.9	20.8	20.9	20.7	20.4	
200	16.8		20.7	20.9	20.8	21.0	20.7	20.4	
300	16.9		20.8	21.0	20.9	20.9	20.8	20.4	
400	16.9		20.9	21.0	20.9	20.9	20.8	20.3	
500	17.0		21.0	21.1	21.0	20.9	20.7		
600	17.0		21.1	21.2	21.1	20.9	20.7		
700	17.0		21.1	21.3	21.0	20.9	20.6		
800	17.2		21.3	21.3	21.1	20.8	20.5		
900	17.1		21.3	21.4	21.1	20.9			
1000	17.2		21.4	21.5	21.1	20.8			
1050	17.5		21.7	21.6	21.2	20.7			

* Averaged over 200mm, 300m and 400mm, long sections.

Test No. 10

Dahl tube manometer reading:	0.530	Q_1	= $0.01868 m^3/s$
Side spill stage	: 6.97cm	Q_w	= $0.00855 m^3/s$
Weir length L	: 110.72cm	Q_2	= $0.01013 m^3/s$
Crest height C	: 35.75cm	V_1	= 0.066m/s
B_1	: 73.50cm	V_2	= 0.064m/s
B_2	: 41.20cm	V_{mean}	= 0.065m/s
Mean head above crest h*	: 2.515cm	C_D (measured)	= 0.655
Mean depth*	: 38.265cm	C_D (Rehbock)	= 0.652

Surface Profiles

X-Section (Distance from start of weir) mm	HEAD ABOVE CREST mm								
	LONG SECTION (DISTANCE BEHIND WEIR) mm								
	0	50	100	200	300	400	500	605	700
0 (50)	20.0	24.5	25.0	25.2	25.2	25.2	24.9	24.7	24.2
100	20.0	24.6	25.0	25.2	25.2	25.2	24.8	24.7	
200	20.3	24.6	25.0	25.2	25.2	25.2	24.8	24.6	
300	20.3	24.6	25.0	25.2	25.2	25.1	24.8	24.6	
400	20.4	24.7	25.0	25.2	25.2	25.1	24.8		
500	20.5	24.8	25.0	25.3	25.2	25.0	24.8		
600	20.5	24.7	25.1	25.3	25.2	25.0	24.7		
700	20.7	24.8	25.2	25.3	25.2	25.0	24.7		
800	20.8	24.8	25.2	25.3	25.2	25.0			
900	20.8	24.9	25.2	25.3	25.2	24.9			
1000	20.8	25.0	25.3	25.3	25.0	24.8			
1050	20.8	25.0	25.3	25.4	25.0	24.8			

* Averaged over 200mm, 300m and 400mm, long sections.

Test No. 11.

Dahl tube manometer reading:	0.720	Q_1	= $0.02170 m^3/s$
Side spill stage :	7.51cm	Q_W	= $0.00964 m^3/s$
Weir length L :	110.72cm	Q_2	= $0.01206 m^3/s$
Crest height C :	35.75cm	V_1	= 0.077m/s
B_1 :	73.50cm	V_2	= 0.076m/s
B_2 :	41.20cm	V_{mean}	= 0.076m/s
Mean head above crest h* :	2.752cm	C_D (measured)	= 0.646
Mean depth* :	38.502cm	C_D (Rehbock)	= 0.649

Surface Profiles

X-Section (Distance from start of weir) mm	HEAD ABOVE CREST mm								
	LONG SECTION (DISTANCE BEHIND WEIR) mm								
	0	50	100	200	300	400	500	605	700
0 (50)	22.2	27.0	27.3	27.6	27.6	27.5	27.3	27.2	27.0
100	22.3	26.9	27.3	27.5	27.6	27.5	27.3	27.1	
200	22.5	26.9	27.3	27.5	27.6	27.5	27.3	27.1	
300	22.5	26.9	27.3	27.6	27.6	27.5	27.3	27.0	
400	22.5	26.9	27.4	27.6	27.6	27.5	27.3		
500	22.5	27.0	27.5	27.6	27.6	27.5	27.2		
600	22.5	27.0	27.5	27.6	27.5	27.4	27.2		
700	22.6	27.0	27.5	27.6	27.5	27.4	27.2		
800	22.7	27.1	27.5	27.7	27.5	27.3			
900	22.8	27.1	27.5	27.7	27.4	27.3			
1000	22.9	27.3	27.6	27.7	27.4	27.3			
1050	23.1	27.4	27.7	27.7	27.4	27.2			

* Averaged over 200mm, 300m and 400mm, long sections.

Test No. 12.

Dahl tube manometer reading:	0.94	Q_1	=	$0.02474 m^3/s$
Side spill stage	: 8.09cm	Q_W	=	$0.01087 m^3/s$
Weir length L	: 110.72cm	Q_2	=	$0.01387 m^3/s$
Crest height C	: 35.75cm	V_1	=	0.087m/s
B_1	: 73.50cm	V_2	=	0.087m/s
B_2	: 41.20cm	V_{mean}	=	0.087m/s
Mean head above crest h*	: 2.993	C_D (measured)	=	0.642
Mean depth*	: 38.743	C_D (Rehbock)	=	0.646

Surface Profiles

X-Section (Distance from start of weir) mm	HEAD ABOVE CREST mm								
	LONG SECTION (DISTANCE BEHIND WEIR) mm								
	0	50	100	200	300	400	500	605	700
0 (50)	23.9	29.2	29.6	30.0	29.9	30.0	29.9	29.7	29.4
100	24.2	29.1	29.6	30.0	29.9	30.0	29.8	29.5	
200	24.4	29.1	29.7	30.0	30.0	30.0	29.7	29.5	
300	24.3	29.2	29.7	30.0	30.0	30.0	29.8	29.5	
400	24.4	29.2	29.8	30.0	29.9	30.0	29.7		
500	24.5	29.2	29.9	30.0	29.9	29.9	29.6		
600	24.5	29.2	29.9	30.0	30.0	29.8	29.6		
700	24.5	29.3	29.9	30.0	30.0	29.7	29.5		
800	24.6	29.4	29.9	30.0	30.0	29.7			
900	24.6	29.4	30.0	30.0	30.0	29.6			
1000	24.7	29.5	30.1	30.1	29.9	29.6			
1050	24.8	29.8	30.2	30.2	29.9	29.5			

* Averaged over 200mm, 300m and 400mm, long sections.

Test No. 13.

Dahl tube manometer reading:	1.20	Q_1	$= 0.02788 m^3/s$
Side spill stage :	8.77cm	Q_W	$= 0.01238 m^3/s$
Weir length L :	110.72cm	Q_2	$= 0.01558 m^3/s$
Crest height C :	35.75cm	V_1	= 0.097m/s
B_1 :	73.50cm	V_2	= 0.097m/s
B_2 :	41.20cm	V_{mean}	= 0.097m/s
Mean head above crest h* :	3.238cm	C_D (measured)	= 0.649
Mean depth* :	38.988cm	C_D (Rehbock)	= 0.644

Surface Profiles

X-Section (Distance from start of weir) mm	HEAD ABOVE CREST mm								
	LONG SECTION (DISTANCE BEHIND WEIR) mm								
	0	50	100	200	300	400	500	605	700
0 (50)→	26.2	31.8	32.3	32.5	32.5	32.3	32.3	32.1	31.9
100	26.8	31.7	32.2	32.5	32.4	32.3	32.3	32.1	
200	26.9	31.8	32.2	32.5	32.4	32.3	32.3	32.0	
300	26.9	31.7	32.2	32.4	32.4	32.3	32.3	31.9	
400	26.9	31.7	32.3	32.5	32.5	32.2	32.3		
500	27.0	31.7	32.3	32.5	32.5	32.2	32.2		
600	27.1	31.7	32.3	32.5	32.5	32.2	32.0		
700	27.1	31.7	32.4	32.5	32.5	32.2			
800	27.1	31.7	32.4	32.5	32.5	32.2			
900	27.1	31.8	32.5	32.5	32.4	32.1			
1000	27.2	31.9	32.5	32.5	32.4	32.0			
1050	27.4	32.1	32.6	32.6	32.3	32.0			

* Averaged over 200mm, 300m and 400mm, long sections.

Test No. 14.

Dahl tube manometer reading:	1.51	Q_I	=	0.03122m^3/s
Side spill stage	: 9.33cm	Q_W	=	0.01367m^3/s
Weir length L	: 110.72cm	Q_2	=	0.01755m^3/s
Crest height C	: 35.75cm	V_1	=	0.108m/s
B_1	: 73.50cm	V_2	=	0.109m/s
B_2	: 41.20cm	V_{mean}	=	0.108m/s
Mean head above crest h*	: 3.496cm	C_D (measured)	=	0.640
Mean depth*	: 39.246cm	C_D (Rehbock)	=	0.642

Surface Profiles

X-Section (Distance from start of weir) mm	HEAD ABOVE CREST mm								
	LONG SECTION (DISTANCE BEHIND WEIR) mm								
	0	50	100	200	300	400	500	605	700
0 (50)-	-28.2	33.9	34.6	35.0	35.0	35.0	35.0	34.6	34.5
100	28.5	33.7	34.5	35.0	35.0	35.0	34.9	34.6	
200	28.7	33.9	34.6	35.0	35.0	35.0	34.9	34.6	
300	28.9	33.9	34.6	35.1	35.0	35.0	34.8	34.5	
400	28.9	34.0	34.7	35.1	35.0	35.0	34.7		
500	28.9	34.0	34.8	35.1	35.0	34.9	34.6		
600	28.8	34.1	34.9	35.1	35.0	34.9	34.6		
700	29.0	34.1	34.8	35.1	35.0	34.8	34.5		
800	29.0	34.1	34.9	35.1	35.0	34.8			
900	29.1	34.2	35.0	35.1	35.0	34.6			
1000	29.1	34.5	35.0	35.1	34.9	34.4			
1050	29.3	34.9	35.3	35.1	34.9	34.4			

* Averaged over 200mm, 300m and 400mm, long sections.

Test No. 15

Dahl tube manometer reading:	2.27	Q_1	=	$0.03815 m^3/s$
Side spill stage :	10.63cm	Q_w	=	$0.01687 m^3/s$
Weir length L :	110.72cm	Q_2	=	$0.02128 m^3/s$
Crest height C :	35.75cm	V_1	=	0.131m/s
B_1 :	73.50cm	V_2	=	0.130m/s
B_2 :	41.20 cm	V_{mean}	=	0.130m/s
Mean head above crest h* :	3.995cm	C_D (measured)	=	0.646
Mean depth* :	39.745cm	C_D (Rehbock)	=	0.639

Surface Profiles

X-Section (Distance from start of weir) mm	HEAD ABOVE CREST mm								
	LONG SECTION (DISTANCE BEHIND WEIR) mm								
	0	50	100	200	300	400	500	605	700
0 (50)→	31.5	38.7	39.5	39.9	40.0	40.1	40.1	39.9	39.8
100	32.3	38.7	39.5	39.9	40.0	40.0	39.9	39.7	
200	32.8	38.8	39.6	39.9	40.0	40.0	39.9	39.6	
300	32.9	38.8	39.6	39.9	40.0	40.0	39.9	39.6	
400	33.0	38.8	39.7	40.0	40.0	40.0	39.8		
500	33.0	38.8	39.7	40.0	40.0	39.9	39.8		
600	33.1	38.8	39.8	40.0	40.0	39.9	39.6		
700	33.2	38.9	39.8	40.0	39.9	39.7	39.5		
800	33.2	38.9	39.8	40.0	39.9	39.6			
900	33.3	39.0	39.8	40.0	39.8	39.5			
1000	33.3	39.2	39.9	40.1	39.8	39.3			
1050	33.9	39.9	40.1	40.1	39.7	39.1			

* Averaged over 200mm, 300m and 400mm, long sections.

Test No. 16.

Dahl tube manometer reading: 1.87 Q_1 = 0.03468m^3/s

Side spill stage : 9.93cm Q_W = 0.01512m^3/s

Weir length L : 110.72cm Q_2 = 0.01956m^3/s

Crest height C : 35.75cm V_1 = 0.119m/s

B_1 : 73.50cm V_2 = 0.120m/s

B_2 : 41.20cm V_{mean} = 0.120m/s

Mean head above crest h* : 3.746cm C_D (measured) = 0.638

Mean depth* : 39.496cm C_D (Rehbock) = 0.640

Surface Profiles

X-Section (Distance from start of weir) mm	HEAD ABOVE CREST mm								
	LONG SECTION (DISTANCE BEHIND WEIR) mm								
	0	50	100	200	300	400	500	605	700
0 (50)→	29.9	36.3	37.2	37.5	37.5	37.6	37.6	37.3	37.3
100	29.7	36.3	37.2	37.5	37.5	37.6	37.5	37.2	
200	29.8	36.4	37.2	37.5	37.5	37.7	37.5	37.0	
300	29.9	36.4	37.2	37.5	37.5	37.6	37.4	37.0	
400	30.0	36.4	37.2	37.5	37.5	37.5	37.3		
500	30.0	36.5	37.2	37.5	37.5	37.5	37.1		
600	30.0	36.5	37.2	37.5	37.5	37.4	37.0		
700	30.0	36.5	37.2	37.6	37.5	37.3	37.0		
800	30.1	36.5	37.3	37.6	37.5	37.3			
900	30.1	36.6	37.4	37.6	37.5	37.1			
1000	30.2	36.8	37.4	37.6	37.3	37.0			
1050	30.8	37.3	37.8	37.6	37.2	36.9			

* Averaged over 200mm, 300m and 400mm, long sections.

Test No. 17.

Dahl tube manometer reading:	2.74	Q_1 =	$0.04185 m^3/s$
Side spill stage :	11.15cm	Q_w =	$0.01822 m^3/s$
Weir length L :	110.72cm	Q_2 =	$0.02363 m^3/s$
Crest height C :	35.75cm	V_1 =	0.142m/s
B_1 :	73.50cm	V_2 =	0.143m/s
B_2 :	41.20cm	V_{mean} =	0.143m/s
Mean head above crest h* :	4.251cm	C_D (measured) =	0.636
Mean depth* :	40.001cm	C_D (Rehbock) =	0.638

Surface Profiles

X-Section (Distance from start of weir) mm	HEAD ABOVE CREST mm								
	LONG SECTION (DISTANCE BEHIND WEIR) mm								
	0	50	100	200	300	400	500	605	700
0 (50) →	33.1	41.0	42.1	42.5	42.7	42.7	42.6	42.3	42.3
100	34.3	41.0	42.1	42.5	42.7	42.7	42.6	42.1	
200	34.7	41.2	42.1	42.5	42.6	42.6	42.6	42.1	
300	34.9	41.3	42.2	42.5	42.6	42.6	42.4	42.0	
400	34.9	41.3	42.3	42.6	42.6	42.5	42.2		
500	35.0	41.3	42.3	42.6	42.6	42.4	42.2		
600	35.0	41.3	42.3	42.6	42.6	42.4	42.1		
700	35.1	41.3	42.3	42.7	42.6	42.4	42.0		
800	35.3	41.4	42.3	42.7	42.5	42.3			
900	35.4	41.4	42.4	42.7	42.4	42.1			
1000	35.4	41.7	42.5	42.8	42.3	42.0			
1050	36.0	42.2	42.6	42.7	42.3	41.9			

* Averaged over 200mm, 300m and 400mm, long sections.

Test No. 18.

Dahl tube manometer reading:	3.25	Q_1	=	$0.04549 m^3/s$
Side spill stage	: 11.88cm	Q_w	=	$0.02018 m^3/s$
Weir length L	: 110.72cm	Q_2	=	$0.02533 m^3/s$
Crest height C	: 35.75cm	V_1	=	0.154m/s
B_1	: 73.50cm	V_2	=	0.153m/s
B_2	: 41.20cm	V_{mean}	=	0.153m/s
Mean head above crest h*	: 4.514cm	C_D (measured)	=	0.644
Mean depth*	: 40.264cm	C_D (Rehbock)	=	0.637

Surface Profiles

X-Section (Distance from start of weir) mm	HEAD ABOVE CREST mm								
	LONG SECTION (DISTANCE BEHIND WEIR) mm								
	0	50	100	200	300	400	500	605	700
0 (50)→	35.9	43.2	44.4	45.2	45.2	45.3	45.3	45.1	45.2
100	37.6	43.1	44.4	45.2	45.2	45.2	45.2	45.1	
200	37.9	43.3	44.5	45.2	45.2	45.2	45.1	45.0	
300	37.9	43.4	44.6	45.2	45.2	45.2	45.0	45.0	
400	37.8	43.5	44.6	45.2	45.2	45.2	44.9		
500	37.8	43.5	44.7	45.2	45.2	45.2	44.8		
600	37.8	43.5	44.7	45.2	45.2	45.2	44.8		
700	37.8	43.6	44.7	45.2	45.2	45.1	44.8		
800	37.8	43.6	44.8	45.2	45.2	45.0			
900	38.1	43.7	44.9	45.2	45.2	44.9			
1000	38.1	44.2	45.3	45.2	45.1	44.6			
1050	38.1	44.8	45.4	45.3	44.9	44.5			

* Averaged over 200mm, 300m and 400mm, long sections.

Test No. 19.

Dahl tube manometer reading:	0.80	Q_1	= 0.022851m^3/s
Side spill stage	: 6.28cm	Q_W	= 0.007225m^3/s
Weir length L	: 110.72cm	Q_2	= 0.01562m^3/s
Crest height C	: 35.75cm	V_1	= 0.082m/s
B_1	: 73.50cm	V_2	= 0.081m/s
B_2	: 50.92cm	V_{mean}	= 0.081m/s
Mean head above crest h*	: 2.242cm	C_D (measured)	= 0.658
Mean depth*	: 37.992cm	C_D (Rehbock)	= 0.657

Surface Profiles

X-Section (Distance from start of weir) mm	HEAD ABOVE CREST mm								
	LONG SECTION (DISTANCE BEHIND WEIR) mm								
	0	50	100	200	300	400	500	605	700
0 (50)→	18.3	21.7	22.3	22.3	22.3	22.3	22.4	22.1	22.0
100	18.3	21.9	22.3	22.3	22.3	22.3	22.3	22.0	
200	18.2	22.0	22.3	22.3	22.4	22.3	22.3	21.9	
300	18.2	22.0	22.3	22.4	22.5	22.3	22.3	21.9	
400	18.3	22.1	22.4	22.4	22.5	22.3	22.3	21.9	
500	18.2	22.1	22.5	22.4	22.5	22.3	22.2		
600	18.2	22.1	22.5	22.4	22.5	22.3	22.2		
700	18.2	22.1	22.5	22.5	22.5	22.3	22.1		
800	18.4	22.3	22.6	22.6	22.5	22.3	22.1		
900	18.3	22.3	22.6	22.6	22.6	22.3	22.0		
1000	18.3	22.3	22.7	22.7	22.6	22.3			
1050	18.5	22.5	22.8	22.8	22.6	22.3			

* Averaged over 200mm, 300m and 400mm, long sections.

Test No. 20.

Dahl tube manometer reading:	1.04	Q_1	= 0.02600m^3/s
Side spill stage :	6.89cm	Q_w	= 0.008390m^3/s
Weir length L :	110.72cm	Q_2	= 0.01761m^3/s
Crest height C :	35.75cm	V_1	= 0.093m/s
B_1 :	73.50cm	V_2	= 0.090m/s
B_2 :	50.92cm	V_{mean}	= 0.092m/s
Mean head above crest h* :	2.498cm	C_D (measured)	= 0.650
Mean depth* :	38.248cm	C_D (Rehbock)	= 0.652

Surface Profiles

X-Section (Distance from start of weir) mm	HEAD ABOVE CREST mm								
	LONG SECTION (DISTANCE BEHIND WEIR) mm								
	0	50	100	200	300	400	500	605	700
0 (50)→	20.1	24.4	24.9	25.0	25.0	25.0	24.8	24.6	24.3
100	20.4	24.5	24.9	24.9	24.9	24.9	24.9	24.5	
200	20.5	24.5	24.9	24.9	24.9	24.9	24.8	24.5	
300	20.5	24.6	25.0	25.0	25.0	24.9	24.8	24.4	
400	20.5	24.6	25.0	25.0	25.0	24.9	24.7	24.4	
500	20.6	24.7	25.0	25.0	25.0	24.9	24.7		
600	20.6	24.7	25.0	25.1	25.0	24.9	24.6		
700	20.7	24.7	25.1	25.1	25.0	24.9	24.6		
800	20.7	24.8	25.1	25.1	25.0	24.9	24.5		
900	20.9	24.9	25.1	25.2	25.0	24.9	24.5		
1000	21.0	25.0	25.2	25.2	25.0	24.8			
1050	21.1	25.1	25.3	25.2	25.0	24.7			

* Averaged over 200mm, 300m and 400mm, long sections.

Test No. 21

Dahl tube manometer reading:	1.32	Q_1	=	$0.02923 m^3/s$
Side spill stage	: 7.27cm	Q_w	=	$0.009147 m^3/s$
Weir length L	: 110.72cm	Q_2	=	$0.02008 m^3/s$
Crest height C	: 35.75cm	V_1	=	0.104m/s
B_1	: 73.50cm	V_2	=	0.103m/s
B_2	: 50.92cm	V_{mean}	=	0.103m/s
Mean head above crest h*	: 2.648cm	C_D (measured)	=	0.649
Mean depth*	: 38.398cm	C_D (Rehbock)	=	0.650

Surface Profiles

X-Section (Distance from start of weir) mm	HEAD ABOVE CREST mm								
	LONG SECTION (DISTANCE BEHIND WEIR) mm								
	0	50	100	200	300	400	500	605	700
0 (50)	21.4	25.9	26.4	26.5	26.5	26.6	26.5	26.3	26.3
100	21.5	25.8	26.4	26.5	26.5	26.5	26.4	26.2	
200	21.6	25.9	26.4	26.5	26.5	26.5	26.4	26.2	
300	21.7	26.0	26.5	26.5	26.5	26.5	26.4	26.1	
400	21.8	26.0	26.5	26.5	26.5	26.5	26.4	26.1	
500	21.8	26.0	26.5	26.5	26.5	26.5	26.3		
600	21.9	26.0	26.5	26.5	26.5	26.4	26.3		
700	21.9	26.1	26.5	26.6	26.5	26.4	26.2		
800	22.0	26.2	26.5	26.6	26.4	26.3	26.0		
900	22.1	26.3	26.6	26.7	26.4	26.2	25.9		
1000	22.1	26.4	26.6	26.7	26.4	26.2			
1050	22.3	26.6	26.8	26.7	26.4	26.1			

* Averaged over 200mm, 300m and 400mm, long sections.

Test No. 22

Dahl tube manometer reading:	1.64	Q_I =	0.03252m^3/s
Side spill stage :	7.80cm	Q_W =	0.010246m^3/s
Weir length L :	110.72cm	Q_2 =	0.02227m^3/s
Crest height C :	35.75cm	V_1 =	0.115m/s
B_1 :	73.50cm	V_2 =	0.113m/s
B_2 :	50.92cm	V_{mean} =	0.114m/s
Mean head above crest h* :	2.867cm	C_D (measured) =	0.646
Mean depth* :	38.617cm	C_D (Rehbock) =	0.647

Surface Profiles

X-Section (Distance from start of weir) mm	HEAD ABOVE CREST mm								
	LONG SECTION (DISTANCE BEHIND WEIR) mm								
	0	50	100	200	300	400	500	605	700
0 (50)→	23.4	27.8	28.4	28.6	28.7	28.6	28.6	28.5	28.5
100	23.6	27.9	28.4	28.5	28.7	28.7	28.5	28.4	
200	23.6	27.9	28.5	28.5	28.8	28.7	28.5	28.4	
300	23.6	28.0	28.5	28.5	28.8	28.7	28.5	28.3	
400	23.7	28.1	28.5	28.5	28.8	28.6	28.5	28.3	
500	23.7	28.1	28.5	28.6	28.8	28.6	28.5		
600	23.7	28.2	28.6	28.7	28.8	28.6	28.4		
700	23.7	28.2	28.6	28.8	28.7	28.6	28.3		
800	23.7	28.2	28.7	28.9	28.7	28.5	28.3		
900	23.7	28.2	28.8	28.9	28.7	28.5	28.2		
1000	23.8	28.4	28.9	29.0	28.7	28.4			
1050	24.0	28.6	28.9	29.0	28.7	28.3			

* Averaged over 200mm, 300m and 400mm, long sections.

Test No. 23

Dahl tube manometer reading:	2.03	Q_I	=	$0.03611 m^3/s$
Side spill stage :	8.28cm	Q_W	=	$0.01128 m^3/s$
Weir length L :	110.72cm	Q_2	=	$0.02483 m^3/s$
Crest height C :	35.75cm	V_1	=	0.127m/s
B_1 :	73.50cm	V_2	=	0.126m/s
B_2 :	50.92cm	V_{mean}	=	0.126m/s
Mean head above crest h* :	3.056cm	C_D (measured)	=	0.646
Mean depth* :	38.806cm	C_D (Rehbock)	=	0.645

Surface Profiles

X-Section (Distance from start of weir) mm	HEAD ABOVE CREST mm								
	LONG SECTION (DISTANCE BEHIND WEIR) mm								
	0	50	100	200	300	400	500	605	700
0 (50)	24.4	29.6	30.3	30.5	30.5	30.6	30.6	30.5	30.5
100	24.9	29.7	30.2	30.5	30.5	30.6	30.5	30.4	
200	25.1	29.8	30.3	30.6	30.5	30.5	30.5	30.3	
300	25.3	29.9	30.3	30.6	30.5	30.5	30.4	30.2	
400	25.3	29.9	30.4	30.7	30.6	30.5	30.3	30.2	
500	25.4	29.9	30.4	30.7	30.6	30.5	30.3		
600	25.5	29.9	30.5	30.6	30.6	30.5	30.3		
700	25.5	30.0	30.5	30.7	30.6	30.5	30.3		
800	25.6	30.0	30.5	30.6	30.6	30.5	30.2		
900	25.6	30.0	30.6	30.7	30.6	30.4	30.1		
1000	25.7	30.1	30.8	30.8	30.6	30.3			
1050	25.9	30.3	30.9	30.9	30.5	30.2			

* Averaged over 200mm, 300m and 400mm, long sections.

Test No. 24

Dahl tube manometer reading:	2.58	Q_1	= 0.04062 m^3/s
Side spill stage :	8.92cm	Q_W	= 0.01272 m^3/s
Weir length L :	110.72cm	Q_2	= 0.02790 m^3/s
Crest height C :	35.75cm	V_1	= 0.141m/s
B_1 :	73.50cm	V_2	= 0.140m/s
B_2 :	50.92cm	V_{mean}	= 0.141m/s
Mean head above crest h* :	3.329cm	C_D (measured)	= 0.641
Mean depth* :	39.079cm	C_D (Rehbock)	= 0.643

Surface Profiles

X-Section (Distance from start of weir) mm	HEAD ABOVE CREST mm								
	LONG SECTION (DISTANCE BEHIND WEIR) mm								
	0	50	100	200	300	400	500	605	700
0 (50)	26.2	32.1	32.9	33.2	33.3	33.3	33.3	33.0	33.0
100	26.9	32.1	32.9	33.2	33.2	33.2	33.2	33.0	
200	27.2	32.2	32.9	33.2	33.2	33.3	33.3	33.0	
300	27.3	32.3	33.0	33.2	33.2	33.2	33.3	33.0	
400	27.3	32.4	33.1	33.3	33.2	33.2	33.2	33.0	
500	27.3	32.4	33.2	33.4	33.2	33.2	33.2		
600	27.4	32.4	33.3	33.3	33.2	33.2	33.0		
700	27.4	32.5	33.3	33.4	33.2	33.2	33.0		
800	27.5	32.7	33.4	33.5	33.3	33.2	32.9		
900	27.8	32.9	33.4	33.5	33.4	33.1	32.9		
1000	27.8	33.0	33.6	33.7	33.4	33.1			
1050	28.2	33.3	33.7	33.8	33.5	33.1			

* Averaged over 200mm, 300m and 400mm, long sections.

Test No. 25

Dahl tube manometer reading:	3.36	Q_1	=	0.04621m^3/s
Side spill stage :	9.56cm	Q_W	=	0.01422 m^3/s
Weir length L :	110.72cm	Q_2	=	0.03199m^3/s
Crest height C :	35.75cm	V_1	=	0.160m/s
B_1 :	73.50cm	V_2	=	0.160m/s
B_2 :	50.92cm	V_{mean}	=	0.160m/s
Mean head above crest h* :	3.597cm	C_D (measured)	=	0.638
Mean depth* :	39.347cm	C_D (Rehbock)	=	0.641

Surface Profiles

X-Section (Distance from start of weir) mm	HEAD ABOVE CREST mm								
	LONG SECTION (DISTANCE BEHIND WEIR) mm								
	0	50	100	200	300	400	500	605	700
0 (50)→	27.8	34.6	35.9	36.1	35.9	36.0	35.9	35.8	35.9
100	29.1	34.8	35.4	35.9	35.9	36.0	35.8	35.7	
200	29.7	34.9	35.5	36.0	35.9	36.0	35.8	35.6	
300	29.8	34.9	35.6	36.0	35.9	36.0	35.9	35.6	
400	29.8	34.9	35.6	36.1	35.9	35.9	35.9	35.6	
500	29.8	35.0	35.6	36.0	36.0	35.9	35.9		
600	29.8	35.0	35.7	36.0	36.0	35.9	35.9		
700	29.9	35.1	35.7	36.0	36.0	35.9	35.7		
800	29.9	35.0	35.8	36.1	36.0	35.9	35.5		
900	30.0	35.1	36.0	36.1	36.0	35.8	35.4		
1000	30.3	35.5	36.1	36.2	36.0	35.6			
1050	30.9	35.8	36.4	36.4	36.1	35.5			

* Averaged over 200mm, 300m and 400mm, long sections.

Test No. 26

Dahl tube manometer reading:			Q_1	=
Side spill stage	:	9.99cm	Q_W	= 0.015268m^3/s
Weir length L	:	110.72cm	Q_2	=
Crest height C	:	35.75cm	V_1	=
B_1	:	73.50cm	V_2	=
B_2	:	50.92cm	V_{mean}	=
Mean head above crest h*	:	3.790cm	C_D (measured)	= 0.633
Mean depth*	:	39.540cm	C_D (Rehbock)	= 0.640

Surface Profiles

X-Section (Distance from start of weir) mm	HEAD ABOVE CREST mm								
	LONG SECTION (DISTANCE BEHIND WEIR) mm								
	0	50	100	200	300	400	500	605	700
0 (50)	29.3	36.4	37.4	37.9	37.8	38.3	37.9	37.9	37.9
100	30.3	36.3	37.3	38.0	37.8	38.0	37.8	37.8	
200	30.8	36.4	37.3	37.9	37.8	38.0	37.8	37.6	
300	30.8	36.5	37.4	38.0	37.8	37.9	37.8	37.5	
400	30.8	36.5	37.5	38.0	37.8	37.9	37.7	37.3	
500	30.9	36.6	37.5	38.0	37.9	37.9	37.7		
600	31.0	36.6	37.5	37.9	37.9	37.8	37.6		
700	31.1	36.6	37.5	38.0	37.9	37.8	37.5		
800	31.2	36.7	37.6	37.9	37.9	37.7	37.5		
900	31.3	36.8	37.7	38.0	37.9	37.6	37.3		
1000	31.5	37.0	38.1	38.2	38.0	37.5			
1050	32.0	37.9	38.1	38.2	38.1	37.5			

* Averaged over 200mm, 300m and 400mm, long sections.

Test No. 27

Dahl tube manometer reading:	4.30	Q_1	=	0.05212m^3/s
Side spill stage :	10.28cm	Q_W	=	0.01599 m^3/s
Weir length L :	110.72cm	Q_2	=	0.03613m^3/s
Crest height C :	35.75cm	V_1	=	0.179m/s
B_1 :	73.50cm	V_2	=	0.179m/s
B_2 :	50.92cm	V_{mean}	=	0.179m/s
Mean head above crest h* :	3.909cm	C_D (measured)	=	0.633
Mean depth* :	39.659cm	C_D (Rehbock)	=	0.639

Surface Profiles

X-Section (Distance from start of weir) mm	HEAD ABOVE CREST mm								
	LONG SECTION (DISTANCE BEHIND WEIR) mm								
	0	50	100	200	300	400	500	605	700
0 (50)→	30.7	37.5	38.6	39.0	39.0	39.1	39.2	39.0	39.1
100	31.8	37.8	38.4	38.9	39.0	39.2	39.1	38.9	
200	32.1	37.8	38.5	39.1	39.1	39.1	38.9	38.9	
300	32.2	37.8	38.6	39.1	39.1	39.0	38.9	38.7	
400	32.2	37.8	38.7	39.1	39.1	39.0	38.9	38.7	
500	32.3	37.9	38.8	39.2	39.1	38.9	38.9		
600	32.4	37.9	38.8	39.3	39.2	38.9	38.9		
700	32.5	37.9	38.9	39.3	39.2	38.8	38.8		
800	32.6	38.0	39.0	39.3	39.2	38.8	38.7		
900	32.6	38.1	39.2	39.2	39.1	38.9	38.5		
1000	32.9	38.5	39.5	39.4	39.3	38.8			
1050	33.4	39.2	39.8	39.7	39.2	38.7			

* Averaged over 200mm, 300m and 400mm, long sections.

Test No. 28

Dahl tube manometer reading:	5.17	Q_1	=	$0.05712 m^3/s$
Side spill stage :	10.79cm	Q_W	=	$0.017286 m^3/s$
Weir length L :	110.72cm	Q_2	=	$0.03983 m^3/s$
Crest height C :	35.75cm	V_1	=	0.195m/s
B_1 :	73.50cm	V_2	=	0.196m/s
B_2 :	50.92cm	V_{mean}	=	0.196m/s
Mean head above crest h* :	4.131cm	C_D (measured)	=	0.630
Mean depth* :	39.881cm	C_D (Rehbock)	=	0.638

Surface Profiles

X-Section (Distance from start of weir) mm	HEAD ABOVE CREST mm								
	LONG SECTION (DISTANCE BEHIND WEIR) mm								
	0	50	100	200	300	400	500	605	700
0 (50)	31.5	39.1	40.7	41.1	41.5	41.3	41.4	41.4	41.3
100	32.7	39.3	40.8	41.2	41.4	41.4	41.4	41.3	
200	33.4	39.5	40.9	41.2	41.4	41.4	41.4	41.2	
300	33.7	39.6	40.9	41.3	41.4	41.4	41.4	41.1	
400	33.8	39.8	41.0	41.3	41.3	41.3	41.3	41.0	
500	34.0	39.8	41.1	41.4	41.4	41.3	41.2		
600	34.0	39.9	41.0	41.4	41.4	41.2	41.0		
700	34.2	40.0	41.1	41.3	41.3	41.2	40.9		
800	34.3	40.1	41.1	41.3	41.3	41.1	40.9		
900	34.4	40.2	41.3	41.4	41.2	41.1	40.9		
1000	34.8	40.7	41.4	41.8	41.2	41.0			
1050	34.8	41.4	42.0	41.8	41.4	40.8			

* Averaged over 200mm, 300m and 400mm, long sections.

(b) Velocity Traverse Readings.

Test No. 2.

LONG SECTION 100 mm BEHIND WEIR : VELOCITY mm/s						
DISTANCE BELOW CREST mm	X SECTION, mm FROM START OF WEIR					
	0	200	400	600	800	1000
30	91.5	95.4	82.1	71.3	72.0	52.3
80	109.8	89.7	70.7	54.0	58.3	57.9
130	103.0	87.6	64.9	48.6	58.6	70.6
180	96.5	80.1	65.4	43.9	60.3	66.9
230	88.1	83.4	61.1	39.9	65.8	71.1
280	59.3	72.1	56.3	38.3	63.0	68.9

LONG SECTION 200 mm BEHIND WEIR : VELOCITY mm/s						
DISTANCE BELOW CREST mm	X SECTION, mm FROM START OF WEIR					
	0	200	400	600	800	1000
30	104.7	98.7	88.1	95.3	102.6	92.8
80	103.8	85.1	92.4	91.9	88.9	97.0
130	92.8	68.5	79.2	86.0	93.2	91.5
180	83.4	85.1	77.5	88.9	76.6	91.9
230	71.5	81.3	79.2	95.3	74.9	94.5
280	68.1	57.9	80.9	86.0	74.0	92.8

Test No. 2.

LONG SECTION 300 mm BEHIND WEIR : VELOCITY mm/s						
DISTANCE BELOW CREST mm	X SECTION, mm FROM START OF WEIR					
	0	200	400	600	800	1000
30	104.3	107.3	100.4	91.1	97.9	103.0
80	98.7	103.4	94.1	83.4	87.2	98.7
130	92.8	94.1	77.9	75.8	89.4	96.6
180	86.4	97.5	66.8	86.0	87.2	93.2
230	91.5	89.8	72.3	93.2	92.8	91.5
280	91.5	83.8	79.2	93.6	89.4	89.4

LONG SECTION 400 mm BEHIND WEIR : VELOCITY mm/s						
DISTANCE BELOW CREST mm	X SECTION, mm FROM START OF WEIR					
	0	200	400	600	800	1000
30	104.7	97.0	95.3	104.3	109.0	114.9
80	92.8	91.9	94.1	103.0	103.8	115.3
130	95.8	90.7	90.2	97.0	106.8	110.2
180	86.8	85.5	86.4	97.5	107.7	113.6
230	83.8	94.1	94.9	96.6	108.1	112.8
280	91.9	95.8	89.8	97.9	104.7	109.8

Test No. 2.

LONG SECTION 500 mm BEHIND WEIR : VELOCITY mm/s						
DISTANCE BELOW CREST mm	X SECTION, mm FROM START OF WEIR					
	0	200	400	600	800	1000
30	79.6	101.7	105.6	110.2	103.8	
80	76.6	101.7	107.3	109.0	106.0	
130	73.2	98.3	106.0	109.4	108.1	
180	76.2	100.0	104.3	110.2	106.0	
230	73.6	97.9	104.7	105.6	100.9	
280	78.3	100.9	100.4	103.0	88.1	

LONG SECTION 635 mm BEHIND WEIR : VELOCITY mm/s						
DISTANCE BELOW CREST mm	X SECTION, mm FROM START OF WEIR					
	0	200	400	600	800	1000
30	89.8	93.6				
80	91.1	89.7				
130	94.5	95.8				
180	91.1	98.8				
230	86.4	87.2				
280	83.0	73.2				

Test No. 3.

LONG SECTION 100 mm BEHIND WEIR : VELOCITY mm/s						
DISTANCE BELOW CREST mm	X SECTION, mm FROM START OF WEIR					
	0	200	400	600	800	1000
30	146.9	114.1	117.5	110.2	107.7	101.7
80	134.5	110.2	110.7	103.4	91.9	88.5
130	128.5	111.9	107.7	91.9	88.9	88.5
180	117.5	110.7	95.8	89.8	87.7	94.5
230	114.5	101.7	88.9	83.4	86.4	95.3
280	101.7	91.5	84.3	75.8	96.2	94.5

LONG SECTION 200 mm BEHIND WEIR : VELOCITY mm/s						
DISTANCE BELOW CREST mm	X SECTION, mm FROM START OF WEIR					
	0	200	400	600	800	1000
30	138.3	133.2	126.8	129.0	123.9	121.3
80	133.2	126.8	119.2	124.3	120.0	122.6
130	128.1	116.6	114.1	111.9	120.9	123.9
180	117.0	111.1	109.4	114.5	115.3	118.3
230	107.3	113.6	109.4	113.2	113.6	118.3
280	103.4	97.9	113.2	116.2	111.5	118.3

Test No. 3.

LONG SECTION 300 mm BEHIND WEIR : VELOCITY mm/s						
DISTANCE BELOW CREST mm	X SECTION, mm FROM START OF WEIR					
	0	200	400	600	800	1000
30	132.8	131.1	135.8	136.2	135.8	133.2
80	129.4	127.7	133.6	131.1	137.5	141.3
130	122.2	123.0	130.2	124.3	130.2	133.2
180	117.9	121.3	121.3	124.3	128.5	132.4
230	112.4	116.6	120.5	124.7	123.9	130.7
280	115.8	120.5	109.4	119.2	116.6	126.0

LONG SECTION 400 mm BEHIND WEIR : VELOCITY mm/s						
DISTANCE BELOW CREST mm	X SECTION, mm FROM START OF WEIR					
	0	200	400	600	800	1000
30	132.8	130.2	134.1	135.8	137.1	142.2
80	124.7	132.8	132.8	137.5	135.8	142.2
130	126.4	126.4	131.5	133.6	135.4	140.9
180	123.0	125.6	130.7	129.4	131.9	137.5
230	121.7	118.3	130.2	123.9	134.5	137.1
280	118.3	117.0	121.3	118.7	123.0	126.4

Test No. 3.

LONG SECTION 500 mm BEHIND WEIR : VELOCITY mm/s						
DISTANCE BELOW CREST mm.	X SECTION, mm FROM START OF WEIR					
	0	200	400	600	800	1000
30	129.8	129.4	132.4	129.0	125.1	
80	125.1	131.1	131.9	135.8	132.4	
130	129.0	128.5	131.9	130.7	135.8	
180	123.9	127.3	131.5	132.4	127.7	
230	122.2	122.6	126.0	132.8	125.6	
280	118.3	111.9	125.6	119.6	121.3	

LONG SECTION 635 mm BEHIND WEIR : VELOCITY mm/s						
DISTANCE BELOW CREST mm	X SECTION, mm FROM START OF WEIR					
	0	200	400	600	800	1000
30	114.9	120.9				
80	117.9	121.7				
130	114.1	120.5				
180	116.2	115.8				
230	105.1	109.4				
280	95.8	101.7				

Test No. 6.

LONG SECTION 100 mm BEHIND WEIR : VELOCITY mm/s						
DISTANCE BELOW CREST mm.	X SECTION, mm FROM START OF WEIR					
	0	200	400	600	800	1000
30	197.0	166.1	153.0	149.9	138.8	131.9
80	181.9	171.1	158.8	138.3	133.6	117.5
130	168.4	162.7	148.4	139.2	126.8	120.9
180	170.0	163.1	158.8	131.9	117.5	128.5
230	158.8	152.3	143.4	122.2	123.4	125.1
280	151.5	160.0	143.0	118.3	122.6	136.6

LONG SECTION 200 mm BEHIND WEIR : VELOCITY mm/s						
DISTANCE BELOW CREST mm	X SECTION, mm FROM START OF WEIR					
	0	200	400	600	800	1000
30	181.6	173.1	165.4	163.8	165.7	160.7
80	164.2	163.8	152.6	156.5	149.9	156.5
130	160.7	154.2	147.2	148.0	149.6	160.7
180	145.7	142.2	141.3	143.0	154.2	163.8
230	132.4	135.8	147.2	139.2	155.0	156.1
280	129.8	127.7	137.1	146.9	157.3	157.7

Test No. 6.

LONG SECTION 300 mm BEHIND WEIR : VELOCITY mm/s						
DISTANCE BELOW CREST mm	X SECTION, mm FROM START OF WEIR					
	0	200	400	600	800	1000
30	168.4	175.0	174.6	175.4	179.6	185.8
80	161.9	171.5	162.3	166.5	176.5	185.0
130	155.3	164.2	160.4	158.8	167.7	181.6
180	146.9	162.7	160.7	161.9	167.7	181.6
230	149.2	153.0	158.0	162.7	167.7	180.8
280	142.2	149.6	165.4	163.1	163.8	178.1

LONG SECTION 400 mm BEHIND WEIR : VELOCITY mm/s						
DISTANCE BELOW CREST mm	X SECTION, mm FROM START OF WEIR					
	0	200	400	600	800	1000
30	171.5	173.1	173.8	177.7	187.0	193.5
80	162.7	168.8	171.1	172.7	176.9	190.8
130	156.9	162.7	167.7	167.3	173.8	191.6
180	149.6	158.0	165.7	166.1	176.2	191.6
230	147.2	155.0	162.3	165.0	171.5	187.3
280	158.8	161.9	161.9	166.9	165.7	178.1

Test No. 6.

LONG SECTION 500 mm BEHIND WEIR : VELOCITY mm/s						
DISTANCE BELOW CREST mm	X SECTION, mm FROM START OF WEIR					
	0	200	400	600	800	1000
30	164.2	172.3	169.2	173.1	176.9	
80	167.3	164.6	165.0	167.7	171.5	
130	158.4	158.8	163.1	164.2	165.4	
180	152.3	157.3	167.7	161.5	162.3	
230	156.5	159.2	166.1	154.2	137.9	
280	155.3	150.3	154.2	140.0	140.0	

LONG SECTION 635 mm BEHIND WEIR : VELOCITY mm/s						
DISTANCE BELOW CREST mm	X SECTION, mm FROM START OF WEIR					
	0	200	400	600	800	1000
30	155.3	162.7				
80	155.0	161.5				
130	149.9	156.9				
180	147.6	145.7				
230	147.2	144.5				
280	115.8	116.2				

Test No. 8.

LONG SECTION 100 mm BEHIND WEIR : VELOCITY mm/s						
DISTANCE BELOW CREST mm	X SECTION, mm FROM START OF WEIR					
	0	200	400	600	800	1000
30	88.5	72.3	68.5	70.2	68.9	58.3
80	81.3	74.0	66.0	53.2	60.4	54.5
130	80.0	70.6	58.7	52.3	56.6	55.7
180	80.0	61.7	62.1	49.4	54.0	62.6
230	75.8	56.6	50.6	48.1	59.1	60.4
280	66.4	57.0	46.4	47.7	58.3	63.4

LONG SECTION 200 mm BEHIND WEIR : VELOCITY mm/s						
DISTANCE BELOW CREST mm	X SECTION, mm FROM START OF WEIR					
	0	200	400	600	800	1000
30	85.5	84.3	76.6	76.1	74.9	74.5
80	81.3	79.2	71.5	72.8	70.2	70.2
130	80.9	75.3	68.9	74.0	69.8	72.8
180	74.0	67.7	68.5	68.5	66.8	72.8
230	68.9	68.1	69.8	69.4	72.3	73.2
280	62.1	67.2	64.7	68.5	70.6	71.9

Test No. 8.

LONG SECTION 300 mm BEHIND WEIR : VELOCITY mm/s						
DISTANCE BELOW CREST mm	X SECTION, mm FROM START OF WEIR					
	0	200	400	600	800	1000
30	85.1	81.3	80.4	80.9	80.9	86.4
80	80.0	81.3	77.9	77.9	77.9	82.6
130	78.3	73.6	75.3	79.6	77.0	85.5
180	73.6	68.5	73.2	72.8	76.6	82.6
230	69.4	74.0	73.2	74.0	75.3	78.3
280	74.0	76.2	73.6	74.5	74.9	77.0

LONG SECTION 400 mm BEHIND WEIR : VELOCITY mm/s						
DISTANCE BELOW CREST mm	X SECTION, mm FROM START OF WEIR					
	0	200	400	600	800	1000
30	80.0	83.0	83.0	83.8	83.0	86.8
80	78.3	80.4	81.3	83.0	86.8	86.4
130	79.2	79.6	79.6	79.6	83.8	86.0
180	73.6	72.3	76.6	83.0	78.7	86.0
230	73.2	73.6	78.3	77.5	79.6	85.1
280	71.1	76.6	74.0	80.4	77.9	83.8

Test No. 8.

LONG SECTION 500 mm BEHIND WEIR : VELOCITY mm/s						
DISTANCE BELOW CREST mm	X SECTION, mm FROM START OF WEIR					
	0	200	400	600	800	1000
30	79.9	79.9	83.0	80.4	79.9	
80	81.3	79.6	78.7	83.0	82.1	
130	73.2	77.0	79.2	81.7	81.3	
180	71.9	74.0	77.5	82.6	77.0	
230	69.8	75.3	77.9	79.9	76.2	
280	75.8	75.8	77.0	81.3	72.8	

LONG SECTION 635 mm BEHIND WEIR : VELOCITY mm/s						
DISTANCE BELOW CREST mm	X SECTION, mm FROM START OF WEIR					
	0	200	400	600	800	1000
30	72.3	73.6				
80	71.5	74.0				
130	70.2	74.9				
180	71.9	75.8				
230	75.3	65.5				
280	67.7	62.1				

Test No. 12.

LONG SECTION 100 mm BEHIND WEIR : VELOCITY mm/s						
DISTANCE BELOW CREST mm	X SECTION, mm FROM START OF WEIR					
	0	200	400	600	800	1000
30	99.6	85.1	80.9	84.2	81.7	71.1
80	98.7	85.5	74.5	74.5	70.6	63.0
130	93.6	85.1	74.5	63.0	61.7	63.4
180	90.2	80.9	63.8	58.2	61.7	64.7
230	86.8	70.2	66.0	59.6	62.6	71.5
280	75.8	61.3	58.7	47.0	68.9	58.2

LONG SECTION 200 mm BEHIND WEIR : VELOCITY mm/s						
DISTANCE BELOW CREST mm	X SECTION, mm FROM START OF WEIR					
	0	200	400	600	800	1000
30	94.9	86.8	86.4	86.8	86.8	90.2
80	94.1	88.1	86.0	84.7	88.9	90.2
130	88.9	83.8	83.0	85.1	84.3	86.4
180	84.7	84.7	82.6	81.3	83.8	86.0
230	80.0	74.9	79.2	77.5	80.0	83.4
280	74.5	63.4	68.9	71.5	80.0	80.0

Test No. 12.

LONG SECTION 300 mm BEHIND WEIR : VELOCITY mm/s						
DISTANCE BELOW CREST mm	X SECTION, mm FROM START OF WEIR					
	0	200	400	600	800	1000
30	94.1	90.2	89.0	88.1	90.2	94.5
80	92.8	93.2	89.4	86.8	89.4	93.6
130	91.1	90.7	89.4	87.3	89.4	94.9
180	91.1	86.0	83.0	81.7	85.5	96.2
230	85.5	81.3	79.6	83.0	86.0	91.5
280	79.6	80.9	75.3	78.7	83.4	85.5

LONG SECTION 400 mm BEHIND WEIR : VELOCITY mm/s						
DISTANCE BELOW CREST mm	X SECTION, mm FROM START OF WEIR					
	0	200	400	600	800	1000
30	90.7	91.5	89.8	89.8	91.5	94.9
80	90.7	89.8	88.5	90.7	90.7	96.2
130	89.4	90.2	87.7	88.5	91.9	99.2
180	89.4	89.0	86.8	88.1	91.5	98.7
230	86.0	86.0	86.8	86.8	88.1	97.9
280	79.2	79.6	82.6	83.4	83.0	86.0

Test No. 12.

LONG SECTION 500 mm BEHIND WEIR : VELOCITY mm/s						
DISTANCE BELOW CREST mm.	X SECTION, mm FROM START OF WEIR					
	0	200	400	600	800	1000
30	87.3	86.0	86.8	89.0		
80	88.1	88.5	86.8	89.0		
130	88.1	87.7	88.1	90.2		
180	85.5	86.4	86.4	89.4		
230	81.7	83.0	84.7	86.8		
280	78.7	80.4	81.3	82.1		

LONG SECTION 600 mm BEHIND WEIR : VELOCITY mm/s						
DISTANCE BELOW CREST mm	X SECTION, mm FROM START OF WEIR					
	0	200	400	600	800	1000
30	85.1	85.5				
80	85.1	85.5				
130	86.4	82.1				
180	85.1	82.1				
230	80.9	81.3				
280	77.5	78.7				

Test No. 12.

LONG SECTION 700 mm BEHIND WEIR : VELOCITY mm/s						
DISTANCE BELOW CREST mm	X SECTION, mm FROM START OF WEIR					
	0	200	400	600	800	1000
30	68.1					
80	68.9					
130	65.5					
180	59.1					
230	59.6					
280	37.6					

LONG SECTION mm BEHIND WEIR : VELOCITY mm/s						
DISTANCE BELOW CREST mm	X SECTION, mm FROM START OF WEIR					
	0	200	400	600	800	1000
30						
80						
130						
180						
230						
280						

Test No. 13.

LONG SECTION 100 mm BEHIND WEIR : VELOCITY mm/s						
DISTANCE BELOW CREST mm.	X SECTION, mm FROM START OF WEIR					
	0	200	400	600	800	1000
30	117.5	100.0	93.6	85.5	92.4	84.7
80	110.7	94.5	86.8	80.9	86.4	84.3
130	103.0	88.1	79.2	79.2	86.4	83.4
180	100.4	80.9	76.2	77.9	79.6	81.7
230	92.8	76.6	66.8	72.4	70.6	80.4
280	81.3	73.2	63.0	65.1	71.9	78.7

LONG SECTION 200 mm BEHIND WEIR : VELOCITY mm/s						
DISTANCE BELOW CREST mm	X SECTION, mm FROM START OF WEIR					
	0	200	400	600	800	1000
30	109.0	103.0	103.4	101.3	103.4	101.3
80	109.4	102.2	98.3	100.0	98.7	98.7
130	101.7	97.5	94.9	97.0	99.6	98.3
180	98.3	95.8	91.9	96.2	97.5	101.3
230	95.3	92.8	91.1	95.3	92.4	97.9
280	86.8	84.3	88.1	92.4	89.4	93.2

Test No. 13.

LONG SECTION 300 mm BEHIND WEIR : VELOCITY mm/s						
DISTANCE BELOW CREST mm.	X SECTION, mm FROM START OF WEIR					
	0	200	400	600	800	1000
30	107.7	103.4	103.4	101.3	103.0	107.3
80	109.0	103.9	102.6	102.6	103.9	106.0
130	103.9	103.9	103.0	103.9	102.2	106.4
180	100.9	98.7	98.3	98.7	100.4	107.7
230	98.7	97.9	95.8	98.3	96.6	101.7
280	92.8	90.2	94.5	93.2	92.4	98.7

LONG SECTION 400 mm BEHIND WEIR : VELOCITY mm/s						
DISTANCE BELOW CREST mm	X SECTION, mm FROM START OF WEIR					
	0	200	400	600	800	1000
30	103.4	100.4	101.7	104.3	104.3	106.0
80	103.4	100.0	99.2	102.6	104.7	110.2
130	103.9	101.7	98.7	102.6	103.0	109.4
180	102.2	97.9	97.9	103.0	102.6	107.7
230	97.0	95.8	94.9	99.6	100.9	107.3
280	89.4	93.2	91.1	90.2	89.4	101.3

Test No. 13.

LONG SECTION 500 mm BEHIND WEIR : VELOCITY mm/s						
DISTANCE BELOW CREST mm	X SECTION, mm FROM START OF WEIR					
	0	200	400	600	800	1000
30	98.7	99.6	99.6	100.0		
80	97.0	99.6	98.3	100.9		
130	98.3	99.6	98.3	99.2		
180	97.5	98.3	97.0	100.4		
230	92.4	94.1	93.2	99.2		
280	89.8	93.4	88.1	88.5		

LONG SECTION 600 mm BEHIND WEIR : VELOCITY mm/s						
DISTANCE BELOW CREST mm	X SECTION, mm FROM START OF WEIR					
	0	200	400	600	800	1000
30	94.5	94.1				
80	92.8	92.4				
130	93.6	92.4				
180	90.2	92.4				
230	86.8	91.1				
280	80.0	71.9				

Test No. 13.

LONG SECTION 700 mm BEHIND WEIR : VELOCITY mm/s						
DISTANCE BELOW CREST mm	X SECTION, mm FROM START OF WEIR					
	0	200	400	600	800	1000
30	76.6					
80	74:5					
130	76.6					
180	72.4					
230	60.0					
280	45.2					

LONG SECTION mm BEHIND WEIR : VELOCITY mm/s						
DISTANCE BELOW CREST mm	X SECTION, mm FROM START OF WEIR					
	0	200	400	600	800	1000
30						
80						
130						
180						
230						
280						

Test No. 16.

LONG SECTION 100 mm BEHIND WEIR : VELOCITY mm/s						
DISTANCE BELOW CREST mm	X SECTION, mm FROM START OF WEIR					
	0	200	400	600	800	1000
30	147.2	126.4	120.0	114.5	111.5	107.3
80	135.4	122.2	108.5	106.0	103.4	101.3
130	124.7	114.9	106.0	97.0	103.0	109.4
180	119.6	111.9	103.4	91.9	94.1	108.2
230	114.1	100.0	95.3	86.0	92.8	104.7
280	101.3	97.0	76.6	77.9	89.4	92.8

LONG SECTION 200 mm BEHIND WEIR : VELOCITY mm/s						
DISTANCE BELOW CREST mm	X SECTION, mm FROM START OF WEIR					
	0	200	400	600	800	1000
30	139.6	134.1	128.1	128.1	131.1	124.3
80	132.8	130.7	125.1	126.8	125.6	123.9
130	129.8	129.4	120.9	124.3	123.9	123.9
180	126.8	120.9	122.2	120.0	117.9	116.2
230	117.5	110.7	117.0	112.8	111.9	114.5
280	99.2	99.2	108.5	110.7	114.9	114.5

Test No. 16.

LONG SECTION 300 mm BEHIND WEIR : VELOCITY mm/s						
DISTANCE BELOW CREST mm	X SECTION, mm FROM START OF WEIR					
	0	200	400	600	800	1000
30	134.5	133.6	130.7	130.7	130.2	136.6
80	131.5	129.4	126.0	127.3	130.7	136.2
130	130.7	128.1	124.3	126.8	126.8	131.9
180	128.5	127.3	117.0	122.6	124.3	130.2
230	125.1	119.6	114.5	115.3	117.9	126.0
280	117.5	120.0	110.2	117.0	109.4	117.5

LONG SECTION 400 mm BEHIND WEIR : VELOCITY mm/s						
DISTANCE BELOW CREST mm	X SECTION, mm FROM START OF WEIR					
	0	200	400	600	800	1000
30	129.4	131.5	126.8	130.2	131.5	134.5
80	127.7	129.0	127.3	129.0	132.4	141.7
130	127.3	129.0	123.4	128.5	129.4	141.3
180	125.1	123.9	123.4	116.6	123.0	138.3
230	119.6	117.0	115.8	115.3	117.0	129.4
280	113.2	112.4	105.1	104.7	108.5	126.0

Test No. 16.

LONG SECTION 500 mm BEHIND WEIR : VELOCITY mm/s						
DISTANCE BELOW CREST mm	X SECTION, mm FROM START OF WEIR					
	0	200	400	600	800	1000
30	125.1	126.8	125.6	126.0		
80	122.2	123.0	126.0	126.4		
130	120.9	119.2	123.9	127.7		
180	117.5	116.6	118.7	120.0		
230	110.7	109.8	114.9	114.1		
280	104.7	102.6	97.9	106.8		

LONG SECTION 600 mm BEHIND WEIR : VELOCITY mm/s						
DISTANCE BELOW CREST mm	X SECTION, mm FROM START OF WEIR					
	0	200	400	600	800	1000
30	115.8	119.6				
80	113.2	120.5				
130	113.6	117.0				
180	108.1	109.8				
230	97.9	100.9				
280	95.8	100.4				

Test No. 16.

LONG SECTION 700 mm BEHIND WEIR : VELOCITY mm/s						
DISTANCE BELOW CREST mm	X SECTION, mm FROM START OF WEIR					
	0	200	400	600	800	1000
30	86.4					
80	88.1					
130	81.3					
180	71.5					
230	62.6					
280	50.6					

LONG SECTION mm BEHIND WEIR : VELOCITY mm/s						
DISTANCE BELOW CREST mm	X SECTION, mm FROM START OF WEIR					
	0	200	400	600	800	1000
30						
80						
130						
180						
230						
280						

Test No. 17.

LONG SECTION 100 mm BEHIND WEIR : VELOCITY mm/s						
DISTANCE BELOW CREST mm	X SECTION, mm FROM START OF WEIR					
	0	200	400	600	800	1000
30	178.9	147.6	139.2	134.5	137.5	129.4
80	165.0	143.8	124.7	118.3	123.4	125.6
130	156.5	139.2	121.3	114.5	122.6	131.6
180	143.8	129.4	117.0	105.1	119.6	133.6
230	135.4	125.6	105.6	104.7	123.4	134.9
280	131.9	117.0	100.9	99.2	119.6	133.2

LONG SECTION 200 mm BEHIND WEIR : VELOCITY mm/s						
DISTANCE BELOW CREST mm	X SECTION, mm FROM START OF WEIR					
	0	200	400	600	800	1000
30	166.9	158.4	151.1	153.8	154.2	151.9
80	158.0	154.6	149.9	151.1	153.0	151.9
130	145.3	143.8	148.0	150.3	150.3	149.6
180	141.3	138.8	144.9	149.6	149.6	152.3
230	126.8	138.8	137.9	146.9	143.8	150.3
280	129.8	128.1	134.9	143.4	144.5	148.4

Test No. 17.

LONG SECTION 300 mm BEHIND WEIR : VELOCITY mm/s						
DISTANCE BELOW CREST mm	X SECTION, mm FROM START OF WEIR					
	0	200	400	600	800	1000
30	158.8	156.9	152.3	152.6	154.6	163.1
80	156.5	156.9	153.0	150.7	153.0	162.3
130	153.4	151.5	152.6	149.9	152.3	158.8
180	146.9	151.1	150.3	149.9	151.1	154.2
230	140.5	145.3	148.4	146.9	148.8	152.3
280	137.9	137.1	148.4	144.5	138.8	151.1

LONG SECTION 400 mm BEHIND WEIR : VELOCITY mm/s						
DISTANCE BELOW CREST mm	X SECTION, mm FROM START OF WEIR					
	0	200	400	600	800	1000
30	153.4	152.3	150.7	149.6	156.5	165.4
80	153.8	151.5	149.6	149.6	154.2	158.4
130	147.6	148.4	143.4	146.9	150.7	155.7
180	145.7	147.6	144.5	140.0	148.5	153.0
230	147.2	148.8	141.7	136.6	146.5	146.1
280	144.2	140.0	140.9	133.2	133.2	131.1

Test No. 17.

LONG SECTION 500 mm BEHIND WEIR : VELOCITY mm/s						
DISTANCE BELOW CREST mm	X SECTION, mm FROM START OF WEIR					
	0	200	400	600	800	1000
30	148.8	146.5	144.9	152.6		
80	146.5	143.8	146.1	149.2		
130	144.9	146.5	144.5	144.5		
180	144.5	142.2	140.5	138.8		
230	140.5	133.6	134.5	139.2		
280	140.9	133.6	126.0	124.3		

LONG SECTION 600 mm BEHIND WEIR : VELOCITY mm/s						
DISTANCE BELOW CREST mm	X SECTION, mm FROM START OF WEIR					
	0	200	400	600	800	1000
30	139.2	142.2				
80	134.5	138.8				
130	134.5	135.8				
180	134.1	134.9				
230	134.1	123.4				
280	123.4	124.7				

Test No. 17,

LONG SECTION 700 mm BEHIND WEIR : VELOCITY mm/s						
DISTANCE BELOW CREST mm	X SECTION, mm FROM START OF WEIR					
	0	200	400	600	800	1000
30	101.7					
80	101.7					
130	89.4					
180	80.0					
230	76.6					
280	46.1					

LONG SECTION mm BEHIND WEIR : VELOCITY mm/s						
DISTANCE BELOW CREST mm	X SECTION, mm FROM START OF WEIR					
	0	200	400	600	800	1000
30						
80						
130						
180						
230						
280						

Test No. 21.

LONG SECTION 100 mm BEHIND WEIR : VELOCITY mm/s						
DISTANCE BELOW CREST mm.	X SECTION, mm FROM START OF WEIR					
	0	200	400	600	800	1000
30	137.89	113.63	105.54	102.14	97.88	90.22
80	129.38	113.63	102.99	93.20	86.39	73.62
130	125.97	113.20	97.45	91.49	79.58	68.93
180	125.55	109.80	94.90	80.85	79.15	76.17
230	118.31	97.03	91.49	68.51	72.34	68.08
280	103.84	95.33	80.43	69.36	64.25	73.62

LONG SECTION 200 mm BEHIND WEIR : VELOCITY mm/s						
DISTANCE BELOW CREST mm	X SECTION, mm FROM START OF WEIR					
	0	200	400	600	800	1000
30	117.89	111.50	110.22	111.50	110.65	106.39
80	117.46	110.22	108.10	105.12	105.12	102.99
130	111.08	108.95	102.14	104.69	97.03	95.75
180	102.99	99.58	100.86	88.94	98.73	100.01
230	94.47	85.96	80.85	88.51	93.20	99.16
280	84.26	78.30	71.49	90.64	97.03	93.20

Test No. 21.

LONG SECTION 300 mm BEHIND WEIR : VELOCITY mm/s						
DISTANCE BELOW CREST mm	X SECTION, mm FROM START OF WEIR					
	0	200	400	600	800	1000
30	114.91	114.48	111.93	116.18	114.05	114.48
80	111.93	113.20	110.22	108.95	113.20	114.91
130	107.67	109.37	109.37	109.37	109.37	114.48
180	103.84	100.86	101.71	104.69	108.52	110.22
230	97.88	102.14	103.41	106.39	105.12	106.39
280	89.79	88.51	95.75	96.18	106.82	106.39

LONG SECTION 400 mm BEHIND WEIR : VELOCITY mm/s						
DISTANCE BELOW CREST mm	X SECTION, mm FROM START OF WEIR					
	0	200	400	600	800	1000
30	116.61	112.78	116.18	114.05	114.48	120.87
80	109.37	110.22	112.35	109.37	117.46	121.29
130	105.97	109.80	110.22	111.50	114.91	120.87
180	105.97	102.99	105.97	111.50	110.65	117.89
230	102.99	98.31	105.12	104.69	105.12	114.91
280	97.45	97.03	103.41	104.69	106.39	114.05

Test No. 21.

LONG SECTION 500 mm BEHIND WEIR : VELOCITY mm/s						
DISTANCE BELOW CREST mm	X SECTION, mm FROM START OF WEIR					
	0	200	400	600	800	1000
30	109.37	111.93	104.69	112.35	108.10	114.91
80	111.08	109.80	113.63	111.93	114.91	117.46
130	104.69	108.52	110.65	112.78	112.78	121.29
180	103.41	108.95	109.37	111.93	114.05	120.87
230	100.86	104.26	105.54	111.50	114.05	119.16
280	96.18	104.69	103.41	108.10	107.24	108.52

LONG SECTION 600 mm BEHIND WEIR : VELOCITY mm/s						
DISTANCE BELOW CREST mm	X SECTION, mm FROM START OF WEIR					
	0	200	400	600	800	1000
30	103.84	107.67	105.12			
80	106.82	108.52	109.37			
130	103.41	108.95	106.82			
180	100.86	107.67	106.39			
230	102.99	105.54	104.69			
280	99.58	105.12	98.31			

Test No. 21.

LONG SECTION 700 mm BEHIND WEIR : VELOCITY mm/s						
DISTANCE BELOW CREST mm	X SECTION, mm FROM START OF WEIR					
	0	200	400	600	800	1000
30	90.64					
80	91.92					
130	92.35					
180	80.43					
230	78.72					
280	67.66					

LONG SECTION mm BEHIND WEIR : VELOCITY mm/s						
DISTANCE BELOW CREST mm	X SECTION, mm FROM START OF WEIR					
	0	200	400	600	800	1000
30						
80						
130						
180						
230						
280						

Test No. 23.

LONG SECTION 100 mm BEHIND WEIR : VELOCITY mm/s						
DISTANCE BELOW CREST mm.	X SECTION, mm FROM START OF WEIR					
	0	200	400	600	800	1000
30	148.40	132.36	122.99	127.25	118.31	113.63
80	145.31	125.55	123.85	117.03	103.41	96.18
130	137.47	124.70	120.44	114.48	100.43	99.58
180	132.36	120.44	111.08	108.10	97.45	91.49
230	119.16	111.93	109.37	98.73	84.26	99.16
280	105.12	101.28	102.14	85.11	85.11	94.90

LONG SECTION 200 mm BEHIND WEIR : VELOCITY mm/s						
DISTANCE BELOW CREST mm	X SECTION, mm FROM START OF WEIR					
	0	200	400	600	800	1000
30	146.86	141.72	137.47	133.64	140.45	136.19
80	144.16	140.87	136.19	130.66	126.40	137.04
130	137.89	138.32	124.27	128.53	127.68	131.51
180	128.10	124.27	118.74	123.85	127.25	132.78
230	119.59	122.14	110.65	121.72	122.99	127.25
280	116.61	103.84	107.24	116.18	121.72	126.82

Test No. 23.

LONG SECTION 300 mm BEHIND WEIR : VELOCITY mm/s						
DISTANCE BELOW CREST mm	X SECTION, mm FROM START OF WEIR					
	0	200	400	600	800	1000
30	145.31	144.54	143.00	146.47	144.16	145.70
80	143.39	141.30	139.59	139.17	143.77	144.93
130	134.06	139.17	134.91	138.74	139.17	142.57
180	127.68	128.95	135.34	135.76	134.06	141.72
230	125.97	122.99	131.93	135.76	137.47	137.89
280	122.14	131.08	124.70	129.80	132.36	131.93

LONG SECTION 400 mm BEHIND WEIR : VELOCITY mm/s						
DISTANCE BELOW CREST mm	X SECTION, mm FROM START OF WEIR					
	0	200	400	600	800	1000
30	142.57	139.17	141.30	140.02	142.15	148.79
80	140.87	140.45	137.89	140.45	143.39	146.86
130	137.47	137.47	138.32	142.15	142.15	146.86
180	135.76	135.76	137.04	134.06	140.45	145.70
230	134.91	134.49	135.34	135.76	132.78	136.19
280	134.91	133.64	131.51	133.21	130.23	139.59

Test No. 23.

LONG SECTION 500 mm BEHIND WEIR : VELOCITY mm/s						
DISTANCE BELOW CREST mm	X SECTION, mm FROM START OF WEIR					
	0	200	400	600	800	1000
30	137.04	137.04	140.02	141.72	143.39	143.39
80	134.49	136.62	132.78	140.87	144.16	148.40
130	130.66	136.19	133.21	137.89	138.32	143.77
180	131.93	132.78	132.78	137.89	135.76	136.62
230	131.08	131.51	128.95	130.23	128.10	133.64
280	127.68	125.55	123.85	119.16	120.01	124.70

LONG SECTION 600 mm BEHIND WEIR : VELOCITY mm/s						
DISTANCE BELOW CREST mm	X SECTION, mm FROM START OF WEIR					
	0	200	400	600	800	1000
30	130.66	129.80	137.04			
80	126.82	134.49	135.34			
130	126.82	133.64	135.34			
180	125.55	128.10	132.36			
230	123.85	122.99	119.59			
280	111.08	115.76	102.99			

Test No. 23.

LONG SECTION 700 mm BEHIND WEIR : VELOCITY mm/s						
DISTANCE BELOW CREST mm.	X SECTION, mm FROM START OF WEIR					
	0	200	400	600	800	1000
30	96.60					
80	97.03					
130	97.03					
180	85.96					
230	67.66					
280	62.55					

LONG SECTION mm BEHIND WEIR : VELOCITY mm/s						
DISTANCE BELOW CREST mm	X SECTION, mm FROM START OF WEIR					
	0	200	400	600	800	1000
30						
80						
130						
180						
230						
280						

Test No. 25.

LONG SECTION 100 mm BEHIND WEIR : VELOCITY mm/s						
DISTANCE BELOW CREST mm	X SECTION, mm FROM START OF WEIR					
	0	200	400	600	800	1000
30	188.89	168.45	159.58	150.33	146.47	122.14
80	177.32	162.67	153.80	136.62	139.59	111.50
130	172.31	164.60	159.58	151.48	147.63	127.68
180	165.75	167.68	160.74	145.31	144.54	119.16
230	161.13	167.30	165.75	158.04	137.89	120.87
280	157.27	156.11	150.71	137.89	114.05	110.65

LONG SECTION 200 mm BEHIND WEIR : VELOCITY mm/s						
DISTANCE BELOW CREST mm	X SECTION, mm FROM START OF WEIR					
	0	200	400	600	800	1000
30	181.95	173.85	165.37	162.67	162.28	160.74
80	169.61	167.68	158.04	155.73	149.56	151.87
130	162.28	168.07	152.26	144.93	147.24	147.63
180	158.43	155.73	143.00	142.15	140.87	146.09
230	151.10	143.77	133.64	134.49	144.93	161.13
280	136.19	127.68	128.95	118.31	151.87	164.21

Test No. 25.

LONG SECTION 300 mm BEHIND WEIR : VELOCITY mm/s						
DISTANCE BELOW CREST mm	X SECTION, mm FROM START OF WEIR					
	0	200	400	600	800	1000
30	178.10	172.70	174.24	172.70	176.17	180.02
80	170.38	170.00	168.45	168.07	167.68	180.41
130	153.80	154.96	155.34	156.88	161.13	171.15
180	153.41	151.10	156.88	163.83	167.30	168.07
230	151.48	161.51	162.28	161.13	165.75	178.10
280	147.63	144.16	156.88	158.43	166.91	177.71

LONG SECTION 400 mm BEHIND WEIR : VELOCITY mm/s						
DISTANCE BELOW CREST mm	X SECTION, mm FROM START OF WEIR					
	0	200	400	600	800	1000
30	172.70	173.47	171.93	178.10	182.72	187.74
80	168.45	171.54	171.93	174.24	175.01	184.27
130	163.05	168.07	172.70	173.85	175.40	183.11
180	156.50	167.30	168.07	172.70	177.71	180.80
230	156.11	163.83	165.75	166.53	176.94	187.74
280	163.05	163.44	166.91	170.38	169.61	180.80

Test No. 25.

LONG SECTION 500 mm BEHIND WEIR : VELOCITY mm/s						
DISTANCE BELOW CREST mm	X SECTION, mm FROM START OF WEIR					
	0	200	400	600	800	1000
30	171.15	175.01	178.48	181.95	184.65	185.81
80	174.62	174.62	178.10	181.95	181.95	189.67
130	166.91	174.24	171.93	178.87	182.34	190.44
180	164.98	170.00	174.62	173.85	181.18	180.80
230	158.81	170.00	178.10	171.93	174.62	185.04
280	157.66	164.21	173.47	163.44	164.60	161.13

LONG SECTION 600 mm BEHIND WEIR : VELOCITY mm/s						
DISTANCE BELOW CREST mm	X SECTION, mm FROM START OF WEIR					
	0	200	400	600	800	1000
30	171.15	175.40	174.24			
80	174.62	174.62	176.94			
130	169.23	175.40	170.00			
180	164.60	177.32	171.15			
230	165.74	175.78	159.20			
280	155.34	151.87	146.47			

Test No. 25.

LONG SECTION 700 mm BEHIND WEIR : VELOCITY mm/s						
DISTANCE BELOW CREST mm	X SECTION, mm FROM START OF WEIR					
	0	200	400	600	800	1000
30	132.78					
80	137.04					
130	129.38					
180	120.44					
230	103.41					
280	85.11					

LONG SECTION mm BEHIND WEIR : VELOCITY mm/s						
DISTANCE BELOW CREST mm	X SECTION, mm FROM START OF WEIR					
	0	200	400	600	800	1000
30						
80						
130						
180						
230						
280						

Test No. 27.

LONG SECTION 100 mm BEHIND WEIR : VELOCITY mm/s						
DISTANCE BELOW CREST mm	X SECTION, mm FROM START OF WEIR					
	0	200	400	600	800	1000
30	215.89	199.31	185.04	179.64	172.31	145.31
80	210.49	196.99	182.72	168.45	165.37	149.56
130	196.61	194.29	180.41	163.05	161.13	140.02
180	195.07	191.21	180.80	166.14	150.33	137.89
230	186.97	180.02	175.01	157.66	142.57	135.76
280	181.18	178.48	173.08	151.87	133.64	139.17

LONG SECTION 200 mm BEHIND WEIR : VELOCITY mm/s						
DISTANCE BELOW CREST mm	X SECTION, mm FROM START OF WEIR					
	0	200	400	600	800	1000
30	208.18	198.92	192.37	190.82	193.52	197.38
80	190.05	192.37	185.81	183.11	182.72	188.89
130	184.65	173.47	158.43	185.81	181.57	176.55
180	170.77	174.24	170.77	174.62	169.23	177.71
230	168.84	151.87	163.44	166.14	171.15	175.40
280	145.70	150.33	160.74	170.00	169.23	174.62

Test No. 27.

LONG SECTION 300 mm BEHIND WEIR : VELOCITY mm/s						
DISTANCE BELOW CREST mm.	X SECTION, mm FROM START OF WEIR					
	0	200	400	600	800	1000
30	198.92	196.99	196.22	191.21	189.67	200.85
80	195.07	187.35	178.87	182.72	189.28	194.29
130	176.55	175.78	178.87	186.19	186.19	188.89
180	175.78	168.07	178.48	173.85	180.02	189.28
230	170.77	163.83	166.91	168.07	175.40	182.72
280	158.43	162.28	165.37	168.07	181.18	182.34

LONG SECTION 400 mm BEHIND WEIR : VELOCITY mm/s						
DISTANCE BELOW CREST mm	X SECTION, mm FROM START OF WEIR					
	0	200	400	600	800	1000
30	194.29	191.21	193.52	193.14	196.22	208.95
80	190.05	189.67	189.28	196.22	196.61	204.32
130	183.50	186.19	186.97	191.98	182.72	205.86
180	173.08	179.25	186.58	181.18	185.81	199.31
230	173.08	173.08	171.54	179.64	188.12	197.38
280	172.31	169.61	170.38	179.64	187.74	189.28

Test No. 27.

LONG SECTION 500 mm BEHIND WEIR : VELOCITY mm/s						
DISTANCE BELOW CREST mm.	X SECTION, mm FROM START OF WEIR					
	0	200	400	600	800	1000
30	190.82	192.37	196.61	191.98	196.99	200.08
80	184.65	195.07	186.97	196.22	196.22	209.72
130	175.78	178.48	180.02	193.52	195.84	201.62
180	170.38	179.64	176.17	191.21	190.05	194.29
230	161.90	170.38	179.64	181.57	188.89	181.18
280	168.45	174.62	178.48	177.32	175.40	169.61

LONG SECTION 600 mm BEHIND WEIR : VELOCITY mm/s						
DISTANCE BELOW CREST mm	X SECTION, mm FROM START OF WEIR					
	0	200	400	600	800	1000
30	185.81	192.75	190.05			
80	178.10	186.19	189.28			
130	170.00	180.80	183.88			
180	169.61	182.72	178.48			
230	170.00	177.71	180.41			
280	172.31	161.90	144.93			

Test No. 27.

LONG SECTION 700 mm BEHIND WEIR : VELOCITY mm/s						
DISTANCE BELOW CREST mm	X SECTION, mm FROM START OF WEIR					
	0	200	400	600	800	1000
30	161.90					
80	150.33					
130	141.72					
180	128.95					
230	115.76					
280	97.45					

LONG SECTION mm BEHIND WEIR : VELOCITY mm/s						
DISTANCE BELOW CREST mm	X SECTION, mm FROM START OF WEIR					
	0	200	400	600	800	1000
30						
80						
130						
180						
230						
280						

(c) Details of the Method of Computing α and β Values.

V.1 Velocity energy coefficients α and momentum flux correction factors β are used to allow for the effects of non-uniform velocity distribution when computing values of velocity energy and momentum flux. They are defined by the following equations,

$$\alpha \cdot \frac{1}{2} \rho Q v^2 = \int_A \frac{1}{2} \rho u^3 \cdot dA$$

$$\therefore \quad \alpha = \frac{\int_A u^3 \cdot dA}{Q v^2}$$

$$Q = \int_A u \cdot dA$$

and $$v = Q/A$$

$$\therefore \quad \alpha = \frac{A^2 \int_A u^3 \cdot dA}{\left(\int_A u \cdot dA \right)^3} \qquad \text{............(V.1)}$$

Similarly $$\beta \cdot \rho A V^2 = \int_A \rho u^2 \, dA$$

$$\beta = \frac{A \int_A u^2 \cdot dA}{\left(\int_A u \cdot dA \right)^2} \qquad \text{............(V.2)}$$

V.2 Calculation of β.

Values of β were initially computed using a graphical method, as described below, for each cross-section at which velocity traverses were made.

For each vertical section values of u were plotted against y (Figs. 6.2 to 6.6 are examples). The area contained by the distribution curve of u was denoted Area 1 (Fig. V.1).

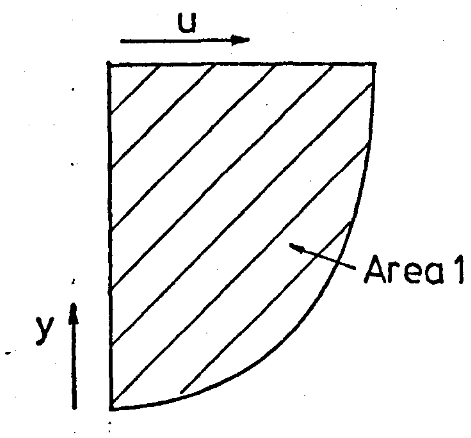

$$\text{Area } 1 = \int_{o}^{y} u \cdot dy$$

Fig. V.1

Vertical Distribution of u.

Velocity distributions were plotted and Area 1 values measured at each vertical section along a cross-section. The cross-sectional distribution of Area 1 values was then plotted (Fig. V.2).

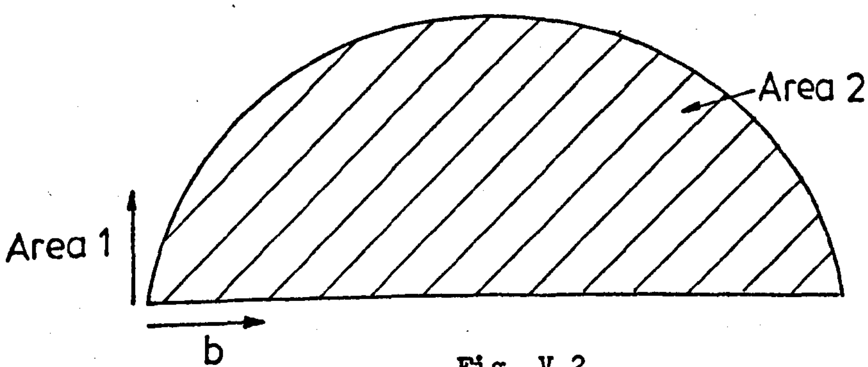

$$\text{Area } 2 = \int_{A} u \cdot dA$$

Fig. V.2

Cross-sectional Distribution of Area 1.

The area under this curve was denoted Area 2 and is equal to $\int_A u \cdot dA$. Values of u^2 were then computed and a similar exercise undertaken with distributions of u^2 with y, the two areas now being denoted Area 3 and Area 4. By a similar argument Area 4 = $\int_A u^2 \cdot dA$.

The cross-sectional area of flow, A, was obtained by plotting the head measurements across the section, and β was calculated from

$$\beta = \frac{A \cdot \text{Area } 4}{(\text{Area } 2)^2} \qquad \text{..............(V.3)}$$

An example of the method is given in Table V.1 below.

TABLE V.1
Computed Values of Momentum Flux Correction Factor β

Reading No. 2 Cross-section 0 mm

Distance behind weir mm	Area 1 Graph m^2/s	Area 1 Computed m^2/s	Area 2 Graph m^3/s^2 x10^{-3}	Area 2 Computed m^3/s^2 x10^{-3}
100	0.03184	0.03304	2.9318	3.0448
200	0.03212	0.03267	2.8612	2.9216
300	0.03573	0.03571	3.3260	3.3986
400	0.03544	0.03527	3.2932	3.3203
500	0.02909	0.02892	2.2102	2.2230
600	0.03325	0.03340	2.9296	2.9653
Cross-section Area m^2	**Area 2 Graph m^3/s**	**Area 2 Computed m^3/s**	**Area 4 Graph m^4/s x10^{-3}**	**Area 4 Computed m^4/s^2 x10^{-3}**
0.02839	0.02419	0.02439	2.1530	2.1916

β_{Graph} = 1.045 β_{Computed} = 1.046

It was found, however, that this method became tedious when applied to all the velocity traverse readings. A numerical method was therefore developed by approximating the velocity distribution and the other graphs to stepped distributions. An example is shown below for a typical velocity distribution.

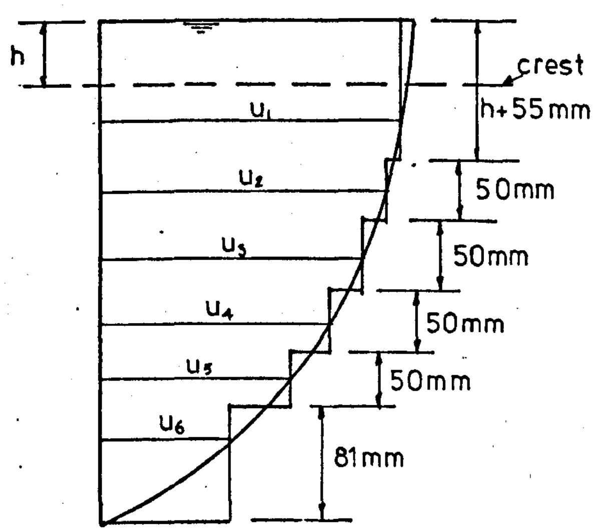

Fig. V3 Stepped Approximation to Velocity Distribution Curve

Thus,

$$\text{Area } 1 = (h + 0.055)\, u_1 + 0.05\, (u_2 + u_3 + u_4 + u_5) + 0.031\, u_6 \qquad \text{..............(V.5)}$$

Similar approximations were made for Areas 2 to 6. Values of β and α were then calculated using equations (V.3) and (V.4) respectively, using the computed values of the Areas. Since the method only involves the use of simple numerical expressions it can be readily programmed for computation by a digital computer. A Hewlett Packard desk top computer was used to perform the computations, and Table V.1 also contains the computed values of Areas 1, 2, 3 and 4, and β , for comparison with the graphical values. There is clearly very little difference between the two sets of results, the values of β being virtually identical.

The computed values of α and β are given in Table 6.2 and plotted in Figure 6.7.

APPENDIX VI

Error Analysis for the Coefficient of Discharge.

VI.1 Analysis of the Possible Error in Measured C_D values due to the Possible Errors in Scale Readings.

For a typical reading in the centre of the range,

Head above crest, h	=	0.03496	± 0.0001	m
Side spill stage, H	=	9.33	± 0.01	cm
Length of Weir, L	=	1.1072	± 0.001	m

$$C_D = \frac{Qw}{{}^2/_3 \sqrt{2g}\, L\, h^{3/2}}$$

∴ Proportional error in C_D =

$$\frac{dC_D}{C_D} = \left\{\left(\frac{dQw}{Qw}\right)^2 + \left(\frac{dL}{L}\right)^2 + \left(\frac{3}{2}\frac{dh}{h}\right)^2\right\}^{\frac{1}{2}}$$

Now, from the calibration data for the side spill channel,

$$Qw = 0.000374\ H^{1.6116}$$

$$\therefore \frac{dQw}{Qw} = 1.6116\ \frac{dH}{H}$$

$$\therefore \frac{d\,C_D}{C_D} = \left\{\left(1.6116\ \frac{dH}{H}\right)^2 + \left(\frac{dL}{L}\right)^2 + \left(1.5\ \frac{dh}{h}\right)^2\right\}^{\frac{1}{2}}$$

$$= \left\{\left(\frac{1.6116\ .\ 0.01}{9.33}\right)^2 + \left(\frac{0.001}{1.1072}\right)^2 + \left(\frac{1.5\ .\ 0.0001}{0.03496}\right)^2\right\}^{\frac{1}{2}}$$

$$= \pm\ 0.0047$$

or ± 0.5%

APPENDIX VII

Results of the Main Experimental Investigation.

(a) Depth and Dishcarge Measurements.

(b) Longitudinal Surface Profiles.

(c) Transverse Surface Profiles.

(a) Depth and Discharge Measurements.

SUBCRITICAL FLOW PROFILES EXCEPT WHERE STATED.

Weir No. 1. Channel Width = 0.1016 m   Crest Height = 80.0 mm   Weir Length = 0.6096m

TEST No.	UPSTREAM DISCHARGE Q_1 l/s	SIDE SPILL DISCHARGE Q_w l/s	DOWNSTREAM DISCHARGE Q_2 l/s	DEPTH AT UPSTREAM END OF WEIR Y_1 mm	DEPTH AT 428 mm DOWNSTREAM OF WEIR Y_3 mm	VISCOCITY ν 10^{-6} kg/ms	BED SLOPE	REMARKS
15	6.59	4.31	2.28	95.4	112.0	0.963	Horizontal	Downstream sluice open 25.4mm
16	5.94	3.74	2.20	94.9	108.7	0.957	Horizontal	" " "
17	5.34	3.18	2.16	93.8	105.1	0.955	Horizontal	" " "
18	4.63	2.53	2.10	92.4	100.9	0.953	Horizontal	" " "
19	4.19	2.13	2.06	91.1	98.1	0.951	Horizontal	" " "
20	3.53	1.90	1.63	91.1	95.6	0.967	Horizontal	Downstream sluice open 19.1mm
21	4.27	2.62	1.65	93.3	100.3	0.964	Horizontal	" " "
22	4.56	2.90	1.66	94.1	101.8	0.962	Horizontal	" " "
23	5.40	3.69	1.71	95.9	106.6	0.962	Horizontal	" " "
24	5.94	4.21	1.73	97.1	109.9	0.960	Horizontal	" " "
25	6.43	4.68	1.75	97.2	112.7	0.951	Horizontal	" " "
26	7.02	5.24	1.78	97.9	115.8	0.951	Horizontal	" " "
27	7.46	5.67	1.79	99.5	119.2	0.951	Horizontal	" " "
28	6.66	5.43	1.23	100.2	114.9	1.012	Horizontal	Downstream sluice open 12.7mm

SUBCRITICAL FLOW PROFILES EXCEPT WHERE STATED

Weir No. 1. Channel Width = 0.1016 m   Crest Height = 80.0 mm   Weir Length = 0.6096m

TEST No.	UPSTREAM DISCHARGE Q_1 l/s	SIDE SPILL DISCHARGE Q_w l/s	DOWNSTREAM DISCHARGE Q_2 l/s	DEPTH AT UPSTREAM END OF WEIR Y_1 mm	DEPTH AT 428 mm DOWNSTREAM OF WEIR Y_3 mm	VISCOCITY $\nu 10^{-6}$ kg/ms	BED SLOPE	REMARKS
29	5.99	4.81	1.18	99.1	111.4	1.007	Horizontal	Downstream sluice open 12.7mm
30	5.34	4.20	1.14	97.8	108.0	0.997	Horizontal	" " "
31	4.70	3.60	1.10	96.8	103.6	0.997	Horizontal	" " "
32	3.88	2.79	1.09	94.5	99.9	0.992	Horizontal	" " "
33	3.02	1.92	1.10	91.6	94.9	0.988	Horizontal	" " "
34	2.19	1.82	0.37	91.7	93.3	1.022	Horizontal	Downstream weir
35	2.93	2.44	0.49	93.9	96.9	1.017	Horizontal	" "
36	3.69	3.08	0.61	95.9	100.6	1.009	Horizontal	" "
37	4.38	3.64	0.74	97.2	104.0	1.009	Horizontal	" "
38	5.54	4.49	1.05	98.7	109.3	1.007	Horizontal	" "
39	6.49	5.11	1.38	99.4	113.7	0.995	Horizontal	" "
40	7.61	5.95	1.66	99.9	119.6	0.997	Horizontal	" "
41	3.46	1.84	1.62	88.7	101.3	0.921	0.00758	Downstream sluice open 19.1mm
42	4.33	2.70	1.63	91.5	106.6	0.915	0.00758	" " "

SUBCRITICAL FLOW PROFILES EXCEPT WHERE STATED

Weir No. 1. Channel Width = 0.1016 m Crest Height = 80.0 mm Weir Length = 0.6096 m

TEST No.	UPSTREAM DISCHARGE Q_1 l/s	SIDE SPILL DISCHARGE Q_w l/s	DOWNSTREAM DISCHARGE Q_2 l/s	DEPTH AT UPSTREAM END OF WEIR y_1 mm	DEPTH AT 428 mm DOWNSTREAM OF WEIR y_3 mm	VISCOCITY $\nu\ 10^{-6}$ kg/ms	BED SLOPE	REMARKS
43	5.33	3.67	1.66	93.9	112.5	0.913	0.00758	Downstream sluice open 19.1mm
44	6.21	4.47	1.74	95.4	117.7	0.909	0.00758	" " "
45	6.50	4.71	1.79	95.6	119.4	0.889	0.00758	" " "
46	7.50	5.67	1.83	95.7	125.7	0.881	0.00758	" " "
48	5.86	4.75	1.11	97.2	117.4	0.870	0.00758	Downstream weir
49	5.20	4.32	0.88	96.6	114.0	0.868	0.00758	" "
50	4.56	3.85	0.71	95.9	111.3	0.868	0.00758	" "
51	3.77	3.24	0.53	94.6	107.7	0.866	0.00758	" "
52	3.06	2.62	0.44	92.8	104.1	0.866	0.00758	" "
53	2.60	2.23	0.37	91.6	101.7	0.864	0.00758	" "
54	13.42	2.39	11.03	111.9	85.3+	0.862	0.00758	Supercritical flow
55	7.58	5.82	1.76	98.8	122.6	0.909	0.00379	Downstream sluice open 19.1mm
56	6.56	4.83	1.73	97.2	116.8	0.901	0.00379	" " "
57	5.77	4.14	1.63	96.2	112.2	0.895	0.00379	" " "

+ Depth at downstream end of weir, y_2, mm.

SUBCRITICAL FLOW PROFILES EXCEPT WHERE STATED

Weir No. 1. Channel Width = 0.1016 m Crest Height = 80.0 mm Weir Length = 0.6096 m

TEST No.	UPSTREAM DISCHARGE Q_1 l/s	SIDE SPILL DISCHARGE Q_w l/s	DOWNSTREAM DISCHARGE Q_2 l/s	DEPTH AT UPSTREAM END OF WEIR y_1 mm	DEPTH AT 428 mm DOWNSTREAM OF WEIR y_3 mm	VISCOSITY $\nu \, 10^{-6}$ kg/ms	BED SLOPE	REMARKS
58	4.83	3.17	1.66	94.5	106.7	0.893	0.00379	Downstream sluice open 19.1mm
59	4.07	2.46	1.61	92.5	102.2	0.889	0.00379	" " "
60	3.33	1.80	1.53	89.7	97.5	0.885	0.00379	" " "
61	14.25	2.59	11.66	115.0	85.4+	1.084	0.00379	Supercritical flow

+ Depth at downstream end of weir, y_2, mm.

SUBCRITICAL FLOW PROFILES.

Weir No. 2. Channel Width = 0.1016 m Crest Height = 118.0 mm Weir Length = 0.6096 m

TEST No.	UPSTREAM DISCHARGE Q_1 l/s	SIDE SPILL DISCHARGE Q_w l/s	DOWNSTREAM DISCHARGE Q_2 l/s	DEPTH AT UPSTREAM END OF WEIR y_1 mm	DEPTH AT 428 mm DOWNSTREAM OF WEIR y_3 mm	VISCOCITY $\nu\ 10^{-6}$ kg/ms	BED SLOPE	REMARKS
62	3.68	1.85	1.83	129.0	134.5	1.054	0.00379	Downstream sluice open 19.1mm
63	3.95	2.07	1.88	129.9	135.9	1.087	0.00379	" " "
64	4.95	3.05	1.90	133.6	141.2	1.071	0.00379	" " "
65	6.02	4.07	1.95	136.9	146.3	1.065	0.00379	" " "
66	6.79	4.80	1.99	138.9	149.9	1.060	0.00379	" " "
67	7.31	5.32	1.99	140.4	152.3	1.050	0.00379	" " "
68	7.74	5.71	2.03	141.5	154.4	1.004	0.00379	" " "
69	9.83	7.79	2.04	145.8	163.2	1.002	0.00379	" " "
70	8.44	6.42	2.02	143.2	157.8	1.044	0.00379	" " "

SUPERCRITICAL FLOW PROFILES.

Weir No. 3. Channel Width = 0.1016 m Crest Height = 36.0 mm Weir Length = 0.6096m

TEST No.	UPSTREAM DISCHARGE Q_1 l/s	SIDE SPILL DISCHARGE Q_w l/s	DOWNSTREAM DISCHARGE Q_2 l/s	DEPTH AT UPSTREAM END OF WEIR Y_1 mm	DEPTH AT DOWNSTREAM END OF WEIR Y_2 mm	VISCOCITY $\nu 10^{-6}$ kg/ms	BED SLOPE	REMARKS
71	13.20	6.20	7.00	105.0	46.2	1.123	Horizontal	Upstream flow subcritical
72	11.69	5.24	6.45	98.0	44.7	1.129	Horizontal	" " "
73	10.03	4.15	5.88	90.5	42.7	1.121	Horizontal	" " "
74	8.03	2.91	5.12	79.2	41.6	1.112	Horizontal	" " "
75	9.37	3.74	5.63	86.6	42.6	1.098	Horizontal	" " "
76	10.86	4.77	6.09	94.7	43.6	1.092	Horizontal	" " "
77	12.64	5.63	7.01	96.2	47.0	1.135	Horizontal	Upstream flow supercritical sluice open 116mm
78	12.59	4.64	7.95	80.7	48.1	1.117	Horizontal	Upstream flow supercritical sluice open 98mm
79	12.53	3.69	8.84	69.9	49.0	1.109	Horizontal	Upstream flow supercritical sluice open 84.5mm
132	13.82	6.37	7.45	106.7	46.0	1.004	0.00376	Upstream flow subcritical
133	13.11	5.98	7.13	102.8	46.0	1.035	0.00376	" " "
134	12.25	5.43	6.82	99.4	45.2	1.017	0.00376	" " "
135	11.42	4.86	6.56	95.7	44.0	0.960	0.00376	" " "
136	10.41	4.21	6.20	90.5	43.1	1.076	0.00376	" " "

SUPERCRITICAL FLOW PROFILES

Weir No. 3. Channel Width = 0.1016 m Crest Height = 36.0 mm Weir Length = 0.6096m

TEST No.	UPSTREAM DISCHARGE Q_1 l/s	SIDE SPILL DISCHARGE Q_w l/s	DOWNSTREAM DISCHARGE Q_2 l/s	DEPTH AT UPSTREAM END OF WEIR Y_1 mm	DEPTH AT DOWNSTREAM END OF WEIR Y_2 mm	VISCOCITY $\nu 10^{-6}$ kg/ms	BED SLOPE	REMARKS
137	9.47	3.63	5.84	85.5	42.5	1.055	0.00376	Upstream flow subcritical
138	12.63	5.14	7.49	89.0	46.6	1.032	0.00376	Upstream flow supercritical sluice open 116mm.
139	12.52	4.24	8.28	76.2	47.7	1.022	0.00376	Upstream flow supercritical sluice open 98mm.
140	12.60	3:32	9.28	68.0	48.0	1.017	0.00376	Upstream flow supercritical sluice open 84.5mm.
141	14.01	6.23	7.78	105.5	47.2	1.063	0.00694	Upstream flow subcritical
142	13.27	5.81	7.46	103.0	46.7	1.042	0.00694	" " "
143	12.16	5.14	7.02	97.4	45.8	1.045	0.00694	" " "
144	11.32	4.66	6.66	93.1	44.9	1.027	0.00694	" " "
145	10.33	4.03	6.30	88.4	43.9	1.007	0.00694	" " "
146	9.29	3.40	5.89	83.5	42.4	0.997	0.00694	" " "
147	12.50	4.75	7.75	85.2	47.4	1.014	0.00694	Upstream flow supercritical sluice open 116mm.
148	12.50	3.82	8.68	73.5	48.1	1.019	0.00694	Upstream flow supercritical sluice open 98mm.

SUPERCRITICAL FLOW PROFILES

Weir No. 3. Channel Width = 0.1016 m Crest Height = 36.0 mm Weir Length = 0.6096 m

TEST No.	UPSTREAM DISCHARGE Q_1 l/s	SIDE SPILL DISCHARGE Q_w l/s	DOWNSTREAM DISCHARGE Q_2 l/s	DEPTH AT UPSTREAM END OF WEIR y_1 mm	DEPTH AT DOWNSTREAM END OF WEIR y_2 mm	VISCOCITY $\nu 10^{-6}$ kg/ms	BED SLOPE	REMARKS
149	12.47	3.05	9.42	66.2	48.4	1.002	0.00694	Upstream flow supercritical sluice open 84.5mm.

SUBCRITICAL FLOW PROFILES

Weir No. 4 Channel Width = 0.1016 m Crest Height = 79.5 mm Weir Length = 0.4572m

TEST No.	UPSTREAM DISCHARGE Q_1 l/s	SIDE SPILL DISCHARGE Q_w l/s	DOWNSTREAM DISCHARGE Q_2 l/s	DEPTH AT UPSTREAM END OF WEIR y_1 mm	DEPTH AT 505 mm DOWNSTREAM OF WEIR y_3 mm	VISCOCITY $\nu 10^{-6}$ kg/ms	BED SLOPE	REMARKS
80	3.09	1.49	1.60	92.4	97.9	1.087	0.00366	Downstream sluice open 19.1mm.
81	4.44	2.82	1.62	98.4	107.4	1.079	0.00366	" " "
82	5.24	3.60	1.64	101.6	112.9	1.076	0.00366	" " "
83	5.86	4.15	1.71	103.6	117.1	1.073	0.00366	" " "
84	6.22	4.47	1.75	104.8	119.1	1.068	0.00366	" " "
85	6.69	4.93	1.76	106.4	122.3	1.060	0.00366	" " "
86	7.27	5.49	1.78	108.0	125.7	1.055	0.00366	" " "
87	7.74	5.93	1.81	109.6	128.7	1.050	0.00366	" " "
88	8.10	6.91	1.19	113.6	132.5	1.057	0.00366	Downstream sluice open 12.7mm.
89	5.30	4.15	1.15	104.2	115.5	1.055	0.00366	" " "
90	4.29	3.16	1.13	100.4	109.0	1.052	0.00366	" " "
91	3.52	2.39	1.13	97.2	103.5	1.050	0.00366	" " "
92	2.62	1.50	1.12	92.8	97.4	1.047	0.00366	" " "
93	5.88	4.72	1.16	95.9	119.0	1.045	0.00366	" " "

SUBCRITICAL FLOW PROFILES

Weir No. 4 Channel Width = 0.1016 m Crest Height = 79.5 mm Weir Length = 0.4572 m

TEST No.	UPSTREAM DISCHARGE Q_1 l/s	SIDE SPILL DISCHARGE Q_w l/s	DOWNSTREAM DISCHARGE Q_2 l/s	DEPTH AT UPSTREAM END OF WEIR y_1 mm	DEPTH AT 505 mm DOWNSTREAM OF WEIR y_3 mm	VISCOCITY $\nu\, 10^{-6}$ kg/ms	BED SLOPE	REMARKS
94	7.47	6.29	1.18	111.2	128.4	1.019	0.00366	Downstream sluice open 12.7mm.
95	8.23	5.91	2.32	107.8	130.3	1.012	0.00366	Downstream sluice open 25.4mm.
96	7.45	5.14	2.31	105.8	125.3	1.009	0.00366	" " "
97	6.35	4.07	2.28	102.6	118.2	1.007	0.00366	" " "
98	5.24	3.07	2.17	98.8	110.4	1.007	0.00366	" " "
99	4.37	2.27	2.10	95.6	104.4	1.004	0.00366	" " "
100	3.55	1.48	2.07	91.9	98.5	1.004	0.00366	" " "
101	2.87	1.31	1.56	90.9	93.6	1.076	Horizontal	Downstream sluice open 19.1mm.
102	4.29	2.72	1.57	97.7	104.1	1.071	Horizontal	" " "
103	4.83	3.24	1.59	99.8	107.8	1.057	Horizontal	" " "
104	6.14	4.45	1.69	104.2	115.8	1.052	Horizontal	" " "
105	7.20	5.47	1.73	107.6	122.1	1.050	Horizontal	" " "
106	8.03	6.28	1.75	110.8	127.8	1.045	Horizontal	" " "

SUBCRITICAL FLOW PROFILES

Weir No. 4. Channel Width = 0.1016 m Crest Height = 79.5 mm Weir Length = 0.4572 m

TEST No.	UPSTREAM DISCHARGE Q_1 l/s	SIDE SPILL DISCHARGE Q_w l/s	DOWNSTREAM DISCHARGE Q_2 l/s	DEPTH AT UPSTREAM END OF WEIR Y_1 mm	DEPTH AT 505 mm DOWNSTREAM OF WEIR Y_3 mm	VISCOCITY $\nu 10^{-6}$ kg/ms	BED SLOPE	REMARKS
107	3.22	1.56	1.66	90.5	102.0	1.029	0.00713	Downstream sluice open 19.1mm.
108	4.35	2.69	1.66	95.6	110.0	1.027	0.00713	" " "
109	5.20	3.52	1.68	98.7	116.0	1.024	0.00713	" " "
110	6.16	4.37	1.79	101.7	121.8	1.014	0.00713	" " "
111	7.00	5.17	1.83	104.0	127.3	1.009	0.00713	" " "
112	7.53	5.66	1.87	106.4	130.6	0.999	0.00713	" " "

WEIR NO. 4.

SUPPLEMENTARY RESULTS : TEST NOS. 101 TO 112.

Reading No.	Depth 76.2 mm Downstream of Weir. mm
101	94.1
102	104.1
103	107.6
104	115.2
105	121.1
106	125.8
107	99.1
108	106.8
109	112.1
110	117.7
111	122.6
112	125.8

SUBCRITICAL FLOW PROFILES

Weir No. 5. Channel Width = 0.1016 m Crest Height = 80.5 mm Weir Length = 0.7620 m

TEST No.	UPSTREAM DISCHARGE Q_1 l/s	SIDE SPILL DISCHARGE Q_w l/s	DOWNSTREAM DISCHARGE Q_2 l/s	DEPTH AT UPSTREAM END OF WEIR y_1 mm	DEPTH AT 352 mm DOWNSTREAM OF WEIR y_3 mm	VISCOCITY $\nu\ 10^{-6}$ kg/ms	BED SLOPE	REMARKS
113	4.25	2.59	1.66	90.0	104.8	0.976	0.00713	Downstream sluice open 19.1mm.
114	5.20	3.51	1.69	91.3	110.4	0.976	0.00713	" " "
115	5.96	4.17	1.79	91.5	114.3	0.976	0.00713	" " "
116	7.09	5.19	1.90	90.9	121.2	0.976	0.00713	" " "
117	7.54	5.63	1.91	90.7	123.5	0.974	0.00713	" " "
119	3.74	2.15	1.59	90.1	99.4	0.988	0.00356	" " "
120	4.58	2.94	1.64	91.4	104.1	0.988	0.00356	" " "
121	5.40	3.70	1.70	93.1	108.3	0.985	0.00356	" " "
122	6.08	4.35	1.73	93.2	112.0	0.983	0.00356	" " "
123	6.69	4.89	1.80	93.6	115.3	0.983	0.00356	" " "
124	7.29	5.43	1.86	92.9	119.2	0.979	0.00356	" " "
125	7.73	5.85	1.88	92.9	121.8	0.976	0.00356	" " "
126	3.02	1.46	1.56	89.5	92.4	0.993	Horizontal	" " "
127	4.36	2.78	1.58	92.6	99.9	0.993	Horizontal	" " "
128	5.34	3.72	1.62	94.3	105.2	0.990	Horizontal	" " "

SUBCRITICAL FLOW PROFILES

Weir No. 5. Channel Width = 0.1016m Crest Height = 80.5 mm Weir Length = 0.7620m

TEST No.	UPSTREAM DISCHARGE Q_1 l/s	SIDE SPILL DISCHARGE Q_w l/s	DOWNSTREAM DISCHARGE Q_2 l/s	DEPTH AT UPSTREAM END OF WEIR y_1 mm	DEPTH AT 352 mm DOWNSTREAM OF WEIR y_3 mm	VISCOCITY $\nu 10^{-6}$ kg/ms	BED SLOPE	REMARKS
129	6.13	4.43	1.70	94.6	109.1	0.988	Horizontal	Downstream sluice open 19.1mm.
130	6.81	5.04	1.77	94.6	113.1	0.981	Horizontal	" " "
131	7.49	5.70	1.79	94.5	117.1	0.972	Horizontal	" " "

(b) Longitudinal Surface Profiles.

WEIR NO. 1

LONGITUDINAL PROFILE CO-ORDINATES

Reading No. 16	Chainage, ins	76	78	80	82	84	86	88	90	92	94	96+	98	100	102	104	106
	Depth, mm	-	-	-	-	-	-	-	-	-	95.5	94.7	94.7	94.3	97.3	102.5	100.3
	Chainage, ins	108	110	112	114	116	118	120ƒ	122	124	126	128	130	132	134	136	138
	Depth, mm	100.6	104.0	104.1	105.1	106.3	106.6	107.3	107.7	-	-	-	-	-	-	-	-
Reading No. 19	Chainage, ins	76	78	80	82	84	86	88	90	92	94	96+	98	100	102	104	106
	Depth, mm	-	-	-	-	-	-	-	-	-	91.3	91.1	90.7	92.5	92.9	93.0	94.6
	Chainage, ins	108	110	112	114	116	118	120ƒ	122	124	126	128	130	132	134	136	138
	Depth, mm	94.5	95.5	95.7	96.8	96.9	97.0	97.7	98.2	-	-	-	-	-	-	-	-
Reading No. 21	Chainage, ins	76	78	80	82	84	86	88	90	92	94	96+	98	100	102	104	106
	Depth, mm	-	-	-	-	-	-	-	-	-	93.7	93.0	93.5	94.1	95.8	95.2	95.9
	Chainage, ins	108	110	112	114	116	118	120ƒ	122	124	126	128	130	132	134	136	138
	Depth, mm	96.9	97.8	98.1	99.0	99.2	99.8	100.0	100.0	100.6	100.5	100.3	100.7	100.8	101.0	101.0	100.7

+ **Start of Weir**

ƒ **End of Weir**

WEIR NO. 1

LONGITUDINAL PROFILE CO-ORDINATES

Reading No.																	
24	Chainage,ins	76	78	80	82	84	86	88	90	92	94	96+	98	100	102	104	106
	Depth,mm	-	-	-	-	-	-	-	-	-	97.1	96.8	96.3	95.6	100.1	103.9	102.6
	Chainage,ins	108	110	112	114	116	118	120∤	122	124	126	128	130	132	134	136	138
	Depth,mm	103.9	105.5	105.6	106.7	107.8	108.6	109.0	109.4	109.4	109.9	110.0	110.0	110.1	110.0	110.2	110.0
29	Chainage,ins	76	78	80	82	84	86	88	90	92	94	96+	98	100	102	104	106
	Depth,mm	-	-	-	-	-	-	-	-	-	99.1	98.6	97.3	99.4	104.0	106.0	104.0
	Chainage,ins	108	110	112	114	116	118	120∤	122	124	126	128	130	132	134	136	138
	Depth,mm	106.6	107.7	108.1	108.9	109.8	109.4	111.1	110.9	111.3	110.9	111.1	111.4	111.5	111.5	111.5	111.4
32	Chainage,ins	76	78	80	82	84	86	88	90	92	94	96+	98	100	102	104	106
	Depth,mm	-	-	-	-	-	-	-	-	-	94.4	94.3	94.0	95.5	96.2	97.0	97.4
	Chainage,ins	108	110	112	114	116	118	120∤	122	124	126	128	130	132	134	136	138
	Depth,mm	97.4	98.0	98.6	99.4	99.5	99.9	100.0	99.8	99.8	100.3	100.1	100.3	100.0	100.1	100.1	100.3

+ Start of Weir

∤ End of Weir

WEIR NO. 1

LONGITUDINAL PROFILE CO-ORDINATES

Reading No. 35	Chainage,ins	76	78	80	82	84	86	88	90	92	94	96 +	98	100	102	104	106
	Depth,mm	-	-	-	-	-	-	-	-	-	94.2	93.9	94.3	94.9	95.2	95.6	95.8
	Chainage,ins	108	110	112	114	116	118	120 ƒ	122	124	126	128	130	132	134	136	138
	Depth,mm	95.9	96.5	96.6	96.9	97.2	97.3	97.3	97.6	97.5	97.4	97.6	97.6	97.8	97.5	97.4	97.5
Reading No. 38	Chainage,ins	76	78	80	82	84	86	88	90	92	94	96 +	98	100	102	104	106
	Depth,mm	-	-	-	-	-	-	-	-	-	98.9	98.5	97.6	98.9	101.7	102.6	102.6
	Chainage,ins	108	110	112	114	116	118	120 ƒ	122	124	126	128	130	132	134	136	138
	Depth,mm	105.3	105.9	106.8	107.3	108.0	108.6	108.8	109.1	108.9	109.5	109.1	109.1	109.7	109.1	109.2	109.5
Reading No. 42	Chainage,ins	76	78	80	82	84	86	88	90	92	94	96 +	98	100	102	104	106
	Depth,mm	-	-	-	-	-	-	-	-	-	91.3	91.1	91.5	93.5	94.1	95.3	97.0
	Chainage,ins	108	110	112	114	116	118	120 ƒ	122	124	126	128	130	132	134	136	138
	Depth,mm	97.8	99.0	99.4	100.2	101.8	102.2	103.1	103.5	103.8	104.5	104.2	104.7	104.7	105.1	105.5	106.2

+ Start of Weir

ƒ End of Weir

WEIR NO. 1 LONGITUDINAL PROFILE CO-ORDINATES

Reading No.																	
45	Chainage,ins	76	78	80	82	84	86	88	90	92	94	96+	98	100	102	104	106
	Depth,mm	-	-	-	-	-	-	-	-	-	94.1	93.9	94.5	97.1	99.8	105.0	104.9
	Chainage,ins	108	110	112	114	116	118	120≠	122	124	126	128	130	132	134	136	138
	Depth,mm	105.3	108.9	108.8	110.4	111.8	113.9	115.2	115.5	116.3	116.6	116.6	116.2	116.4	117.2	117.8	117.8
54	Chainage,ins	76	78	80	82	84	86	88	90	92	94	96+	98	100	102	104	106
	Depth,mm	132.9	130.4	129.5	129.1	128.7	127.9	126.9	125.0	123.8	121.2	117.9	113.3	107.8	101.7	97.5	93.9
	Chainage,ins	108	110	112	114	116	118	120≠	122	124	126	128	130	132	134	136	138
	Depth,mm	91.0	88.7	87.2	86.4	85.2	84.7	83.7	84.7	84.9	86.5	86.3	87.8	87.4	86.5	87.0	86.6
56	Chainage,ins	76	78	80	82	84	86	88	90	92	94	96+	98	100	102	104	106
	Depth,mm	-	-	-	-	-	-	-	-	-	96.5	95.9	96.3	97.1	100.2	106.1	106.3
	Chainage,ins	108	110	112	114	116	118	120≠	122	124	126	128	130	132	134	136	138
	Depth,mm	105.0	108.5	109.8	110.1	111.2	112.8	113.4	114.7	114.9	115.3	115.1	115.5	115.8	115.4	115.4	116.2

+ Start of Weir

≠ End of Weir

WEIR NO. 1 LONGITUDINAL PROFILE CO-ORDINATES

Reading No. 59	Chainage,ins	76	78	80	82	84	86	88	90	92	94	96+	98	100	102	104	106
	Depth,mm	-	-	-	-	-	-	-	-	-	92.1	91.4	92.1	93.5	95.1	95.5	96.2
	Chainage,ins	108	110	112	114	116	118	120∤	122	124	126	128	130	132	134	136	138
	Depth,mm	96.7	97.5	97.9	98.8	99.3	100.1	100.6	100.7	101.1	100.8	101.1	101.7	101.7	101.8	101.8	101.7
Reading No. 61	Chainage,ins	76	78	80	82	84	86	88	90	92	94	96+	98	100	102	104	106
	Depth,mm	142.4	139.1	136.3	134.0	132.5	131.1	129.0	127.5	125.7	122.7	119.8	114.3	108.0	102.4	97.2	92.9
	Chainage,ins	108	110	112	114	116	118	120∤	122	124	126	128	130	132	134	136	138
	Depth,mm	90.1	88.2	86.6	85.6	83.7	83.7	83.5	83.9	85.3	86.3	88.2	88.2	88.1	87.0	87.6	89.6
Reading No.	Chainage,ins	76	78	80	82	84	86	88	90	92	94	96+	98	100	102	104	106
	Depth,mm																
	Chainage,ins	108	110	112	114	116	118	120∤	122	124	126	128	130	132	134	136	138
	Depth,mm																

+ **Start of Weir**

∤ **End of Weir**

WEIR NO. 2 LONGITUDINAL PROFILE CO-ORDINATES

Reading No. 63	Chainage,ins	76	78	80	82	84	86	88	90	92	94	96+	98	100	102	104	106
	Depth,mm	-	-	-	-	-	-	-	-	-	129.2	129.4	129.6	130.2	131.0	131.2	131.8
	Chainage,ins	108	110	112	114	116	118	120 ƒ	122	124	126	128	130	132	134	136	138
	Depth,mm	132.1	132.6	133.0	133.2	133.7	134.4	134.6	134.3	134.6	134.9	135.4	135.4	135.4	135.5	135.6	135.7
Reading No. 66	Chainage,ins	76	78	80	82	84	86	88	90	92	94	96+	98	100	102	104	106
	Depth,mm	-	-	-	-	-	-	-	-	-	137.8	137.5	137.3	139.6	141.5	141.7	142.8
	Chainage,ins	108	110	112	114	116	118	120 ƒ	122	124	126	128	130	132	134	136	138
	Depth,mm	143.8	145.2	145.3	146.1	146.2	146.8	147.9	148.4	148.9	148.8	149.3	149.2	149.4	149.3	149.8	149.4
Reading No.	Chainage,ins	76	78	80	82	84	86	88	90	92	94	96+	98	100	102	104	106
	Depth,mm																
	Chainage,ins	108	110	112	114	116	118	120 ƒ	122	124	126	128	130	132	134	136	138
	Depth,mm																

\+ **Start of Weir**

ƒ **End of Weir**

WEIR NO. 3

LONGITUDINAL PROFILE CO-ORDINATES

Reading No. 71	Chainage,ins	76	78	80	82	84	86	88	90	92	94	96 +	98	100	102	104	106
	Depth,mm	135.0	132.7	132.3	131.6	129.8	127.5	124.4	121.7	117.4	112.2	105.0	96.3	87.7	78.4	71.0	64.4
	Chainage,ins	108	110	112	114	116	118	120 ǂ	122	124	126	128	130	132	134	136	138
	Depth,mm	59.4	55.1	52.7	49.8	47.9	46.7	46.2	45.6	45.7	45.8	46.7	48.2	50.8	50.0	48.3	47.4
Reading No. 72	Chainage,ins	76	78	80	82	84	86	88	90	92	94	96 +	98	100	102	104	106
	Depth,mm	128.3	126.0	123.3	121.9	118.9	117.3	114.9	112.3	108.6	103.9	98.0	90.0	81.7	73.2	64.8	59.8
	Chainage,ins	108	110	112	114	116	118	120 ǂ	122	124	126	128	130	132	134	136	138
	Depth,mm	56.1	52.1	50.0	49.1	47.0	45.8	44.7	44.0	44.2	44.6	46.0	47.4	48.9	48.1	46.1	46.0
Reading No. 73	Chainage,ins	76	78	80	82	84	86	88	90	92	94	96 +	98	100	102	104	106
	Depth,mm	113.5	111.7	111.0	110.5	109.2	108.3	106.3	104.3	100.7	96.6	90.5	82.7	74.8	66.1	60.1	55.3
	Chainage,ins	108	110	112	114	116	118	120 ǂ	122	124	126	128	130	132	134	136	138
	Depth,mm	52.1	49.4	47.4	46.2	44.1	43.6	42.7	42.5	42.9	44.1	45.5	47.0	45.8	44.5	44.1	45.9

+ Start of Weir

ǂ End of Weir

WEIR NO. 3 LONGITUDINAL PROFILE CO-ORDINATES

Reading No.																	
74	Chainage, ins	76	78	80	82	84	86	88	90	92	94	96+	98	100	102	104	106
	Depth, mm	101.1	99.0	98.4	97.8	96.9	96.3	93.8	91.2	87.7	84.3	79.2	73.7	66.5	59.5	54.4	51.0
	Chainage, ins	108	110	112	114	116	118	120ƒ	122	124	126	128	130	132	134	136	138
	Depth, mm	48.1	46.2	44.6	43.6	42.3	42.0	41.6	41.5	43.1	43.3	44.0	44.1	44.2	44.0	44.6	46.0
75	Chainage, ins	76	78	80	82	84	86	88	90	92	94	96+	98	100	102	104	106
	Depth, mm	110.7	109.9	109.8	108.2	107.3	105.7	102.7	99.9	96.2	91.8	86.6	79.4	71.4	64.2	58.1	54.2
	Chainage, ins	108	110	112	114	116	118	120ƒ	122	124	126	128	130	132	134	136	138
	Depth, mm	50.6	48.6	46.6	45.3	43.8	43.0	42.6	42.7	43.3	44.4	45.4	46.1	45.0	44.3	44.5	45.9
76	Chainage, ins	76	78	80	82	84	86	88	90	92	94	96+	98	100	102	104	106
	Depth, mm	121.0	118.8	116.1	114.7	113.1	111.2	109.4	107.4	104.4	99.9	94.7	87.2	78.9	71.3	64.1	57.7
	Chainage, ins	108	110	112	114	116	118	120ƒ	122	124	126	128	130	132	134	136	138
	Depth, mm	53.7	50.7	48.7	46.8	45.9	44.1	43.6	43.1	43.4	44.4	46.0	47.1	46.5	45.7	45.1	45.3

+ **Start of Weir**

ƒ **End of Weir**

WEIR NO. 3 LONGITUDINAL PROFILE CO-ORDINATES

Reading No. 77	Chainage,ins	76	78	80	82	84	86	88	90	92	94	96 +	98	100	102	104	106
	Depth,mm	97.6	97.4	99.0	100.8	101.6	101.8	101.8	102.0	102.0	100.0	96.2	91.7	84.8	77.5	71.2	64.7
	Chainage,ins	108	110	112	114	116	118	120 ≠	122	124	126	128	130	132	134	136	138
	Depth,mm	59.7	55.5	53.3	50.3	48.8	47.4	47.0	46.3	46.0	46.1	46.9	48.5	49.6	50.7	49.6	47.9
Reading No. 78	Chainage,ins	76	78	80	82	84	86	88	90	92	94	96 +	98	100	102	104	106
	Depth,mm	79.0	79.1	79.3	79.3	79.5	79.4	79.6	80.6	80.7	80.7	80.7	78.7	75.6	71.8	68.1	65.1
	Chainage,ins	108	110	112	114	116	118	120 ≠	122	124	126	128	130	132	134	136	138
	Depth,mm	61.1	58.2	55.4	52.6	50.6	49.3	48.1	47.1	47.2	47.3	48.1	49.2	50.6	52.7	52.0	50.2
Reading No. 79	Chainage,ins	76	78	80	82	84	86	88	90	92	94	96 +	98	100	102	104	106
	Depth,mm	67.4	67.5	67.8	68.0	67.8	67.7	67.9	69.0	70.4	70.3	69.9	68.3	66.8	65.0	63.5	60.0
	Chainage,ins	108	110	112	114	116	118	120 ≠	122	124	126	128	130	132	134	136	138
	Depth,mm	58.1	56.9	54.8	52.9	51.1	50.0	49.0	48.8	48.9	49.0	49.1	49.2	51.4	53.9	53.3	51.8

+ Start of Weir

≠ End of Weir

WEIR NO. 3 LONGITUDINAL PROFILE CO-ORDINATES

Reading No.																	
132	Chainage,ins	76	78	80	82	84	86	88	90	92	94	96+	98	100	102	104	106
	Depth,mm	136.2	129.7	129.1	126.7	125.5	123.3	120.7	119.5	116.7	112.5	106.7	98.3	88.6	78.7	70.2	63.2
	Chainage,ins	108	110	112	114	116	118	120∤	122	124	126	128	130	132	134	136	138
	Depth,mm	59.3	55.0	52.5	50.4	48.8	47.1	46.0	45.4	45.3	46.4	47.0	50.4	50.5	48.3	47.3	47.0
133	Chainage,ins	76	78	80	82	84	86	88	90	92	94	96+	98	100	102	104	106
	Depth,mm	130.7	127.0	124.0	122.8	120.4	119.5	117.1	115.3	112.1	108.0	102.8	94.7	86.4	78.2	70.7	64.1
	Chainage,ins	108	110	112	114	116	118	120∤	122	124	126	128	130	132	134	136	138
	Depth,mm	58.8	54.9	42.0	49.9	48.3	46.9	46.0	45.4	45.2	45.4	46.5	47.9	49.6	49.1	47.8	46.6
134	Chainage,ins	76	78	80	82	84	86	88	90	92	94	96+	98	100	102	104	106
	Depth,mm	122.2	120.4	118.8	118.3	117.0	116.2	114.2	112.4	109.1	105.1	99.4	91.6	83.2	75.4	68.1	62.2
	Chainage,ins	108	110	112	114	116	118	120∤	122	124	126	128	130	132	134	136	138
	Depth,mm	57.3	53.7	51.1	48.9	47.3	46.2	45.2	44.6	44.7	44.9	45.9	47.1	48.8	48.8	46.1	45.9

+ Start of Weir

∤ End of Weir

WEIR NO. 3

LONGITUDINAL PROFILE CO-ORDINATES

Reading No.																	
135	Chainage,ins	76	78	80	82	84	86	88	90	92	94	96 +	98	100	102	104	106
	Depth,mm	118.0	115.7	115.1	114.3	113.1	112.0	110.4	108.2	105.2	101.1	95.7	88.1	79.9	71.6	64.5	59.2
	Chainage,ins	108	110	112	114	116	118	120 ≠	122	124	126	128	130	132	134	136	138
	Depth,mm	55.3	51.8	49.6	47.8	46.6	45.0	44.0	43.8	43.5	44.4	45.5	47.2	48.1	46.8	45.2	45.1
136	Chainage,ins	76	78	80	82	84	86	88	90	92	94	96 +	98	100	102	104	106
	Depth,mm	115.2	113.7	113.2	111.8	109.7	108.2	106.0	103.4	100.5	95.9	90.5	83.3	75.6	68.5	61.6	56.5
	Chainage,ins	108	110	112	114	116	118	120 ≠	122	124	126	128	130	132	134	136	138
	Depth,mm	53.2	50.3	48.4	46.8	45.2	44.1	43.1	42.9	43.1	43.8	45.6	46.9	46.5	44.4	44.1	44.9
137	Chainage,ins	76	78	80	82	84	86	88	90	92	94	96 +	98	100	102	104	106
	Depth,mm	108.7	106.8	105.4	103.5	101.8	100.5	98.4	96.2	93.7	90.4	85.5	79.2	72.2	64.8	59.1	54.4
	Chainage,ins	108	110	112	114	116	118	120 ≠	122	124	126	128	130	132	134	136	138
	Depth,mm	51.2	48.8	47.1	45.6	44.3	42.9	42.5	42.2	42.6	43.6	44.6	45.7	45.4	43.5	43.4	44.2

+ Start of Weir

≠ End of Weir

WEIR NO. 3 LONGITUDINAL PROFILE CO-ORDINATES

Reading No.																	
138	Chainage, ins	76	78	80	82	84	86	88	90	92	94	96 +	98	100	102	104	106
	Depth, mm	89.9	90.3	90.2	91.2	92.2	93.1	93.0	92.9	92.3	90.9	89.0	85.7	81.0	75.3	69.7	64.5
	Chainage, ins	108	110	112	114	116	118	120 ∤	122	124	126	128	130	132	134	136	138
	Depth, mm	60.3	56.0	53.1	51.0	49.0	47.4	46.6	45.9	46.0	45.8	46.5	47.9	49.6	50.2	48.5	47.3
139	Chainage, ins	76	78	80	82	84	86	88	90	92	94	96 +	98	100	102	104	106
	Depth, mm	74.6	75.3	75.8	75.8	75.6	75.5	75.6	75.7	76.3	76.6	76.2	75.0	72.4	69.4	65.3	62.6
	Chainage, ins	108	110	112	114	116	118	120 ∤	122	124	126	128	130	132	134	136	138
	Depth, mm	59.3	56.5	54.4	52.3	50.2	48.8	47.7	47.3	47.4	47.4	47.9	49.0	50.2	51.7	50.7	49.4
140	Chainage, ins	76	78	80	82	84	86	88	90	92	94	96 +	98	100	102	104	106
	Depth, mm	66.0	65.9	65.8	65.3	65.1	64.5	64.9	66.2	67.5	68.0	68.0	66.6	64.4	62.8	60.2	58.1
	Chainage, ins	108	110	112	114	116	118	120 ∤	122	124	126	128	130	132	134	136	138
	Depth, mm	56.4	54.5	53.2	51.6	50.3	48.7	48.0	47.5	47.3	47.5	47.9	48.6	50.0	51.8	52.1	50.7

\+ Start of Weir

∤ End of Weir

WEIR NO. 3 LONGITUDINAL PROFILE CO-ORDINATES

Reading No.																	
141	Chainage,ins	76	78	80	82	84	86	88	90	92	94	96+	98	100	102	104	106
	Depth,mm	128.2	125.1	123.3	122.7	122.8	121.1	120.6	117.7	114.5	111.0	105.5	98.3	89.3	79.2	71.1	64.2
	Chainage,ins	108	110	112	114	116	118	120≠	122	124	126	128	130	132	134	136	138
	Depth,mm	59.5	55.7	53.2	51.0	49.5	48.4	47.2	45.7	45.6	46.1	47.9	49.3	50.8	49.2	47.6	47.3
142	Chainage,ins	76	78	80	82	84	86	88	90	92	94	96+	98	100	102	104	106
	Depth,mm	126.1	124.9	124.9	124.6	123.7	121.6	119.6	116.4	112.9	108.4	103.0	95.1	86.5	78.1	71.1	65.0
	Chainage,ins	108	110	112	114	116	118	120≠	122	124	126	128	130	132	134	136	138
	Depth,mm	59.6	56.0	52.6	50.4	49.0	47.7	46.7	45.9	45.5	45.7	46.6	47.8	49.7	49.8	47.9	46.7
143	Chainage,ins	76	78	80	82	84	86	88	90	92	94	96+	98	100	102	104	106
	Depth,mm	124.3	121.5	120.4	118.5	116.3	114.3	112.4	109.8	106.6	102.3	97.4	90.2	82.3	74.6	68.0	62.1
	Chainage,ins	108	110	112	114	116	118	120≠	122	124	126	128	130	132	134	136	138
	Depth,mm	57.5	53.9	51.3	49.2	47.9	46.8	45.8	45.1	44.8	45.1	45.8	47.1	48.6	48.8	46.9	45.8

+ Start of Weir

≠ End of Weir

WEIR NO. 3 LONGITUDINAL PROFILE CO-ORDINATES

Reading No.																	
144	Chainage,ins	76	78	80	82	84	86	88	90	92	94	96 +	98	100	102	104	106
	Depth,mm	118.1	116.0	114.2	112.0	110.2	108.1	106.7	104.3	101.6	97.8	93.1	86.5	78.9	71.6	64.9	59.6
	Chainage,ins	108	110	112	114	116	118	120 ǂ	122	124	126	128	130	132	134	136	138
	Depth,mm	55.6	52.2	50.1	48.2	46.9	45.9	44.9	44.4	44.1	44.3	45.1	46.7	48.2	47.8	45.8	44.9
145	Chainage,ins	76	78	80	82	84	86	88	90	92	94	96 +	98	100	102	104	106
	Depth,mm	109.4	106.6	105.0	104.2	102.7	101.8	100.4	98.7	96.2	93.2	88.4	82.5	75.6	68.3	62.3	57.7
	Chainage,ins	108	110	112	114	116	118	120 ǂ	122	124	126	128	130	132	134	136	138
	Depth,mm	53.6	50.5	48.7	47.1	46.1	44.9	43.9	42.8	43.3	43.5	43.8	46.2	46.9	46.4	44.7	44.1
146	Chainage,ins	76	78	80	82	84	86	88	90	92	94	96 +	98	100	102	104	106
	Depth,mm	99.9	98.5	97.9	97.3	96.6	95.3	94.5	93.4	90.9	87.8	83.5	77.8	71.4	64.3	58.4	54.5
	Chainage,ins	108	110	112	114	116	118	120 ǂ	122	124	126	128	130	132	134	136	138
	Depth,mm	50.9	48.9	47.4	45.8	44.4	43.5	42.4	42.2	42.6	43.2	44.0	45.3	45.3	43.9	43.4	43.8

+ Start of Weir

ǂ End of Weir

WEIR NO. 3

LONGITUDINAL PROFILE CO-ORDINATES

Reading No. 147	Chainage,ins	76	78	80	82	84	86	88	90	92	94	96+	98	100	102	104	106
	Depth,mm	86.4	86.2	86.1	86.1	87.0	88.2	88.5	88.6	87.6	86.7	85.2	82.1	78.2	74.1	68.7	64.5
	Chainage,ins	108	110	112	114	116	118	120⨍	122	124	126	128	130	132	134	136	138
	Depth,mm	60.3	56.8	53.7	51.2	49.4	48.2	47.4	46.4	46.4	46.7	47.1	48.2	49.7	50.8	49.4	47.8
Reading No. 148	Chainage,ins	76	78	80	82	84	86	88	90	92	94	96+	98	100	102	104	106
	Depth,mm	72.3	72.6	73.0	72.9	72.8	72.9	73.1	73.1	73.3	73.5	73.5	72.3	70.5	67.5	64.7	60.9
	Chainage,ins	108	110	112	114	116	118	120⨍	122	124	126	128	130	132	134	136	138
	Depth,mm	58.6	55.6	53.9	52.0	50.6	49.1	48.1	48.1	47.4	47.7	48.2	49.2	50.1	51.7	50.8	49.5
Reading No. 149	Chainage,ins	76	78	80	82	84	86	88	90	92	94	96+	98	100	102	104	106
	Depth,mm	64.6	64.4	64.4	64.3	63.6	63.4	63.9	63.6	65.7	65.7	66.2	64.7	63.7	61.4	60.0	57.7
	Chainage,ins	108	110	112	114	116	118	120⨍	122	124	126	128	130	132	134	136	138
	Depth,mm	55.5	54.3	52.5	51.5	50.3	49.0	48.4	47.7	47.5	47.7	48.2	48.6	49.7	51.2	52.1	51.5

+ Start of Weir

⨍ End of Weir

(c) Transverse Surface Profiles.

Transverse Surface Profile Coordinates

Subcritical Profile : Case II

Reading No. 24.	Depth in mm.				
Station Chainage ins.	Distance from back face of Weir, mm.				
	0	25	50	75	100
+ 96	95.4	95.8	96.8	97.7	99.1
100	93.0	95.0	96.6	99.0	99.9
104	97.3	101.6	103.9	104.6	104.6
108	99.2	102.5	103.9	106.0	107.3
112	100.7	104.6	105.6	106.8	108.2
116	102.9	106.5	107.8	109.2	109.6
≁ 120	110.6	109.0	109.0	109.5	109.5

+ Start of Weir

≁ End of Weir

Transverse Surface Profile Coordinates

Supercritical Profile : Case I

Reading No. 143.	Depth in mm.				
Station Chainage ins.	Distance from back face of Weir, mm.				
	0	25	50	75	100
+ 96	94.3	95.9	97.4	98.4	99.0
100	65.6	77.2	82.3	84.9	86.3
104	59.2	64.0	68.0	70.7	71.2
108	55.3	56.6	57.5	58.6	60.0
112	52.4	52.4	51.3	50.5	52.4
116	49.1	49.7	47.9	47.5	48.1
≠ 120	45.7	45.9	45.8	45.2	45.7

\+ Start of Weir

≠ End of Weir

APPENDIX VIII

Performance of the Mathematical Model.

Weir No. 1. PERFORMANCE OF THE MATHEMATICAL MODEL: SUBCRITICAL FLOW, CASE II.

TEST No.	UPSTREAM DISCHARGE Q_1 l/s			SIDE SPILL DISCHARGE Q_w l/s			UPSTREAM DEPTH y_1 mm		
	measured	computed	% error	measured	computed	% error	measured	computed	% error
15	6.590	6.307	-4.29	4.310	4.027	-6.57	95.40	90.96	-4.65
16	5.940	5.796	-2.42	3.740	3.596	-3.85	94.90	91.41	-3.68
17	5.340	5.251	-1.67	3.180	3.091	-2.80	93.80	91.31	-2.65
18	4.630	4.601	-0.63	2.530	2.501	-1.15	92.40	90.72	-1.82
19	4.190	4.170	-0.48	2.130	2.110	-0.94	91.10	90.05	-1.15
20	3.530	3.467	-1.78	1.900	1.837	-3.32	91.10	89.89	-1.33
21	4.270	4.184	-2.01	2.620	2.534	-3.28	93.30	91.49	-1.94
22	4.560	4.420	-3.07	2.900	2.760	-4.83	94.10	91.86	-2.38
23	5.400	5.193	-3.83	3.690	3.483	-5.61	95.90	92.58	-3.46
24	5.940	5.711	-3.86	4.210	3.981	-5.44	97.10	92.69	-4.54
25	6.430	6.145	-4.43	4.680	4.395	-6.09	97.20	92.48	-4.86
26	7.020	6.616	-5.75	5.240	4.836	-7.71	97.90	91.83	-6.20
27	7.460	7.098	-4.85	5.670	5.308	-6.38	99.50	90.61	-8.93
28	6.660	6.247	-6.20	5.430	5.017	-7.61	100.20	93.80	-6.39
29	5.990	5.663	-5.46	4.810	4.483	-6.80	99.10	94.24	-4.90
30	5.340	5.084	-4.79	4.200	3.944	-6.10	97.80	94.20	-3.68

Weir No. 1. PERFORMANCE OF THE MATHEMATICAL MODEL: SUBCRITICAL FLOW, CASE II.

TEST No.	UPSTREAM DISCHARGE Q_1 l/s			SIDE SPILL DISCHARGE Q_w l/s			UPSTREAM DEPTH y_1 mm		
	measured	computed	% error	measured	computed	% error	measured	computed	% error
31	4.700	4.330	-7.87	3.600	3.230	-10.28	96.80	93.56	-3.35
32	3.880	3.714	-4.28	2.790	2.624	- 5.95	94.50	92.52	-2.10
33	3.020	2.927	-3.08	1.920	1.827	- 4.84	91.60	90.42	-1.29
34	2.190	2.072	-5.39	1.820	1.702	- 6.48	91.70	90.73	-1.06
35	2.930	2.769	-5.49	2.440	2.279	- 6.60	93.90	92.49	-1.50
36	3.690	3.494	-5.31	3.080	2.884	- 6.36	95.90	93.80	-2.19
37	4.380	4.169	-4.82	3.640	3.429	- 5.80	97.20	94.53	-2.75
38	5.540	5.251	-5.22	4.490	4.201	- 6.44	98.70	94.55	-4.20
39	6.490	6.125	-5.62	5.110	4.745	- 7.14	99.40	93.49	-5.95
40	7.610	7.109	-6.58	5.950	5.449	- 8.42	99.90	90.93	-8.98
41	3.460	3.416	-1.27	1.840	1.796	- 2.39	88.70	87.32	-1.56
42	4.330	4.207	-2.84	2.700	2.577	- 4.56	91.50	89.03	-2.70
43	5.330	5.123	-3.88	3.670	3.463	- 5.64	93.90	89.91	-4.25
44	6.210	5.944	-4.28	4.470	4.204	- 5.95	95.40	89.53	-6.15
45	6.500	6.214	-4.40	4.710	4.424	- 6.07	95.60	89.05	-6.85
46	7.500	7.087	-5.51	5.670	5.257	- 7.28	95.70	86.10	-10.03

Weir No. 1. PERFORMANCE OF THE MATHEMATICAL MODEL: SUBCRITICAL FLOW, CASE II.

TEST No.	UPSTREAM DISCHARGE Q_1 l/s			SIDE SPILL DISCHARGE Q_w l/s			UPSTREAM DEPTH Y_1 mm		
	measured	computed	% error	measured	computed	% error	measured	computed	% error
48	5.860	5.608	-4.30	4.750	4.498	-5.31	97.20	91.55	-5.81
49	5.200	4.939	-5.02	4.320	4.059	-6.04	96.60	92.21	-4.54
50	4.560	4.391	-3.71	3.850	3.681	-4.39	95.90	92.35	-3.70
51	3.770	3.662	-2.86	3.240	3.132	-3.33	94.60	91.96	-2.79
52	3.060	2.980	-2.61	2.620	2.540	-3.05	92.80	90.87	-2.08
53	2.600	2.520	-3.08	2.230	2.150	-3.59	91.60	89.89	-1.87
55	7.580	7.098	-6.36	5.820	5.338	-8.28	98.80	88.62	-10.30
56	6.560	6.272	-4.39	4.830	4.542	-5.96	97.20	90.81	-6.57
57	5.770	5.531	-4.14	4.140	3.901	-5.77	96.20	91.53	-4.85
58	4.830	4.703	-2.63	3.170	3.043	-4.01	94.50	90.94	-3.77
59	4.070	3.982	-2.16	2.460	2.372	-3.58	92.50	89.97	-2.74
60	3.330	3.225	-3.15	1.800	1.695	-5.83	89.70	88.36	-1.49

	% error Q_1	% error Q_w	% error Y_1
Mean	-3.99	-5.41	-4.05
Standard Deviation	1.63	1.90	2.42

Weir No. 2. PERFORMANCE OF THE MATHEMATICAL MODEL: SUBCRITICAL FLOW, CASE II.

TEST No.	UPSTREAM DISCHARGE Q_1 l/s			SIDE SPILL DISCHARGE Q_w l/s			UPSTREAM DEPTH y_1 mm		
	measured	computed	% error	measured	computed	% error	measured	computed	% error
62	3.680	3.543	-3.72	1.850	1.713	-7.41	129.00	127.76	-0.96
63	3.950	3.820	-3.29	2.070	1.940	-6.28	129.90	128.63	-0.98
64	4.950	4.768	-3.68	3.050	2.868	-5.97	133.60	131.72	-1.41
65	6.020	5.767	-4.20	4.070	3.817	-6.22	136.90	134.11	-2.04
66	6.790	6.499	-4.29	4.800	4.509	-6.06	138.90	135.48	-2.46
67	7.310	6.974	-4.60	5.320	4.984	-6.32	140.40	136.28	-2.93
68	7.740	7.420	-4.13	5.710	5.390	-5.60	141.50	136.82	-3.31
69	9.830	9.199	-6.42	7.790	7.159	-8.10	145.80	138.38	-5.09
70	8.440	8.098	-4.05	6.420	6.078	-5.33	143.20	137.65	-3.88
Mean			-4.26			-6.37			-2.56
Standard Deviation			0.90			0.87			1.39

Weir No. 4. PERFORMANCE OF THE MATHEMATICAL MODEL: SUBCRITICAL FLOW, CASE II.

TEST No.	UPSTREAM DISCHARGE Q_1 l/s			SIDE SPILL DISCHARGE Q_w l/s			UPSTREAM DEPTH y_1 mm		
	measured	computed	% error	measured	computed	% error	measured	computed	% error
80	3.090	3.105	0.49	1.490	1.505	1.01	92.40	90.15	-2.44
81	4.440	4.401	-0.88	2.820	2.781	-1.38	98.40	94.73	-3.73
82	5.240	5.213	-0.52	3.600	3.573	-0.75	101.60	95.72	-5.79
83	5.860	5.876	0.27	4.150	4.166	0.39	103.60	97.20	-6.18
84	6.220	6.194	-0.42	4.470	4.444	-0.58	104.80	97.33	-7.13
85	6.690	6.669	-0.31	4.930	4.909	-0.43	106.40	97.43	-8.43
86	7.270	7.170	-1.38	5.490	5.390	-1.82	108.00	97.07	-10.12
87	7.740	7.603	-1.77	5.930	5.793	-2.31	109.60	96.18	-12.24
88	8.100	7.920	-2.22	6.910	6.730	-2.60	113.60	97.85	-13.86
89	5.300	5.299	-0.02	4.150	4.149	-0.02	104.20	98.61	-5.36
90	4.290	4.283	-0.16	3.160	3.153	-0.22	100.40	96.56	-3.82
91	3.520	3.469	-1.45	2.390	2.339	-2.13	97.20	94.05	-3.24
92	2.620	2.623	0.11	1.500	1.503	0.20	92.80	90.55	-2.42
93	5.880	5.853	-0.46	4.720	4.693	-0.57	95.90	99.29	3.53
94	7.470	7.315	-2.07	6.290	6.135	-2.46	111.20	99.21	-10.78
95	8.230	7.989	-2.93	5.910	5.669	-4.08	107.80	92.28	-14.40

Weir No. 4. PERFORMANCE OF THE MATHEMATICAL MODEL: SUBCRITICAL FLOW, CASE II.

TEST No.	UPSTREAM DISCHARGE Q_1 l/s			SIDE SPILL DISCHARGE Q_w l/s			UPSTREAM DEPTH y_1 mm		
	measured	computed	% error	measured	computed	% error	measured	computed	% error
96	7.450	7.346	-1.40	5.140	5.036	-2.02	105.80	94.72	-10.47
97	6.350	6.361	0.17	4.070	4.081	0.27	102.60	95.39	-7.03
98	5.240	5.212	-0.53	3.070	3.042	-0.91	98.80	94.34	-4.51
99	4.370	4.354	-0.37	2.270	2.254	-0.70	95.60	92.44	-3.31
100	3.550	3.586	1.01	1.480	1.516	2.43	91.90	89.75	-2.34
101	2.870	2.896	0.91	1.310	1.336	1.98	90.90	90.19	-0.78
102	4.290	4.307	0.40	2.720	2.737	0.63	97.70	95.57	-2.18
103	4.830	4.858	0.58	3.240	3.268	0.86	99.80	96.91	-2.90
104	6.140	6.111	-0.47	4.450	4.421	-0.65	104.20	98.53	-5.44
105	7.200	7.064	-1.89	5.470	5.334	-2.49	107.60	98.58	-8.38
106	8.030	7.883	-1.83	6.280	6.133	-2.34	110.80	97.16	-12.31
107	3.220	3.328	3.35	1.560	1.668	6.92	90.50	90.01	-0.54
108	4.350	4.408	1.33	2.690	2.748	2.16	95.60	93.71	-1.98
109	5.200	5.285	1.63	3.520	3.605	2.41	98.70	95.55	-3.19
110	6.160	6.198	0.62	4.370	4.408	0.87	101.70	96.15	-5.46
111	7.000	7.010	0.14	5.170	5.180	0.19	104.00	95.82	-7.87

Weir No. 4. PERFORMANCE OF THE MATHEMATICAL MODEL: SUBCRITICAL FLOW, CASE II.

TEST No.	UPSTREAM DISCHARGE Q_1 l/s			SIDE SPILL DISCHARGE Q_w l/s			UPSTREAM DEPTH y_1 mm		
	measured	computed	% error	measured	computed	% error	measured	computed	% error
112	7.530	7.485	-0.60	5.660	5.615	-0.80	106.40	94.80	-10.90
Mean			-0.32			-0.27			- 5.94
Standard Deviation			1.27			2.04			4.24

Weir No. 5. PERFORMANCE OF THE MATHEMATICAL MODEL: SUBCRITICAL FLOW, CASE II.

TEST No.	UPSTREAM DISCHARGE Q_1 l/s			SIDE SPILL DISCHARGE Q_w l/s			UPSTREAM DEPTH y_1 mm		
	measured	computed	% error	measured	computed	% error	measured	computed	% error
113	4.250	4.257	0.16	2.590	2.597	0.27	90.00	86.50	-3.89
114	5.200	5.153	-0.90	3.510	3.463	-1.34	91.30	86.70	-5.04
115	5.960	5.785	-2.94	4.170	3.995	-4.20	91.50	85.97	-6.04
116	7.090	6.751	-4.78	5.190	4.851	-6.53	90.90	82.98	-8.71
117	7.540	7.020	-6.90	5.630	5.110	-9.24	90.70	80.59	-11.15
119	3.740	3.810	1.87	2.150	2.220	3.26	90.10	87.67	-2.70
120	4.580	4.601	0.46	2.940	2.961	0.71	91.40	88.36	-3.33
121	5.400	5.299	-1.87	3.700	3.599	-2.73	93.10	88.33	-5.12
122	6.080	5.877	-3.34	4.350	4.147	-4.67	93.20	87.82	-5.77
123	6.690	6.378	-4.66	4.890	4.578	-6.38	93.60	86.79	-7.28
124	7.290	6.908	-5.24	5.430	5.048	-7.03	92.90	84.95	-8.56
125	7.730	7.217	-6.64	5.850	5.337	-8.77	92.90	83.20	-10.44
126	3.020	3.170	4.97	1.460	1.610	10.27	89.50	88.17	-1.49
127	4.360	4.412	1.19	2.780	2.832	1.87	92.60	90.30	-2.48
128	5.340	5.311	-0.54	3.720	3.691	-0.78	94.30	90.71	-3.81
129	6.130	5.973	-2.56	4.430	4.273	-3.54	94.60	90.33	-4.51

Weir No. 5. PERFORMANCE OF THE MATHEMATICAL MODEL: SUBCRITICAL FLOW, CASE II.

TEST No.	UPSTREAM DISCHARGE Q_1 l/s			SIDE SPILL DISCHARGE Q_w l/s			UPSTREAM DEPTH y_1 mm		
	measured	computed	% error	measured	computed	% error	measured	computed	% error
130	6.810	6.600	-3.08	5.040	4.830	-4.17	94.60	89.42	-5.48
131	7.490	7.155	-4.47	5.700	5.365	-5.88	94.50	88.06	-6.81
Mean			-2.18			-2.71			-5.70
Standard Deviation			3.15			4.82			2.71

PERFORMANCE OF THE MATHEMATICAL MODEL: SUPERCRITICAL FLOW, CASE I:

Weir No. 3. NO ALLOWANCE FOR CURVATURE.

TEST No.	DOWNSTREAM DISCHARGE Q_2 l/s			SIDE SPILL DISCHARGE Q_w l/s			DOWNSTREAM DEPTH y_2 mm		
	measured	computed	% error	measured	computed	% error	measured	computed	% error
71	7.000	7.622	8.89	6.200	5.578	-10.03	46.20	48.09	4.09
72	6.450	7.025	8.91	5.240	4.665	-10.97	44.70	46.77	4.63
73	5.880	6.337	7.77	4.150	3.693	-11.01	42.70	45.23	5.93
74	5.120	5.471	6.86	2.910	2.559	-12.06	41.60	43.26	3.99
75	5.630	6.061	7.66	3.740	3.309	-11.52	42.60	44.59	4.67
76	6.090	6.682	9.72	4.770	4.178	-12.41	43.60	45.99	5.48
132	7.450	7.925	6.38	6.370	5.895	- 7.46	46.00	48.44	5.30
133	7.130	7.661	7.45	5.980	5.449	- 8.88	46.00	47.85	4.02
134	6.820	7.313	7.23	5.430	4.937	- 9.08	45.20	47.07	4.14
135	6.560	6.978	6.37	4.860	4.442	- 8.60	44.00	46.29	5.20
136	6.200	6.561	5.82	4.210	3.849	- 8.57	43.10	45.37	5.27
137	5.840	6.165	5.57	3.630	3.305	- 8.95	42.50	44.45	4.59
141	7.780	8.069	3.71	6.230	5.941	- 4.64	47.20	48.52	2.80
142	7.460	7.767	4.12	5.810	5.503	- 5.28	46.70	47.85	2.46
143	7.020	7.338	4.53	5.140	4.822	- 6.19	45.80	46.87	2.34
144	6.660	7.004	5.17	4.660	4.316	- 7.38	44.90	46.09	2.65

PERFORMANCE OF THE MATHEMATICAL MODEL: SUPERCRITICAL FLOW, CASE I:
NO ALLOWANCE FOR CURVATURE.

Weir No. 3.

TEST No.	DOWNSTREAM DISCHARGE Q_2 l/s			SIDE SPILL DISCHARGE Q_w l/s			DOWNSTREAM DEPTH y_2 mm		
	measured	computed	% error	measured	computed	% error	measured	computed	% error
145	6.300	6.591	4.62	4.030	3.739	- 7.22	43.90	45.12	2.78
146	5.890	6.140	4.24	3.400	3.150	- 7.35	42.40	44.06	3.92
Mean			6.39			- 8.76			4.13
Standard Deviation			1.80			2.27			1.12

PERFORMANCE OF THE MATHEMATICAL MODEL: SUPERCRITICAL FLOW, CASE IV: NO ALLOWANCE FOR CURVATURE.

Weir No. 3.

TEST No.	DOWNSTREAM DISCHARGE Q_2 l/s			SIDE SPILL DISCHARGE Q_w l/s			DOWNSTREAM DEPTH y_2 mm		
	measured	computed	% error	measured	computed	% error	measured	computed	% error
77	7.010	7.527	7.38	5.630	5.113	- 9.18	47.00	47.77	1.64
78	7.950	8.119	2.13	4.640	4.471	- 3.64	48.10	48.23	0.27
79	8.840	8.826	-0.16	3.690	3.704	0.38	49.00	48.26	-1.51
138	7.490	7.794	4.06	5.140	4.836	- 5.91	46.60	47.79	2.55
139	8.280	8.385	1.27	4.240	4.135	- 2.48	47.70	48.06	0.75
140	9.280	9.076	-2.20	3.320	3.524	6.14	48.00	48.08	0.17
147	7.750	7.908	2.04	4.750	4.592	- 3.33	47.40	47.63	0.49
148	8.680	8.586	-1.08	3.820	3.914	2.46	48.10	47.92	-0.37
149	9.420	9.157	-2.79	3.050	3.313	8.62	48.40	47.74	-1.36
Mean			1.18			- 0.77			0.29
Standard Deviation			3.21			5.73			1.30

Weir No. 3.

PERFORMANCE OF THE MATHEMATICAL MODEL: SUPERCRITICAL FLOW, CASE I: WITH ALLOWANCE FOR CURVATURE.

TEST No.	DOWNSTREAM DISCHARGE Q_2 l/s			SIDE SPILL DISCHARGE Q_w l/s			DOWNSTREAM DEPTH y_2 mm		
	measured	computed	% error	measured	computed	% error	measured	computed	% error
71	7.000	7.366	5.23	6.200	5.834	- 5.90	46.20	47.31	2.40
72	6.450	6.822	5.76	5.240	4.868	- 7.10	44.70	46.14	3.22
73	5.880	6.165	4.85	4.150	3.865	- 6.87	42.70	44.65	4.57
74	5.120	5.350	4.49	2.910	2.680	- 7.90	41.60	42.97	3.29
75	5.630	5.931	5.34	3.740	3.439	- 8.05	42.60	44.20	3.76
76	6.090	6.508	6.86	4.770	4.352	- 8.76	43.60	45.50	4.36
132	7.450	7.661	- 2.83	6.370	6.159	- 3.31	46.00	47.63	3.54
133	7.130	7.432	- 4.24	5.980	5.678	- 5.05	46.00	47.12	2.43
134	6.820	7.133	4.59	5.430	5.117	- 5.76	45.20	46.59	3.08
135	6.560	6.796	3.60	4.860	4.624	- 4.86	44.00	45.71	3.89
136	6.200	6.401	3.24	4.210	4.009	- 4.77	43.10	44.80	3.94
137	5.840	6.049	3.58	3.630	3.421	- 5.76	42.50	44.08	3.71
141	7.780	7.827	- 0.60	6.230	6.183	- 0.75	47.20	47.75	1.17
142	7.460	7.540	- 1.07	5.810	5.730	- 1.38	46.70	47.12	0.90
143	7.020	7.096	- 1.08	5.140	5.064	- 1.48	45.80	46.19	0.85
144	6.660	6.867	3.11	4.660	4.453	- 4.44	44.90	45.70	1.78

Weir No. 3.

PERFORMANCE OF THE MATHEMATICAL MODEL: SUPERCRITICAL FLOW, CASE I: WITH ALLOWANCE FOR CURVATURE.

TEST No.	DOWNSTREAM DISCHARGE Q_2 l/s			SIDE SPILL DISCHARGE Q_w l/s			DOWNSTREAM DEPTH Y_2 mm		
	measured	computed	% error	measured	computed	% error	measured	computed	% error
145	6.300	6.458	2.51	4.030	3.872	- 3.92	43.90	44.66	1.73
146	5.890	6.044	2.61	3.400	3.246	- 4.53	42.40	43.79	3.28
Mean			3.64			- 5.03			2.88
Standard Deviatinn			1.71			2.30			1.18

Weir No. 3.

PERFORMANCE OF THE MATHEMATICAL MODEL: SUPERCRITICAL FLOW, CASE IV: WITH ALLOWANCE FOR CURVATURE.

	TEST No.	DOWNSTREAM DISCHARGE Q_2 l/s			SIDE SPILL DISCHARGE Q_w l/s			DOWNSTREAM DEPTH Y_2 mm		
		measured	computed	% error	measured	computed	% error	measured	computed	% error
	77	7.010	7.347	4.81	5.630	5.293	- 5.98	47.00	47.13	0.28
+	78	7.950	8.119	2.13	4.640	4.471	- 3.64	48.10	47.92	- 0.37
+	79	8.840	8.825	- 0.17	3.690	3.705	0.41	49.00	47.98	- 2.08
	138	7.490	7.671	2.41	5.140	4.959	- 3.52	46.60	47.31	1.52
+	139	8.280	8.385	1.27	4.240	4.135	- 2.48	47.70	47.75	0.10
+	140	9.280	9.075	- 2.21	3.320	3.525	6.17	48.00	48.08	0.17
	147	7.750	7.908	2.04	4.750	4.592	- 3.33	47.40	47.30	- 0.21
+	148	8.680	8.585	- 1.09	3.820	3.915	2.49	48.10	47.62	- 1.00
+	149	9.420	9.156	- 2.80	3.050	3.314	8.66	48.40	47.47	- 1.92
	Mean			0.71			- 0.14			- 0.39
	Standard Deviation			2.47			4.97			1.13

+ Curvature not significant - no allowance made in computation.

APPENDIX IX

(a) Effect of Changing the Position of the Starting Station.

(b) Effect of Fixing the Value of the Surface Slope at the Upstream End of the Weir.

(c) Effect of Using the Manning Equation for Computing the Friction Gradient.

(a) Effect of Changing the Position of the Starting Station.

WEIR NO. 4. PERFORMANCE OF THE MATHEMATICAL MODEL : CHANGE IN STARTING STATION POSITION.

Test No.	Measured Q_1 l/s	Measured y_1 mm	Computed Values: Starting 505 mm d/s of weir				Computed Values: Starting 76.2 mm d/s of weir			
			Q_1 l/s	% error	y_1 mm	% error	Q_1 l/s	% error	y_1 mm	% error
101	2.870	90.90	2.896	0.91	90.19	-0.78	2.942	2.51	90.23	-0.74
102	4.290	97.70	4.307	0.40	95.57	-2.18	4.293	0.07	95.08	-2.68
103	4.830	99.80	4.858	0.58	96.91	-2.90	4.815	-0.31	96.23	-3.58
104	6.140	104.20	6.111	-0.47	98.53	-5.44	6.008	-2.15	97.52	-6.41
105	7.200	107.60	7.064	-1.89	98.58	-8.38	6.906	-4.08	97.37	-9.51
106	8.030	110.80	7.883	-1.83	97.16	-12.31	7.593	-5.44	96.14	-13.23
Mean				-0.38		-5.33		-1.57		-6.03
Standard Deviation				1.23		4.35		2.92		4.68

(b) Effect of Fixing the Value of the Surface Slope at the Upstream End of the Weir.

PERFORMANCE OF THE MATHEMATICAL MODEL: EFFECT OF FIXING THE SURFACE

Weir No. 3. SLOPE AT THE UPSTREAM END OF THE WEIR.

TEST No.	DOWNSTREAM DISCHARGE Q_2 l/s			SIDE SPILL DISCHARGE Q_w l/s			DOWNSTREAM DEPTH y_2 mm		
	measured	computed	% error	measured	computed	% error	measured	computed	% error
71	7.000	7.366	5.23	6.200	5.834	- 5.90	46.20	47.31	2.40
72	6.450	6.822	5.76	5.240	4.868	- 7.10	44.70	46.14	3.22
73	5.880	6.165	4.85	4.150	3.865	- 6.87	42.70	44.65	4.57
74	5.120	5.350	4.49	2.910	2.680	- 7.90	41.60	42.97	3.29
75	5.630	5.931	5.34	3.740	3.439	- 8.05	42.60	44.20	3.76
76	6.090	6.508	6.86	4.770	4.352	- 8.76	43.60	45.50	4.36
77	7.010	7.347	4.81	5.630	5.293	- 5.98	47.00	47.13	0.28
78	7.950	8.119	2.13	4.640	4.471	- 3.64	48.10	47.92	- 0.37
79	8.840	8.825	- 0.17	3.690	3.705	0.41	49.00	47.98	- 2.08
Mean			4.37			- 5.98			2.16
Standard Deviation			2.12			2.83			2.33

With initial slope = -0.12.

PERFORMANCE OF THE MATHEMATICAL MODEL: EFFECT OF FIXING THE SURFACE

Weir No. 3. SLOPE AT THE UPSTREAM END OF THE WEIR.

TEST No.	DOWNSTREAM DISCHARGE Q_2 l/s			SIDE SPILL DISCHARGE Q_w l/s			DOWNSTREAM DEPTH y_2 mm		
	measured	computed	% error	measured	computed	% error	measured	computed	% error
71	7.000	7.409	5.84	6.200	5.791	- 6.60	46.20	47.37	2.53
72	6.450	6.829	5.88	5.240	4.861	- 7.23	44.70	46.08	3.09
73	5.880	6.179	5.09	4.150	3.851	- 7.20	42.70	44.67	4.61
74	5.120	5.344	4.38	2.910	2.686	- 7.70	41.60	42.97	3.29
75	5.630	5.932	5.36	3.740	3.438	- 8.07	42.60	44.20	3.76
76	6.090	6.512	6.93	4.770	4.348	- 8.85	43.60	45.51	4.38
77	7.010	7.289	3.98	5.680	5.351	- 4.96	47.00	47.13	0.28
78	7.950	8.119	2.13	4.640	4.471	- 3.64	48.10	47.92	- 0.37
79	8.840	8.825	- 0.17	3.690	3.705	0.41	49.00	47.98	- 2.08
Mean			4.38			- 5.98			2.17
Standard Deviation			2.19			2.88			2.33

With measured initial slopes.

(c) Effect of Using the Manning Equation for Computing the Friction Gradient.

Weir No. 1. PERFORMANCE OF THE MATHEMATICAL MODEL, s_f COMPUTED FROM MANNING.

TEST No.	UPSTREAM DISCHARGE Q_1 l/s			SIDE SPILL DISCHARGE Q_w l/s			UPSTREAM DEPTH y_1 mm		
	measured	computed	% error	measured	computed	% error	measured	computed	% error
15	6.590	6.323	- 4.05	4.310	4.043	- 6.19	95.40	91.60	- 3.98
16	5.940	5.808	- 2.22	3.740	3.608	- 3.53	94.90	91.88	- 3.18
17	5.340	5.260	- 1.50	3.180	3.100	- 2.52	93.80	91.65	- 2.29
18	4.630	4.607	- 0.50	2.530	2.507	- 0.91	92.40	90.96	- 1.56
19	4.190	4.175	- 0.36	2.130	2.115	- 0.70	91.10	90.24	- 0.94
20	3.530	3.468	- 1.76	1.900	1.838	- 3.26	91.10	89.99	- 1.22
21	4.270	4.186	- 1.97	2.620	2.536	- 3.21	93.30	91.65	- 1.77
22	4.560	4.423	- 3.00	2.900	2.763	- 4.72	94.10	92.05	- 2.18
23	5.400	5.199	- 3.72	3.690	3.489	- 5.45	95.90	92.88	- 3.15
24	5.940	5.720	- 3.70	4.210	3.990	- 5.23	97.10	93.10	- 4.12
25	6.430	6.157	- 4.25	4.680	4.407	- 5.83	97.20	93.00	- 4.32
26	7.020	6.631	- 5.54	5.240	4.851	- 7.42	97.90	92.55	- 5.46
27	7.460	7.118	- 4.58	5.670	5.328	- 6.03	99.50	91.68	- 7.86
28	6.660	6.255	- 6.08	5.430	5.025	- 7.46	100.20	94.29	- 5.90
29	5.990	5.669	- 5.36	4.810	4.489	- 6.67	99.10	94.58	- 4.56
30	5.340	5.087	- 4.74	4.200	3.947	- 6.02	97.80	94.44	- 3.44

Weir No. 1. PERFORMANCE OF THE MATHEMATICAL MODEL, s_f COMPUTED FROM MANNING.

TEST No.	UPSTREAM DISCHARGE Q_1 l/s			SIDE SPILL DISCHARGE Q_w l/s			UPSTREAM DEPTH y_1 mm		
	measured	computed	% error	measured	computed	% error	measured	computed	% error
31	4.700	4.331	- 7.85	3.600	3.231	-10.25	96.80	93.72	- 3.18
32	3.880	3.714	- 4.28	2.790	2.624	- 5.95	94.50	92.62	- 1.99
33	3.020	2.925	- 3.15	1.920	1.825	- 4.95	91.60	90.47	- 1.23
34	2.190	2.070	- 6.71	1.820	1.700	- 6.59	91.70	90.74	- 1.05
35	2.930	2.768	- 5.53	2.440	2.278	- 6.64	93.90	92.52	- 1.47
36	3.690	3.493	- 5.34	3.080	2.883	- 6.40	95.90	93.88	- 2.11
37	4.380	4.169	- 4.82	3.640	3.429	- 5.80	97.20	94.66	- 2.61
38	5.540	5.254	- 5.16	4.490	4.204	- 6.37	98.70	94.81	- 3.94
39	6.490	6.134	- 5.49	5.110	4.754	- 6.97	99.40	93.97	- 5.46
40	7.610	7.127	- 6.35	5.950	5.467	- 8.12	99.90	91.96	- 7.95
Mean			- 4.15			- 5.51			- 3.34
Standard Deviation			1.91			2.14			1.97

APPENDIX X

Performance of the Mathematical Model using the Data of Engels and Gentilini.

Weir No. PERFORMANCE OF THE MATHEMATICAL MODEL, DATA BY ENGELS (SUBCRITICAL FLOW, CASE II)

TEST No.	UPSTREAM DISCHARGE Q_1 l/s			SIDE SPILL DISCHARGE Q_w l/s			UPSTREAM DEPTH y_1 mm		
	measured	computed	% error	measured	computed	% error	measured	computed	% error
E 4	14.700	14.198	- 3.41	3.500	2.998	- 14.34	110.00	110.59	0.54
E 5	14.700	13.908	- 5.39	4.400	3.608	- 18.00	101.00	100.35	-0.64
E 7	125.500	146.980	17.12	23.400	44.880	91.79	180.00	177.33	-1.48
E 9	180.000	180.548	0.30	10.000	10.548	5.48	283.00	299.84	5.95
E10	180.000	182.375	1.32	14.000	16.375	16.96	285.00	389.36	1.53
E12	153.500	155.936	1.59	31.300	33.736	7.78	356.00	355.64	-0.10
E13	153.500	152.317	- 0.77	50.600	49.417	- 2.34	297.00	298.34	0.45
E14	153.500	152.198	- 0.85	56.300	54.998	- 2.31	278.00	278.44	0.16
E15	153.500	156.003	1.63	58.400	60.903	4.29	271.00	270.40	-0.22
E16	153.500	156.995	2.28	60.100	63.595	5.82	276.00	266.10	-3.59
E17	153.500	156.114	1.70	60.500	63.114	4.32	266.00	264.69	-0.49
E18	153.500	150.440	- 1.99	62.600	59.540	- 4.89	262.00	263.67	0.64
E19	103.700	105.243	1.49	8.200	9.743	18.82	300.00	299.62	-0.13
E20	103.700	108.308	4.44	10.700	15.308	43.07	290.00	291.40	0.48
E21	103.700	108.101	4.24	14.800	19.201	29.74	278.00	279.60	0.58
E22	103.700	111.297	7.33	17.400	24.997	43.66	271.00	270.93	-0.03

Weir No. PERFORMANCE OF THE MATHEMATICAL MODEL, DATA BY ENGELS (SUBCRITICAL FLOW, CASE II)

TEST No.	UPSTREAM DISCHARGE Q_1 l/s			SIDE SPILL DISCHARGE Q_w l/s			UPSTREAM DEPTH y_1 mm		
	measured	computed	% error	measured	computed	% error	measured	computed	% error
E23	103.700	111.541	7.56	18.900	26.741	41.49	266.00	266.20	0.08
E24	103.700	114.074	10.00	19.700	30.074	52.66	262.00	263.86	0.71
E25	103.700	115.790	11.66	20.000	32.090	60.45	262.00	262.20	0.08
Mean			3.17			20.23			0.24
Standard Deviation			5.53			28.68			1.74

Weir No. PERFORMANCE OF THE MATHEMATICAL MODEL, DATA BY GENTILINI (SUBCRITICAL FLOW)

TEST No.	UPSTREAM DISCHARGE Q_1 l/s			SIDE SPILL DISCHARGE Q_w l/s			UPSTREAM DEPTH y_1 mm		
	measured	computed	% error	measured	computed	% error	measured	computed	% error
G 1	21.650	21.071	- 2.67	21.650	21.071	- 2.67	298.40	296.39	- 0.67
G 2	18.850	18.579	- 1.44	14.280	14.009	- 1.90	287.10	285.99	- 0.39
G 3	16.050	15.490	- 3.49	13.050	12.490	- 4.29	285.30	283.95	- 0.47
G 4	21.650	21.588	- 0.29	7.680	7.618	- 1.09	274.20	274.18	- 0.01
G 5	17.720	17.515	- 1.16	3.820	3.615	- 5.37	265.80	265.61	- 0.07
G 6	12.450	12.007	- 3.56	10.850	10.407	- 4.08	118.50	114.72	- 3.19
G 7	18.250	18.278	0.15	4.950	4.978	0.57	158.90	157.62	- 0.81
G 8	14.650	14.841	1.30	7.000	7.191	2.73	168.30	166.13	- 1.29
Mean			- 1.40			- 2.01			- 0.86
Standard Deviation			1.76			2.70			1.03

Weir No.

PERFORMANCE OF THE MATHEMATICAL MODEL, DATA BY GENTILINI (SUPERCRITICAL FLOW, UPSTREAM DEPTHS OBTAINED FROM FIG. 6.56)

TEST No.	DOWNSTREAM DISCHARGE Q_2 l/s			SIDE SPILL DISCHARGE Q_w l/s			DOWNSTREAM DEPTH y_2 mm		
	measured	computed	% error	measured	computed	% error	measured	computed	% error
G 9	18.670	19.297	3.36	7.750	7.123	- 8.09	66.10	64.45	- 2.50
G10	17.650	17.956	1.73	6.050	5.744	- 5.06	65.50	68.41	4.44
G11	20.650	21.106	2.21	6.200	5.744	- 7.35	73.00	70.01	- 4.10
G12	18.150	18.624	2.61	4.800	4.326	- 9.88	69.00	66.45	- 3.70

	% error Q_2	% error Q_w	% error y_2
Mean	2.48	- 7.60	- 1.41
Standard Deviation	0.69	2.00	3.99

PERFORMANCE OF THE MATHEMATICAL MODEL, DATA BY GENTILINI

Weir No.

(SUPERCRITICAL FLOW, MEASURED UPSTREAM DEPTHS)

TEST No.	DOWNSTREAM DISCHARGE Q_2 l/s			SIDE SPILL DISCHARGE Q_w l/s			DOWNSTREAM DEPTH y_2 mm		
	measured	computed	% error	measured	computed	% error	measured	computed	% error
G 9	18.670	19.456	4.21	7.750	6.964	-10.14	66.10	64.63	- 2.22
G10	17.650	18.114	2.63	6.050	5.586	- 7.67	65.50	63.32	- 3.33
G11	20.650	21.130	2.32	6.200	5.720	- 7.74	73.00	69.76	- 4.44
G12	18.150	18.632	2.66	4.800	4.318	-10.04	69.00	66.41	- 3.75
Mean			2.96			- 8.90			- 3.44
Standard Deviation			0.85			1.38			0.93

APPENDIX XI

Performance of De Marchi's Method and Chow's Numerical Integration Method.

Weir No. 1. PERFORMANCE OF DE MARCHI's METHOD: SUBCRITICAL FLOW, CASE II.

TEST No.	UPSTREAM DISCHARGE Q_1 l/s			SIDE SPILL DISCHARGE Q_w l/s			UPSTREAM DEPTH y_1 mm		
	measured	computed	% error	measured	computed	% error	measured	computed	% error
15	6.590	6.270	- 4.86	4.310	3.990	- 7.42	95.40	90.18	- 5.47
16	5.940	5.764	- 2.96	3.740	3.564	- 4.71	94.90	90.85	- 4.27
17	5.340	5.217	- 2.30	3.180	3.057	- 3.87	93.80	90.93	- 3.06
18	4.630	4.563	- 1.45	2.530	2.463	- 2.65	92.40	90.48	- 2.08
19	4.190	4.128	- 1.48	2.130	2.068	- 2.91	91.10	89.86	- 1.36
20	3.530	3.441	- 2.52	1.900	1.811	- 4.68	91.10	89.78	- 1.45
21	4.270	4.169	- 2.37	2.620	2.519	- 3.85	93.30	91.35	- 2.09
22	4.560	4.409	- 3.31	2.900	2.749	- 5.21	94.10	91.70	- 2.55
23	5.400	5.189	- 3.91	3.690	3.479	- 5.72	95.90	92.25	- 3.81
24	5.940	5.709	- 3.89	4.210	3.979	- 5.49	97.10	92.18	- 5.07
25	6.430	6.142	- 4.48	4.680	4.392	- 6.15	97.20	91.77	- 5.59
26	7.020	6.607	- 5.88	5.240	4.827	- 7.88	97.90	90.85	- 7.20
27	7.460	7.079	- 5.11	5.670	5.289	- 6.72	99.50	89.26	-10.29
28	6.660	6.272	- 5.83	5.430	5.042	- 7.15	100.20	93.02	- 7.17
29	5.990	5.692	- 4.97	4.810	4.512	- 6.20	99.10	93.75	- 5.40
30	5.340	5.111	- 4.29	4.200	3.971	- 5.45	97.80	93.93	- 3.96

Weir No. 1. PERFORMANCE OF DE MARCHI's METHOD: SUBCRITICAL FLOW, CASE II.

TEST No.	UPSTREAM DISCHARGE Q_1 l/s			SIDE SPILL DISCHARGE Q_w l/s			UPSTREAM DEPTH y_1 mm		
	measured	computed	% error	measured	computed	% error	measured	computed	% error
31	4.700	4.350	- 7.45	3.600	3.250	- 9.72	96.80	93.46	- 3.45
32	3.880	3.725	- 3.99	2.790	2.635	- 5.56	94.50	92.48	- 2.14
33	3.020	2.904	- 3.84	1.920	1.804	- 6.04	91.60	90.48	- 1.22
34	2.190	2.090	- 4.57	1.820	1.720	- 5.49	91.70	90.76	- 1.03
35	2.930	2.786	- 4.91	2.440	2.296	- 5.90	93.90	92.55	- 1.44
36	3.690	3.508	- 4.93	3.080	2.898	- 5.91	95.90	93.89	- 2.10
37	4.380	4.205	- 4.00	3.640	3.465	- 4.81	97.20	94.47	- 2.81
38	5.540	5.284	- 4.62	4.490	4.234	- 5.70	98.70	94.23	- 4.53
39	6.490	6.143	- 5.35	5.110	4.763	- 6.79	99.40	92.79	- 6.65
40	7.610	7.097	- 6.74	5.950	5.437	- 8.62	99.90	89.53	-10.38
41	3.460	4.304	24.39	1.840	2.684	45.87	88.70	91.68	3.36
42	4.330	5.145	18.82	2.700	3.515	30.19	91.50	92.47	1.06
43	5.330	6.074	13.96	3.670	4.414	20.27	93.90	92.10	- 1.92
44	6.210	6.857	10.42	4.470	5.117	14.47	95.40	90.32	- 5.32
45	6.500	7.106	9.32	4.710	5.316	12.87	95.60	89.12	- 6.78
46	7.500	N/C	N/C	5.670	N/C	N/C	95.70	N/C	N/C

Weir No. 1. PERFORMANCE OF DE MARCHI's METHOD: SUBCRITICAL FLOW, CASE II.

TEST No.	UPSTREAM DISCHARGE Q_1 l/s			SIDE SPILL DISCHARGE Q_w l/s			UPSTREAM DEPTH y_1 mm		
	measured	computed	% error	measured	computed	% error	measured	computed	% error
48	5.860	6.618	12.94	4.750	5.508	15.96	97.20	92.65	- 4.68
49	5.200	5.995	15.29	4.320	5.115	18.40	96.60	94.37	- 2.31
50	4.560	5.469	19.93	3.850	4.759	23.61	95.90	95.21	- 0.72
51	3.770	4.749	25.97	3.240	4.219	30.23	94.60	95.65	1.11
52	3.060	4.031	31.73	2.620	3.591	37.06	92.80	95.37	2.77
53	2.600	3.556	36.77	2.230	3.186	42.87	91.60	94.82	3.52
55	7.580	7.500	- 1.06	5.820	5.740	- 1.37	98.80	86.45	-12.50
56	6.560	6.732	2.62	4.830	5.002	3.56	97.20	90.65	- 6.74
57	5.770	6.016	4.26	4.140	4.386	5.94	96.20	92.24	- 4.12
58	4.830	5.177	7.18	3.170	3.517	10.95	94.50	92.40	- 2.22
59	4.070	4.439	9.07	2.460	2.829	15.00	92.50	91.91	- 0.64
60	3.330	3.652	9.67	1.800	2.122	17.89	89.70	90.71	1.13
Mean			3.29			4.49			- 3.29
Standard Deviation			11.42			15.32			3.47

Weir No. 2. PERFORMANCE OF DE MARCHI's METHOD : SUBCRITICAL FLOW, CASE II.

TEST No.	UPSTREAM DISCHARGE Q_1 l/s			SIDE SPILL DISCHARGE Q_w l/s			UPSTREAM DEPTH y_1 mm		
	measured	computed	% error	measured	computed	% error	measured	computed	% error
62	3.680	4.007	8.89	1.850	2.177	17.68	129.00	130.78	1.38
63	3.950	4.295	8.73	2.070	2.415	16.67	129.90	131.59	1.30
64	4.950	5.331	7.70	3.050	3.431	12.49	133.60	134.32	0.54
65	6.020	6.374	5.88	4.070	4.424	8.70	136.90	136.40	-0.37
66	6.790	7.129	4.99	4.800	5.139	7.06	138.90	137.50	-1.01
67	7.310	7.619	4.23	5.320	5.629	5.81	140.40	138.12	-1.62
68	7.740	8.074	4.32	5.710	6.044	5.85	141.50	138.46	-2.15
69	9.830	9.875	0.46	7.790	7.835	0.58	145.80	139.08	-4.61
70	8.440	8.766	3.86	6.420	6.746	5.08	143.20	138.96	-2.96

Mean	5.45	8.88	-1.06
Standard Deviation	2.70	5.66	2.01

Weir No. 4. PERFORMANCE OF DE MARCHI's METHOD : SUBCRITICAL FLOW, CASE II.

TEST No.	UPSTREAM DISCHARGE Q_1 l/s			SIDE SPILL DISCHARGE Q_w l/s			UPSTREAM DEPTH y_1 mm		
	measured	computed	% error	measured	computed	% error	measured	computed	% error
80	3.090	3.422	10.74	1.490	1.822	22.28	92.40	92.46	0.06
81	4.440	4.800	8.11	2.820	3.180	12.77	98.40	96.24	- 2.20
82	5.240	5.627	7.39	3.600	3.987	10.75	101.60	97.50	- 4.04
83	5.860	6.307	7.63	4.150	4.597	10.77	103.60	97.49	- 5.90
84	6.220	6.637	6.70	4.470	4.887	9.33	104.80	97.10	- 7.35
85	6.690	7.105	6.20	4.930	5.345	8.42	106.40	96.63	- 9.18
86	7.270	7.601	4.55	5.490	5.821	6.03	108.00	95.24	-11.81
87	7.740	8.019	3.60	5.930	6.209	4.70	109.60	92.85	-15.28
88	8.100	8.362	3.23	6.910	7.172	3.79	113.60	92.84	-18.27
89	5.300	5.760	8.68	4.150	4.610	11.08	104.20	99.42	- 4.59
90	4.290	4.710	9.79	3.160	3.580	13.29	100.40	98.17	- 2.22
91	3.520	3.862	9.72	2.390	2.732	14.31	97.20	96.12	- 1.11
92	2.620	2.973	13.47	1.500	1.853	23.53	92.80	93.01	0.23
93	5.880	6.326	7.59	4.720	5.166	9.45	95.90	99.52	3.77
94	7.470	7.785	4.22	6.290	6.605	5.01	111.20	97.04	12.73
95	8.230	N/C	N/C	5.910	N/C	N/C	107.80	N/C	N/C

Weir No. 4. PERFORMANCE OF DE MARCHI's METHOD : SUBCRITICAL FLOW, CASE II.

TEST No.	UPSTREAM DISCHARGE Q_1 l/s			SIDE SPILL DISCHARGE Q_w l/s			UPSTREAM DEPTH y_1 mm		
	measured	computed	% error	measured	computed	% error	measured	computed	% error
96	7.450	7.733	3.80	5.140	5.423	5.51	105.80	92.37	-12.69
97	6.350	6.755	6.38	4.070	4.475	9.95	102.60	95.15	- 7.26
98	5.240	5.591	6.70	3.070	3.421	11.43	98.80	95.32	- 3.52
99	4.370	4.706	7.69	2.270	2.606	14.80	95.60	94.03	- 1.64
100	3.550	3.899	9.83	1.480	1.829	23.58	91.90	91.76	- 0.15
101	2.870	2.841	- 1.01	1.310	1.281	- 2.21	90.90	90.06	- 0.92
102	4.290	4.282	- 0.19	2.720	2.712	- 0.29	97.70	95.25	- 2.51
103	4.830	4.839	0.19	3.240	3.249	0.28	99.80	96.44	- 3.37
104	6.140	6.098	- 0.68	4.450	4.408	- 0.94	104.20	97.56	- 6.37
105	7.200	7.063	- 1.90	5.470	5.333	- 2.50	107.60	96.81	-10.03
106	8.030	7.881	- 1.86	6.280	6.131	- 2.37	110.80	94.08	-15.09
107	3.220	4.049	25.75	1.560	2.389	53.14	90.50	94.18	4.07
108	4.350	5.213	19.84	2.690	3.553	32.08	95.60	96.81	1.27
109	5.200	6.124	17.77	3.520	4.444	26.25	98.70	97.60	1.11
110	6.160	7.045	14.37	4.370	5.255	20.25	101.70	96.62	- 5.00

Weir No. 4. PERFORMANCE OF DE MARCHI's METHOD : SUBCRITICAL FLOW, CASE II.

TEST No.	UPSTREAM DISCHARGE Q_1 l/s			SIDE SPILL DISCHARGE Q_w l/s			UPSTREAM DEPTH y_1 mm		
	measured	computed	% error	measured	computed	% error	measured	computed	% error
111	7.000	7.837	11.96	5.170	6.007	16.19	104.00	93.98	- 9.63
112	7.530	N/C	N/C	5.660	N/C	N/C	106.40	N/C	N/C

Mean	7.43	11.96	- 4.42
Standard Deviation	6.38	11.73	6.46

Weir No. 5. PERFORMANCE OF DE MARCHI's METHOD : SUBCRITICAL FLOW, CASE II.

TEST No.	UPSTREAM DISCHARGE Q_1 l/s			SIDE SPILL DISCHARGE Q_w l/s			UPSTREAM DEPTH y_1 mm		
	measured	computed	% error	measured	computed	% error	measured	computed	% error
113	4.250	5.148	21.13	2.590	3.488	34.67	90.00	89.81	- 0.21
114	5.200	6.024	15.85	3.510	4.334	23.48	91.30	88.86	- 2.67
115	5.960	6.603	10.79	4.170	4.813	15.42	91.50	87.19	- 4.71
116	7.090	N/C	N/C	5.190	N/C	N/C	90.90	N/C	N/C
117	7.540	N/C	N/C	5.630	N/C	N/C	90.70	N/C	N/C
119	3.740	4.229	13.07	2.150	2.639	22.74	90.10	89.68	- 0.47
120	4.580	5.026	9.74	2.940	3.386	15.17	91.40	89.89	- 1.65
121	5.400	5.713	5.80	3.700	4.013	8.46	93.10	89.31	- 4.07
122	6.080	6.269	3.11	4.350	4.539	4.34	93.20	88.27	- 5.29
123	6.690	6.737	0.70	4.890	4.937	0.96	93.60	86.68	- 7.39
124	7.290	7.214	- 1.04	5.430	5.354	- 1.40	92.90	83.90	- 9.69
125	7.730	N/C	N/C	5.850	N/C	N/C	92.90	N/C	N/C
126	3.020	3.071	1.69	1.460	1.511	3.49	89.50	87.76	- 1.94
127	4.360	4.306	- 1.24	2.780	2.726	- 1.94	92.60	89.78	- 3.05
128	5.340	5.193	- 2.75	3.720	3.573	- 3.95	94.30	89.89	- 4.68
129	6.130	5.834	- 4.83	4.430	4.134	- 6.68	94.60	89.15	- 5.76

Weir No. 5. PERFORMANCE OF DE MARCHI's METHOD : SUBCRITICAL FLOW, CASE II.

TEST No.	UPSTREAM DISCHARGE Q_1 l/s			SIDE SPILL DISCHARGE Q_w l/s			UPSTREAM DEPTH y_1 mm		
	measured	computed	% error	measured	computed	% error	measured	computed	% error
130	6.810	6.435	- 5.51	5.040	4.665	- 7.44	94.60	87.76	- 7.23
131	7.490	6.959	- 7.09	5.700	5.169	- 9.32	94.50	85.68	- 9.33
Mean			3.96			6.54			- 4.54
Standard Deviation			8.47			13.12			2.97

Weir No. 3. PERFORMANCE OF DE MARCHI's METHOD: SUPERCRITICAL FLOW, CASE I.

TEST No.	DOWNSTREAM DISCHARGE Q_2 l/s			SIDE SPILL DISCHARGE Q_w l/s			DOWNSTREAM DEPTH y_2 mm		
	measured	computed	% error	measured	computed	% error	measured	computed	% error
71	7.000	7.691	9.87	6.200	5.509	-11.15	46.20	46.20	0.00
72	6.450	7.124	10.45	5.240	4.566	-12.86	44.70	45.11	0.92
73	5.880	6.502	10.58	4.150	3.528	-14.99	42.70	44.17	3.44
74	5.120	5.613	9.63	2.910	2.417	-16.94	41.60	42.08	1.15
75	5.630	6.215	10.39	3.740	3.155	-15.64	42.60	43.47	2.04
76	6.090	6.790	11.49	4.770	4.070	-14.68	43.60	44.46	1.97
132	7.450	7.938	6.55	6.370	5.882	- 7.66	46.00	46.66	1.43
133	7.130	7.693	7.90	5.980	5.417	- 9.41	46.00	46.20	0.43
134	6.820	7.360	7.92	5.430	4.890	- 9.94	45.20	45.57	0.82
135	6.560	7.088	8.05	4.860	4.332	-10.86	44.00	45.34	3.05
136	6.200	6.666	7.52	4.210	3.744	-11.07	43.10	44.36	2.92
137	5.840	6.261	7.21	3.630	3.209	-11.60	42.50	43.43	2.19
141	7.780	8.052	3.50	6.230	5.958	- 4.37	47.20	46.87	-0.70
142	7.460	7.763	4.06	5.810	5.507	- 5.22	46.70	46.33	-0.79
143	7.020	7.395	5.34	5.140	4.765	- 7.30	45.80	45.84	0.09
144	6.660	7.053	5.90	4.660	4.267	- 8.43	44.90	45.04	0.31

Weir No. 3. PERFORMANCE OF DE MARCHI's METHOD: SUPERCRITICAL FLOW, CASE I.

TEST No.	DOWNSTREAM DISCHARGE Q_2 l/s			SIDE SPILL DISCHARGE Q_w l/s			DOWNSTREAM DEPTH y_2 mm		
	measured	computed	% error	measured	computed	% error	measured	computed	% error
145	6.300	6.637	5.35	4.030	3.693	- 8.36	43.90	44.13	0.52
146	5.890	6.208	5.40	3.400	3.082	- 9.35	42.40	43.35	2.24
Mean			7.62			-10.55			1.22
Standard Deviation			2.40			3.50			1.26

Weir No. 3. PERFORMANCE OF DE MARCHI's METHOD: SUPERCRITICAL FLOW, CASE IV.

TEST No.	DOWNSTREAM DISCHARGE Q_2 l/s			SIDE SPILL DISCHARGE Q_w l/s			DOWNSTREAM DEPTH y_2 mm		
	measured	computed	% error	measured	computed	% error	measured	computed	% error
77	7.010	7.635	8.92	5.630	5.005	-11.10	47.00	46.12	- 1.87
78	7.950	8.271	4.04	4.640	4.319	- 6.92	48.10	46.83	- 2.64
79	8.840	9.015	1.98	3.690	3.515	- 4.74	49.00	47.01	- 4.06
138	7.490	7.882	5.23	5.140	4.748	- 7.63	46.60	46.49	- 0.24
139	8.280	8.516	2.85	4.240	4.004	- 5.57	47.70	46.93	- 1.61
140	9.280	9.260	- 0.22	3.320	3.340	0.60	48.00	47.16	- 1.75
147	7.750	7.984	3.02	4.750	4.516	- 4.93	47.40	46.61	- 1.67
148	8.680	8.700	0.23	3.820	3.800	- 0.52	48.10	46.98	- 2.33
149	9.420	9.317	-1.09	3.050	3.153	3.38	48.40	46.95	- 3.00
Mean			2.77			- 4.16			- 2.13
Standard Deviation			3.09			4.52			1.06

Weir No. 1. PERFORMANCE OF CHOW's NUMERICAL INTEGRATION METHOD : SUBCRITICAL FLOW, CASE II.

TEST No.	UPSTREAM DISCHARGE Q_1 l/s			SIDE SPILL DISCHARGE Q_w l/s			UPSTREAM DEPTH y_1 mm		
	measured	computed	% error	measured	computed	% error	measured	computed	% error
15	6.590	6.346	- 3.70	4.310	4.066	- 5.66	95.40	91.26	- 4.34
16	5.940	5.824	- 1.95	3.740	3.624	- 3.10	94.90	91.70	- 3.37
17	5.340	5.269	- 1.33	3.180	3.109	- 2.23	93.80	91.60	- 2.34
18	4.630	4.600	- 0.65	2.530	2.500	- 1.19	92.40	90.91	- 1.61
19	4.190	4.166	- 0.57	2.130	2.106	- 1.13	91.10	90.19	- 1.00
20	3.530	3.464	- 1.87	1.900	1.834	- 3.47	91.10	89.99	- 1.22
21	4.270	4.194	- 1.78	2.620	2.544	- 2.90	93.30	91.66	- 1.76
22	4.560	4.433	- 2.79	2.900	2.773	- 4.38	94.10	92.07	- 2.16
23	5.400	5.218	- 3.37	3.690	3.508	- 4.93	95.90	92.87	- 3.16
24	5.940	5.750	- 3.20	4.210	4.020	- 4.51	97.10	93.01	- 4.21
25	6.430	6.195	- 3.65	4.680	4.445	- 5.02	97.20	92.80	- 4.53
26	7.020	6.676	- 4.90	5.240	4.896	- 6.56	97.90	92.12	- 5.90
27	7.460	7.171	- 3.87	5.670	5.381	- 5.10	99.50	90.87	- 8.67
28	6.660	6.314	- 5.20	5.430	5.084	- 6.37	100.20	94.13	- 6.06
29	5.990	5.717	- 4.56	4.810	4.537	- 5.68	99.10	94.59	- 4.55
30	5.340	5.127	- 3.99	4.200	3.987	- 5.07	97.80	94.53	- 3.34

Weir No. **1.** **PERFORMANCE OF CHOW's NUMERICAL INTEGRATION METHOD : SUBCRITICAL FLOW, CASE II.**

TEST No.	UPSTREAM DISCHARGE Q_1 l/s			SIDE SPILL DISCHARGE Q_w l/s			UPSTREAM DEPTH y_1 mm		
	measured	computed	% error	measured	computed	% error	measured	computed	% error
31	4.700	4.355	- 7.34	3.600	3.255	- 9.58	96.80	93.80	- 3.10
32	3.880	3.729	- 3.89	2.790	2.639	- 5.41	94.50	92.70	- 1.90
33	3.020	2.933	- 2.88	1.920	1.833	- 4.53	91.60	90.53	- 1.17
34	2.190	2.086	- 4.75	1.820	1.716	- 5.71	91.70	90.85	- 0.93
35	2.930	2.787	- 4.88	2.440	2.297	- 5.86	93.90	92.64	- 1.34
36	3.690	3.515	- 4.74	3.080	2.905	- 5.68	95.90	94.00	- 1.98
37	4.380	4.197	- 4.18	3.640	3.457	- 5.03	97.20	94.77	- 2.50
38	5.540	5.293	- 4.46	4.490	4.243	- 5.50	98.70	94.87	- 3.88
39	6.490	6.185	- 4.70	5.110	4.805	- 5.97	99.40	93.83	- 5.58
40	7.610	7.191	- 5.51	5.950	5.531	- 7.04	99.90	91.18	- 8.73
41	3.460	3.922	13.35	1.840	2.302	25.11	88.70	88.68	- 0.02
42	4.330	4.747	9.63	2.700	3.117	15.44	91.50	89.99	- 1.65
43	5.330	5.635	6.66	3.670	4.025	9.67	93.90	90.27	- 3.87
44	6.210	6.495	4.59	4.470	4.755	6.38	95.40	89.06	- 6.65
45	6.500	6.758	3.97	4.710	4.968	5.48	95.60	88.24	- 7.70
46	7.500	6.758	- 9.89	5.670	4.928	-13.09	95.70	88.24	- 7.80

Weir No. 1. PERFORMANCE OF CHOW's NUMERICAL INTEGRATION METHOD : SUBCRITICAL FLOW, CASE II.

TEST No.	UPSTREAM DISCHARGE Q_1 l/s			SIDE SPILL DISCHARGE Q_w l/s			UPSTREAM DEPTH y_1 mm		
	measured	computed	% error	measured	computed	% error	measured	computed	% error
48	5.860	6.209	5.96	4.750	5.099	7.35	97.20	91.37	- 6.00
49	5.200	5.555	6.83	4.320	4.675	8.22	96.60	92.60	- 4.14
50	4.560	5.012	9.91	3.850	4.302	11.74	95.90	93.08	- 2.94
51	3.770	4.282	13.58	3.240	3.752	15.80	94.60	93.03	- 1.66
52	3.060	3.587	17.22	2.620	3.147	20.11	92.80	92.29	- 0.55
53	2.600	3.118	19.92	2.230	2.748	23.23	91.60	91.58	- 0.02
55	7.580	7.401	- 2.36	5.820	5.512	- 5.29	98.80	87.61	-11.33
56	6.560	6.579	0.29	4.830	4.849	0.39	97.20	90.68	- 6.71
57	5.770	5.836	1.14	4.140	4.206	1.59	96.20	91.80	- 4.57
58	4.830	4.989	3.29	3.170	3.329	5.02	94.50	91.48	- 3.20
59	4.070	4.252	4.47	2.460	2.642	7.40	92.50	90.64	- 2.01
60	3.330	3.478	4.44	1.800	1.948	8.22	89.70	89.21	- 0.55

	% error Q_1	% error Q_w	% error y_1
Mean	0.42	0.57	- 3.65
Standard Deviation	6.76	9.06	2.61

Weir No. 2. PERFORMANCE OF CHOW's NUMERICAL INTEGRATION METHOD : SUBCRITICAL FLOW, CASE II.

TEST No.	UPSTREAM DISCHARGE Q_1 l/s			SIDE SPILL DISCHARGE Q_w l/s			UPSTREAM DEPTH y_1 mm		
	measured	computed	% error	measured	computed	% error	measured	computed	% error
62	3.680	3.827	3.99	1.850	1.997	7.95	129.00	128.96	- 0.03
63	3.950	4.111	4.08	2.070	2.231	7.78	129.90	129.80	- 0.08
64	4.950	5.089	2.81	3.050	3.189	4.56	133.60	132.73	- 0.65
65	6.020	6.114	1.56	4.070	4.164	2.31	136.90	135.02	- 1.37
66	6.790	6.858	1.00	4.800	4.868	1.42	138.90	136.31	- 1.86
67	7.310	7.346	0.49	5.320	5.356	0.68	140.40	137.09	- 2.36
68	7.740	7.805	0.84	5.710	5.775	1.14	141.50	137.59	- 2.76
69	9.830	9.619	- 2.15	7.790	7.579	- 2.71	145.80	138.86	- 4.76
70	8.440	8.500	0.71	6.420	6.480	0.93	143.20	138.35	- 3.39

Mean		
	1.48 (% error, Q_1)	

Statistic	Q_1 % error	Q_w % error	y_1 % error
Mean	1.48	2.67	- 1.92
Standard Deviation	1.94	3.49	1.58

Weir No. 4. PERFORMANCE OF CHOW's NUMERICAL INTEGRATION METHOD : SUBCRITICAL FLOW, CASE II.

TEST No.	UPSTREAM DISCHARGE Q_1 l/s			SIDE SPILL DISCHARGE Q_w l/s			UPSTREAM DEPTH y_1 mm		
	measured	computed	% error	measured	computed	% error	measured	computed	% error
80	3.090	3.350	8.41	1.490	1.750	17.45	92.40	91.00	- 1.52
81	4.440	4.694	5.72	2.820	3.074	9.01	98.40	95.10	- 3.35
82	5.240	5.529	5.52	3.600	3.889	8.03	101.60	96.51	- 5.01
83	5.860	6.209	5.96	4.150	4.499	8.41	103.60	96.82	- 6.54
84	6.220	6.532	5.02	4.470	4.782	6.98	104.80	96.70	- 7.73
85	6.690	7.018	4.90	4.930	5.258	6.65	106.40	96.37	- 9.43
86	7.270	7.526	3.52	5.490	5.746	4.66	108.00	95.35	-11.71
87	7.740	7.962	2.87	5.930	6.152	3.74	109.60	93.48	-14.71
88	8.100	8.312	2.62	6.910	7.122	3.07	113.60	94.07	-17.19
89	5.300	5.646	6.53	4.150	4.496	8.34	104.20	98.52	- 5.45
90	4.290	4.600	7.23	3.160	3.470	9.81	100.40	96.92	- 3.47
91	3.520	3.761	6.85	2.390	2.631	10.08	97.20	94.73	- 2.54
92	2.620	2.881	9.96	1.500	1.761	17.40	92.80	91.55	- 1.35
93	5.880	6.214	5.68	4.720	5.054	7.08	95.90	98.86	3.09
94	7.470	7.705	3.15	6.290	6.525	3.74	111.20	97.24	-12.55
95	8.230	N/C		5.910	N/C		107.80	N/C	

Weir No. 4. PERFORMANCE OF CHOW's NUMERICAL INTEGRATION METHOD : SUBCRITICAL FLOW, CASE II.

TEST No.	UPSTREAM DISCHARGE Q_1 l/s			SIDE SPILL DISCHARGE Q_w l/s			UPSTREAM DEPTH y_1 mm		
	measured	computed	% error	measured	computed	% error	measured	computed	% error
96	7.450	7.674	3.01	5.140	5.364	4.36	105.80	92.65	-12.43
97	6.350	6.676	5.13	4.070	4.396	8.01	102.60	94.69	- 7.71
98	5.240	5.500	4.96	3.070	3.330	8.47	98.80	94.43	- 4.42
99	4.370	4.614	5.58	2.270	2.614	15.15	95.60	92.87	- 2.86
100	3.550	3.818	7.55	1.480	1.748	18.11	91.90	90.47	- 1.56
101	2.870	2.887	0.59	1.310	1.327	1.30	90.90	90.03	- 0.96
102	4.290	4.313	0.54	2.720	2.743	0.85	97.70	95.31	- 2.45
103	4.830	4.873	0.89	3.240	3.283	1.33	99.80	96.58	- 3.23
104	6.140	6.158	0.29	4.450	4.468	0.40	104.20	97.99	- 5.96
105	7.200	7.134	- 0.92	5.470	5.404	1.21	107.60	97.67	- 9.23
106	8.030	7.978	- 0.65	6.280	6.228	- 0.83	110.80	95.53	-13.78
107	3.220	3.827	18.85	1.560	2.167	38.91	90.50	91.59	1.20
108	4.350	4.967	14.18	2.690	3.307	22.94	95.60	94.55	- 1.10
109	5.200	5.879	13.06	3.520	4.199	19.29	98.70	95.68	- 3.06
110	6.160	6.807	10.50	4.370	5.027	15.03	101.70	95.23	- 6.36
111	7.000	7.619	8.84	5.170	5.789	11.97	104.00	93.26	-10.33
112	7.530	8.076	7.25	5.660	6.206	9.65	106.40	89.71	-15.69
Mean			5.74			9.39			- 6.25
Standard Deviation			4.38			8.16			5.19

Weir No. 5. PERFORMANCE OF CHOW's NUMERICAL INTEGRATION METHOD : SUBCRITICAL FLOW, CASE II.

TEST No.	UPSTREAM DISCHARGE Q_1 l/s			SIDE SPILL DISCHARGE Q_w l/s			UPSTREAM DEPTH y_1 mm		
	measured	computed	% error	measured	computed	% error	measured	computed	% error
113	4.250	4.700	10.59	2.590	3.040	17.37	90.00	87.00	- 3.33
114	5.200	5.603	7.75	3.510	3.913	11.48	91.30	86.72	- 5.02
115	5.960	6.218	4.33	4.170	4.428	6.19	91.50	85.50	- 6.56
116	7.090	7.124	0.48	5.190	5.224	0.66	90.90	79.95	-12.05
117	7.540	7.124	- 5.52	5.630	5.214	- 7.39	90.70	79.95	-11.85
119	3.740	4.036	7.91	2.150	2.446	13.77	90.10	88.15	- 2.16
120	4.580	4.844	5.76	2.940	3.204	8.98	91.40	88.73	- 2.92
121	5.400	5.542	2.63	3.700	3.842	3.84	93.10	88.49	- 4.95
122	6.080	6.125	0.74	4.350	4.396	1.06	93.20	87.80	- 5.79
123	6.690	6.623	- 1.00	4.890	4.823	- 1.37	93.60	86.51	- 7.57
124	7.290	7.139	- 2.07	5.430	5.279	- 2.78	92.90	84.24	- 9.32
125	7.730	7.430	- 3.88	5.850	5.550	- 5.13	92.90	80.80	-13.02
126	3.020	3.164	4.77	1.460	1.604	9.86	89.50	88.30	- 1.34
127	4.360	4.421	1.40	2.780	2.841	2.19	92.60	90.51	- 2.26
128	5.340	5.336	- 0.07	3.720	3.716	- 0.11	94.30	90.97	- 3.53
129	6.130	6.013	- 1.91	4.430	4.313	- 2.64	94.60	90.60	- 4.23

Weir No. 5. PERFORMANCE OF CHOW's NUMERICAL INTEGRATION METHOD : SUBCRITICAL FLOW, CASE II.

TEST No.	UPSTREAM DISCHARGE Q_1 l/s			SIDE SPILL DISCHARGE Q_w l/s			UPSTREAM DEPTH y_1 mm		
	measured	computed	% error	measured	computed	% error	measured	computed	% error
130	6.810	6.657	- 2.25	5.040	4.887	- 3.04	94.60	89.67	- 5.21
131	7.490	7.226	- 3.52	5.700	5.436	- 4.63	94.50	88.24	- 6.62
Mean			1.45			2.68			- 5.99
Standard Deviation			4.56			7.11			3.54

Weir No. 3. PERFORMANCE OF CHOW's NUMERICAL INTEGRATION METHOD: SUPERCRITICAL FLOW, CASE I.

TEST No.	DOWNSTREAM DISCHARGE Q_2 l/s			SIDE SPILL DISCHARGE Q_w l/s			DOWNSTREAM DEPTH Y_2 mm		
	measured	computed	% error	measured	computed	% error	measured	computed	% error
71	7.000	7.641	9.16	6.200	5.559	-10.34	46.20	48.07	4.05
72	6.450	7.041	9.16	5.240	4.649	-11.28	44.70	46.75	4.59
73	5.880	6.343	7.87	4.150	3.687	-11.16	42.70	45.20	5.85
74	5.120	5.471	6.86	2.910	2.559	-12.06	41.60	43.24	3.94
75	5.630	6.067	7.76	3.740	3.303	-11.68	42.60	44.57	4.62
76	6.090	6.690	9.85	4.770	4.170	-12.58	43.60	45.97	5.44
132	7.450	7.949	6.70	6.370	5.871	- 7.83	46.00	48.42	5.26
133	7.130	7.686	7.80	5.980	5.424	- 9.30	46.00	47.83	3.98
134	6.820	7.332	7.51	5.430	4.918	- 9.43	45.20	47.05	4.09
135	6.560	6.993	6.60	4.860	4.427	- 8.91	44.00	46.28	5.18
136	6.200	6.574	6.03	4.210	3.836	- 8.88	43.10	45.36	5.24
137	5.840	6.178	5.79	3.630	3.292	- 9.31	42.50	44.44	4.56
141	7.780	8.098	4.09	6.230	5.912	- 5.10	47.20	48.50	2.75
142	7.460	7.792	4.45	5.810	5.478	- 5.71	46.70	47.84	2.44
143	7.020	7.360	4.84	5.140	4.800	- 6.61	45.80	46.86	2.31
144	6.660	7.024	5.47	4.660	4.296	- 7.81	44.90	46.08	2.63

Weir No. 3. PERFORMANCE OF CHOW's NUMERICAL INTEGRATION METHOD: SUPERCRITICAL FLOW, CASE I.

TEST No.	DOWNSTREAM DISCHARGE Q_2 l/s			SIDE SPILL DISCHARGE Q_w l/s			DOWNSTREAM DEPTH y_2 mm		
	measured	computed	% error	measured	computed	% error	measured	computed	% error
145	6.300	6.607	4.87	4.030	3.723	- 7.62	43.90	45.12	2.78
146	5.890	6.153	4.47	3.400	3.137	- 7.74	42.40	44.05	3.89

	% error (Q_2)	% error (Q_w)	% error (y_2)
Mean	6.63	- 8.91	4.09
Standard Deviation	1.76	2.38	1.12

Weir No. 3. PERFORMANCE OF CHOW's NUMERICAL INTEGRATION METHOD: SUPERCRITICAL FLOW, CASE IV.

TEST No.	DOWNSTREAM DISCHARGE Q_2 l/s			SIDE SPILL DISCHARGE Q_w l/s			DOWNSTREAM DEPTH y_2 mm		
	measured	computed	% error	measured	computed	% error	measured	computed	% error
77	7.010	7.559	7.83	5.630	5.081	- 9.75	47.00	47.77	1.64
78	7.950	8.166	2.72	4.640	4.424	- 4.66	48.10	48.24	0.29
79	8.840	8.879	0.44	3.690	3.651	- 1.06	49.00	48.27	- 1.49
138	7.490	7.834	4.59	5.140	4.796	- 6.69	46.60	47.80	2.58
139	8.280	8.435	1.87	4.240	4.085	- 3.66	47.70	48.07	0.21
140	9.280	9.128	- 1.64	3.320	3.472	4.58	48.00	48.09	0.19
147	7.750	7.950	2.58	4.750	4.550	- 4.21	47.40	47.63	0.49
148	8.680	8.635	- 0.52	3.820	3.865	1.18	48.10	47.93	0.35
149	9.420	9.207	- 2.26	3.050	3.263	6.98	48.40	47.75	1.34
Mean			1.73			- 1.92			0.25
Standard Deviation			3.18			5.38			1.29